Photoemission with soft and hard x-rays: Some future perspectives

Chuck Fadley
Dept. of Physics, UC Davis
Materials Sciences Division
Lawrence Berkeley National Laboratory
Soleil Synchrotron

Supported by:
DOE: LBNL Materials Sciences Division
"Nanoscale Magnetic Materials"
ARO-Multi-University Research Initiative:
"Emergent Phenomena at Mott Oxide Interfaces"
Peter Grünberg Institute, PGI 6, Jülich Research Center
LABEX-PALM-APTCOM Project, Triangle de Physique, Paris

Soleil seminars: 21 July, 15 September, 22 September; 2014

The Core Group: Present→Past

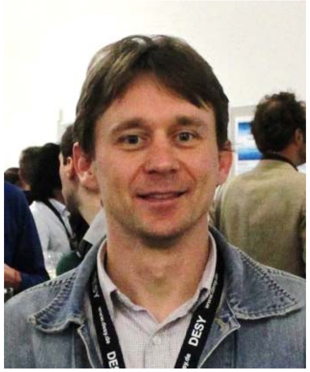

Lukasz Plucinski
→Jülich

Alexander Kaiser
→SPECS

Alex Gray
→Stanford

Julian Rault
(Soleil/LBNL)

Postdocs **Senior Scientist** **Grad students** **External Student Visitors**

Other Institutions and Collaborators

THE UNIVERSITY OF CALIFORNIA
DAVIS

1990-

BERKELEY LAB

1972-1990

UNIVERSITY · OF · HAWAI'I
1907
MĀNOA

1976-1991

SSRL

1978-1988: LURE

Other Institutions and Collaborators

1990-

The Advanced Light Source

PETRA III

Experiments/Data Analysis **Sample Synthesis/Charac.** **Theory/Modeling**

A. Gray[1,2], S. Nemšák[1,2], A. Kaiser[1,2,&], G. Conti[1,2], C. Papp[1,2,*], B. Balke[1,2,+], S. Ueda[3,4], Y. Yamashita[3,4], K. Kobayashi[3,4], M. Gorgoi[5], S.-H. Yang[6], L. Plucinski[7], S. Döring[8], U. Berges[8], M. Huijben[9,10], D. Buergler[7], F. Hellman[2,11], E. Rotenberg[12], A. Bostwick[12], J. Minar[13], J. Braun[13], H. Ebert[13], P. Krüger[14], J. Fujii[15], G. Panaccione[15], C. Caspers[7], M. Mueller[7], B.C. Sell[1,2,#], M. W. West[2], M. Press[2], F. Salmassi[2], J.B. Kortright[2], E. Gullikson[2], S.S.P. Parkin[6], A. Gloskovskii[16], W. Drube[16], F. Kronast[5], C. Westphal[8], V. Strocov[18], M. Kobayashi[18], J. Rault[19], J.-P. Rueff[19], M.-C. Asensio[19], J. Avila[19], A. Taleb-Ibrahim[19], P. Lefevre[19], F. Bertran[19], C.M. Schneider[7], H. Ohno[20], R. Ramesh[2,9,11], J. Son[17], P. Moetakef[17], S. Stemmer[17], M. Bibes[22], A. Janotti[17], C. Van der Welle[17], R. Pentcheva[21], et al.

---

[1]Physics, UC Davis; [2]Mat. Sci. Div., LBNL; [3]SPring-8; [4]NIMS; [5]HZB-BESSY Berlin; [6]IBM Almaden; [7]Research Center Jűlich; [8]Physics, Tech. Univ. Dortmund; Physics; [9]Mat. Sci., UC Berkeley; [10]Univ. of Twente; [11] Physics, UC Berkeley; [12]ALS, LBNL; [13]Phys. Chem., Univ. Munich; [14]Univ. Bourgogne, Dijon; [15]TASC, Trieste; [16]Petra III, Hamburg; [17]UC Santa Barbara; [18]SLS: [19]Soleil; [20]Tohoku Univ., [21] Physics Dept., Duisberg Univ.; [22] CNRS-Thales-U. Paris Sud; Pres. addresses: [&]SPECS; [*]Univ. Erlangen; [+]Univ. Mainz; [#]Wright-Patterson AFB

A few recent overviews

- "X-Ray Photoelectron Spectroscopy and Diffraction in The Hard X-Ray Regime: Fundamental Considerations and Future Possibilities", CSF, Nuc. Inst. & Meth. A 547, 24-41 (2005)
- "X-ray Photoelectron Spectroscopy : Progress and Perspectives", CSF, invited review, J. Electron Spectrosc. 178–179, 2 (2010)
- "Looking Deeper: Angle-Resolved Photoemission with Soft and Hard X-Rays", CSF, Synchrotron Radiation News 25, 26 (2012)
- "Some future perspectives in soft- and hard- x-ray photoemission", CSF and S. Nemšák, J. Electron Spectrosc., online pub.:

http://authors.elsevier.com/sd/article/S036820481400139X

- "Hard X-ray photoemission: an overview and future outlook", CSF, book chapter, in preparation

The Photoelectric Effect, Einstein, 1905

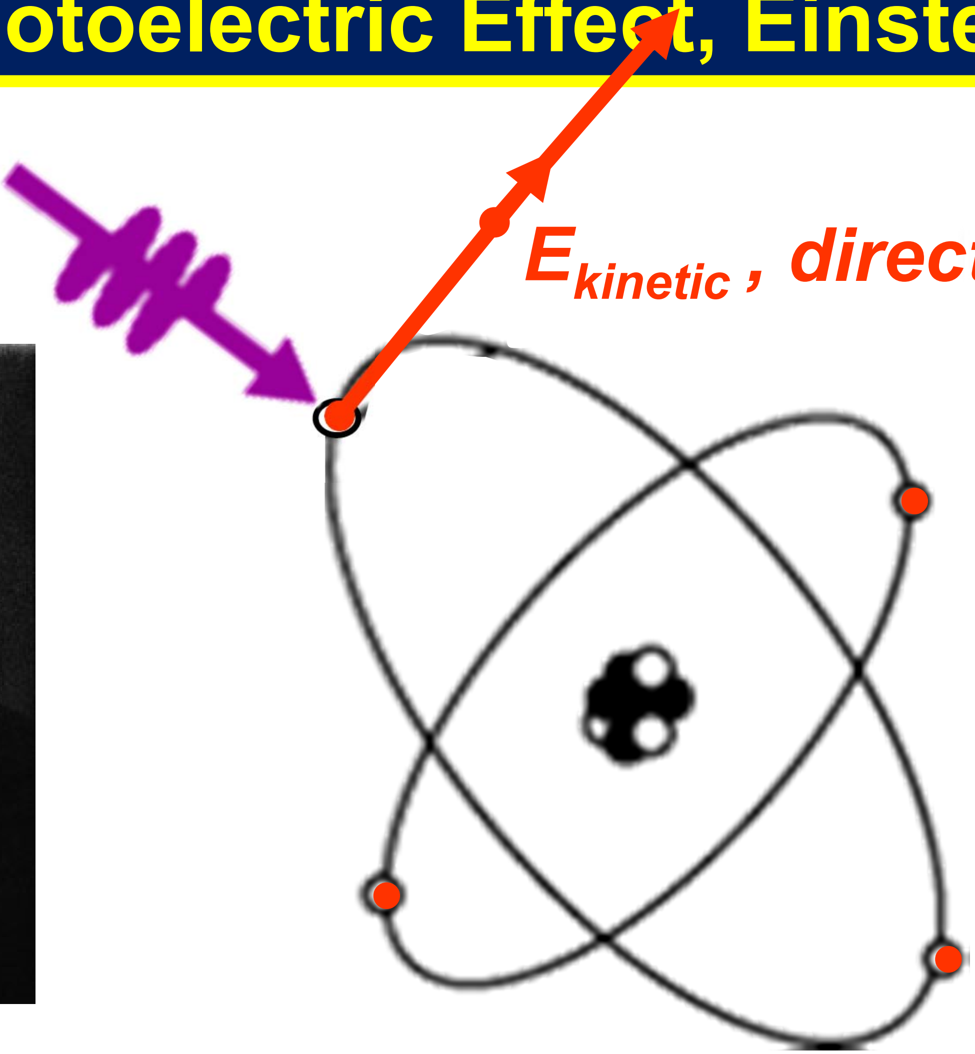

$$h\nu = E_{initial} - E_{final} = E_{binding} + E_{kinetic}$$

ATOMIC (CORE) PHOTOELECTRON INTENSITIES: THE THREE-STEP MODEL

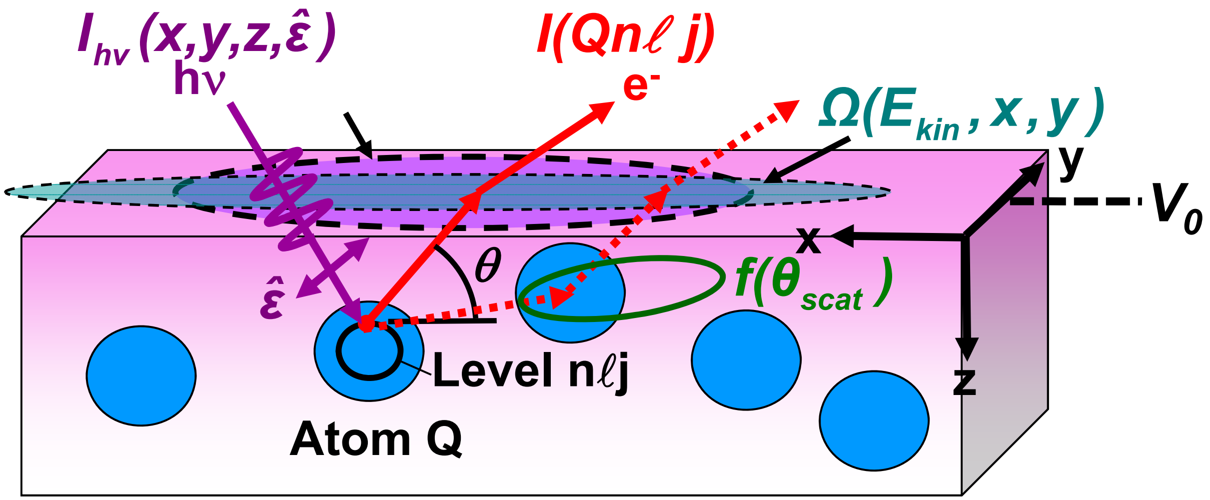

$I(Qn\ell\, j)$ =

$$C\int_0^\infty I_{hv}(x,y,z,\hat{\varepsilon})\rho_Q(x,y,z)\frac{d\sigma_{Qn\ell j}(hv,\hat{\varepsilon})}{d\Omega}\exp\left[-\frac{z}{\Lambda_e(E_{kin})\sin\theta}\right]\Omega(E_{kin},x,y)dxdydz$$

$I_{hv}(x,y,z,\hat{\varepsilon})$ = *x-ray flux*, $\hat{\varepsilon}$ = *polarization*

$\rho_Q(x,y,z)$ = *density of atoms Q* → *quantitative analysis*

$\frac{d\sigma_{Qn\ell j}(hv,\hat{\varepsilon})}{d\Omega}$ = *energy-dependent differential photoelectric cross section for subshell* $Qn\ell\, j$

$\Lambda_e(E_{kin})$ = *energy-dependent inelastic attenuation length* + *elastic scattering:* $f(\theta_{scat})$

→ *Effective Attenuation Length (EAD)* → *Mean Emission Depth (MED)*

$\Omega(E_{kin},x,y)$ = *energy-dependent spectrometer acceptance solid angle = transmission function*

V_0 = *inner potential*

Photoemission from surfaces, complex bulk materials, buried layers, interfaces

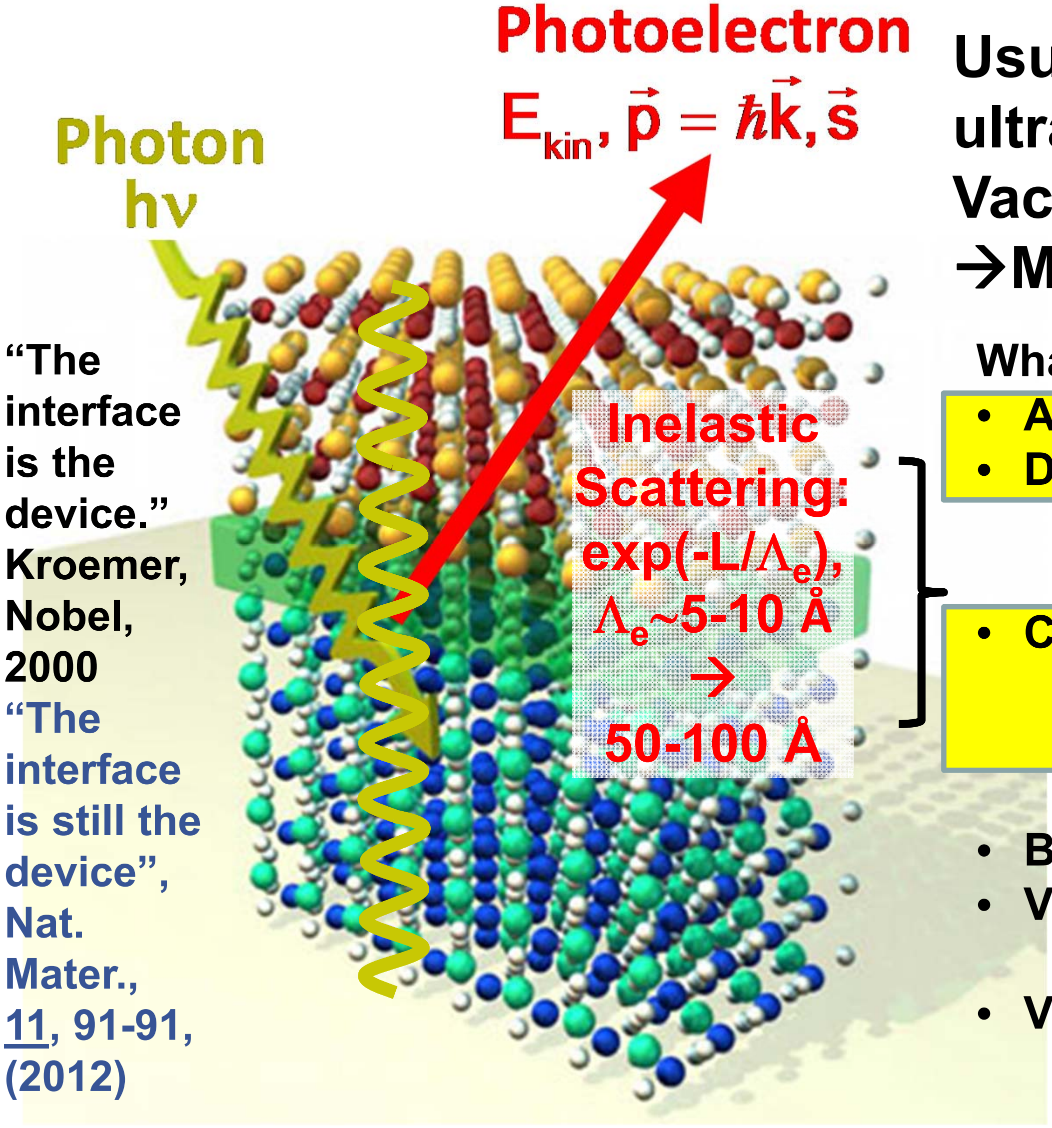

“The interface is the device.” Kroemer, Nobel, 2000

“The interface is still the device”, Nat. Mater., 11, 91-91, (2012)

Usually ultrahigh Vacuum
→Multi-Torr

TEM+EELS+HAADF+…

What do we want to know?

- Atomic structure, lattice distortions
- Depth profiles of composition and optical properties, from surface inward
- Core-levels→element-specific binding energies, charge states electronic configurations, magnetic moments/magnetization
- Band offsets, depth-dependent pot’ls.
- Valence-band densities of states bandgaps, behavior near E_F (XPS)
- Valence-band dispersions, via depth- and angle- resolved photoemission (ARPES)

X-ray photoemission: some key elements

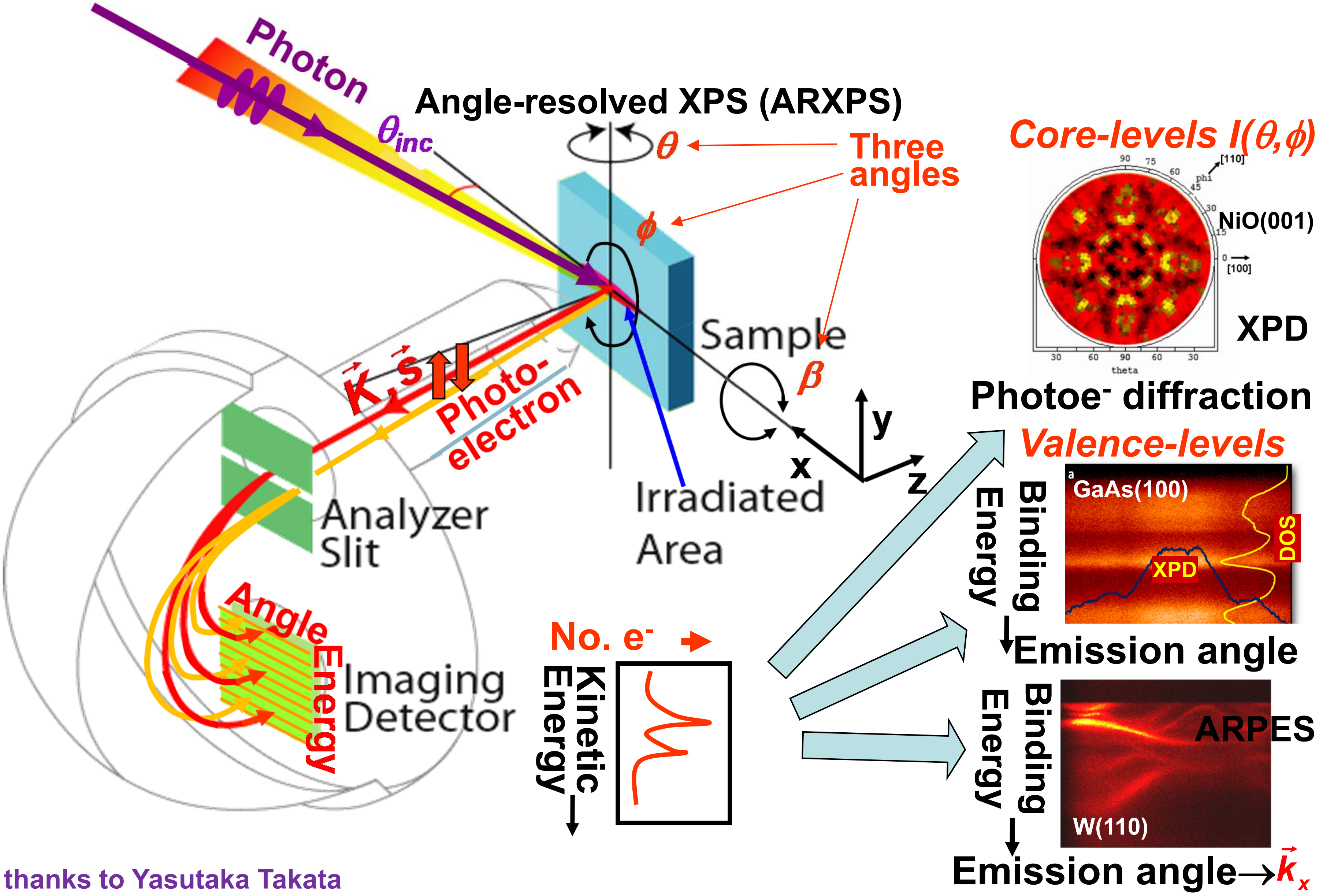

With thanks to Yasutaka Takata

X-ray photoemission: some key elements

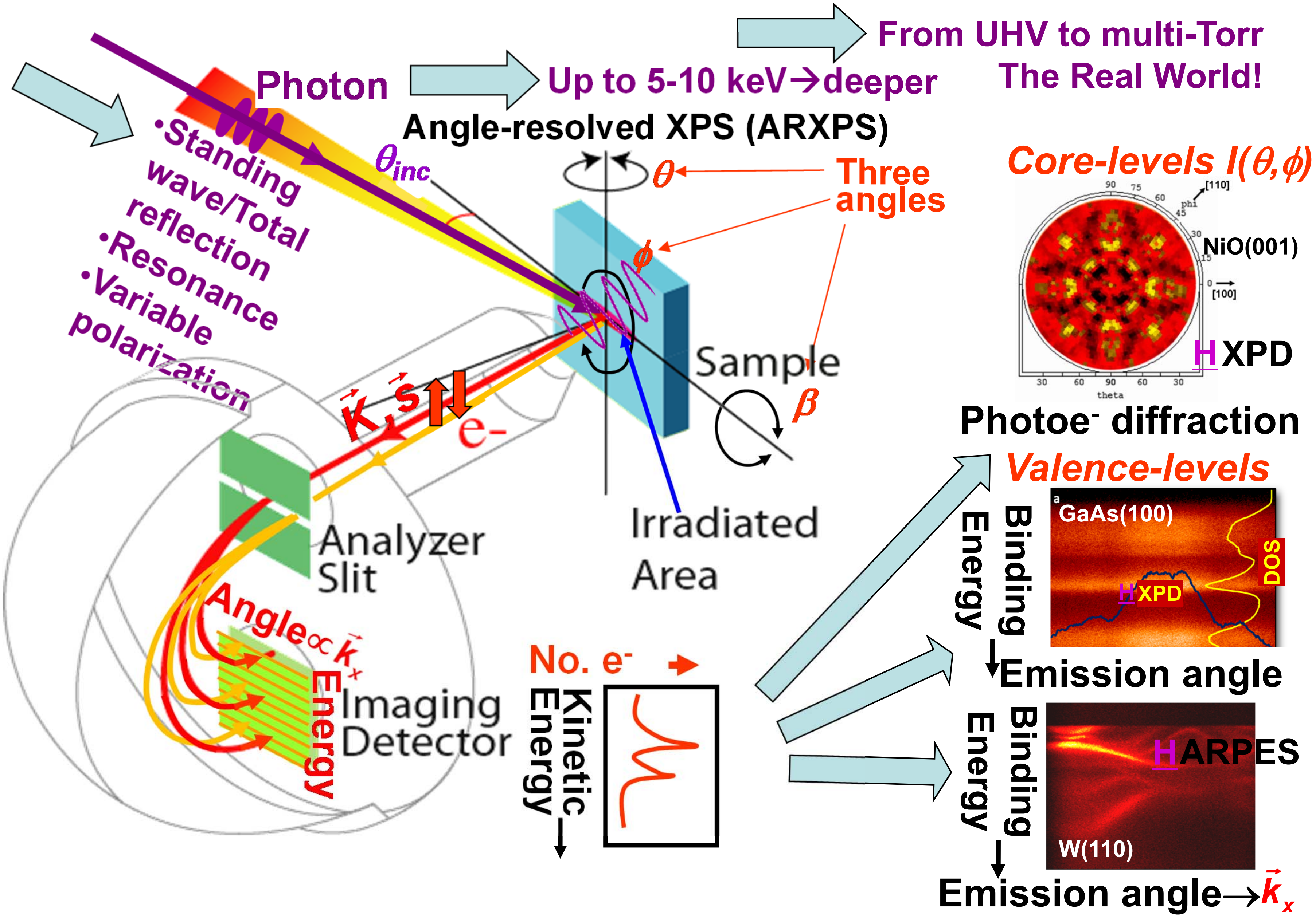

Photon → **Up to 5-10 keV→deeper** → **From UHV to multi-Torr The Real World!**

- •Standing wave/Total reflection
- •Resonance
- •Variable polarization

Angle-resolved XPS (ARXPS)

Three angles

Core-levels $I(\theta,\phi)$

Photoe⁻ diffraction

Valence-levels

Emission angle→$\vec{k}_x$

Photoemission from complex materials, heterostructures, and interfaces

Three ways to address the limitations of traditional photoemission:

- **Use of harder x-ray excitation (SXPS→2 keV, HXPS, HAXPES→10 keV) for deeper probing: core levels and valence DOSs, incl. soft and hard x-ray angle-resolved photoemission (ARPES) and photoelectron diffraction (XPD)**

- **Use of soft and hard x-ray standing waves, total reflection, other x-ray optical effects, resonant excitation, to selectively look below the surface, at buried interfaces, including ARPES**

- **Use of differentially-pumped systems to provide multi-Torr ambient pressure photoemission, more real-world conditions for studying surface chemical processes, catalysis, electrochemistry**

Lectures will be posted at Soleil website and group website:

http://www.physics.ucdavis.edu/fadleygroup/Soleil.Lectures.Fadley.pdf

More bulk sensitivity in photoemission by going to hard x-rays

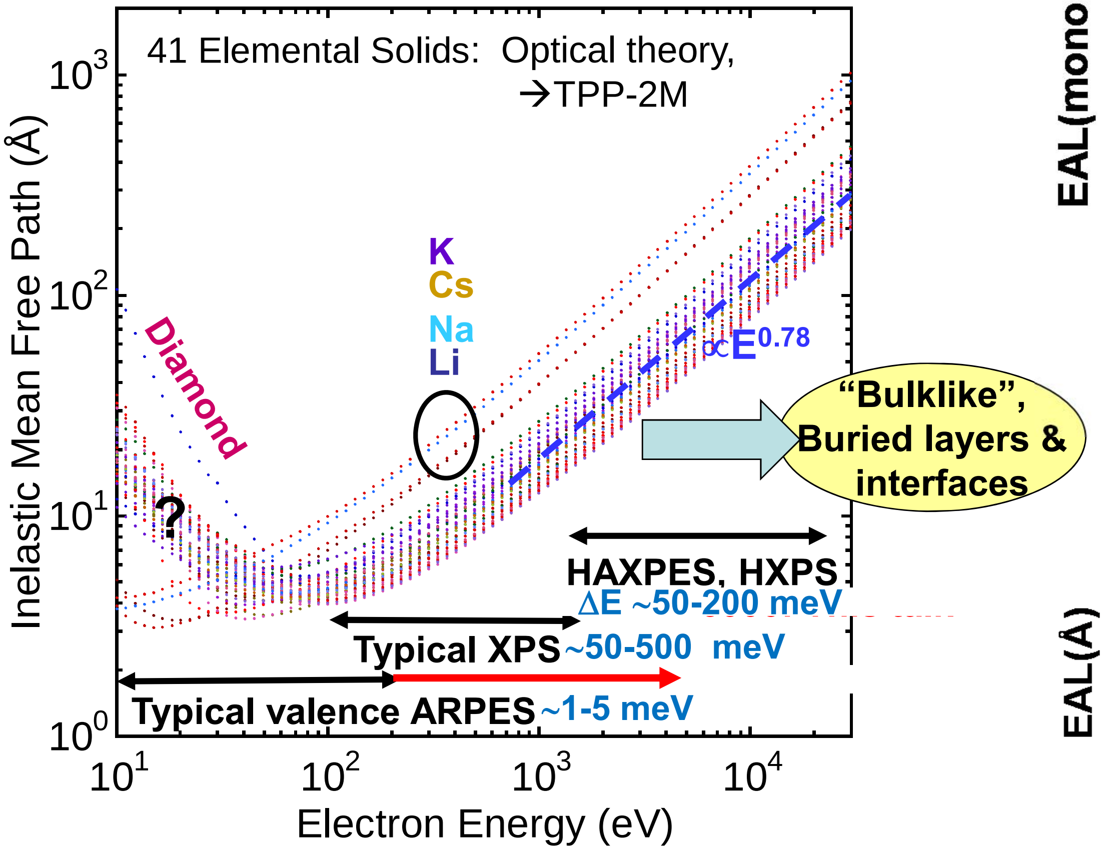

Tanuma, Powell, Penn, Surf. and Interf. Anal. 43, 689 (2011)

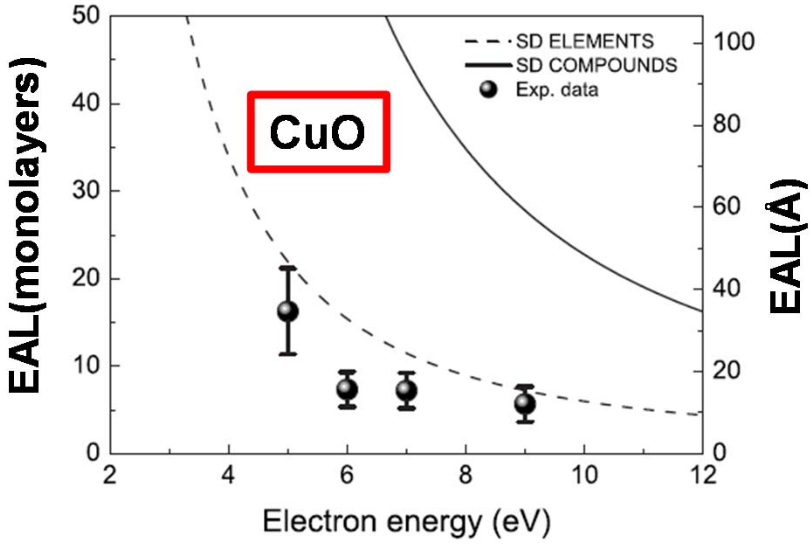

Offi et al., PRB 77, 201101R (2008)

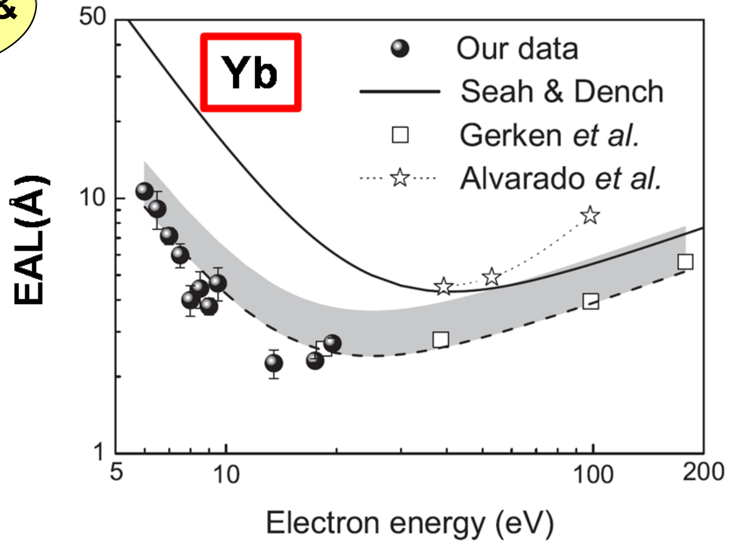

Offi et al., J. Phys.: Cond. Matt. 22 (2010) 305002

→The only certain way to obtain more bulk sensitivity

And with competitive energy resolutions

Soleil--GALAXIES beamline

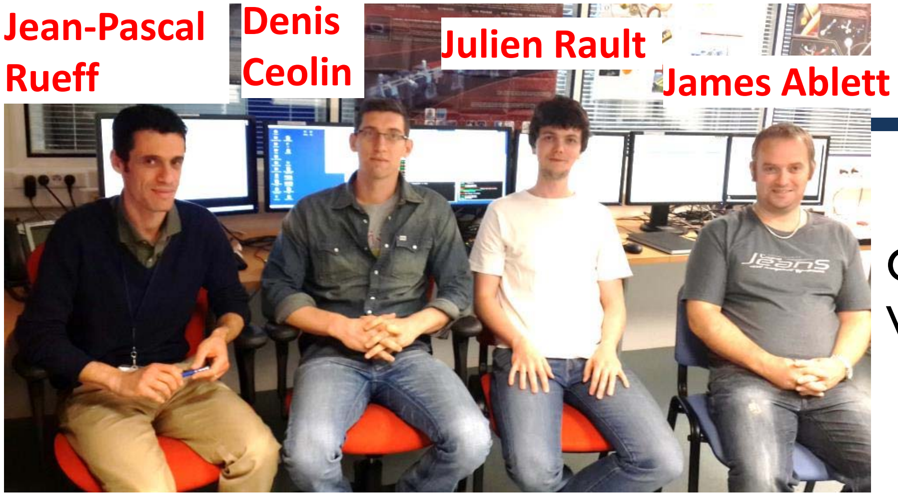

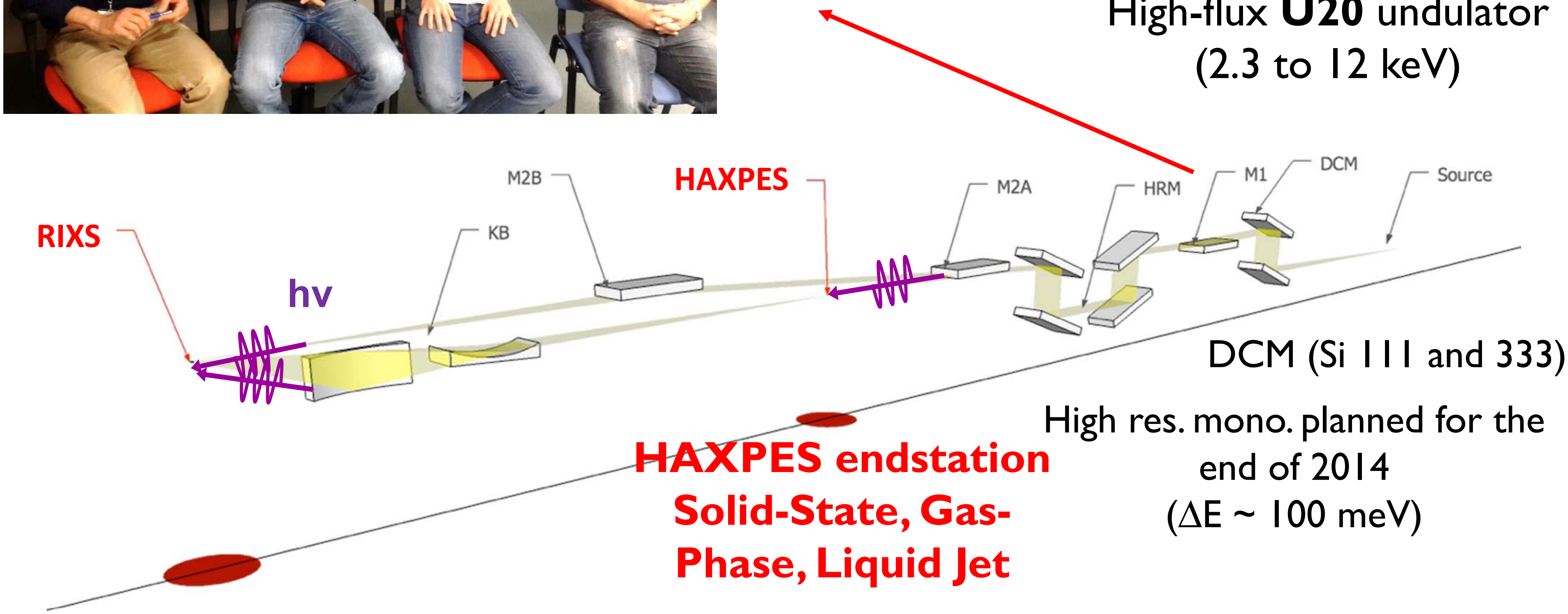

Quarter-wave plate
Variable polarization

High-flux **U20** undulator
(2.3 to 12 keV)

DCM (Si 111 and 333)

High res. mono. planned for the
end of 2014
(ΔE ~ 100 meV)

HAXPES endstation
Solid-State, Gas-Phase, Liquid Jet

30x80 µm² beam spot

RIXS endstation

10x10 µm² beam spot

J.-P. Rueff, J. Rault

Hard x-ray photoemission—plusses and minusses

•**Plusses**

•More bulk sensitive spectra → a versatile tool for any new material or multilayer nanostructure

•Inelastic background less important & Augers more widely spread, less overlap

•Less radiation damage and charging-sort of

•**Minusses**

•Resolution not as good as ~1 meV VUV PS, but as good/better than SX PS, and down to ~50 meV overall, good enough for many applications

Comparison of inelastic mean free paths and energy-loss stopping powers dE/dx

Calculated inelastic mean free paths (Å) [Surf. Interface Anal. 43, 689 (2011)]

Calculated stopping powers dE/dx ÷ density (MeV-cm^2/g) [Nucl. Inst. & Meth. B 270 (2012) 75–92]

H. Shinotsuka, S. Tanuma, C.J. Powell, D.R. Penn

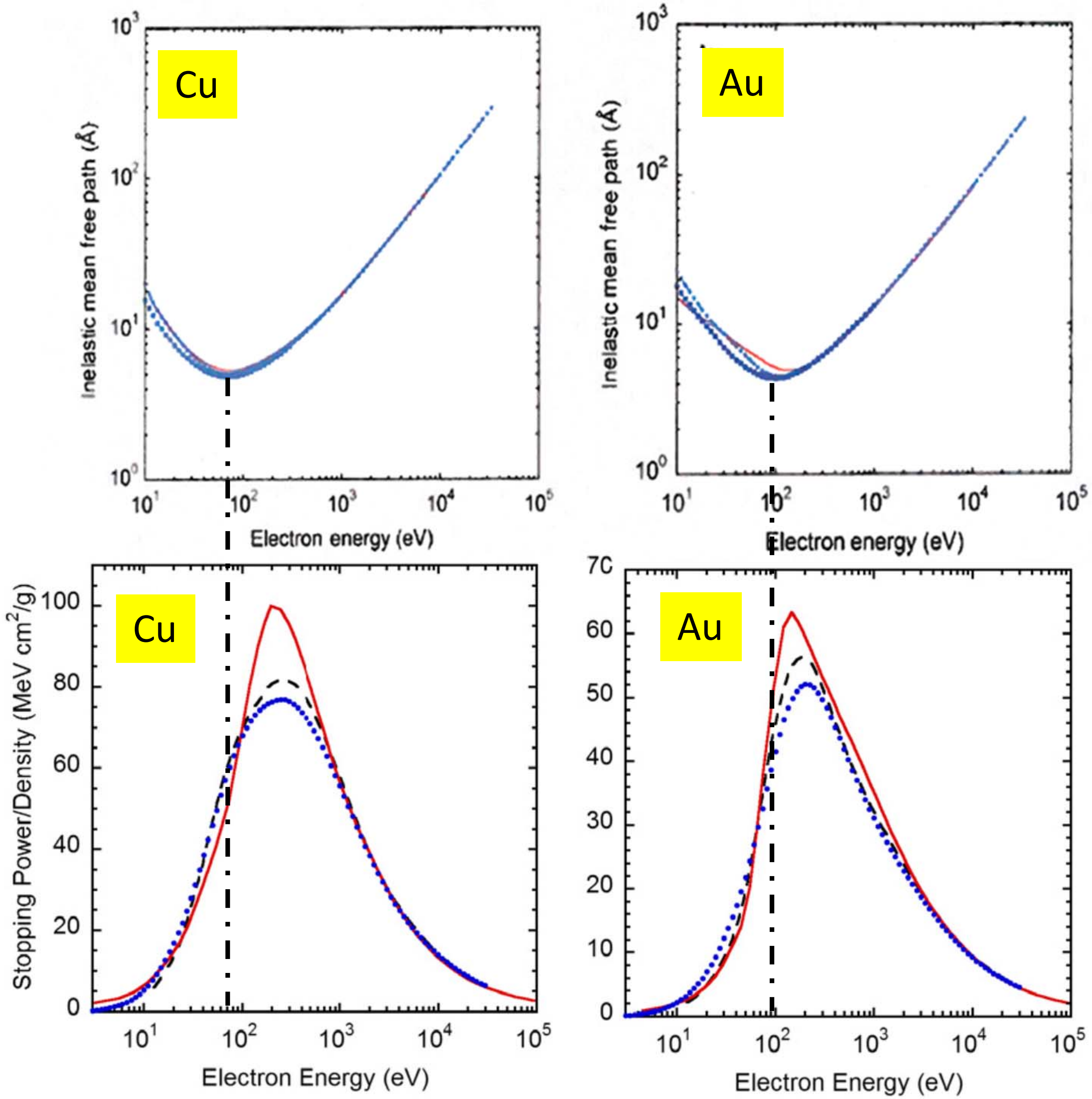

→HXPS/HAXPES spectra have less intense inelastic backgrounds

Hard x-ray photoemission—survey spectrum

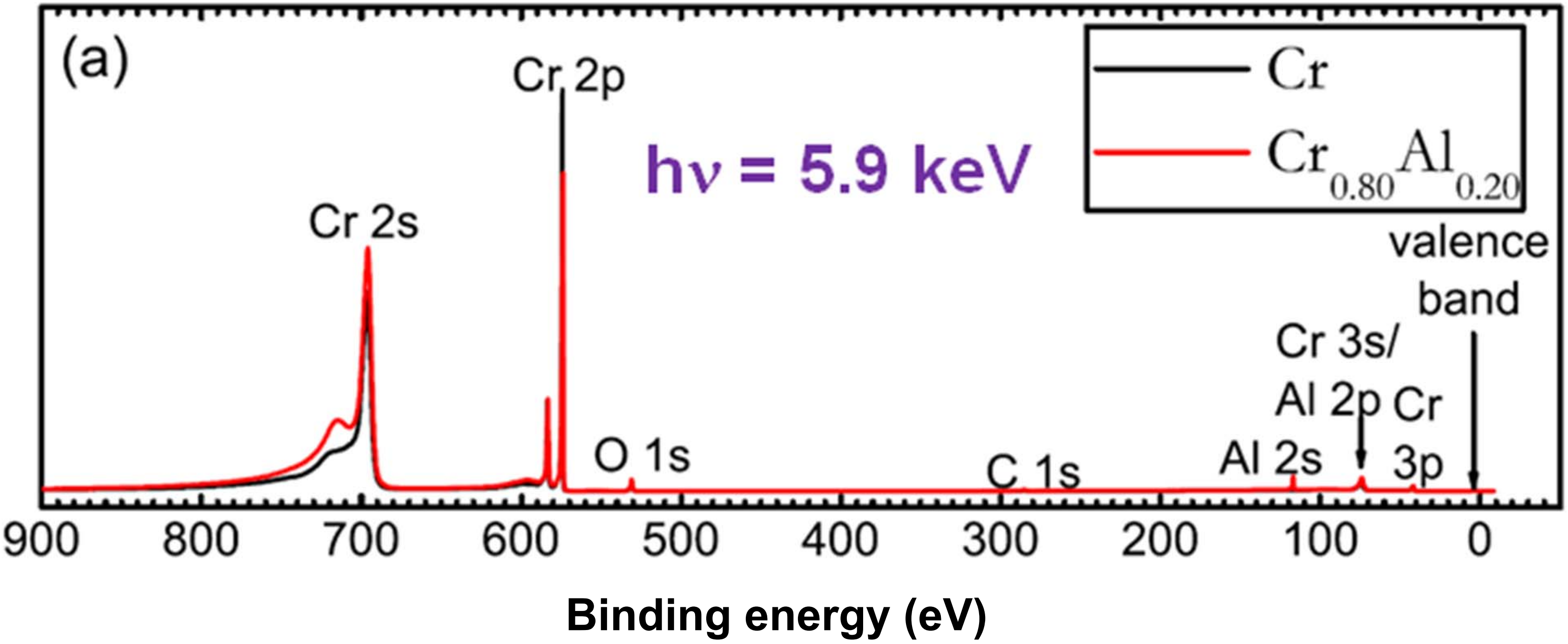

Boekelheide, Gray, et al., PRL 105, 236404 (2010)-SPring-8

How strongly do we expect to see different valence orbital character as a function of photon energy? How deep do we probe? $GdTiO_3/SrTiO_3$ example

Photoelectric cross sections:

- **Soft x-rays: (Yeh, Lindau)**

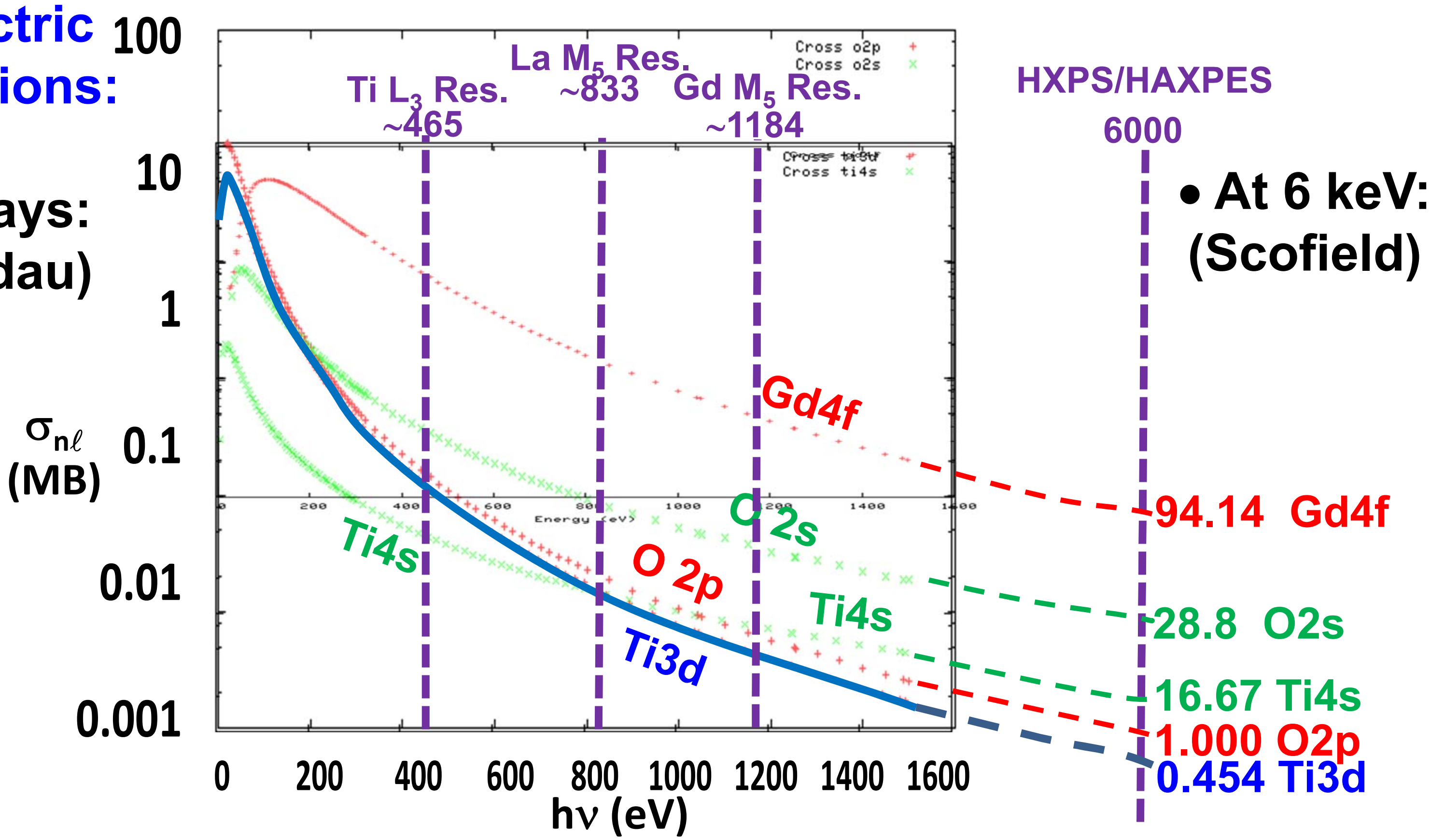

- **At 6 keV: (Scofield)**

Inelastic electron mean free paths → ~ mean depth of photoemission:

STO: 11 Å 16 Å 22 Å 83 Å

GTO: 10 Å 15 Å 20 Å 72 Å

Hard x-ray photoemission—plusses and minusses

- **Plusses**

- More bulk sensitive spectra → a versatile tool for any new material or multilayer nanostructure

- Inelastic background less important & Augers more widely spread, less overlap

- Less radiation damage and charging-sort of

Minusses

- Resolution not as good as ~1 meV VUV PS, but as good/better than SX PS, and down to ~50 meV overall, good enough for many applications

- Photoelectric cross sections low, need special undulator beamline/spectrometer combinations—several solutions→
<1 micron focus and ~50 meV resolution

- High *n,* low-ℓ cross section components strongly favored, but in TM or RE VB they can be more involved in transport , s and p like

-

Hard x-ray photoemission—plusses and minusses

- **Plusses**
- More bulk sensitive spectra → a versatile tool for any new material or multilayer nanostructure
- Inelastic background less important & Augers more widely spread, less overlap
- Less radiation damage and charging-sort of

Minusses

- Resolution not as good as ~1 meV VUV PS, but as good/better than SX PS, and down to ~50 meV overall, good enough for many applications
- Photoelectric cross sections low, need special undulator beamline/spectrometer combinations—several solutions→ <1 micron focus and ~50 meV resolution
- High *n,* low-ℓ cross section components strongly favored, but in TM or RE VB they can be more involved in transport , s and p like
- Recoil energy limits resolution for lighter elements; complex systematics, depending on local bond distances/phonon frequencies→Doppler spectroscopy?

The Photoelectric Effect, Einstein, 1905

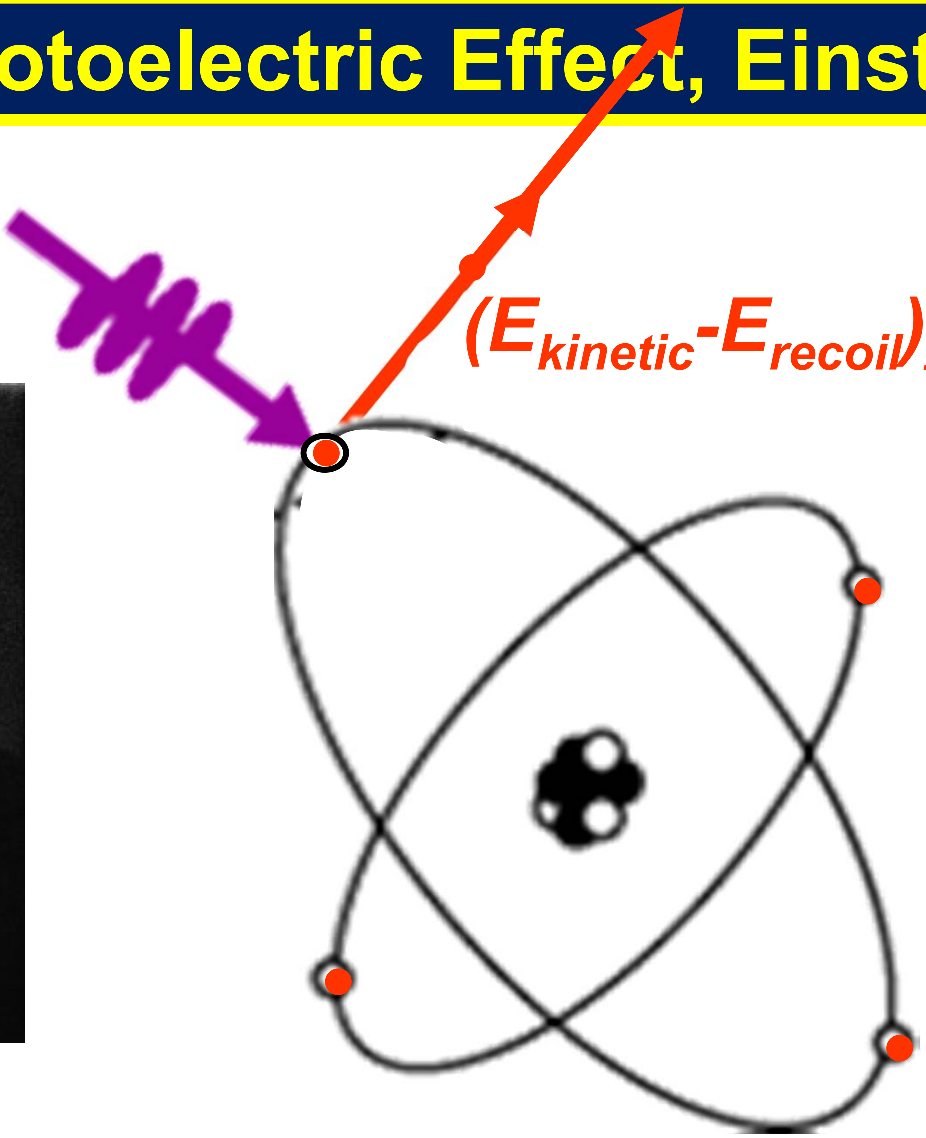

$(E_{kinetic}-E_{recoil})$,direction,spin

$$h\nu = E_{initial} - E_{final} = E_{binding} + (E_{kinetic} - E_{recoil})$$

Well known in free atoms and molecules: Siegbahn et al., ESCA (1967) →→ T.D. Thomas et al. Phys. Rev. Lett. 106, 193009 (2011); M.D. Simon et al., Nat. Comm. 5, 4069 (2014)

Recoil in photoemission from solids

Recoil shift: $\Delta E_{recoil} \approx (m_e/M_{atom})E_{kinetic}$

C 1s in graphite

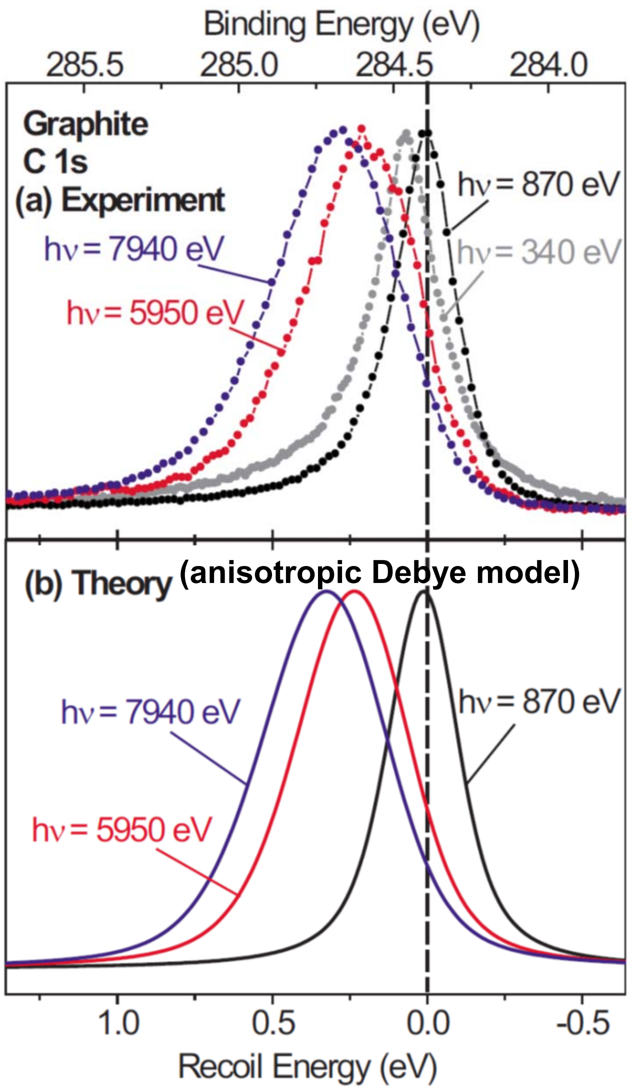

Y. Takata et al.
PRB 75, 233404 (2007)

Al valence bands

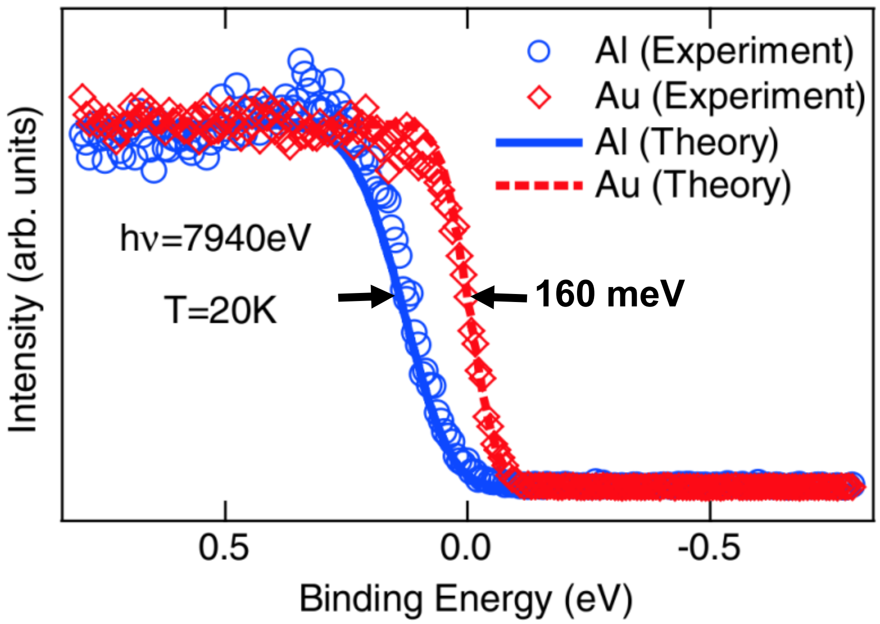

Y. Takata et al.
PRL 101, 137601 (2008)

Approximate recoil-free fraction = Debye-Waller factor--Graphite

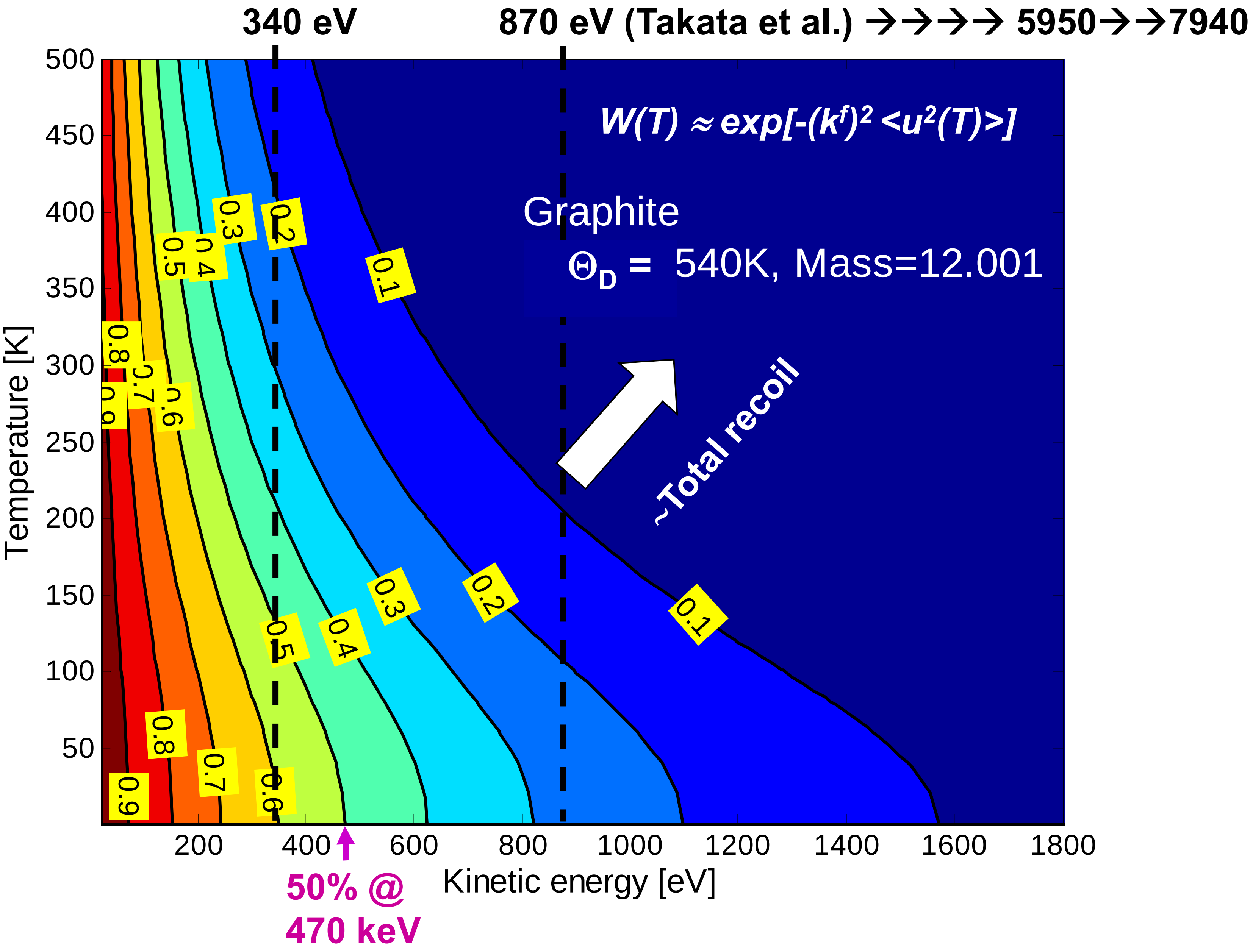

340 eV

870 eV (Takata et al.) →→→→ 5950→→7940

$$W(T) \approx \exp[-(k^f)^2 <u^2(T)>]$$

Graphite

Θ_D = 540K, Mass=12.001

~Total recoil

50% @ 470 keV

L. Plucinski

Recoil energy for all atoms and different photon energies

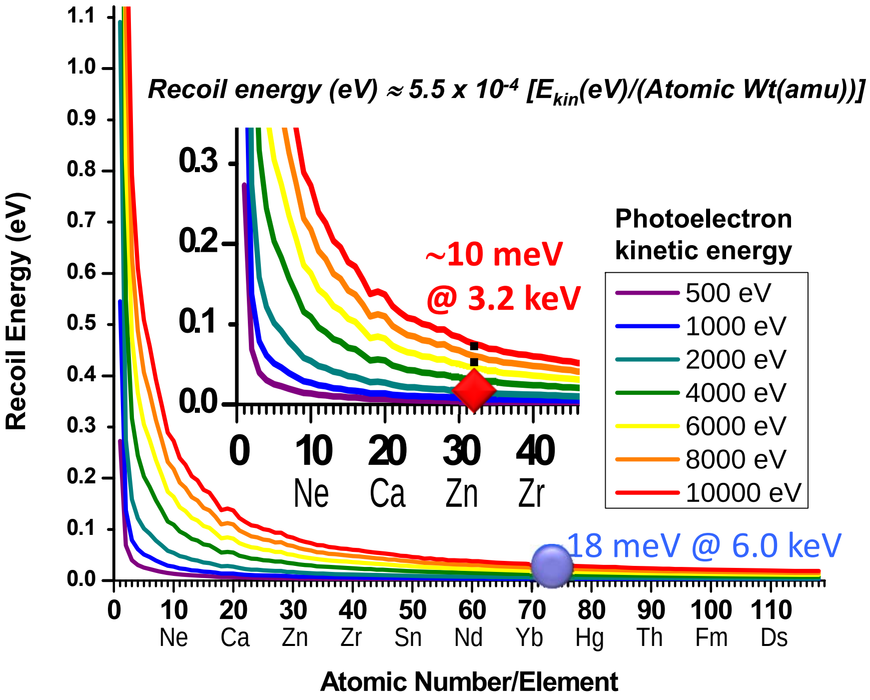

Recoil energy (eV) ≈ 5.5 x 10^{-4} [E_{kin}(eV)/(Atomic Wt(amu))]

~10 meV @ 3.2 keV

18 meV @ 6.0 keV

In solids:
Photon energy for ~50% recoil-free = O.5 Debye-Waller factor @ 20K

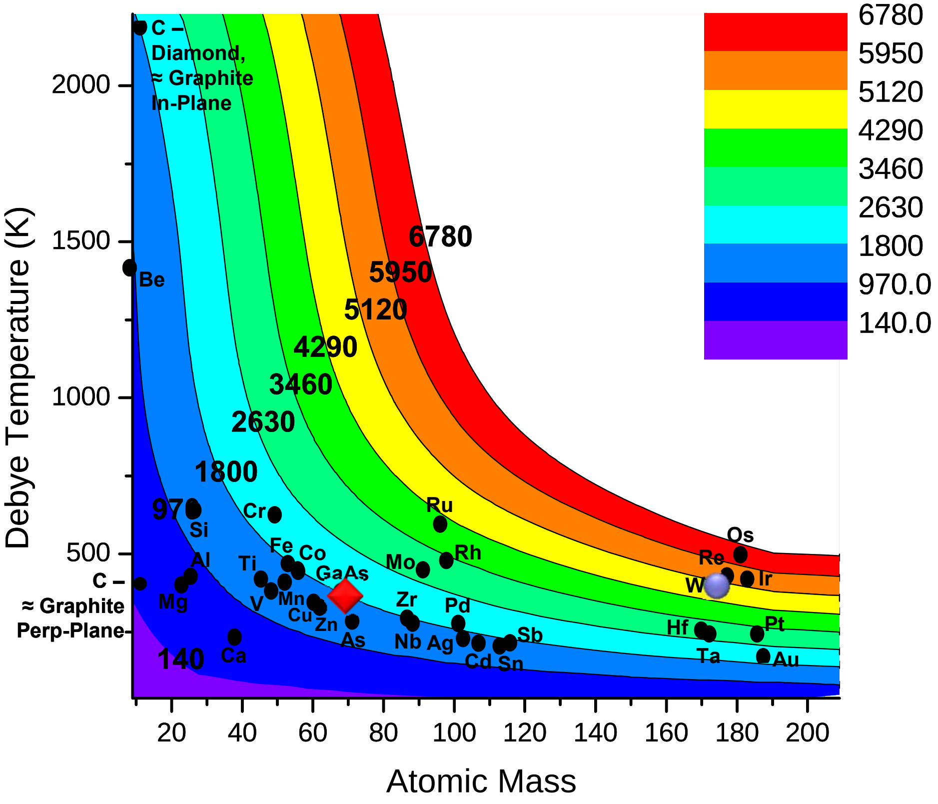

But this depends on local vibrational excitations, can be element-specific

But these estimates seem to be too pessimistic for some systems

C. Papp. L. Plucinski, et al.,
Phys. Rev. B 84, 045433 (2011)
C.S.F., SRN 25, 26 (2012)

A first real application of soft x-ray ARPES: Soft x-ray ARPES from $SrCuO_2$ at $h\nu$ = 700 eV and 300K, photoemission Debye-Waller factor of only 0.03-0.04

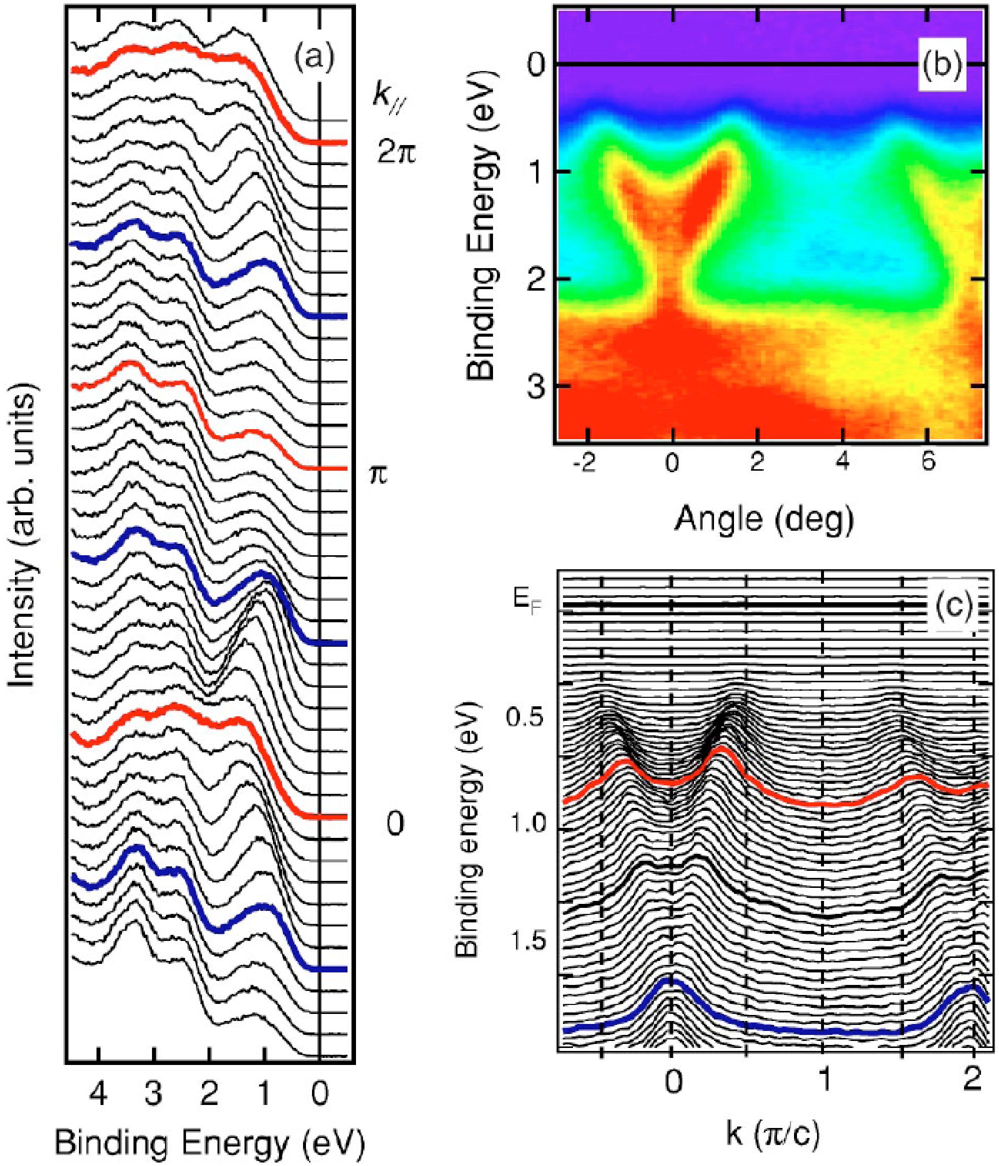

Photoemission DW factors can be too conservative for some systems (lack of correlated vibrations?) →suggests a wider application of SARPES/HARPES

S. Suga, A. Sekiyama, et al., PRB 70, 155106 (2004)

Hard x-ray photoemission—plusses and minusses

•**Plusses**

•More bulk sensitive spectra → a versatile tool for any new material or multilayer nanostructure

•Inelastic background less important & Augers more widely spread, less overlap

•Less radiation damage and charging-sort of

•Easier interpretation of angle-resolved (ARXPS) data → surface and bulk information

Minusses

•Resolution not as good as ~1 meV VUV PS, but as good/better than SX PS, and down to ~50 meV overall, good enough for many applications

•Photoelectric cross sections low, need special undulator beamline/spectrometer combinations—several solutions→
<1 micron focus and ~50 meV resolution

•High *n,* low-ℓ cross section components strongly favored, but in TM or RE VB they can be more involved in transport , s and p like

•Recoil energy limits resolution for lighter elements; complex systematics, depending on local bond distances/phonon frequencies→Doppler spectroscopy?

Varying surface sensitivity for lower electron takeoff angles—ARXPS & ARHXPS

Simplest interpretation:

Average emission depth = $\Lambda_{inelastic}\sin\theta_{takeoff}$

How valid?

$E_{kin} \approx$ 500-1000 eV

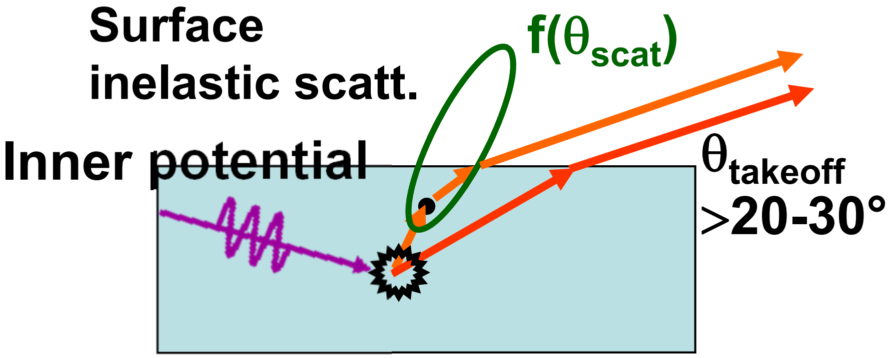

E.g.: A. Jablonski and C. J. Powell, J. Vac. Sci. Tech. A 21, 274 (2003):
→ Mean Emission Depth (MED) more relevant than $\Lambda_{inelastic}$

Varying surface sensitivity for lower electron takeoff angles—ARXPS & ARHXPS

Simplest interpretation:

Average emission depth = $\Lambda_{inelastic}\sin\theta_{takeoff}$

How valid?

$E_{kin} \approx$ 500-1000 eV

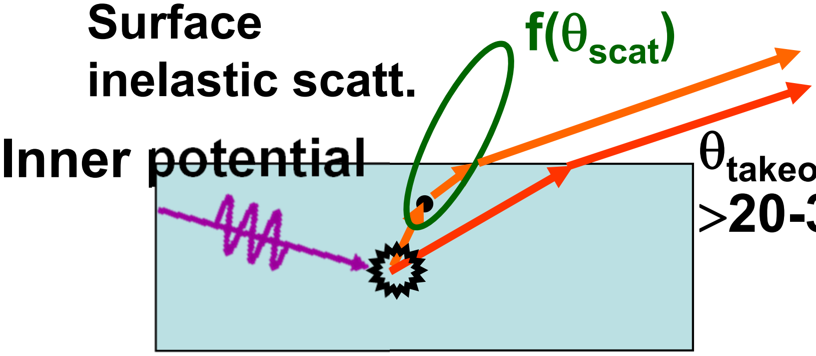

Surface inelastic scatt.

$f(\theta_{scat})$

Inner potential

$\theta_{takeoff}$ >20-30°

E.g.: A. Jablonski and C. J. Powell, J. Vac. Sci. Tech. A 21, 274 (2003):
→ Mean Emission Depth (MED) more relevant than $\Lambda_{inelastic}$

$E_{kin} \approx$ 10,000 eV

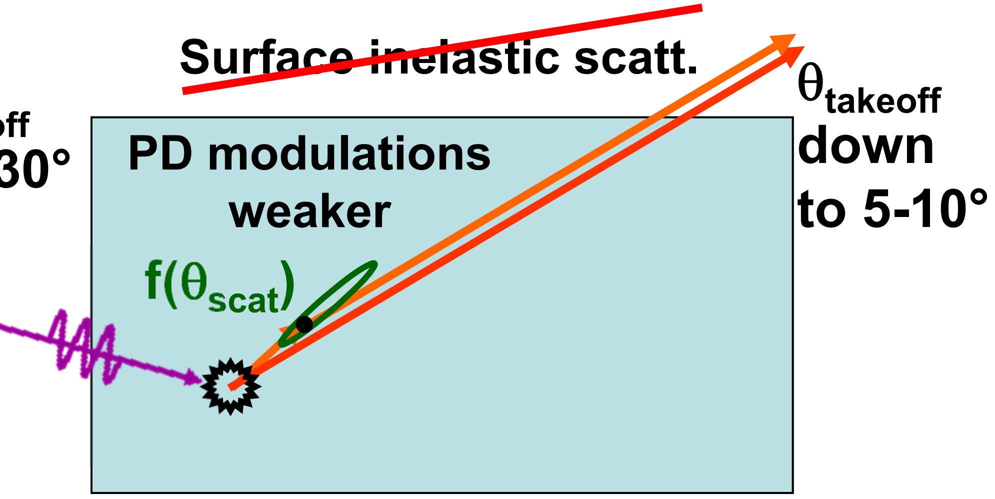

~~Surface inelastic scatt.~~

$\theta_{takeoff}$ down to 5-10°

PD modulations weaker

$f(\theta_{scat})$

Approx. constant analyzer transmission, $\Omega(E_{kin},x,y)$ and Λ_e-IMFP

Cleaner bulk & surface distinction

C.S.F., Nucl. Inst. & Meth. A 547, 24 (2005)

Kover, Werner, Drube, et al., Surf. & Int. Anal. 38, 569 (2006)

Looking into nanoscale devices--Variable takeoff-angle Si 1s photoelectron spectra from NiGe(12-nm)/SiO_2(12-nm)/Si(100)

Average depth ≈ $\Lambda_{IMFP}\sin\Theta$

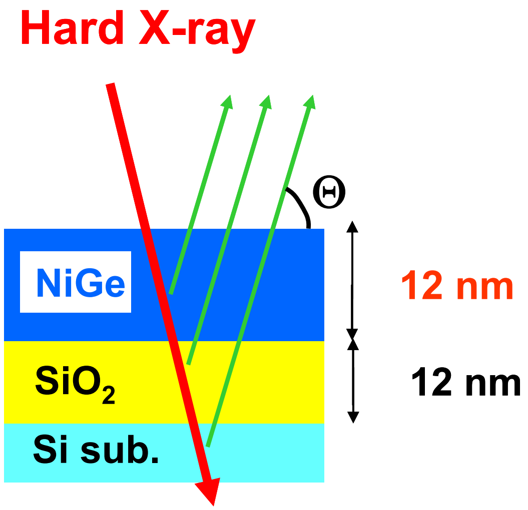

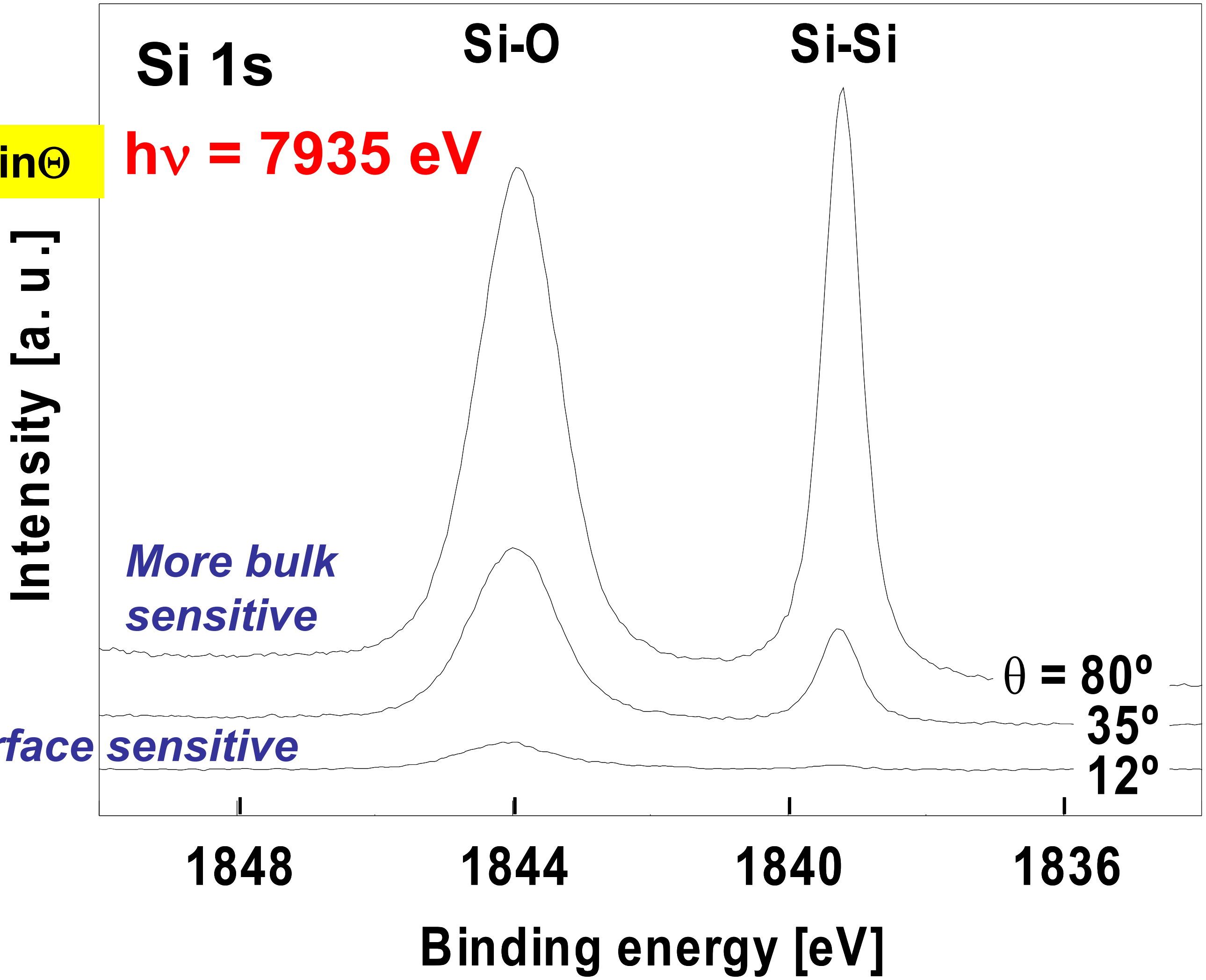

Hattori et al.-SPring8, Int. J. High Speed Electronics 16, 353 (2006)-Spring-8

Hard x-ray photoemission—plusses and minusses

•**Plusses**

- •More bulk sensitive spectra → a versatile tool for any new material or multilayer nanostructure
- •Inelastic background less important & Augers more widely spread, less overlap
- •Less radiation damage and charging-sort of
- •Easier interpretation of angle-resolved (ARXPS) data → surface and bulk information
- •Easier quantitative analysis via core spectra

Minusses

- •Resolution not as good as ~1 meV VUV PS, but as good/better than SX PS, and down to ~50 meV overall, good enough for many applications
- •Photoelectric cross sections low, need special undulator beamline/spectrometer combinations—several solutions→ <1 micron focus and ~50 meV resolution
- •High *n,* low-ℓ cross section components strongly favored, but in TM or RE VB they can be more involved in transport , s and p like
- •Recoil energy limits resolution for lighter elements; complex systematics, depending on local bond distances/phonon frequencies→Doppler spectroscopy?

Hard x-ray photoemission--Quantitative analysis of peak intensities using theoretical cross sections:$La_{0.7}Sr_{0.3}MnO_3$, $h\nu$ = 7700 eV

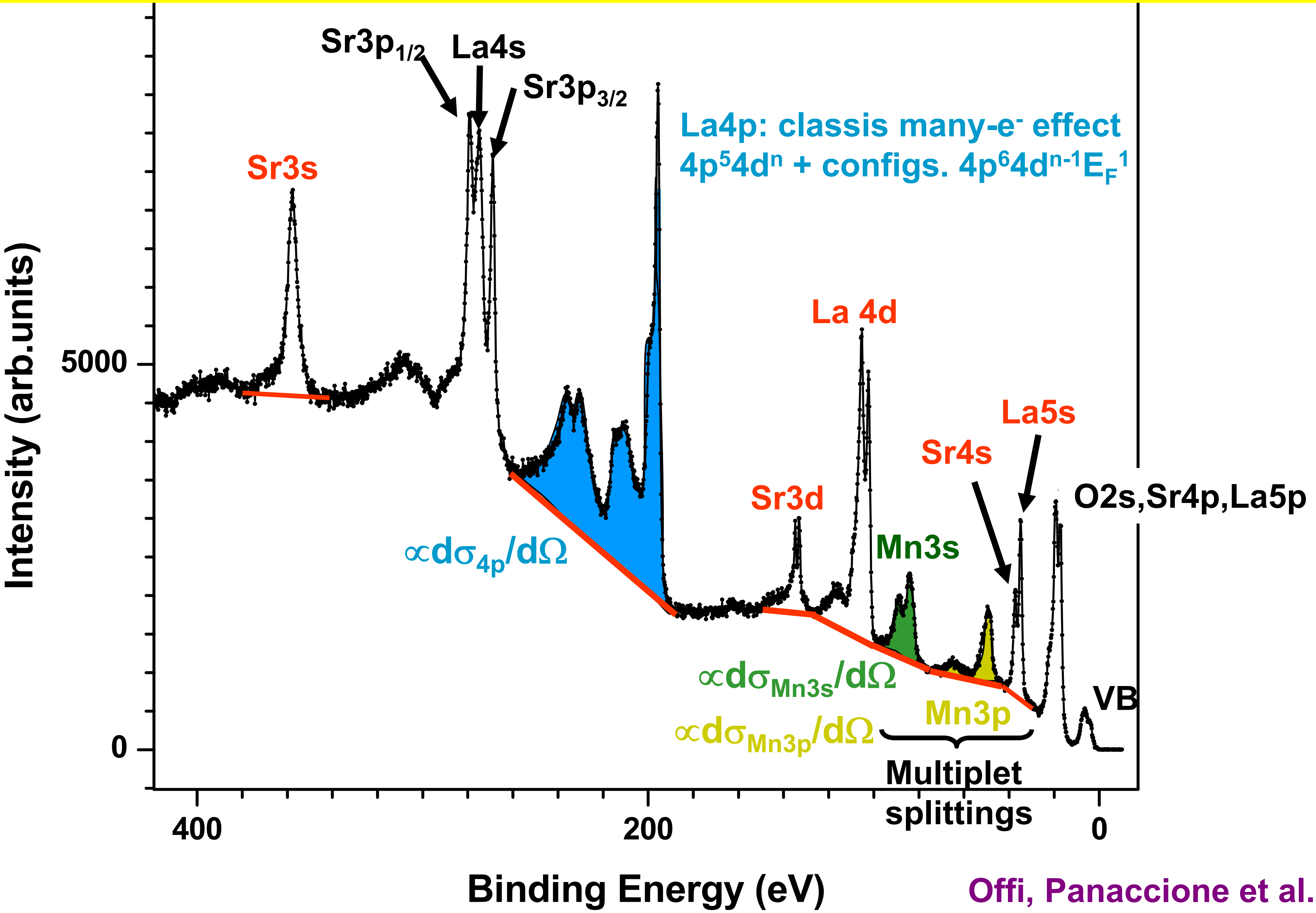

Offi, Panaccione et al., ESRF-VOLPE

Quantitative analysis of peak intensities using theoretical cross sections (Scofield): $La_{0.7}Sr_{0.3}MnO_3$, $h\nu$ = 7700 eV

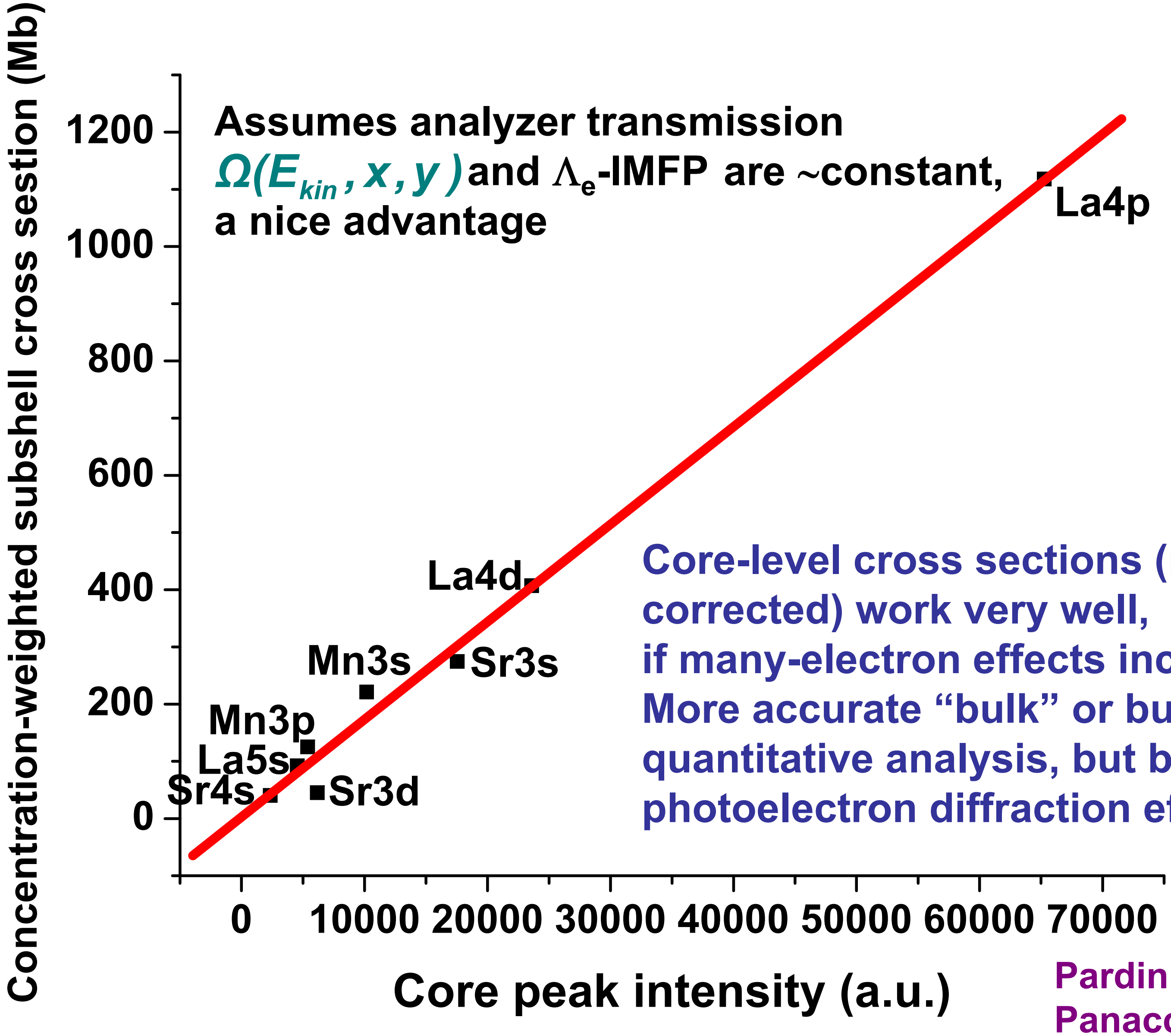

Assumes analyzer transmission $\Omega(E_{kin}, x, y)$ and Λ_e-IMFP are ~constant, a nice advantage

Core-level cross sections (non-dipole corrected) work very well, if many-electron effects included→ More accurate "bulk" or buried layer quantitative analysis, but be careful of photoelectron diffraction effects (later)

Pardini, Offi, Panaccione, CF

Hard x-ray photoemission—plusses and minusses

•Plusses

- More bulk sensitive spectra → a versatile tool for any new material or multilayer nanostructure
- Inelastic background less important & Augers more widely spread, less overlap
- Less radiation damage and charging-sort of
- Easier interpretation of angle-resolved (ARXPS) data → surface and bulk information
- Easier quantitative analysis via core spectra

Minusses

- Resolution not as good as ~1 meV VUV PS, but as good/better than SX PS, and down to ~50 meV overall, good enough for many applications
- Photoelectric cross sections low, need special undulator beamline/spectrometer combinations—several solutions→ <1 micron focus and ~50 meV resolution
- High *n,* low-ℓ cross section components strongly favored, but in TM or RE VB they can be more involved in transport , s and p like
- Recoil energy limits resolution for lighter elements; complex systematics, depending on local bond distances/phonon frequencies→Doppler spectroscopy?
- Intensity calculations must allow for non-dipole effects, photon wave vector, but easy

Differential photoelectric cross sections for filled $n\ell$ subshells

Dipole Non-dipole

$$\frac{d\sigma_{n\ell}(h\nu)}{d\Omega} = \frac{\sigma_{n\ell}(h\nu)}{4\pi}\left[1 + \frac{\beta_{n\ell}}{2}(3\cos^2\theta - 1) + (\delta_{n\ell} + \gamma_{n\ell}\cos^2\theta)\sin\theta\cos\phi\right]^{*}$$

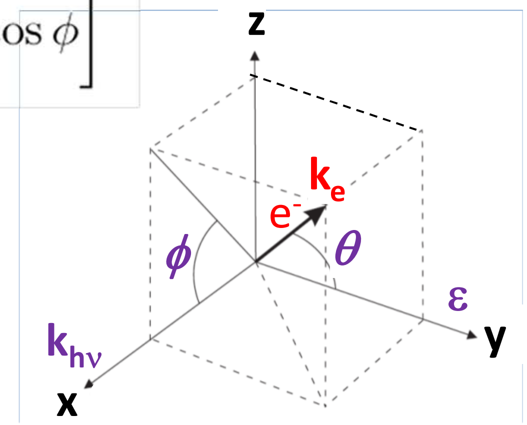

$$\beta_{nl}(E^f) = \frac{\{l(l-1)R_{l-1}{}^2(E^f) + (l+1)(l+2)R_{l+1}{}^2(E^f) - 6l(l+1)R_{l+1}(E^f)R_{l-1}(E^f)\cos[\delta_{l+1}(E^f) - \delta_{l-1}(E^f)]\}}{(2l+1)[lR_{l-1}{}^2(E^f) + (l+1)R_{l+1}{}^2(E^f)]}$$

Dipole $d\sigma_{n\ell}/d\Omega$ calculated from $R_{\ell-1}$, $R_{\ell+1}$, $\delta_{\ell-1}$, and $\delta_{\ell+1}$

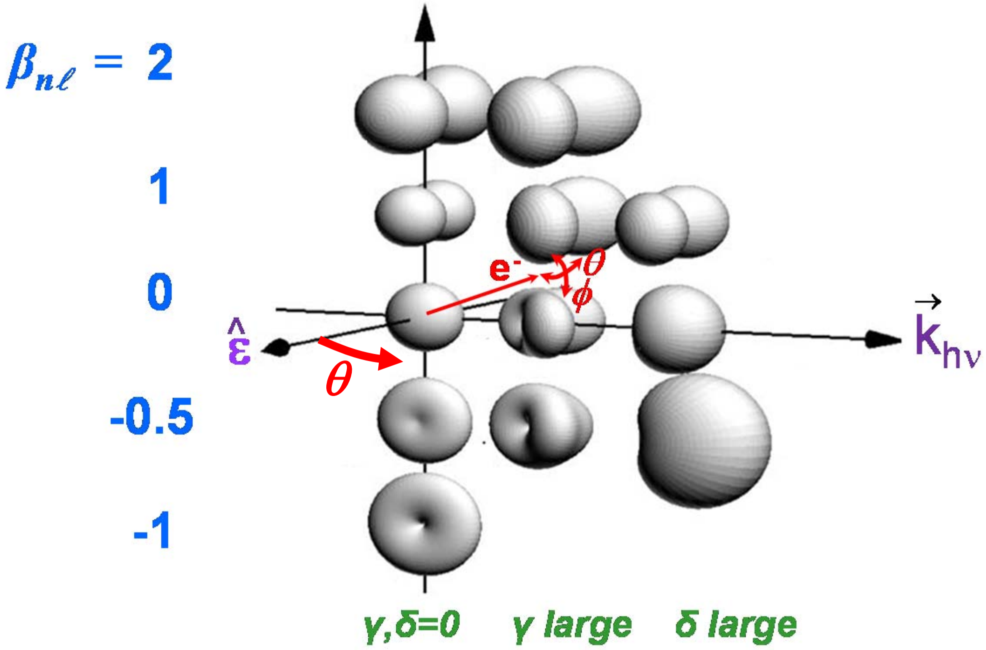

[#] At higher energies, valence cross sections dominated by atomic-like part near the nucleus[#]

*Guilleumin et al., Radiation Physics and Chemistry 75, 2258 (2006)

But what about individual $d\sigma_{2p(x,y,z)}/d\Omega$ or $d\sigma_{3d(xy,yz,xz,z2,x2-y2)}/d\Omega$?[&]

[&] Goldberg, Fadley, Kono, J. Electr. Spectr. 21, 285-363 (1985) → Slavo Nemšák

[#] Gelius, in *Electron Spectroscopy*, D.A. Shirley, Ed. (North Holland, 1971) p. 311; Solterbeck et al., Phys. Rev. Lett. 79, 4681 (1997)

Making use of linear polarization effects on orbital-specific/projected valence-level cross sections Radial matrix elements for and phase shifts for Cu 3d from 40 eV to 5 keV (extrapolated)

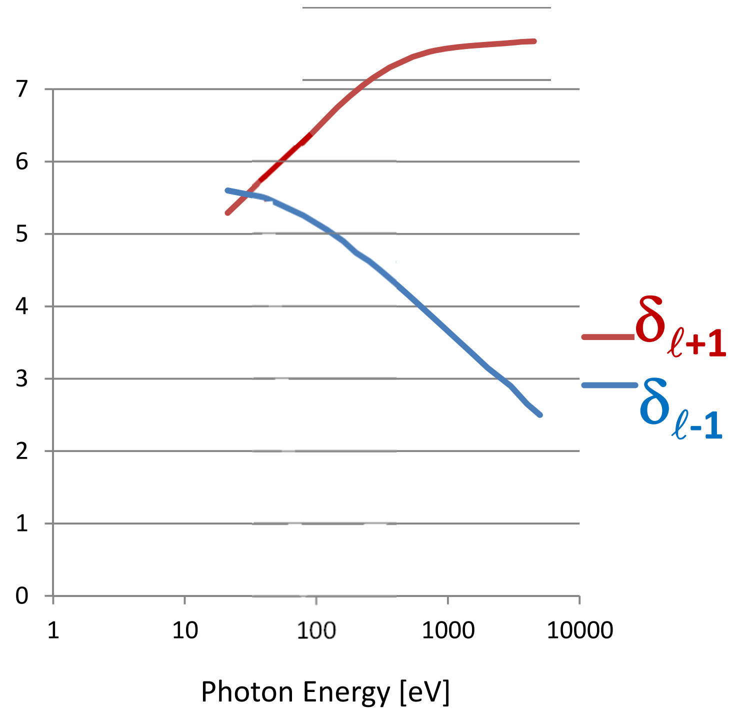

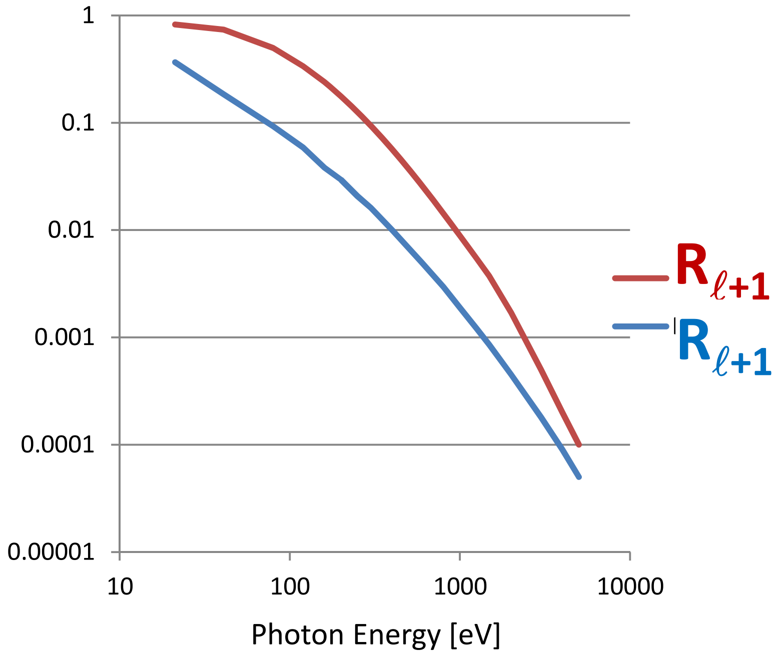

S. Nemšák

Energy dependence of orbital-specific differential cross sections: Cu 3d$_{xy}$ @ 800 and 5000 eV

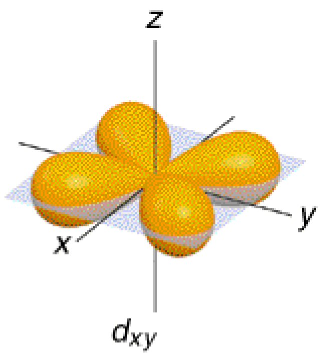

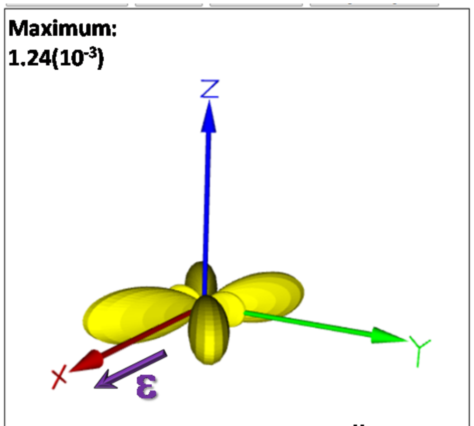

Cu 3d$_{xy}$ (hv=800 eV; E‖[100])

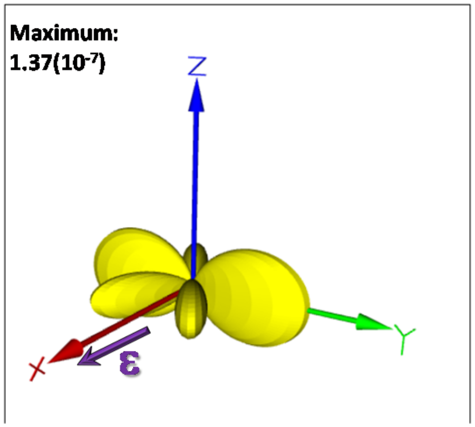

Cu 3d$_{xy}$ (hv=5000 eV; E‖[100])

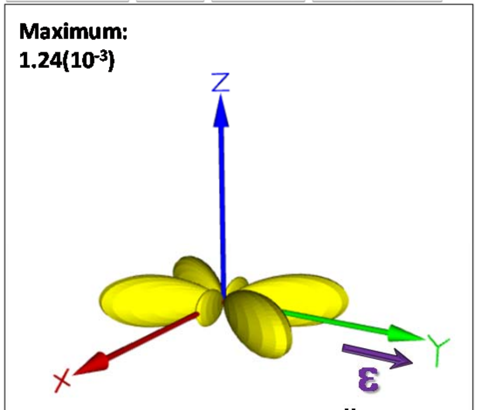

Cu 3d$_{xy}$ (hv=800 eV; E‖[010])

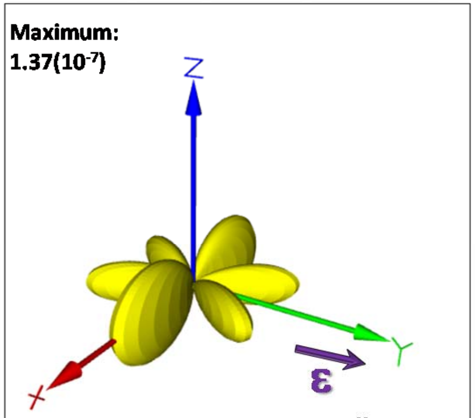

Cu 3d$_{xy}$ (hv=5000 eV; E‖[010])

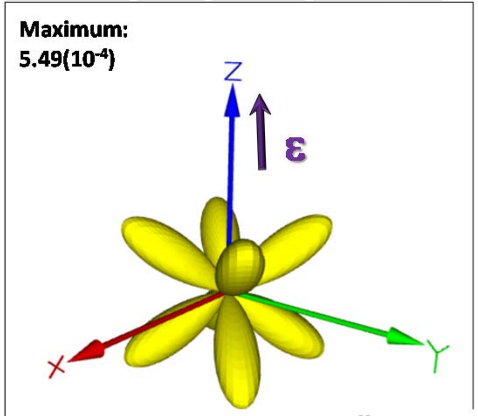

Cu 3d$_{xy}$ (hv=800 eV; E‖[001])

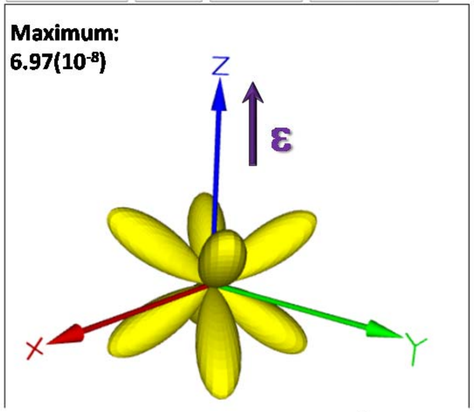

Cu 3d$_{xy}$ (hv=5000 eV; E‖[001])

S. Nemšák

Energy dependence of orbital-specific differential cross sections: Cu 3d$_{x2-y2}$ @ 800 and 5000 eV

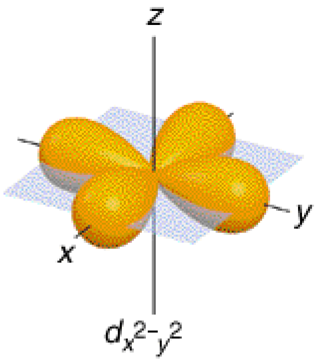

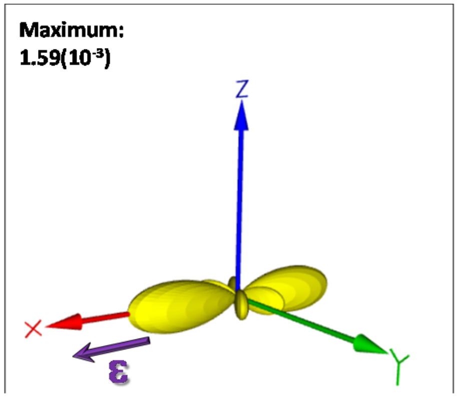

Cu 3d$_{x2-y2}$ (hv=800 eV; E$\parallel$[100])

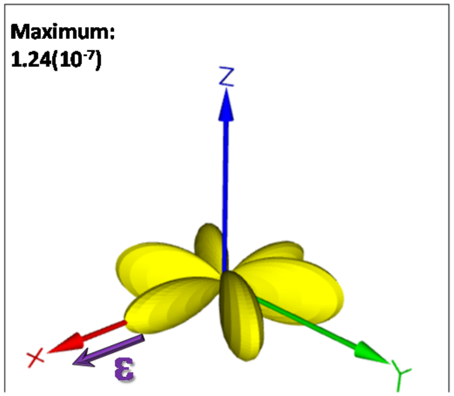

Cu 3d$_{x2-y2}$ (hv=5000 eV; E$\parallel$[100]

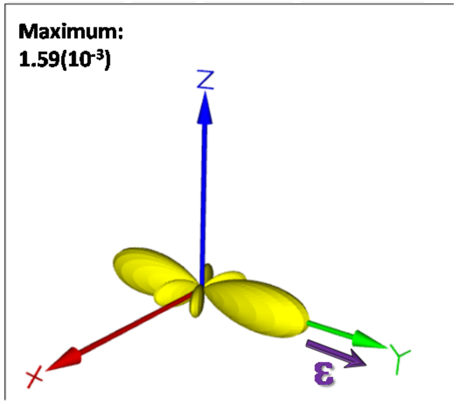

Cu 3d$_{x2-y2}$ (hv=800 eV; E$\parallel$[010]

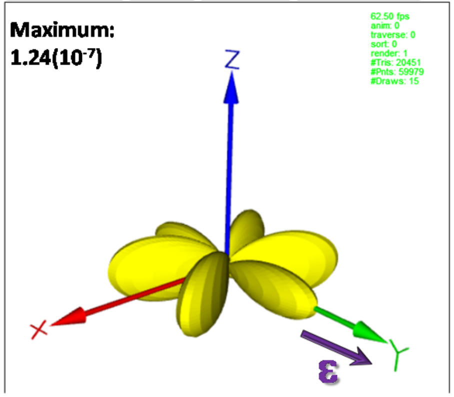

Cu 3d$_{x2-y2}$ (hv=5000 eV; E$\parallel$[010]

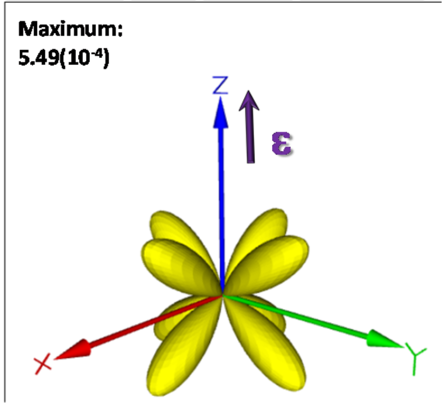

Cu 3d$_{x2-y2}$ (hv=800 eV; E$\parallel$[001

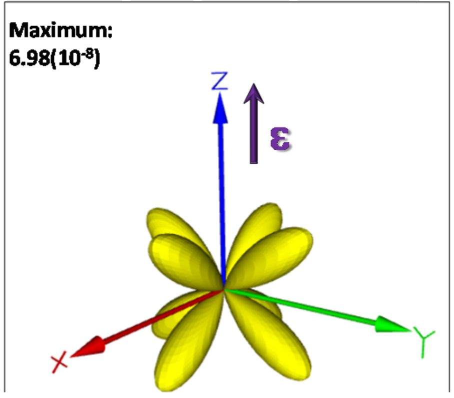

Cu 3d$_{x2-y2}$ (hv=5000 eV; E$\parallel$[001])

S. Nemšák

Energy dependence of orbital-specific differential cross sections: Cu 3d$_{z2}$ @ 800 and 5000 eV

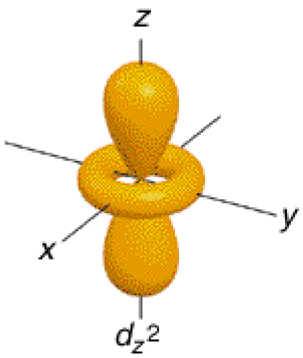

S. Nemšák

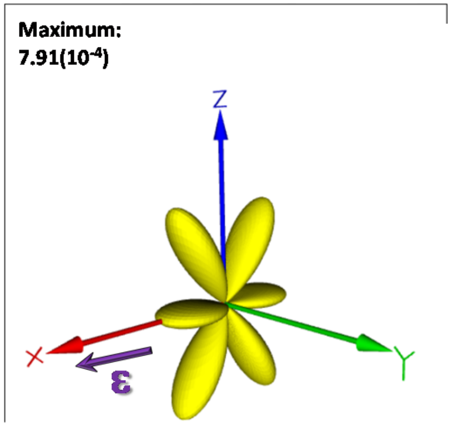

Cu 3d$_{z2}$ (hv=800 eV; E$\|$[100])

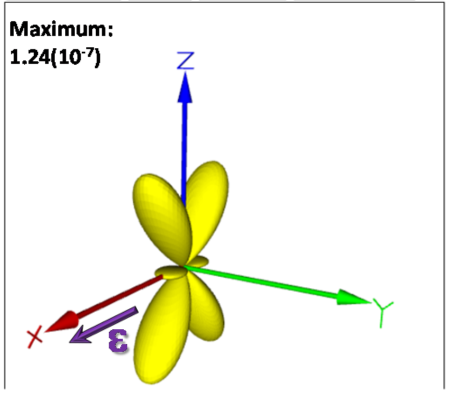

Cu 3d$_{z2}$ (hv=5000 eV; E$\|$[100])

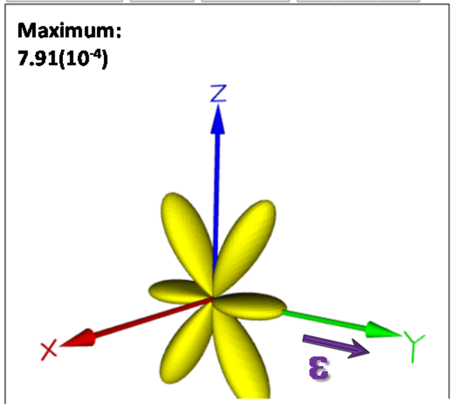

Cu 3d$_{z2}$ (hv=800 eV; E$\|$[010])

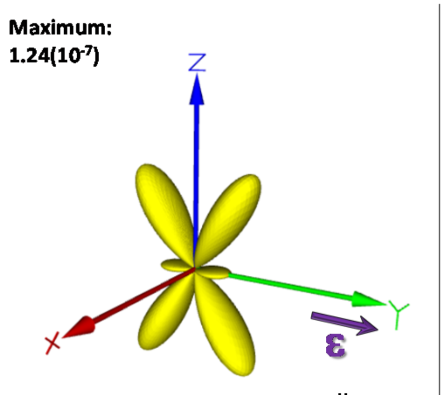

Cu 3d$_{z2}$ (hv=5000 eV; E$\|$[010])

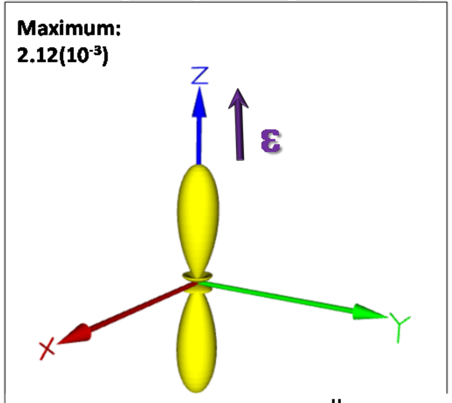

Cu 3d$_{z2}$ (hv=800 eV; E$\|$[001])

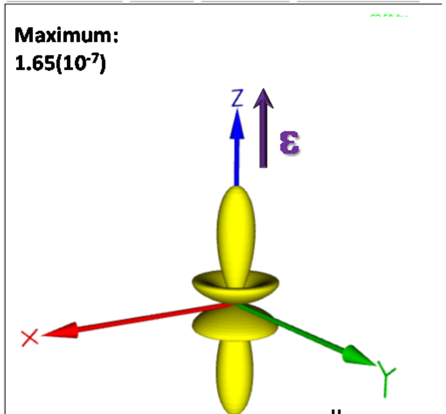

Cu 3d$_{z2}$ (hv=5000 eV; E$\|$[001])

Hard x-ray photoemission—plusses and minusses

•**Plusses**

- More bulk sensitive spectra → a versatile tool for any new material or multilayer nanostructure
- Inelastic background less important & Augers more widely spread, less overlap
- Less radiation damage and charging-sort of
- Easier interpretation of angle-resolved (ARXPS) data → surface <u>and</u> bulk information
- Easier quantitative analysis via core spectra

Minusses

- Resolution not as good as ~1 meV VUV PS, but as good/better than SX PS, and down to ~50 meV overall, good enough for many applications
- Photoelectric cross sections low, need special undulator beamline/spectrometer combinations—several solutions→ <1 micron focus and ~50 meV resolution
- High *n,* low-ℓ cross section components strongly favored, but in TM or RE VB they can be more involved in transport , s and p like
- Recoil energy limits resolution for lighter elements; complex systematics, depending on local bond distances/phonon frequencies→Doppler spectroscopy?
- Intensity calculations must allow for non-dipole effects, photon wave vector, but easy
- Interchannel coupling can complicate high-energy cross sections, but avoidable

High-energy resonant interchannel coupling effects on cross sections

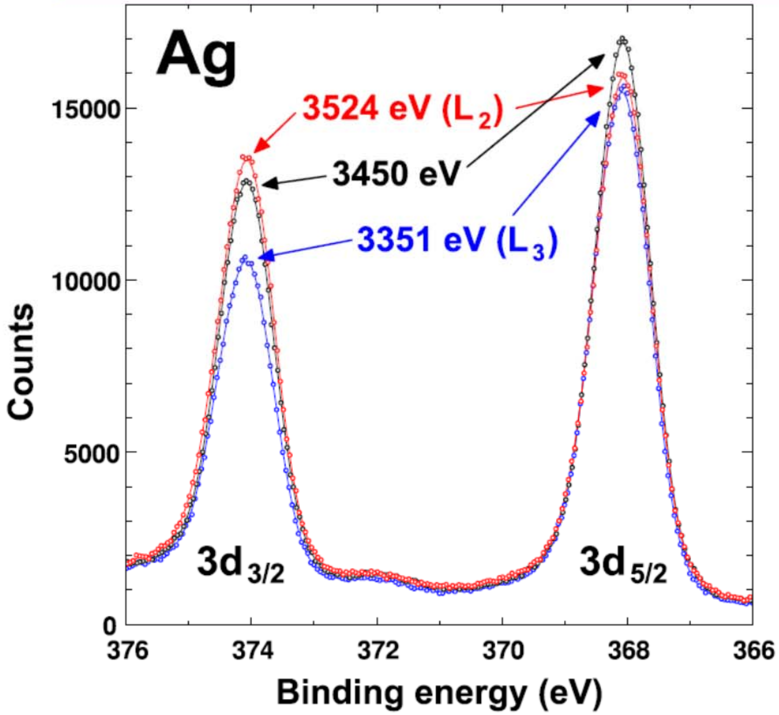

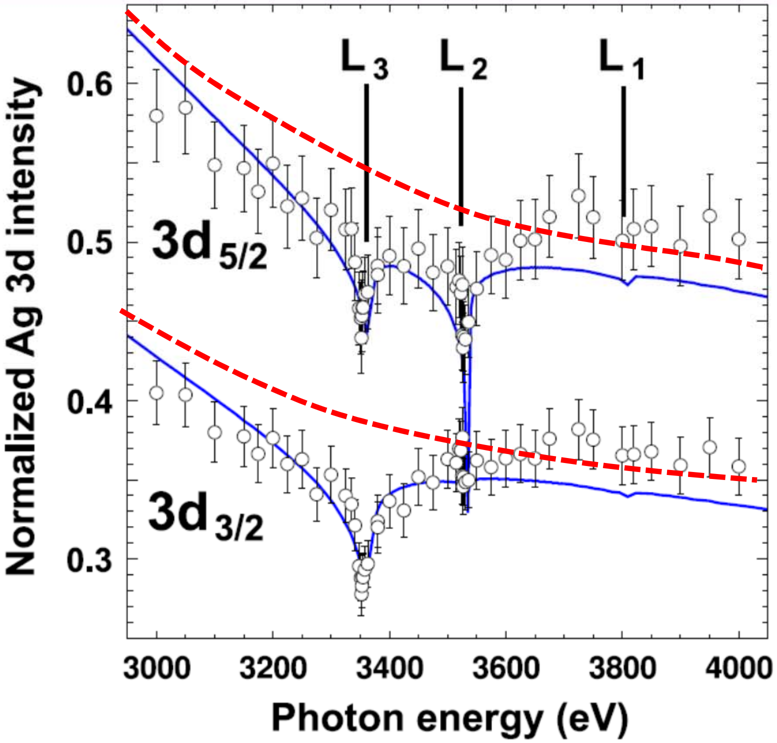

L I	2s	3806
L II	$2p_{1/2}$	3524
L III	$2p_{3/2}$	3351
M I	3s	719
M II	$3p_{1/2}$	604
M III	$3p_{3/2}$	573
M IV	$3d_{3/2}$	374
M V	$3d_{5/2}$	368

Drube, Manson et al., J. Phys. B: At. Mol. Opt. Phys. 46, 245006 (2013)

Hard x-ray photoemission—plusses and minusses

•**Plusses**

•More bulk sensitive spectra → a versatile tool for any new material or multilayer nanostructure

•Inelastic background less important & Augers more widely spread, less overlap

•Less radiation damage and charging-sort of

•Easier interpretation of angle-resolved (ARXPS) data → surface and bulk information

•Easier quantitative analysis via core spectra

•Variable polarization: magnetic circular, linear dichroism, cross section effects

Minusses

•Resolution not as good as ~1 meV VUV PS, but as good/better than SX PS, and down to ~50 meV overall, good enough for many applications

•Photoelectric cross sections low, need special undulator beamline/spectrometer combinations—several solutions→
<1 micron focus and ~50 meV resolution

•High *n,* low-ℓ cross section components strongly favored, but in TM or RE VB they can be more involved in transport , s and p like

•Recoil energy limits resolution for lighter elements; complex systematics, depending on local bond distances/phonon frequencies→Doppler spectroscopy?

•Intensity calculations must allow for non-dipole effects, photon wave vector, but easy

•Interchannel coupling can complicate high-energy cross sections, but avoidable

Magnetic circular dichroism in core-level HXPS

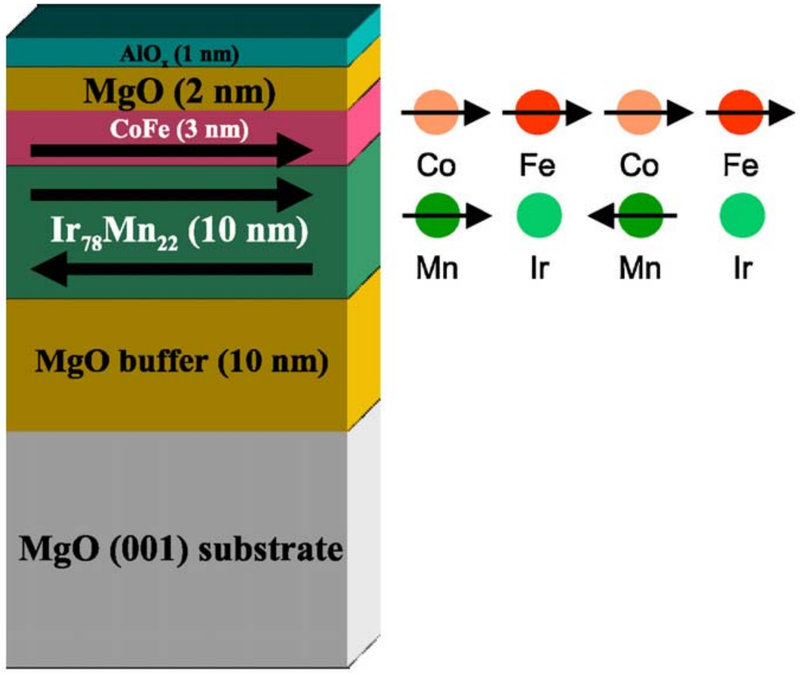

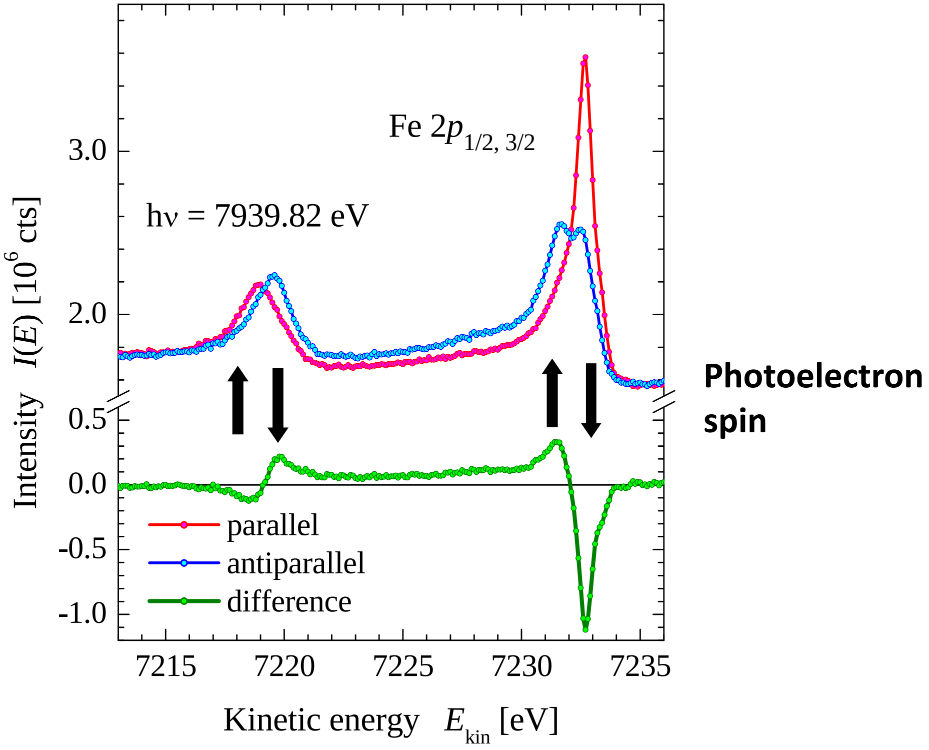

- **Huge dichroism in Fe 2p core level emission is still detected in the deeply buried layer, even at relaxed energy resolution.**

Asymmetry max.: - 40%

- **Element-specific magnetism in buried layers and interfaces**

Kozinya, Fecher et al., Phys. Rev. B 84, 054449 (2011)-SPring-8
(First measurements: S. Ueda et al., Appl. Phys. Express 1, 077003 (2008))

Hard x-ray photoemission—plusses and minusses

•**Plusses**

- More bulk sensitive spectra → a versatile tool for any new material or multilayer nanostructure
- Inelastic background less important & Augers more widely spread, less overlap
- Less radiation damage and charging-sort of
- Easier interpretation of angle-resolved (ARXPS) data → surface and bulk information
- Easier quantitative analysis via core spectra
- Variable polarization: magnetic circular, linear dichroism, cross section effects
- Spin-resolved spectra for magnetic systems

Minusses

- Resolution not as good as ~1 meV VUV PS, but as good/better than SX PS, and down to ~50 meV overall, good enough for many applications
- Photoelectric cross sections low, need special undulator beamline/spectrometer combinations—several solutions→ <1 micron focus and ~50 meV resolution
- High *n,* low-ℓ cross section components strongly favored, but in TM or RE VB they can be more involved in transport , s and p like
- Recoil energy limits resolution for lighter elements; complex systematics, depending on local bond distances/phonon frequencies→Doppler spectroscopy?
- Intensity calculations must allow for non-dipole effects, photon wave vector, but easy
- Interchannel coupling can complicate high-energy cross sections, but avoidable

First spin-resolved HXPS from core levels: buried CoFeAlSi Heusler

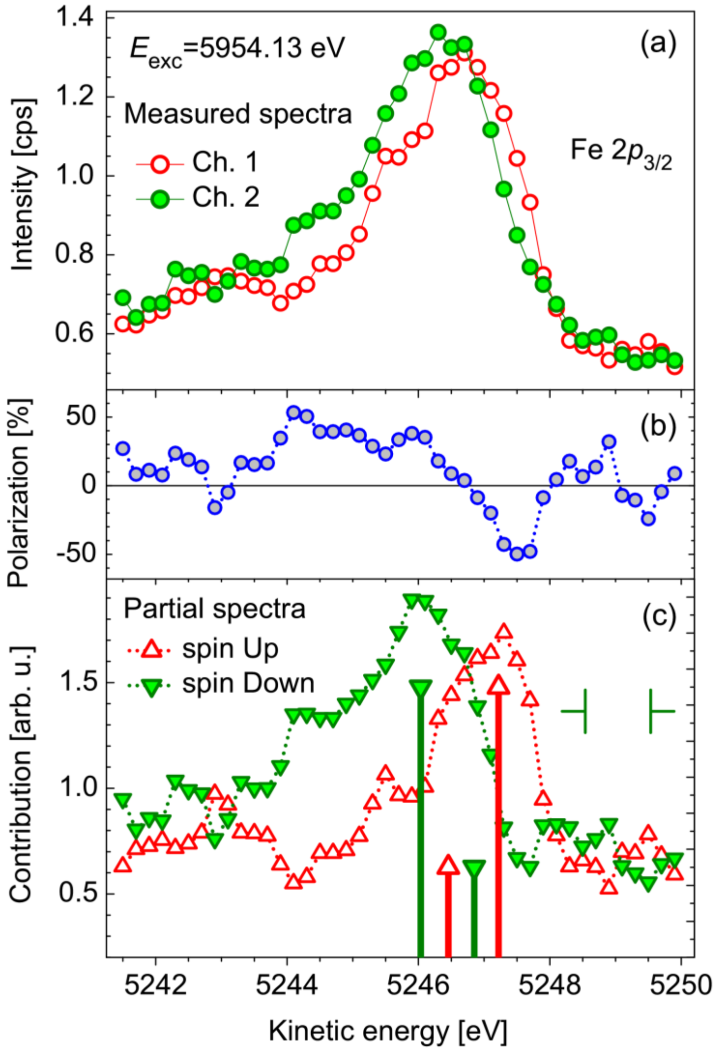

(a) Countrates in the spin detector channels

(b) Spin polarization

(c) Spin-resolved Fe 2$p_{3/2}$ spectra from the buried CoFeAlSi layer.

Stryganyuk, Kozina, Fecher, Felser, Schönhense, Lushchyk, Oelsner, Bernhard, Ikenaga, Sugiyama, Sukegawa, Inomata, Kobayashi, Jpn. J. Appl. Phys. 51, 016602 (2012)

Some first spin-resolved HXPS from core levels: buried CoFe layer

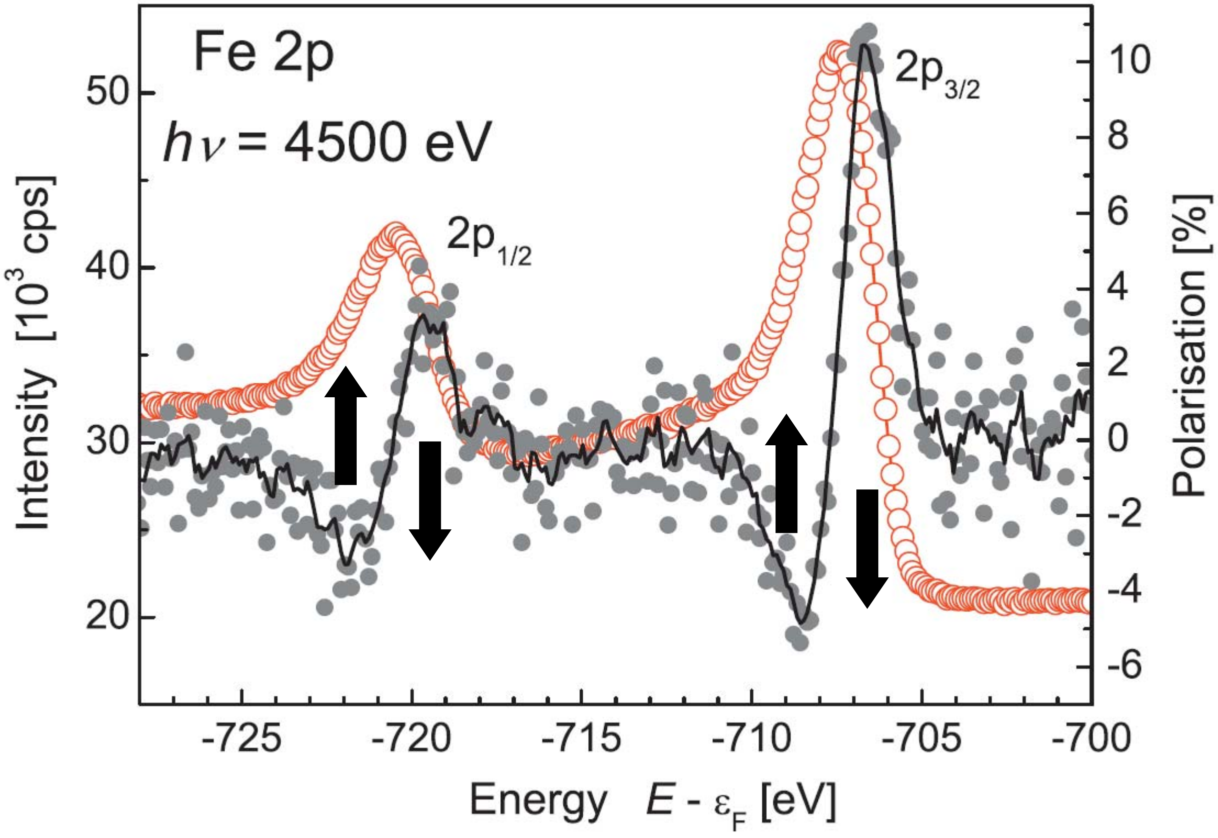

A. Gloskovskiia et al., J. Electron Spect. 185, 47 (2012)-Petra III

+ New spin detectors that will make this 100-1000 times faster:

VLEED), Fe(001)p(1×1)-O surface: Okuda et al., Eur. Phys. J. Special Topics 169, 181–185 (2009)

Jozwiak et al., Rev. Sci. Instrum. 81, 053904 (2010)-Co or Fe exchange scatt

Display: Hahn et al., APL 98,232503 (2011); Tusche et al., APL 99, 032505 (2011)-low-energy spin-orbit from W(100)

Hard x-ray photoemission—plusses and minusses

•**Plusses**

•More bulk sensitive spectra → a versatile tool for any new material or multilayer nanostructure

•Inelastic background less important & Augers more widely spread, less overlap

•Less radiation damage and charging-sort of

•Easier interpretation of angle-resolved (ARXPS) data → surface and bulk information

•Easier quantitative analysis via core spectra

•Variable polarization: magnetic circular, linear dichroism, cross section effects

•Spin-resolved spectra for magnetic systems

•New "bulk fingerprint" satellite effects seen in both core and valence spectra

Minusses

•Resolution not as good as ~1 meV VUV PS, but as good/better than SX PS, and down to ~50 meV overall, good enough for many applications

•Photoelectric cross sections low, need special undulator beamline/spectrometer combinations—several solutions→
<1 micron focus and ~50 meV resolution

•High *n,* low-ℓ cross section components strongly favored, but in TM or RE VB they can be more involved in transport , s and p like

•Recoil energy limits resolution for lighter elements; complex systematics, depending on local bond distances/phonon frequencies→Doppler spectroscopy?

•Intensity calculations must allow for non-dipole effects, photon wave vector, but easy

•Interchannel coupling can complicate high-energy cross sections, but avoidable

Photoemission: The correct energy picture

$$h\nu = E^{Vacuum}_{binding} + E_{kinetic} = E^{Fermi}_{binding} + \varphi_{spectrometer} + E_{kinetic}$$

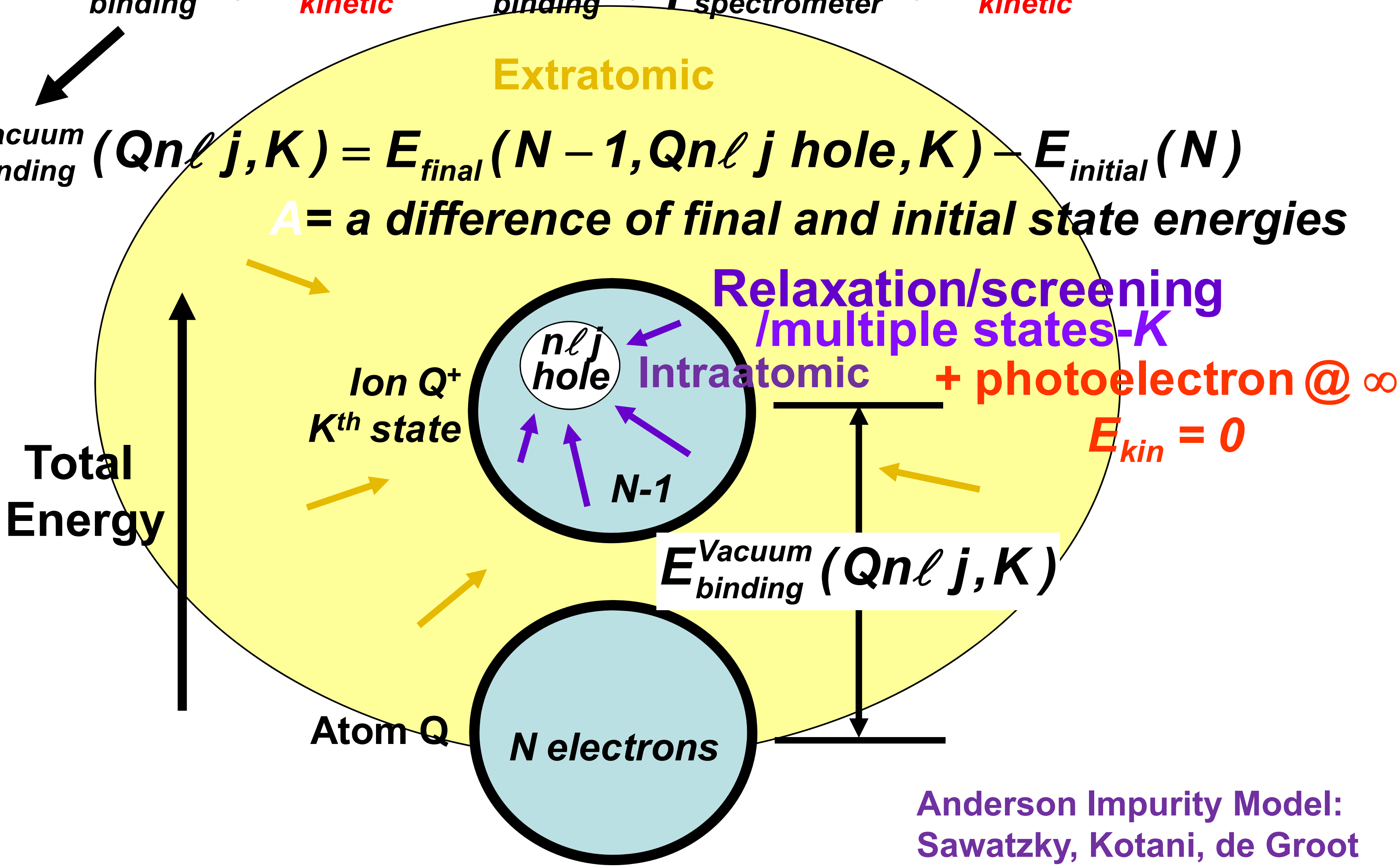

$$E^{Vacuum}_{binding}(Qn\ell\, j,K) = E_{final}(N-1,Qn\ell\, j\ hole,K) - E_{initial}(N)$$

A= a difference of final and initial state energies

Extratomic

Relaxation/screening /multiple states-*K*

Intraatomic

$n\ell j$ hole

Ion Q^+ K^{th} state

N-1

+ photoelectron @ ∞

$E_{kin} = 0$

Total Energy

$E^{Vacuum}_{binding}(Qn\ell\, j,K)$

Atom Q

N electrons

Anderson Impurity Model: Sawatzky, Kotani, de Groot

Electronic Structure of Strained Manganite Thin Films with Room Temperature Ferromagnetism Investigated by Hard X-ray Photoemission Spectroscopy: $La_{0.85}Ba_{0.15}MnO_3$

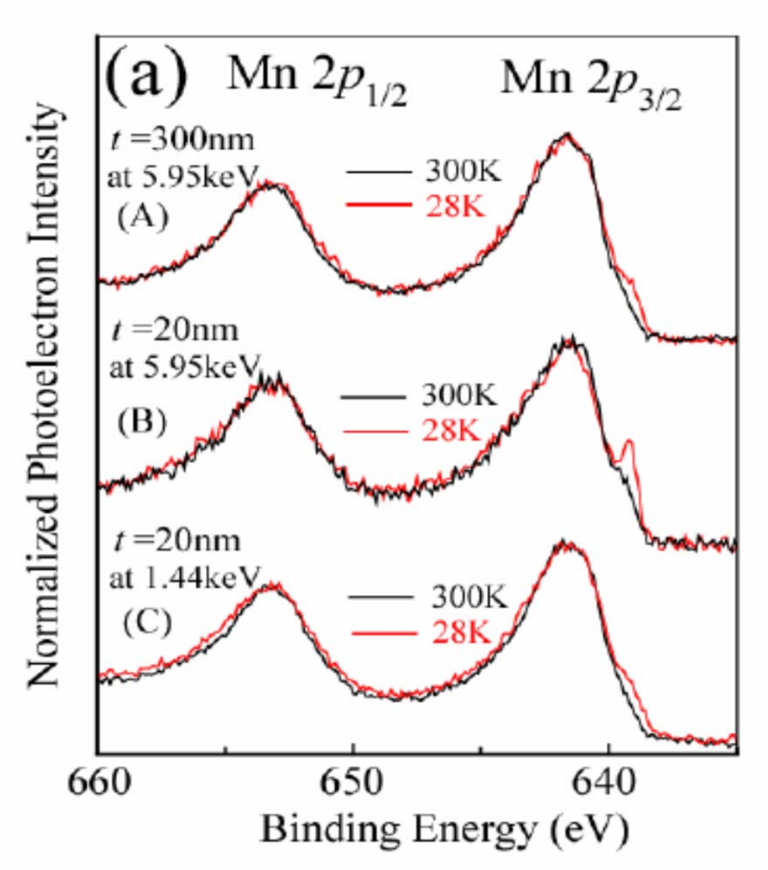

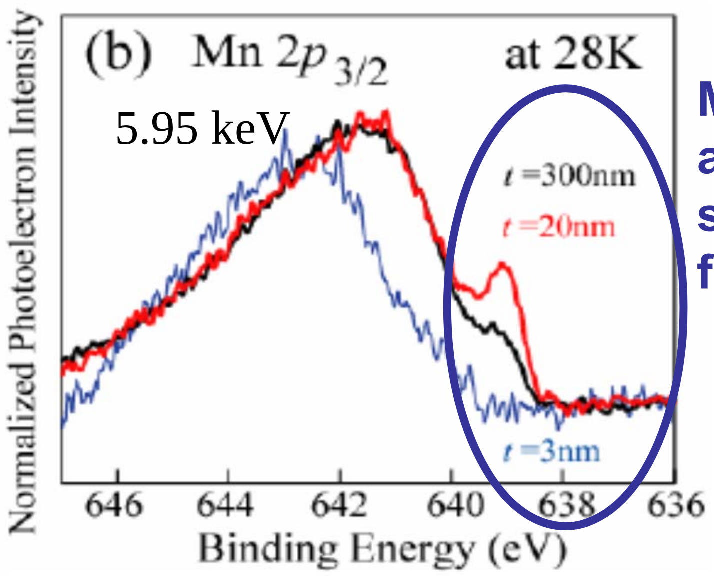

Magnetism-associated screening feature

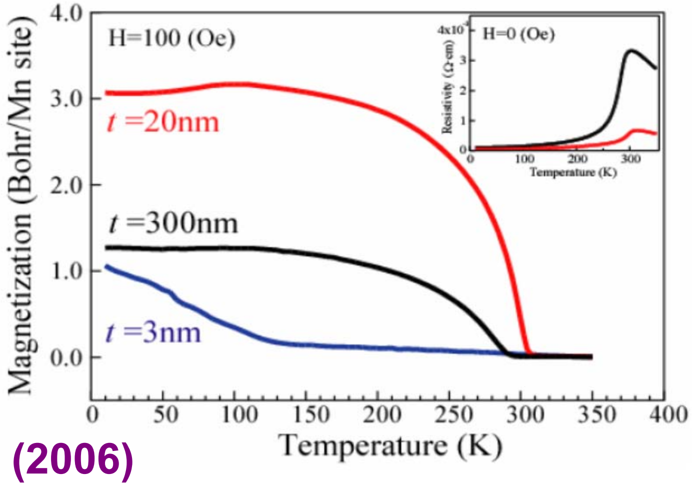

Tanaka et al., SPring8, Phys. Rev. B 73, 094403 (2006)

Temperature dependence of Mn2p spectra: $La_{0.7}Sr_{0.3}MnO_3$
New satellite structures in core spectra

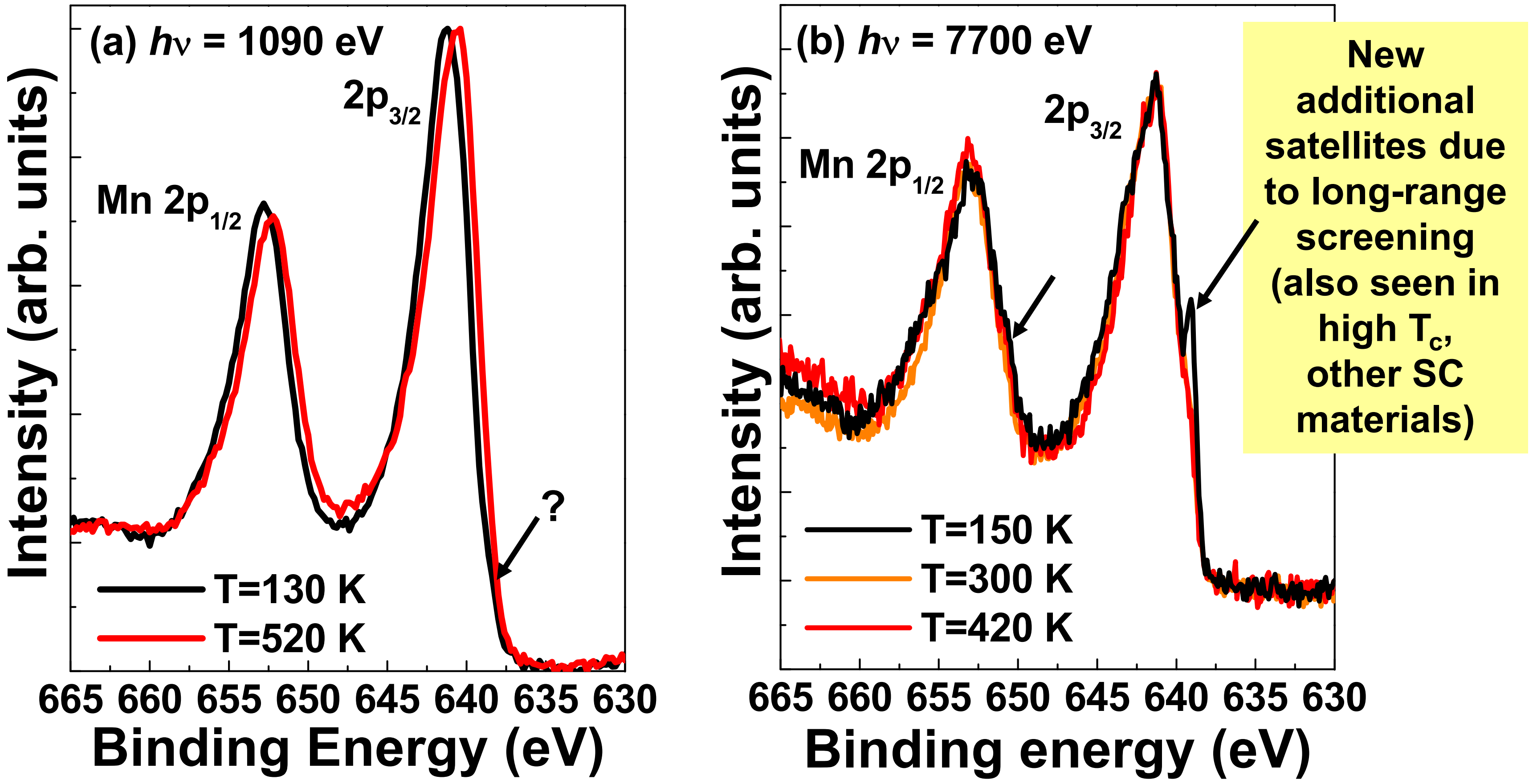

New additional satellites due to long-range screening (also seen in high T_c, other SC materials)

Mean depth: ~1 nm

Mean depth: ~8 nm

→Suggests bulk electronic structure not reached until ca. 8 nm depth

Offi, Mannella, et al., Phys. Rev. B 2008, 77, 174422 - ESRF

Hard x-ray photoemission @ 3.2 keV: GaAs doped with Mn-- $Ga_{0.96}Mn_{0.04}As$, a magnetic semiconductor: T = 20K, Broad Survey

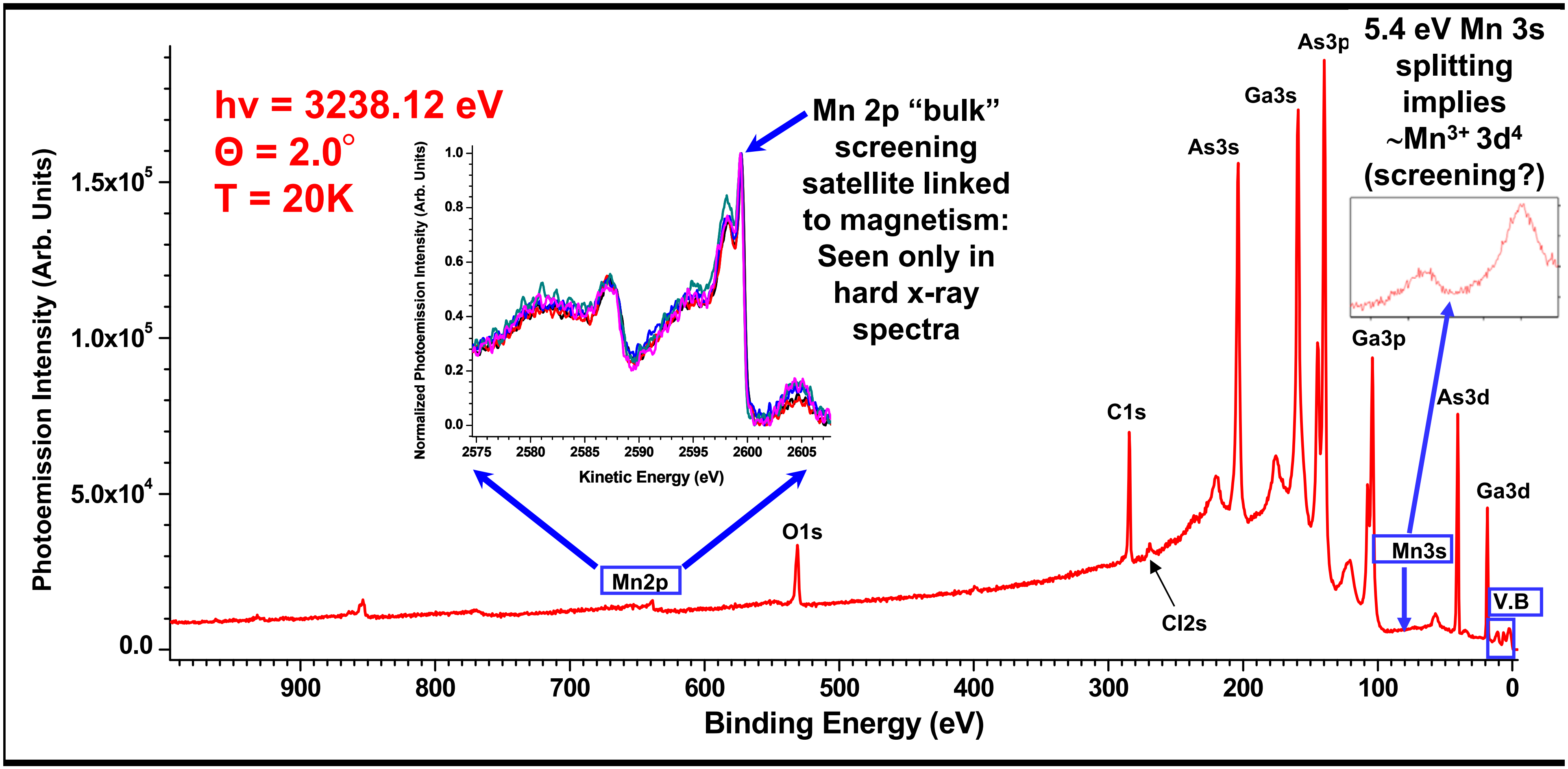

hν = 3238.12 eV
Θ = 2.0°
T = 20K

Mn 2p “bulk” screening satellite linked to magnetism: Seen only in hard x-ray spectra

5.4 eV Mn 3s splitting implies ~Mn^{3+} $3d^4$ (screening?)

Samples: Stone, Dubon
Expt.-Gray, Papp, Ueda, Yamashita, Kobayashi
Theory- Pickett, Ylvisaker, Minar, Braun, Ebert
Nature Materials, 11, 957 (2012)

Plus detailed core-level and VB study: Fujii, Panaccione et al., Phys. Rev. Lett. 111, 097201 (2013)

$Ga_{0.96}Mn_{0.04}As$: Using MCD in screening satellites to determine covalency

MCD Experiment- Below T_C

Anderson Impurity Model calcs. vs d hybridization V

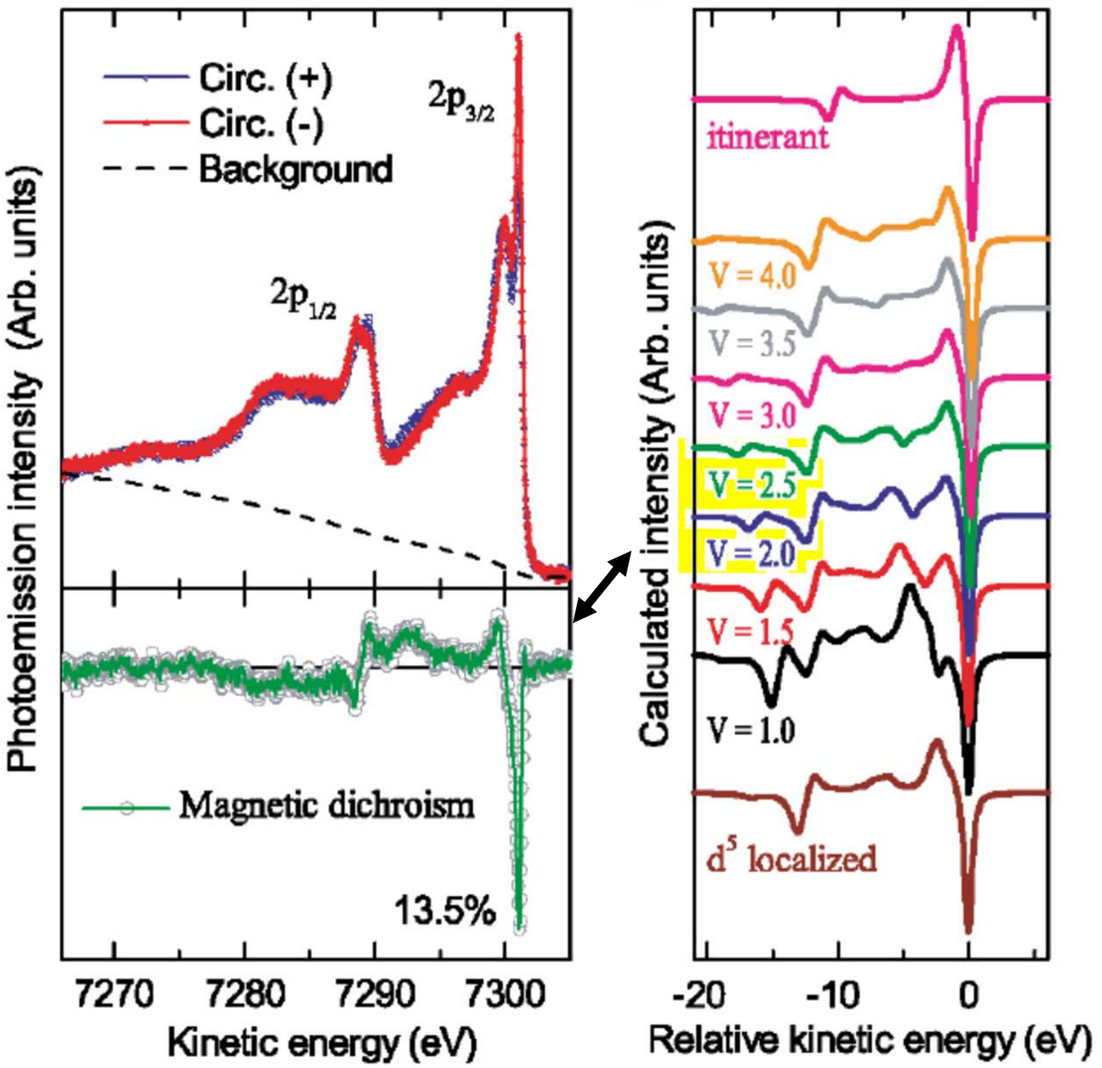

Plus detailed core-level and VB study: Fujii, Panaccione et al., Phys. Rev. Lett. 111, 097201 (2013)

Hard x-ray photoemission—plusses and minusses

•**Plusses**

- •More bulk sensitive spectra → a versatile tool for any new material or multilayer nanostructure
- •Inelastic background less important & Augers more widely spread, less overlap
- •Less radiation damage and charging-sort of
- •Easier interpretation of angle-resolved (ARXPS) data → surface and bulk information
- •Easier quantitative analysis via core spectra
- •Variable polarization: magnetic circular, linear dichroism, cross section effects
- •Spin-resolved spectra for magnetic systems
- •New "bulk fingerprint" satellite effects seen in both core and valence spectra
- • Hard x-ray photoelectron diffraction: dopants, lattice distortions

Minusses

- •Resolution not as good as ~1 meV VUV PS, but as good/better than SX PS, and down to ~50 meV overall, good enough for many applications
- •Photoelectric cross sections low, need special undulator beamline/spectrometer combinations—several solutions→ <1 micron focus and ~50 meV resolution
- •High *n,* low-ℓ cross section components strongly favored, but in TM or RE VB they can be more involved in transport , s and p like
- •Recoil energy limits resolution for lighter elements; complex systematics, depending on local bond distances/phonon frequencies→Doppler spectroscopy?
- •Intensity calculations must allow for non-dipole effects, photon wave vector, but easy
- •Interchannel coupling can complicate high-energy cross sections, but avoidable

X-ray photoemission: some key elements

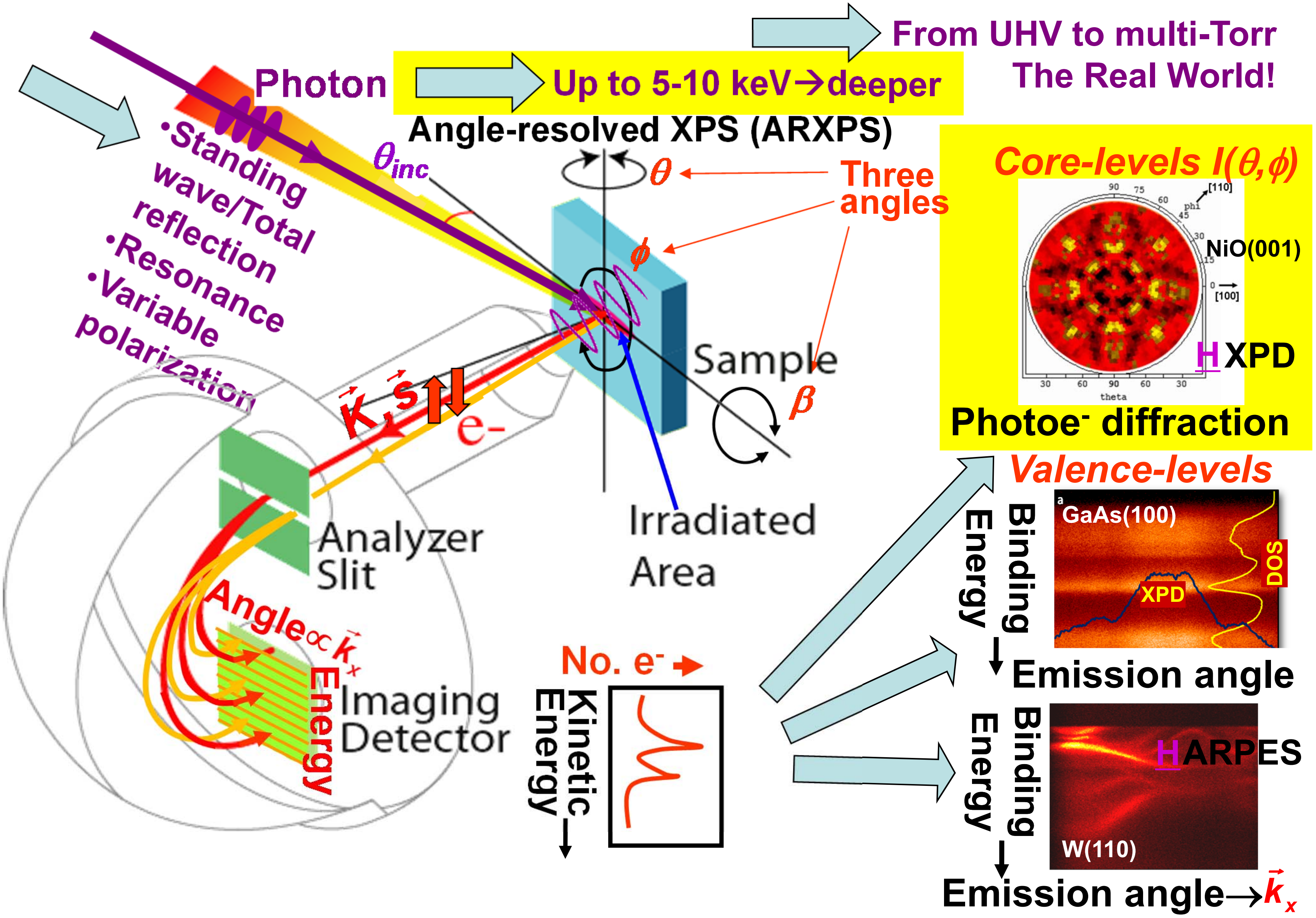

From UHV to multi-Torr
The Real World!

Photon – Up to 5-10 keV→deeper

Angle-resolved XPS (ARXPS)

- Standing wave/Total reflection
- Resonance
- Variable polarization

Three angles

Core-levels $I(\theta,\phi)$

HXPD

Photoe$^-$ diffraction

Valence-levels

HARPES

Soft→Hard X-Ray Photoelectron Diffraction: Basic Systematics and Modeling

The scattering of photoelectrons from localized sources can be described in real space (multiple scattering cluster) and reciprocal space (dynamical theory of electron diffraction)

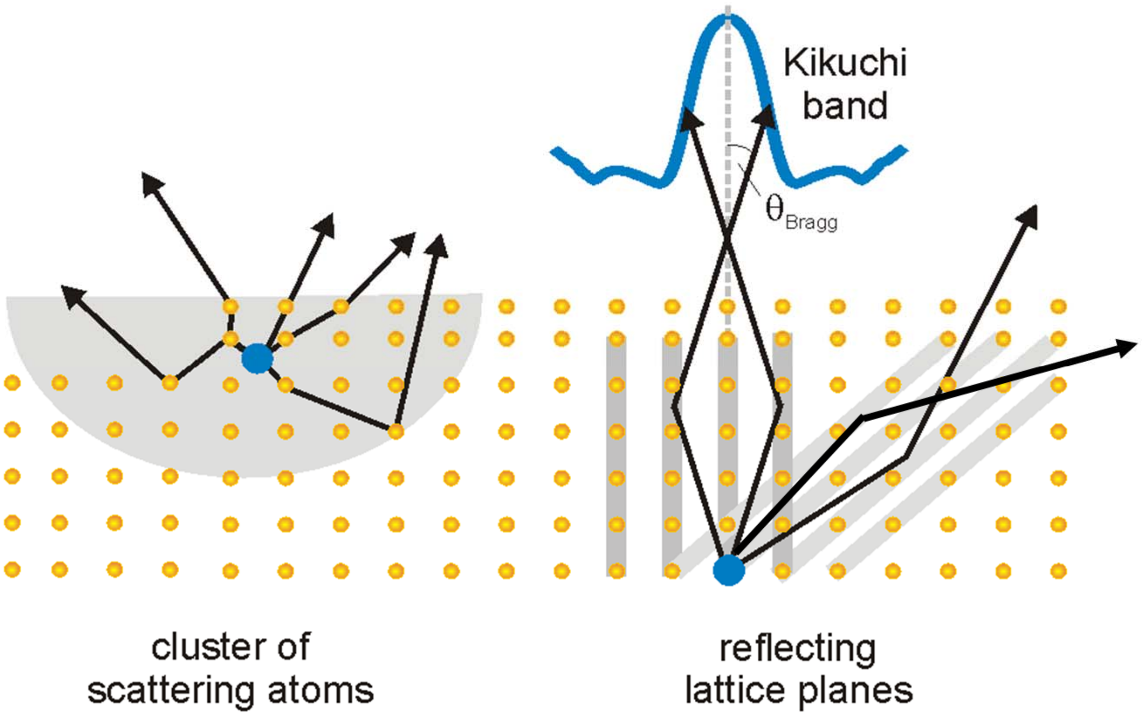

A. Winkelmann, J. Garcia de Abajo, C.F., Journal of Physics 10 (2008) 113002

Photoelectron Diffraction: Single Scattering Theory

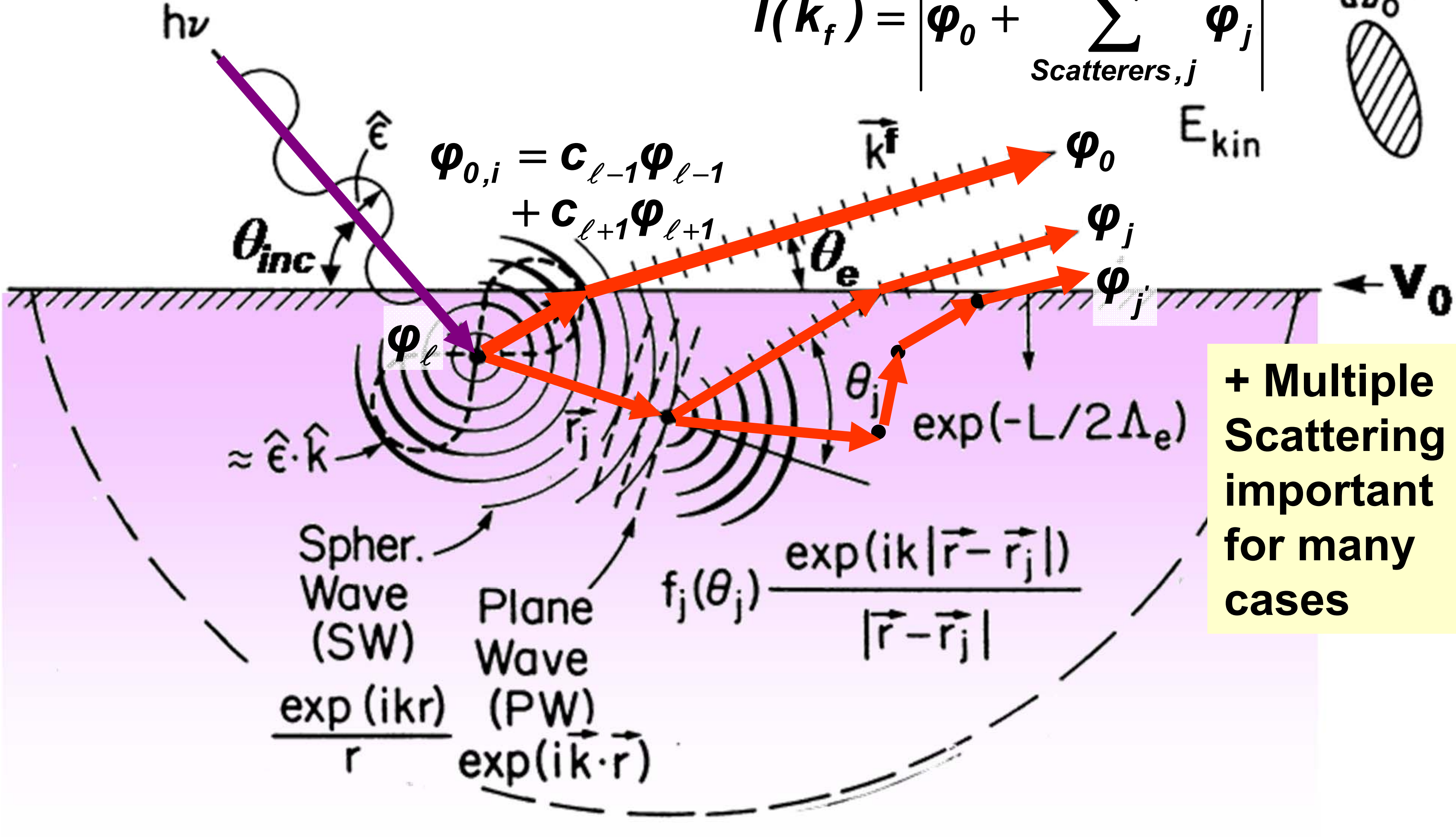

$$I(\vec{k}_f) = \left| \varphi_0 + \sum_{Scatterers,j} \varphi_j \right|^2$$

$$\varphi_{0,i} = c_{\ell-1}\varphi_{\ell-1} + c_{\ell+1}\varphi_{\ell+1}$$

+ Multiple Scattering important for many cases

CSF in Advances in Surface and Interface Science, R. Z. Bachrach, Ed. (Plenum Press, New York, 1992). Online MS program by F. Garcia de Abajo: http://nanophotonics.csic.es/widgets/edac/index.html

ENERGY DEPENDENCE OF ELECTRON ELASTIC SCATTERING

$$f(\theta) = |f(\theta)| e^{i\psi(\theta)}$$

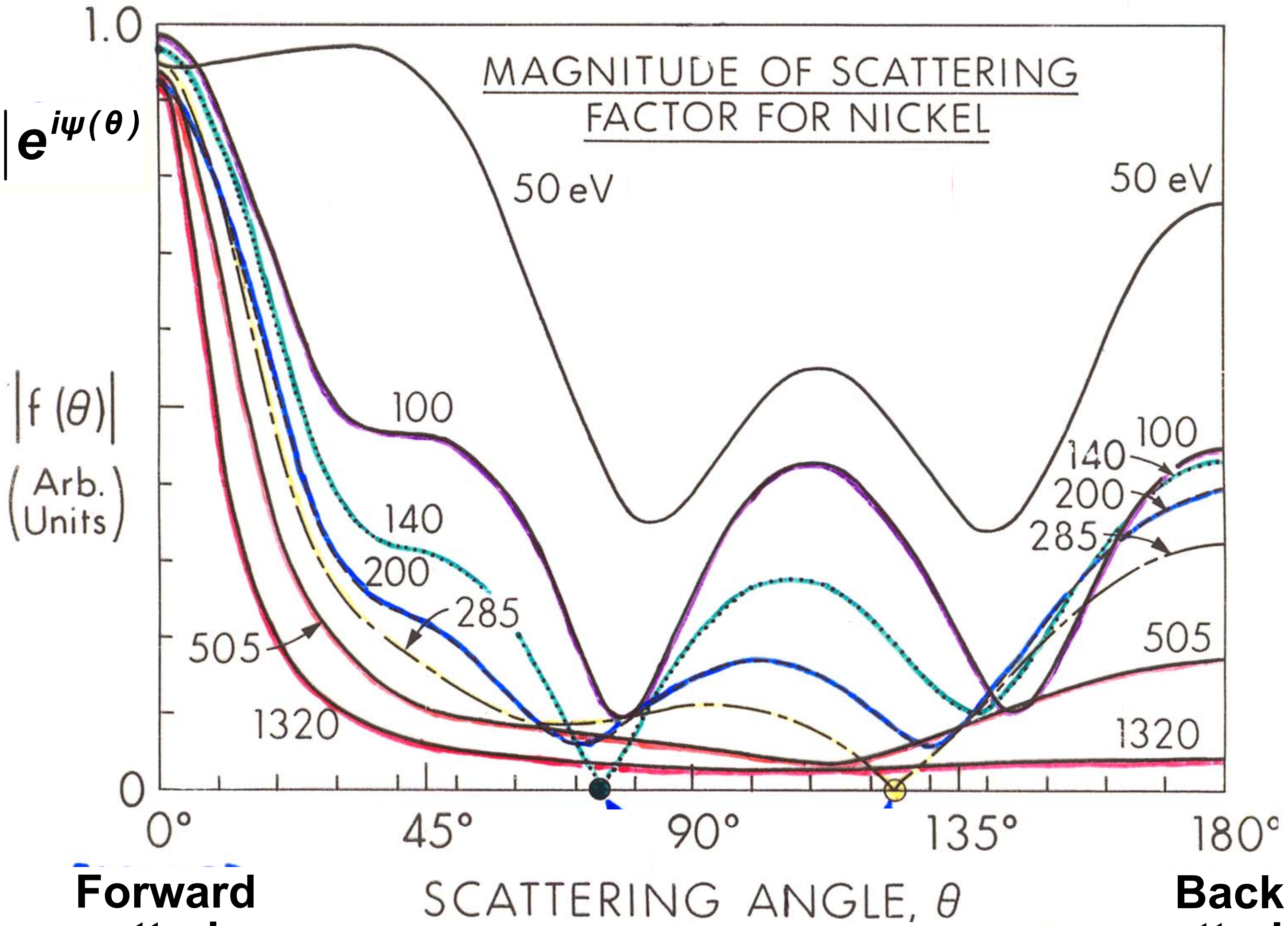

Forward scattering

Back scattering

→ The higher the energy, the more forward scattering dominates

Sagurton et al.
Surf. Sci. 182, 287 ('84)

Photoelectron Diffraction with soft and hard x-ray excitation: two viewpoints, expt. vs. theory at ~1 keV

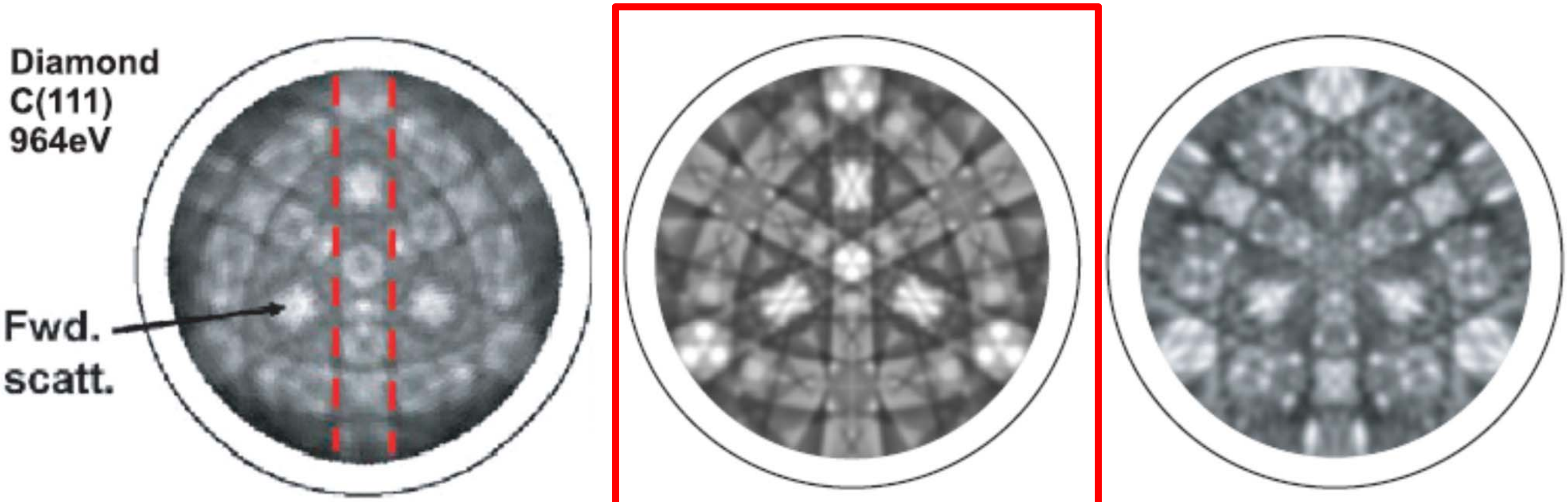

(a) experiment

Osterwalder et al.,
Surf. Sci. 312, 131 (1994)

(b) dynamical simulation

Kikuchi-band approach

(c) multiple scattering simulation (EDAC)

→Most appropriate for higher energies, bulklike emission

A. Winkelmann et al, New J. Phys 10 (2008) 113002

Hard x-ray photoelectron diffraction--Theory:
Sensitivity to lattice distortions and atomic site type?

Si(111)-6 keV: Impurity atom on lattice site (Si) vs. tetrahedral interstitial (T)

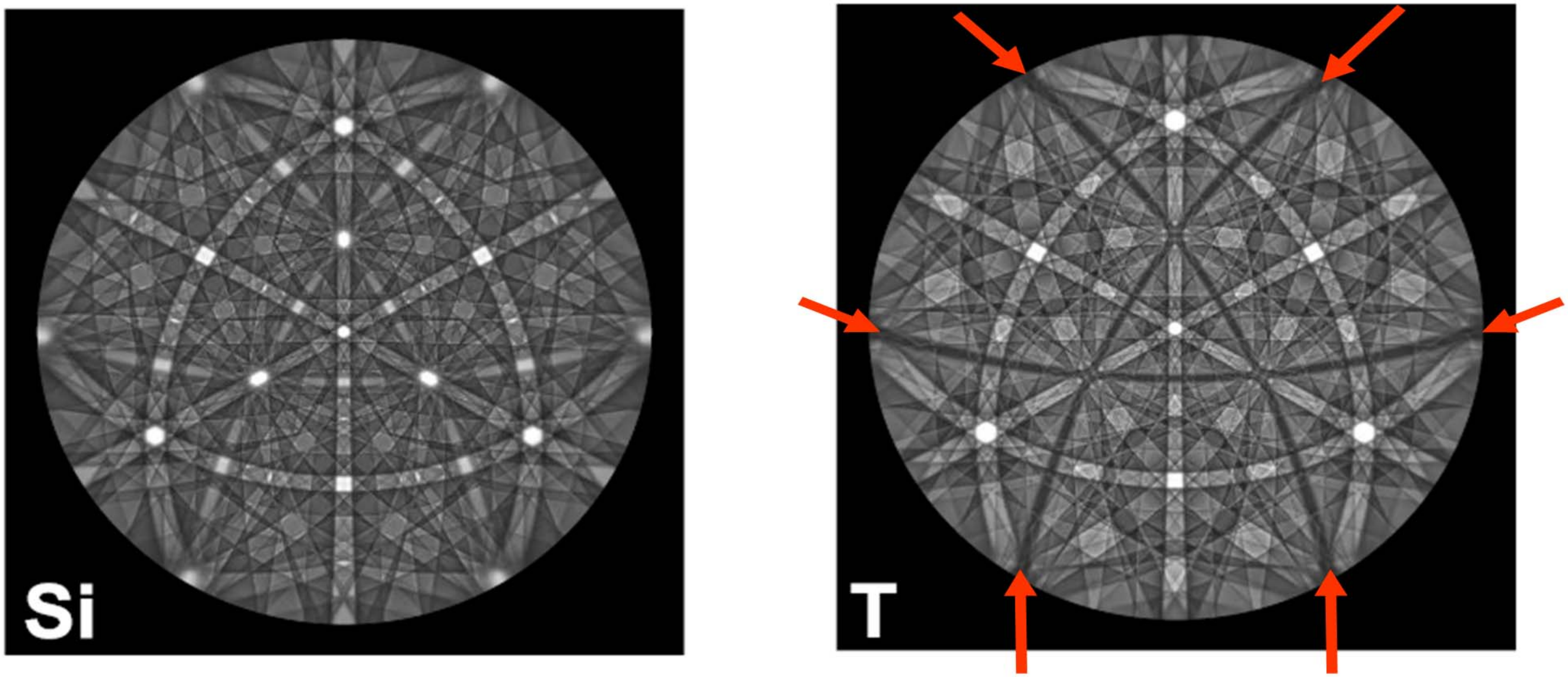

Missing Kikuchi bands-->"forbidden reflections"

A. Winkelman, J. Garcia de Abajo, MPI Halle, CF, New Journal of Physics 10 (2008) 113002

First application to Mn incorporation into GaAs Bartos, Pis, Kobata, Kobayashi, Cukr, Jirıcek, Novak, Ikenaga, Sugiyama, Phys. Rev. B 83, 235327 (2011)-Spring-8

HAXPES @ Soleil: Diamond with nitrogen substitional dopant: ~2:10^4 concentration, as N-vacancy centers ~1:10^4 concentration

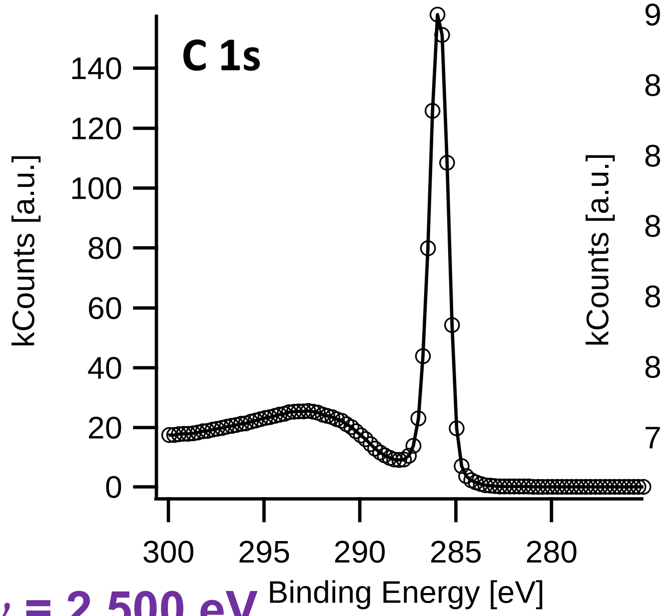

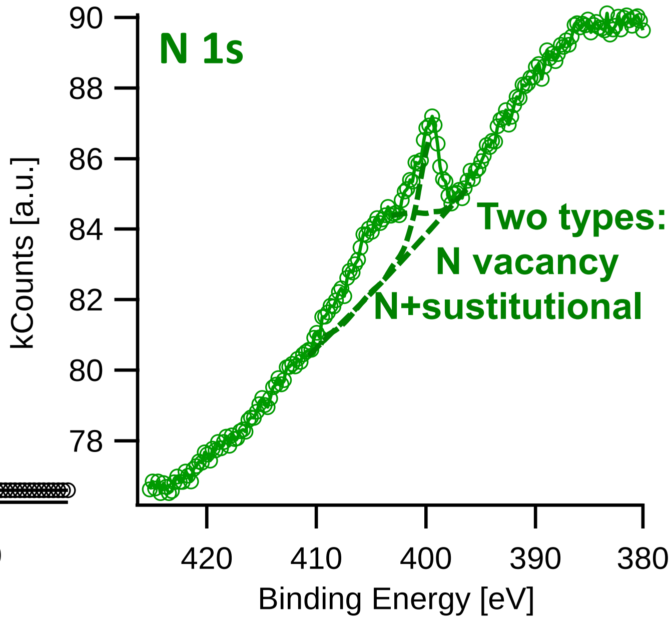

hν = 2,500 eV

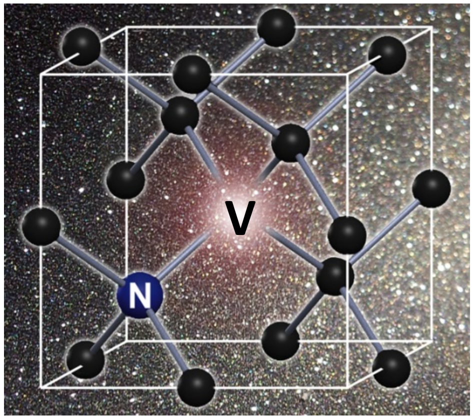

[Quantum computing? http://www.nature.com/ncomms/journal/v4/n4/full/ncomms2771.html](http://www.nature.com/ncomms/journal/v4/n4/full/ncomms2771.html)

Total N at 2.4:10^4 From N 1s and VB to avoid non-linearity in C 1s

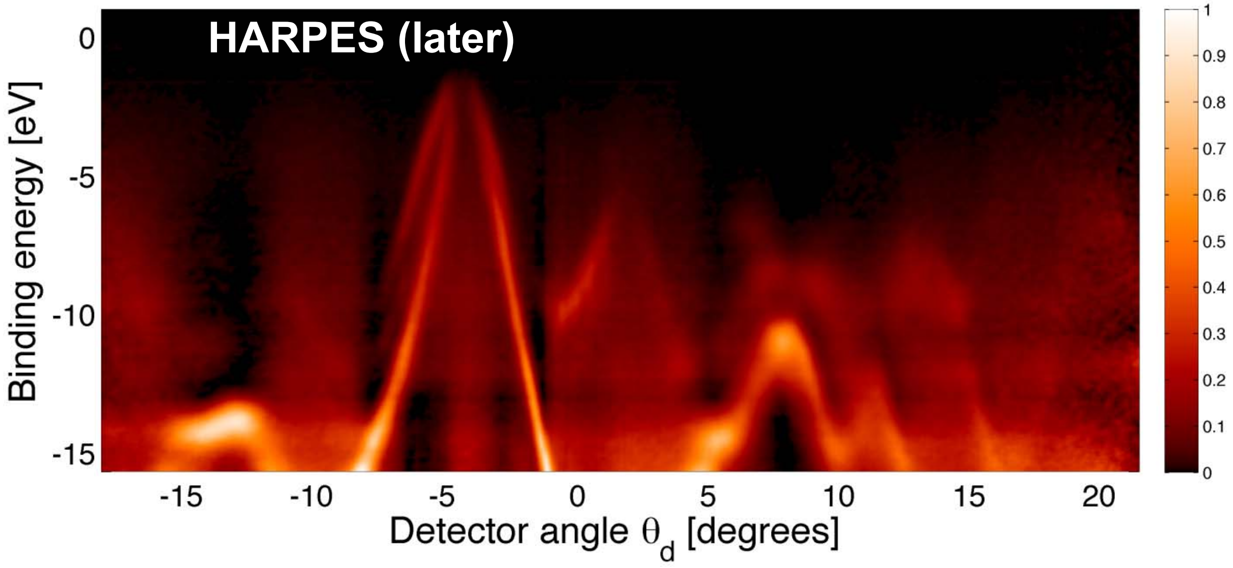

Pálsson, Nemšák, Rueff, Lischner, Conlon, Saw, Eiteneer, Rattanachata, Perona, Conlon, CF

Hard x-ray photoelectron diffraction from C and two N peaks

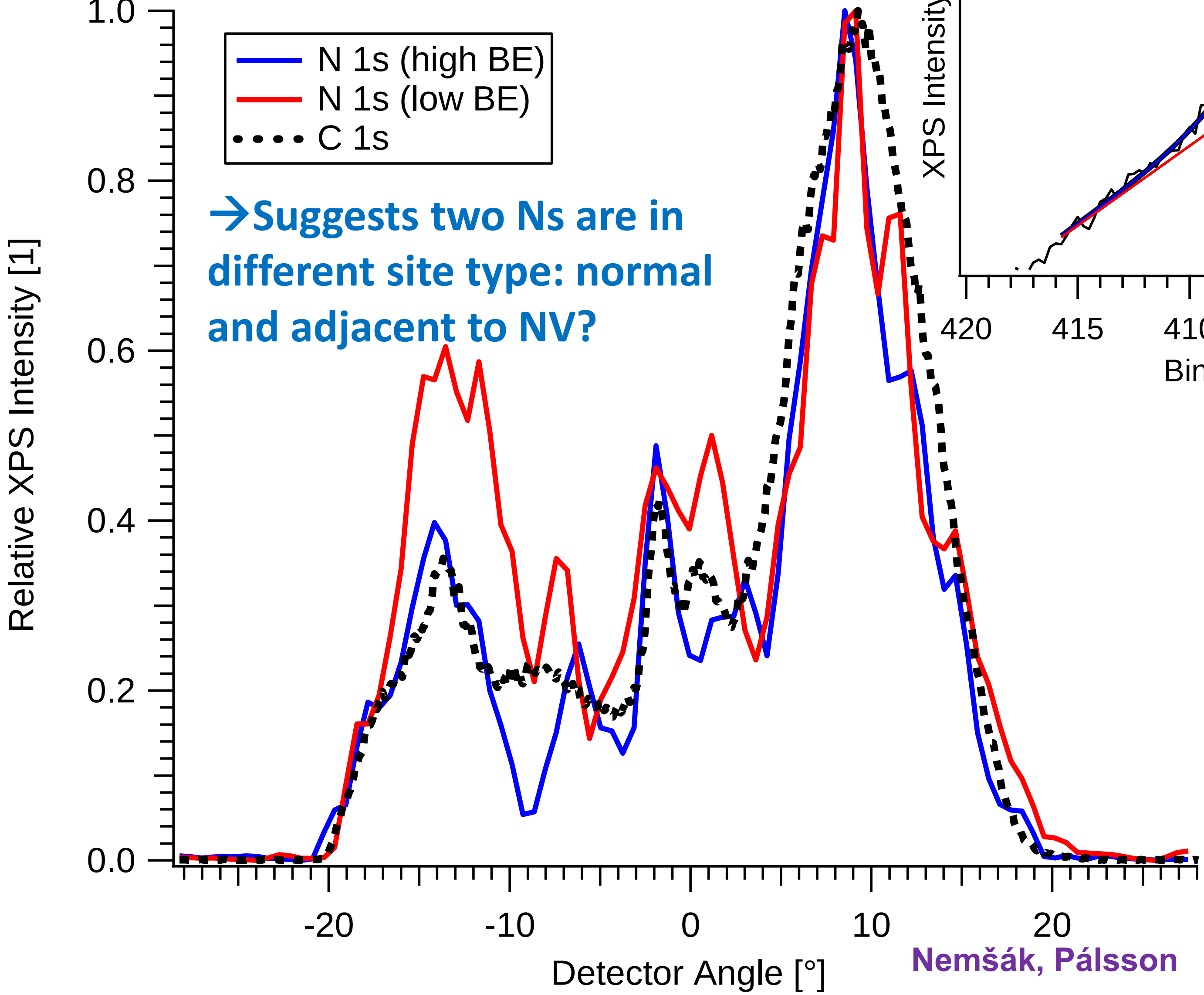

→Suggests two Ns are in different site type: normal and adjacent to NV?

Nemšák, Pálsson

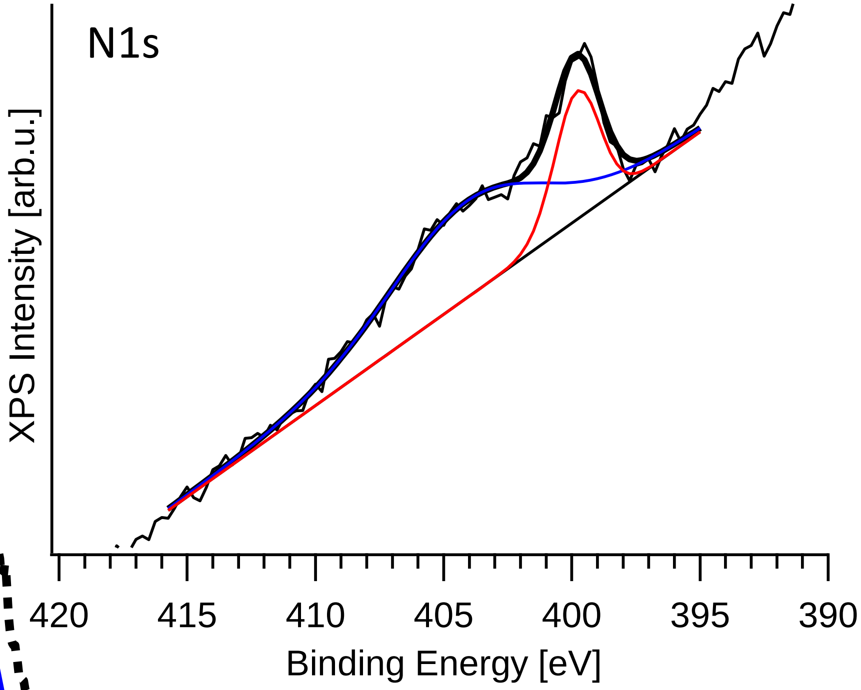

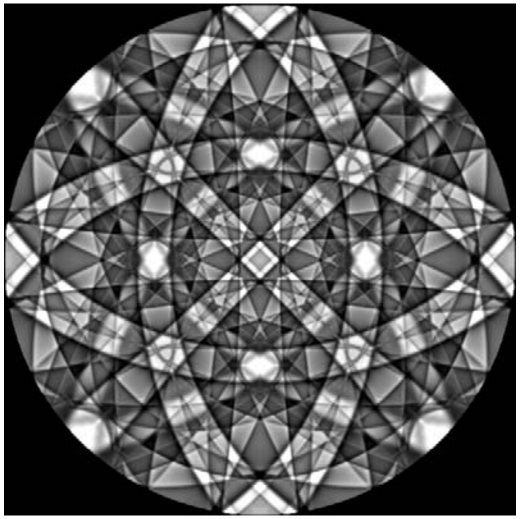

Dynamical (Kikuchi) theory: Winkelmann

Photoemission with soft and hard x-rays:
Some future perspectives

Chuck Fadley
Dept. of Physics, UC Davis
Materials Sciences Division
Lawrence Berkeley National Laboratory
Soleil Synchrotron

Supported by:
DOE: LBNL Materials Sciences Division
"Nanoscale Magnetic Materials"
ARO-Multi-University Research Initiative:
"Emergent Phenomena at Mott Oxide Interfaces"
Peter Grünberg Institute, PGI 6, Jülich Research Center
LABEX-PALM-APTCOM Project, Triangle de Physique, Paris

Soleil seminars: 21 July, 15 September, 22 September; 2014

X-ray photoemission: some key elements

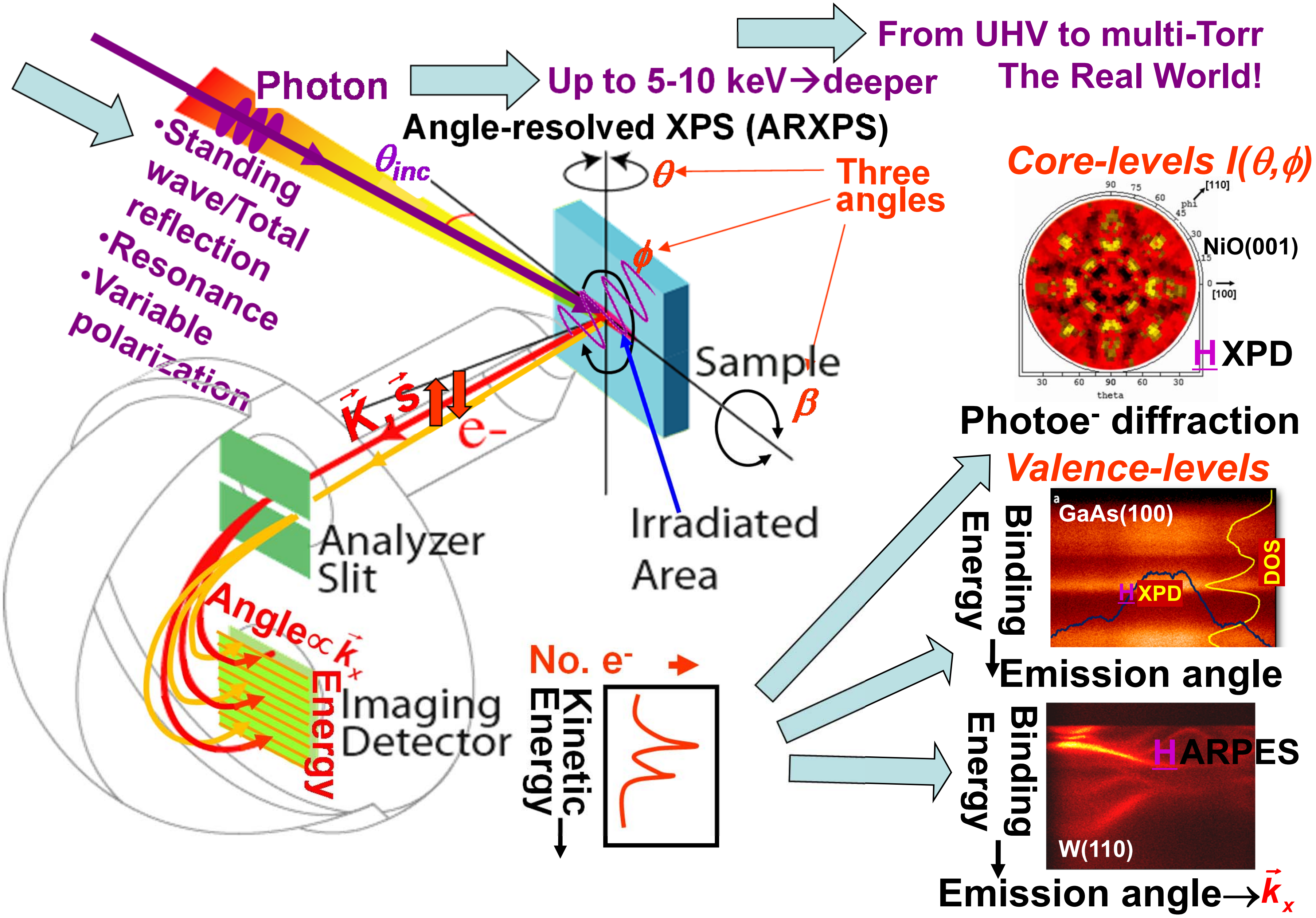

Photon

- Standing wave/Total reflection
- Resonance
- Variable polarization

Up to 5-10 keV→deeper

From UHV to multi-Torr
The Real World!

Angle-resolved XPS (ARXPS)

Three angles

Core-levels I(θ,φ)

Photoe$^-$ diffraction

Valence-levels

Photoemission from complex materials, heterostructures, and interfaces

Three ways to address the limitations of traditional photoemission:

- **Use of harder x-ray excitation (SXPS→2 keV, HXPS, HAXPES→10 keV) for deeper probing: core levels and valence DOSs, incl. soft <u>and</u> hard x-ray angle-resolved photoemission (ARPES) and photoelectron diffraction (XPD)**

- **Use of soft <u>and</u> hard x-ray standing waves, total reflection, other x-ray optical effects, resonant excitation, to selectively look below the surface, at buried interfaces, including ARPES**

- **Use of differentially-pumped systems to provide multi-Torr ambient pressure photoemission, more real-world conditions for studying surface chemical processes, catalysis, electrochemistry**

Lectures posted at Soleil website and group website:

http://www.physics.ucdavis.edu/fadleygroup/Soleil.Lectures.Fadley.pdf

Hard x-ray photoemission—plusses and minusses

•Plusses

•More bulk sensitive spectra → a versatile tool for any new material or multilayer nanostructure

•Inelastic background less important & Augers more widely spread, less overlap

•Less radiation damage and charging-sort of

•Easier interpretation of angle-resolved (ARXPS) data → surface and bulk information

•Easier quantitative analysis via core spectra

•Variable polarization: magnetic circular, linear dichroism, cross section effects

•Spin-resolved spectra for magnetic systems

•New "bulk fingerprint" satellite effects seen in both core and valence spectra

• Hard x-ray photoelectron diffraction: dopants, lattice distortions

•Bulk DOS info. at highest energies and temperatures

•3d "bulk" band mapping SARPES/HARPES capability with cryocooling

Minusses

•Resolution not as good as ~1 meV VUV PS, but as good/better than SX PS, and down to ~50 meV overall, good enough for many applications

•Photoelectric cross sections low, need special undulator beamline/spectrometer combinations—several solutions→
<1 micron focus and ~50 meV resolution

•High *n*, low-ℓ cross section components strongly favored, but in TM or RE VB they can be more involved in transport , s and p like

•Recoil energy limits resolution for lighter elements; complex systematics, depending on local bond distances/phonon frequencies→Doppler spectroscopy?

•Intensity calculations must allow for non-dipole effects, photon wave vector, but easy

•Interchannel coupling can complicate high-energy cross sections, but avoidable

ARPES—How high can we go in energy and temperature?

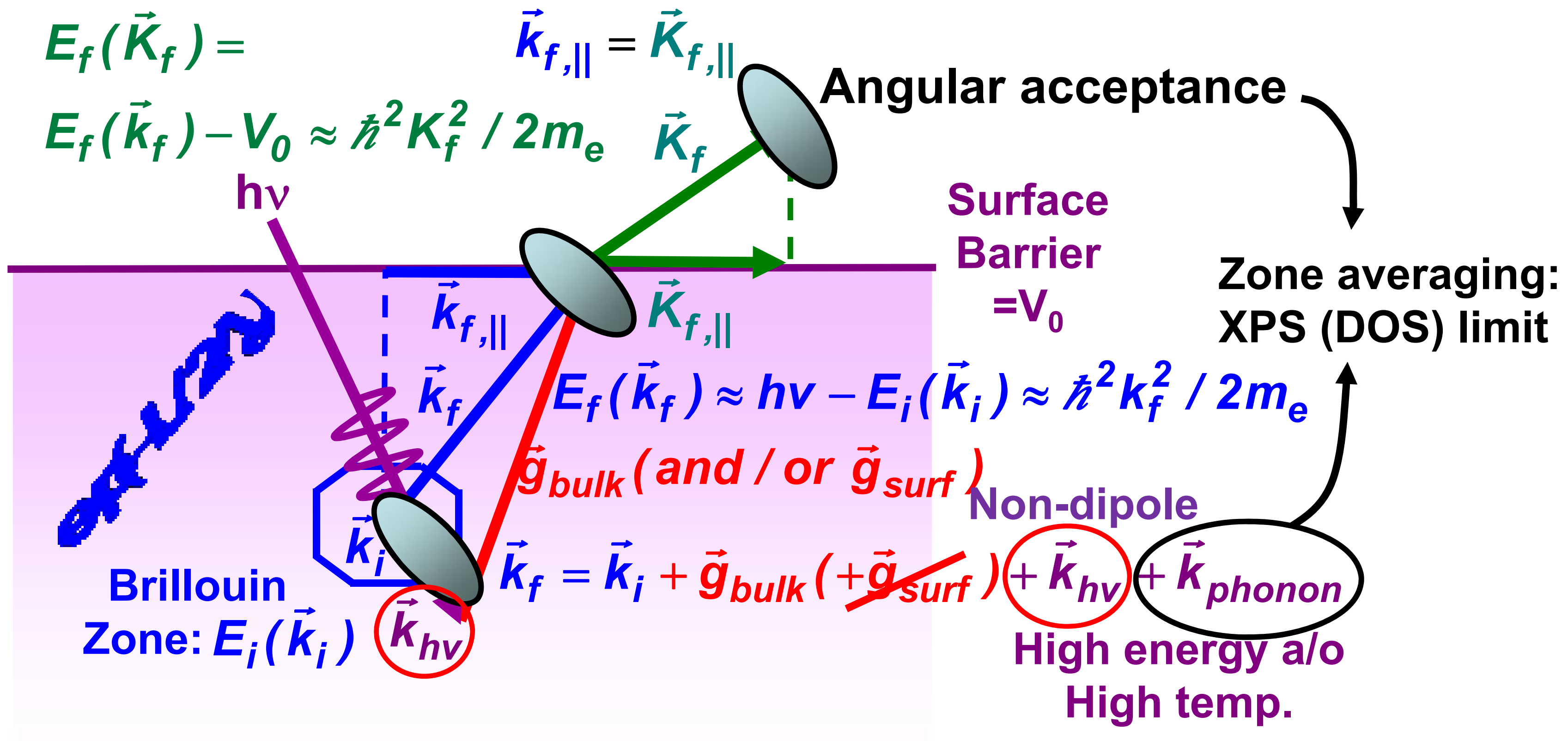

$E_f(\vec{K}_f) =$

$E_f(\vec{k}_f) - V_0 \approx \hbar^2 K_f^2 / 2m_e$

$\vec{k}_{f,||} = \vec{K}_{f,||}$

Surface Barrier $=V_0$

Zone averaging: XPS (DOS) limit

$E_f(\vec{k}_f) \approx h\nu - E_i(\vec{k}_i) \approx \hbar^2 k_f^2 / 2m_e$

$\vec{g}_{bulk}$ (and / or $\vec{g}_{surf}$)

Brillouin Zone: $E_i(\vec{k}_i)$

$\vec{k}_f = \vec{k}_i + \vec{g}_{bulk} (+\cancel{\vec{g}_{surf}}) + \vec{k}_{h\nu} + \vec{k}_{phonon}$

High energy a/o High temp.

Fraction DTs ≈ Debye-Waller factor = $W(T) \approx \exp[-(k^f)^2 \langle u^2(T) \rangle]$

$\approx \exp[-C_1 (k^f)^2 T/(m \Theta_D^2)] \approx \exp(-C_2 E_{kin} T)$

$W \approx 1$

ARPES→bands, quasiparticles (Low hν, Low T, High angul. Res.)

$W \approx 0$

XPS→DOS+XPD (High hν, High T, Low angul. Res.)

Shevchik, Phys. Rev. B 16, 3428 (1977)
Hussain….CF, Phys. Rev. B 34 (1986) 5226

Angle-Resolved Photoemission at High Energy--

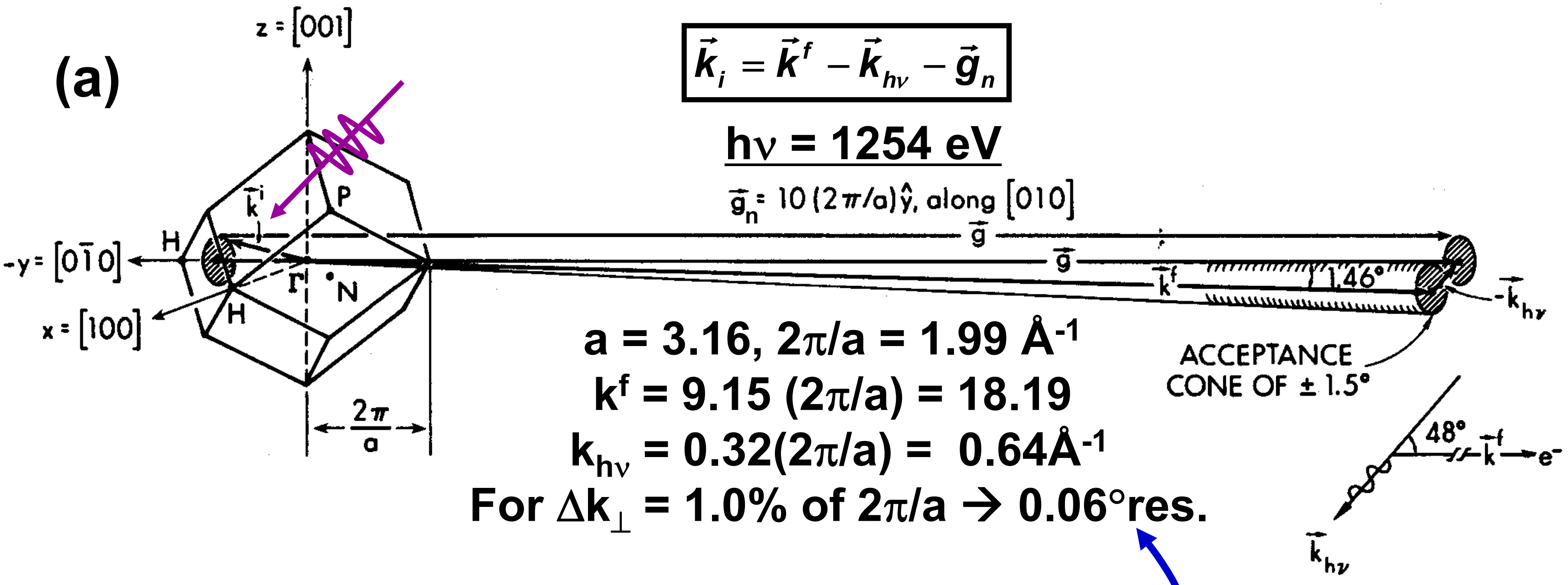

$$\boxed{\vec{k}_i = \vec{k}^f - \vec{k}_{h\nu} - \vec{g}_n}$$

$h\nu$ = 1254 eV

a = 3.16, 2π/a = 1.99 Å^{-1}

k^f = 9.15 (2π/a) = 18.19

$k_{h\nu}$ = 0.32(2π/a) = 0.64Å^{-1}

For $\Delta k_{\perp}$ = 1.0% of 2π/a → 0.06°res.

Hussain et al.....CF, Phys. Rev. B 22 3750 (1980) Phys. Rev. B 34, 5226 (1986)

Shevchik, Phys. Rev. B 16, 3428 (1977)

Additional effects at higher energies:

- **Non-dipole--the photon momentum $k_{h\nu}$ →*easy to allow for***
- **Angular acceptance→B.Z. averaging →*need better angular res.***
- **Lattice recoil→phonon creation→more B.Z. averaging,**

Fraction DTs ≈ Debye-Waller factor = $W(T) \approx \exp[-(k^f)^2 \langle u^2(T)\rangle]$

$\approx \exp[-C_1 (k^f)^2 T/(m\Theta_D{}^2)] \approx \exp(-C_2 E_{kin} T)$ →*need cryocooling*

→the "XPS limit" of full B.Z. averaging and D.O.S. sensitivity

→core-like photoelectron diffraction

- **Recoil →peak shifts and broadening:**

$$E_{recoil}(eV) \approx \left[\frac{m_e}{M}\right] E_{kin} \approx 5.5\ x\ 10^{-4} \left[\frac{E_{kin}(eV)}{M(amu)}\right]$$

Alvarez et al., PR*B* 54, 14703 (1996)

Takata et al., Phys. Rev. B 75, 233404 (2007)

VALENCE-BAND PHOTOELECTRON INTENSITIES IN THE DENSITY-OF-STATES LIMIT

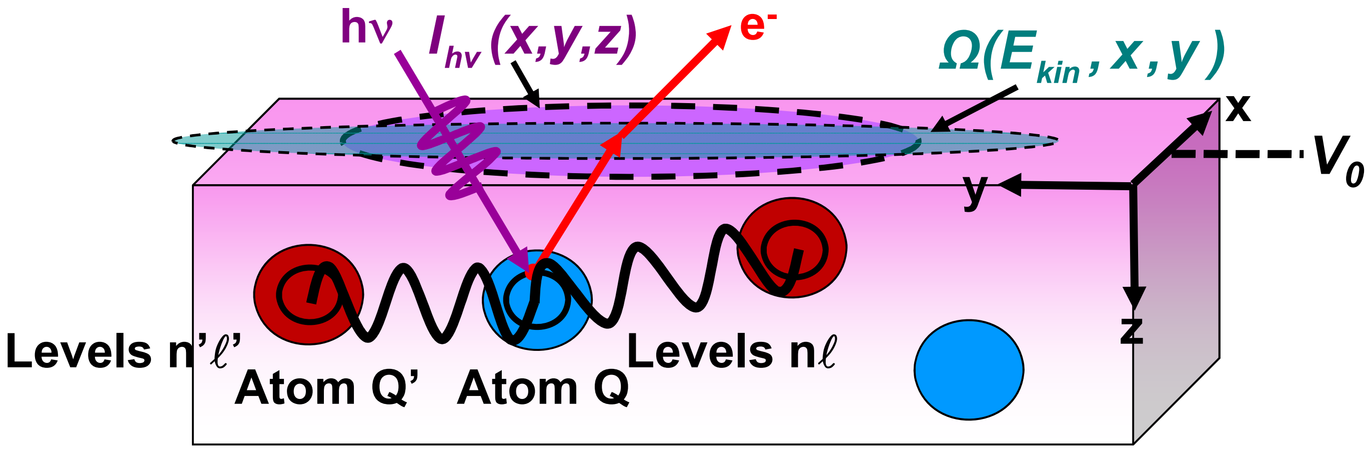

*For a given subshell:**

$I(E_{kin,}Qn\ell) \cong$

$$C'\int_0^\infty I_{h\nu}(x,y,z)\rho_{Qn\ell}(E_b,x,y,z)\frac{d\sigma_{Qn\ell}(h\nu)}{d\Omega}\exp\left[-\frac{z}{\Lambda_e(E_{kin})\sin\theta}\right]\Omega(E_{kin},x,y)dxdydz$$

$I_{h\nu}(x,y,z)$ = *x-ray flux*

$\rho_{Qn\ell}(E_b,x,y,z)$ = *density of states, projected onto Qnℓ character*

$\frac{d\sigma_{Qn\ell}(h\nu)}{d\Omega}$ = *energy-dependent differential photoelectric cross section for subshell Qnℓ*

$\Lambda_e(E_{kin})$ = *energy-dependent inelastic attenuation length*

→ *Mean Emission Depth*

$\Omega(E_{kin},x,y)$ = *energy-dependent spectrometer acceptance solid angle*

*For the total VB intensity:**

$$I_{total}(E_{kin}) = \sum_{Qn\ell} I(E_{kin,}Qn\ell)$$

*** E.g.-Solterbeck et al., Phys. Rev. Lett. 79, 4681 (1997)**

Case study: Temperature dependence of Mn2p spectra: $La_{0.7}Sr_{0.3}MnO_3$
New satellite structures in core spectra

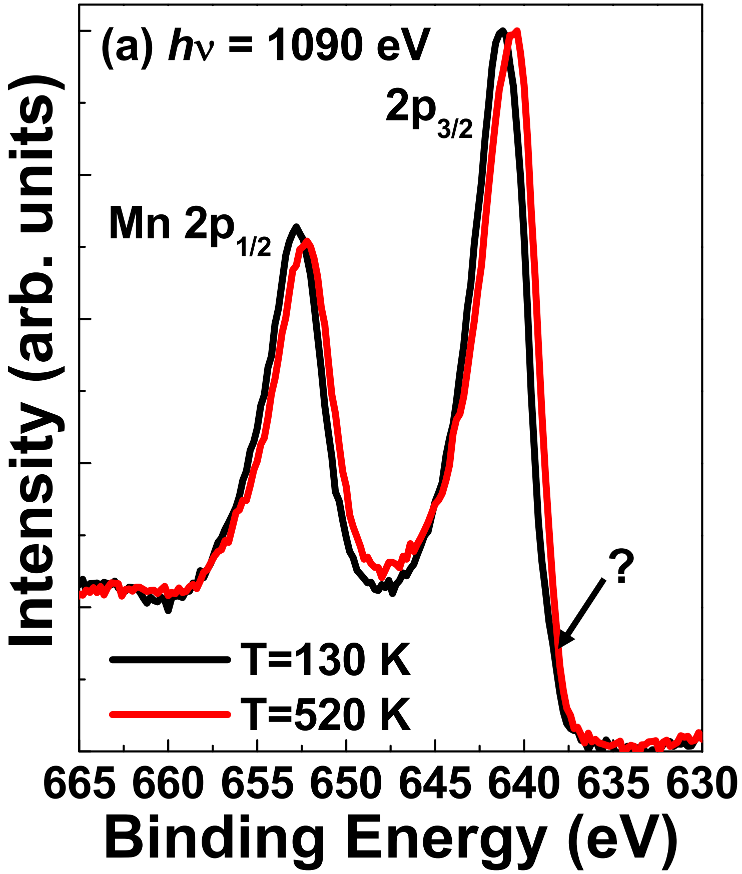

Mean depth: ~1 nm

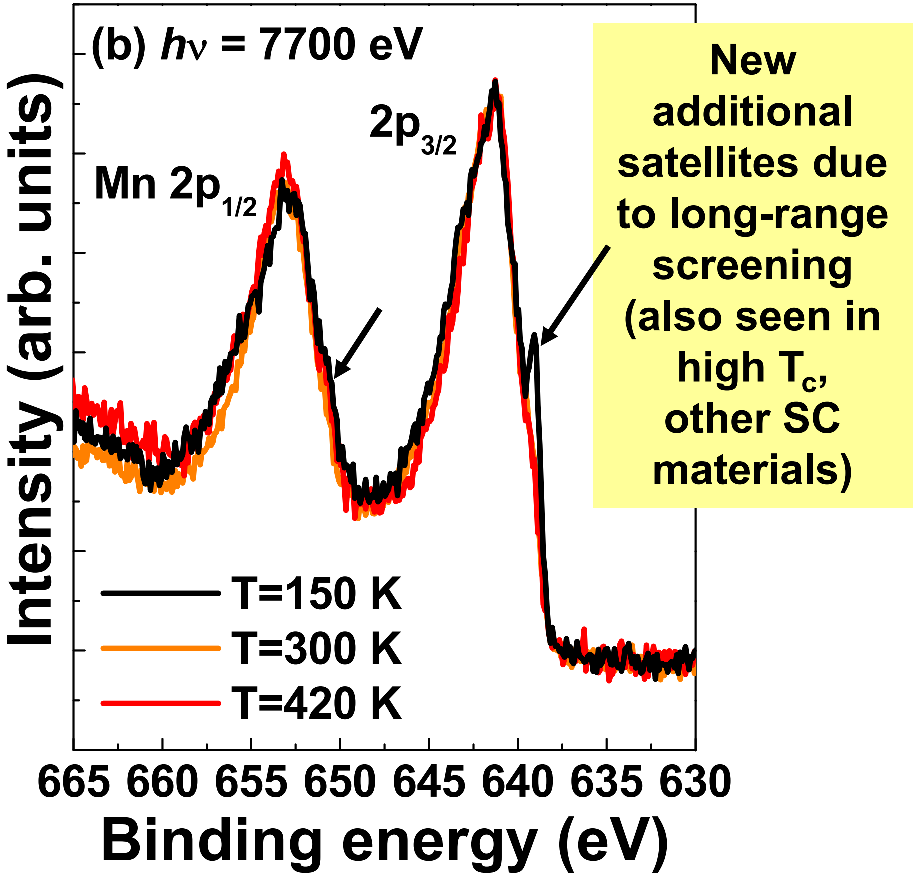

New additional satellites due to long-range screening (also seen in high T_c, other SC materials)

Mean depth: ~8 nm

→ Suggests bulk electronic structure not reached until ca. 8 nm depth

Offi, Mannella, et al., Phys. Rev. B 2008, 77, 174422 - ESRF

$La_{0.7}$ $Sr_{0.3}$ MnO_3: Presence of “bulk” magnetism-associated screening features in both Mn 3s and 3p spectra

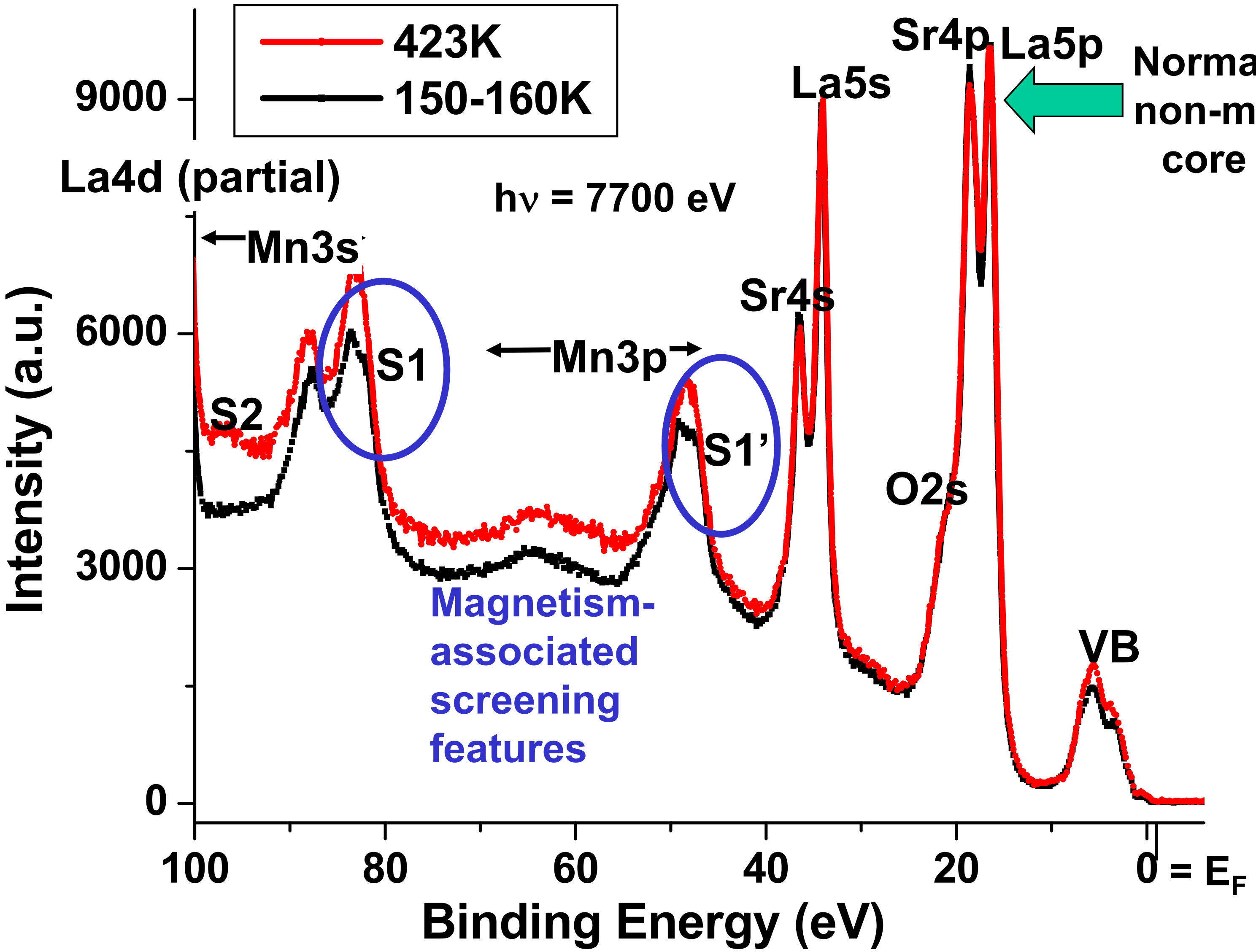

Normalized to non-magnetic core levels

Magnetism-associated screening features

Offi et al., PRB 77, 174422 (‘08)-ESRF

$La_{0.7}$ $Sr_{0.3}$ MnO_3: Derivation of density-of-states information from core-normalized HXPS valence-band spectra

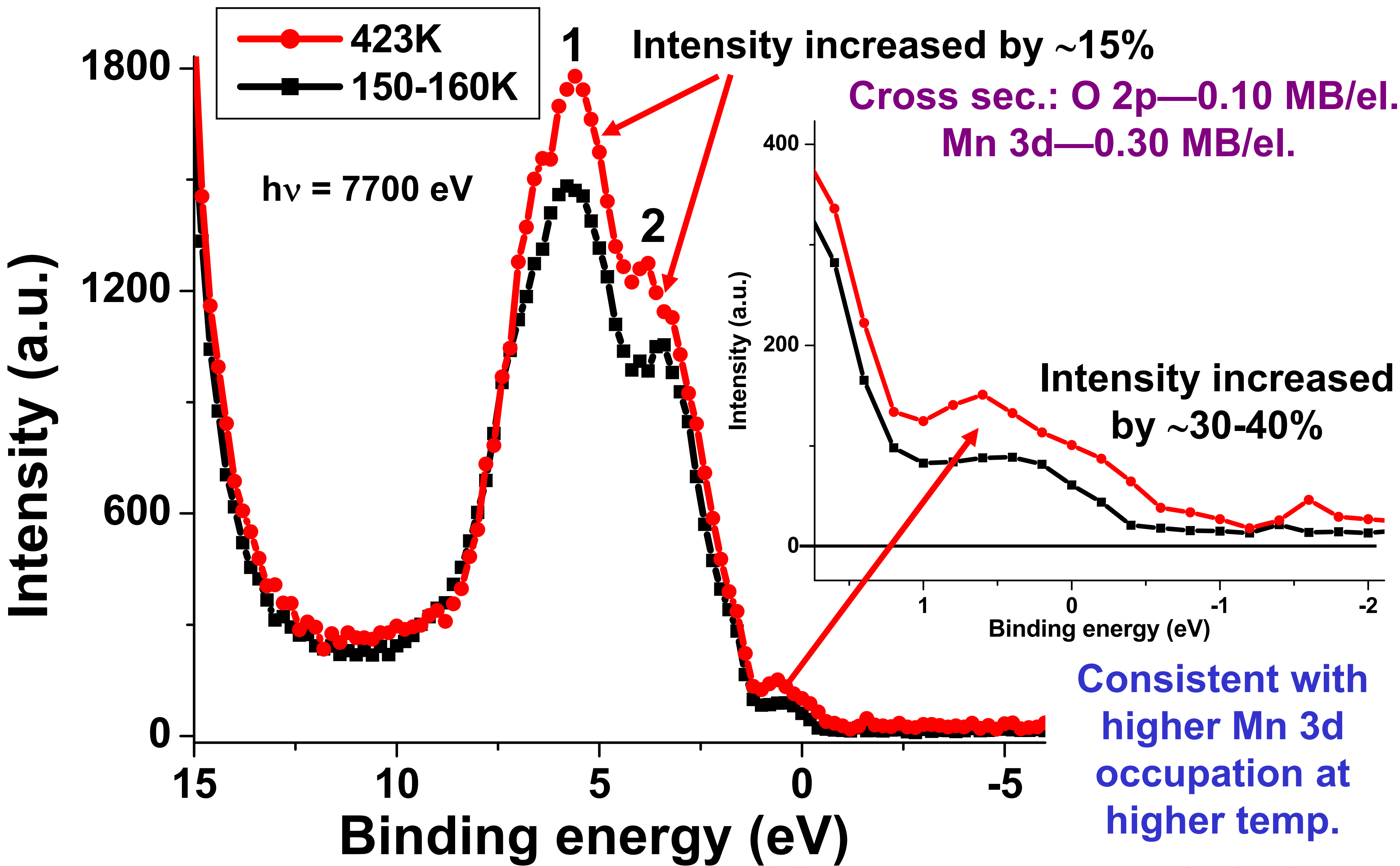

Intensity increased by ~15%

Cross sec.: O 2p—0.10 MB/el.
Mn 3d—0.30 MB/el.

Intensity increased by ~30-40%

Consistent with higher Mn 3d occupation at higher temp.

Offi et al., PRB 77, 174422 ('08)-ESRF

Hard x-ray photoemission @ 5.9 keV: Opening of a semiconducting gap in the “bulk” of a magnetic CrAl alloy

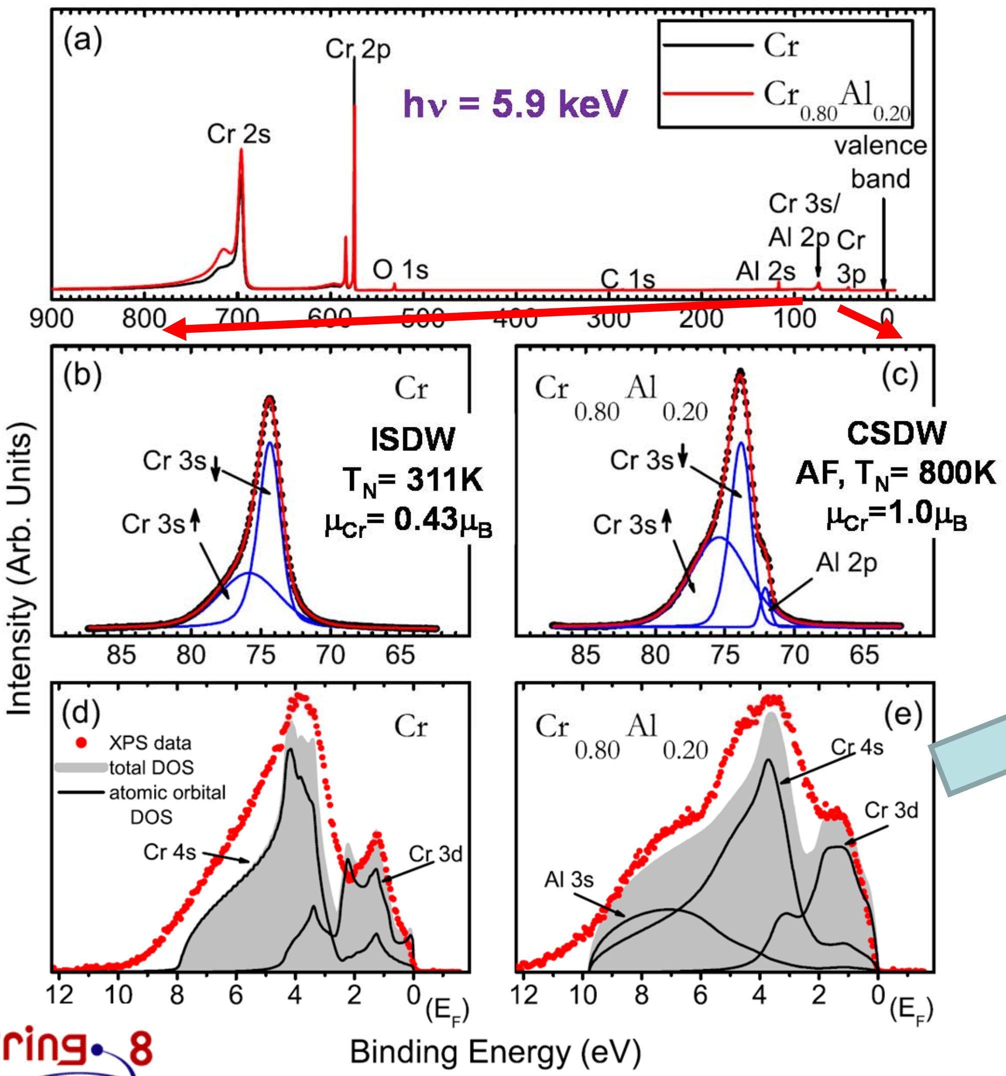

Resistivity

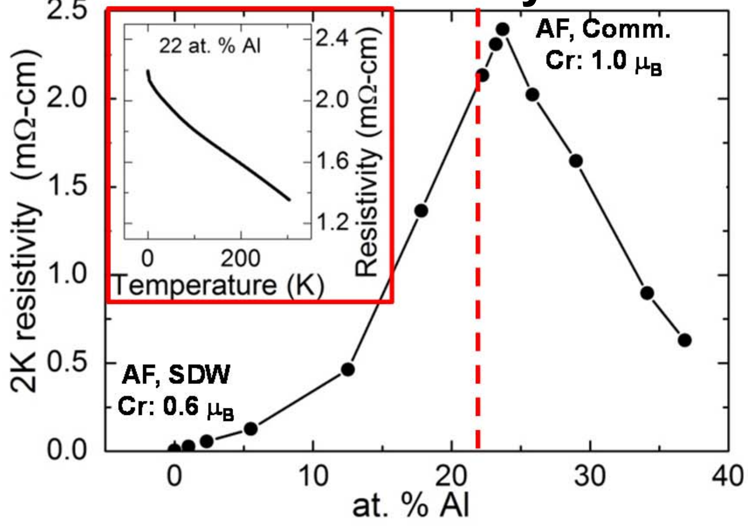

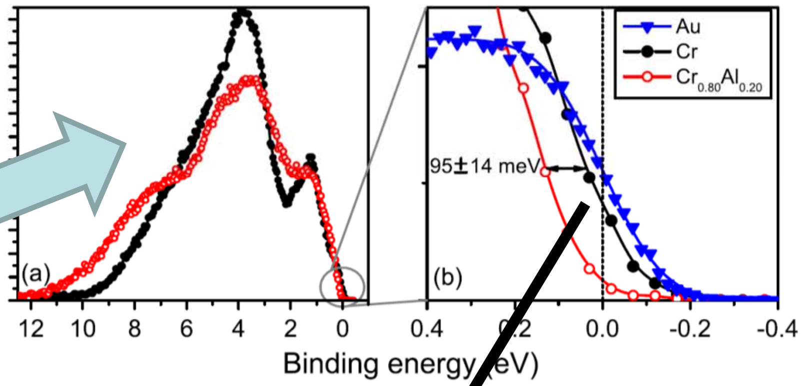

Opening of ~90 meV semiconducting gap

Boekelheide, Gray et al. (Hellman, Fadley Groups) PRL 105, 236404 (2010)

Hard x-ray photoemission—plusses and minusses

•**Plusses**

- More bulk sensitive spectra → a versatile tool for any new material or multilayer nanostructure
- Inelastic background less important & Augers more widely spread, less overlap
- Less radiation damage and charging-sort of
- Easier interpretation of angle-resolved (ARXPS) data → surface and bulk information
- Easier quantitative analysis via core spectra
- Variable polarization: magnetic circular, linear dichroism, cross section effects
- Spin-resolved spectra for magnetic systems
- New "bulk fingerprint" satellite effects seen in both core and valence spectra
- Hard x-ray photoelectron diffraction: dopants, lattice distortions
- Bulk DOS info. at highest energies and temperatures
- 3d "bulk" band mapping SARPES/HARPES capability with cryocooling

Minusses

- Resolution not as good as ~1 meV VUV PS, but as good/better than SX PS, and down to ~50 meV overall, good enough for many applications
- Photoelectric cross sections low, need special undulator beamline/spectrometer combinations—several solutions→
  <1 micron focus and ~50 meV resolution
- High *n*, low-ℓ cross section components strongly favored, but in TM or RE VB they can be more involved in transport , s and p like
- Recoil energy limits resolution for lighter elements; complex systematics, depending on local bond distances/phonon frequencies→Doppler spectroscopy?
- Intensity calculations must allow for non-dipole effects, photon wave vector, but easy
- Interchannel coupling can complicate high-energy cross sections, but avoidable
- Phonon effects reduce capability for ARPES at higher energies/temperatures

Tungsten--Debye-Waller Factors and Recoil Energies

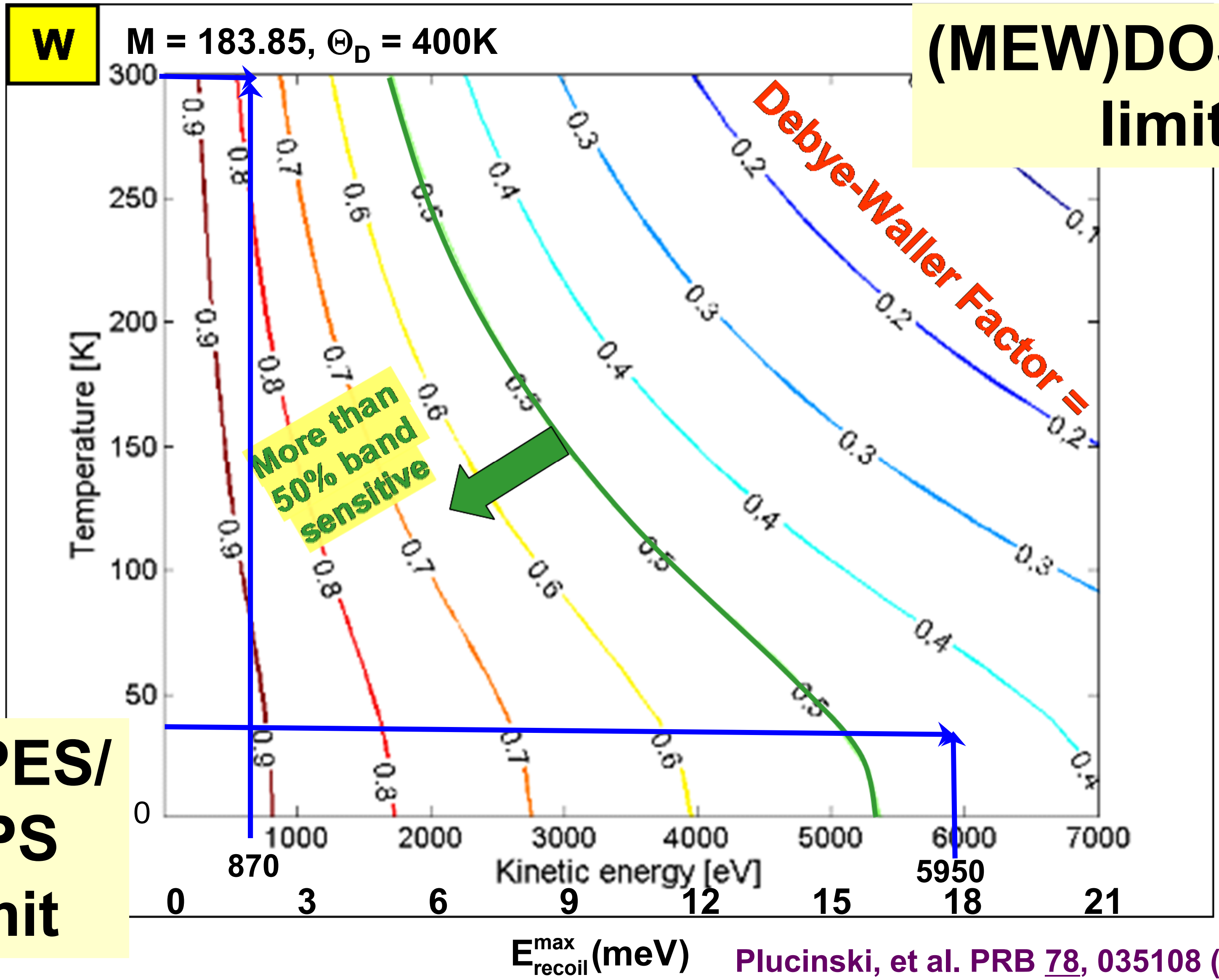

(MEW)DOS/XPS limit

ARPES/ UPS limit

Plucinski, et al. PRB 78, 035108 (2008);
Phys. Rev. B 84, 045433 (2011)-ALS;
Gray, Minar et al., Nature Mat. 10, 759 (2011)-SPring-8

ARPES→HARPES-How high can we go? Photoemission Debye-Waller Factors and Recoil Energies

Photon energy for ~50% DTs = O.5 D-W @ 20K

Recoil energy for all atoms and different photon energies

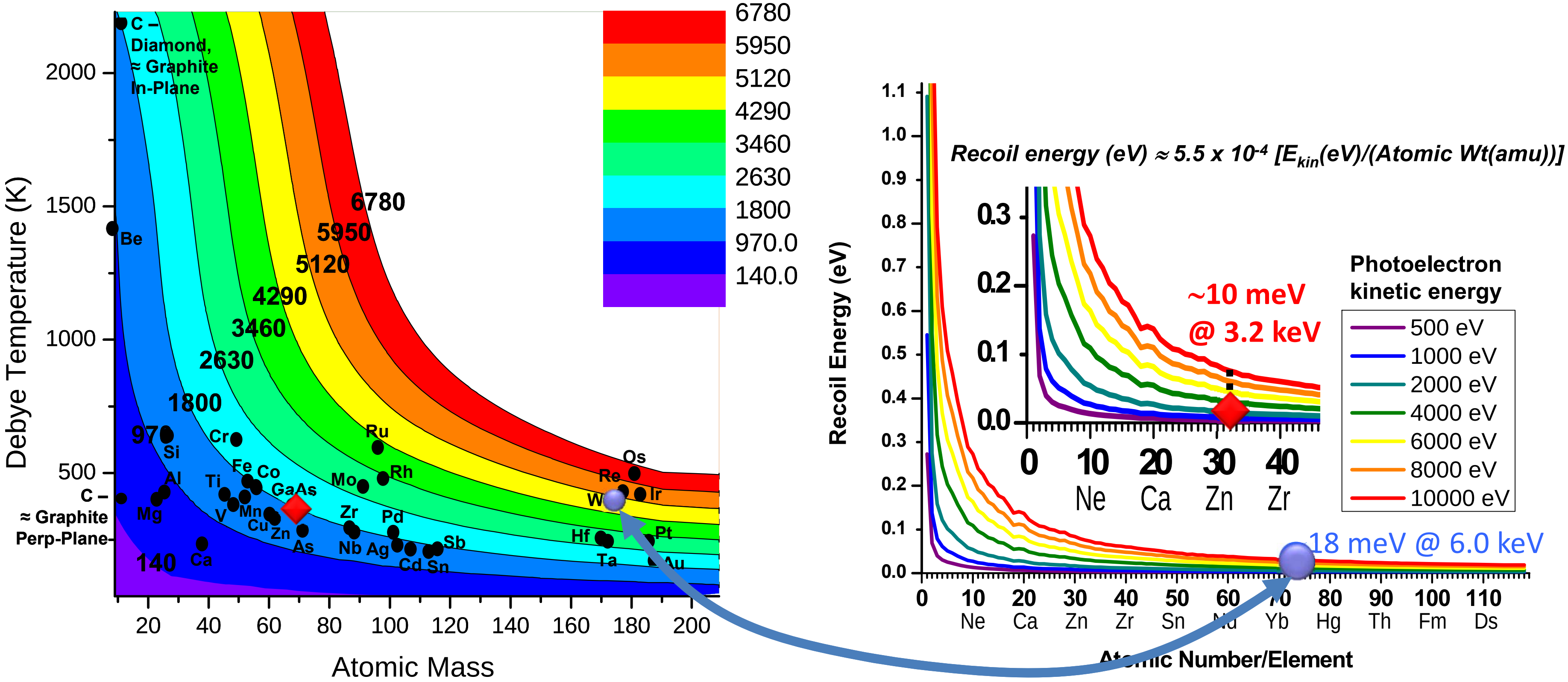

C. Papp. L. Plucinski, et al., Phys. Rev. B 84, 045433 (2011)

Hard x-ray ARPES for W(110): 6.0 keV

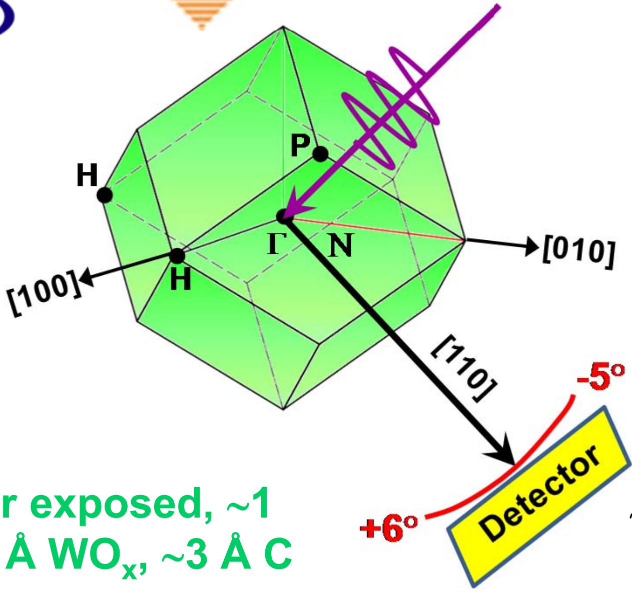

W(110)-air exposed, ~1 year, ~12 Å WO_x, ~3 Å C

Ang. Res.:
~0.2°→0.02°
in future

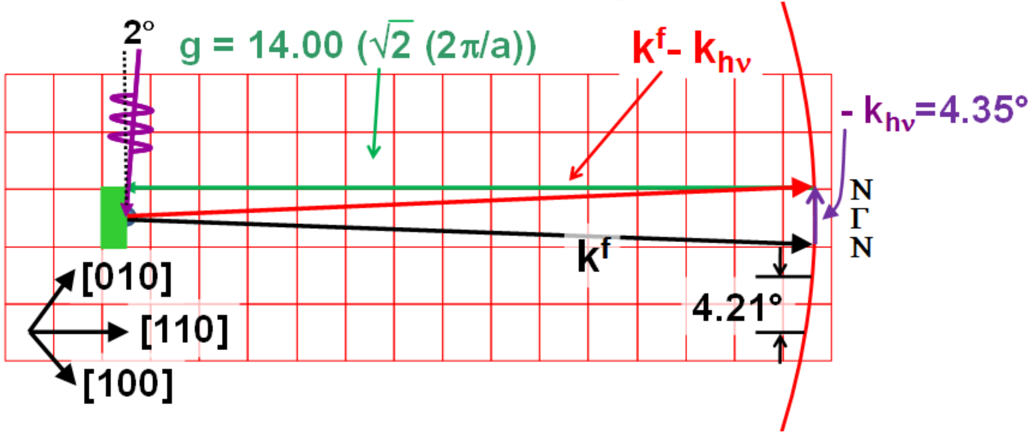

Gray, Minar et al., Nature Materials 10, 759 (2011-SPring-8)

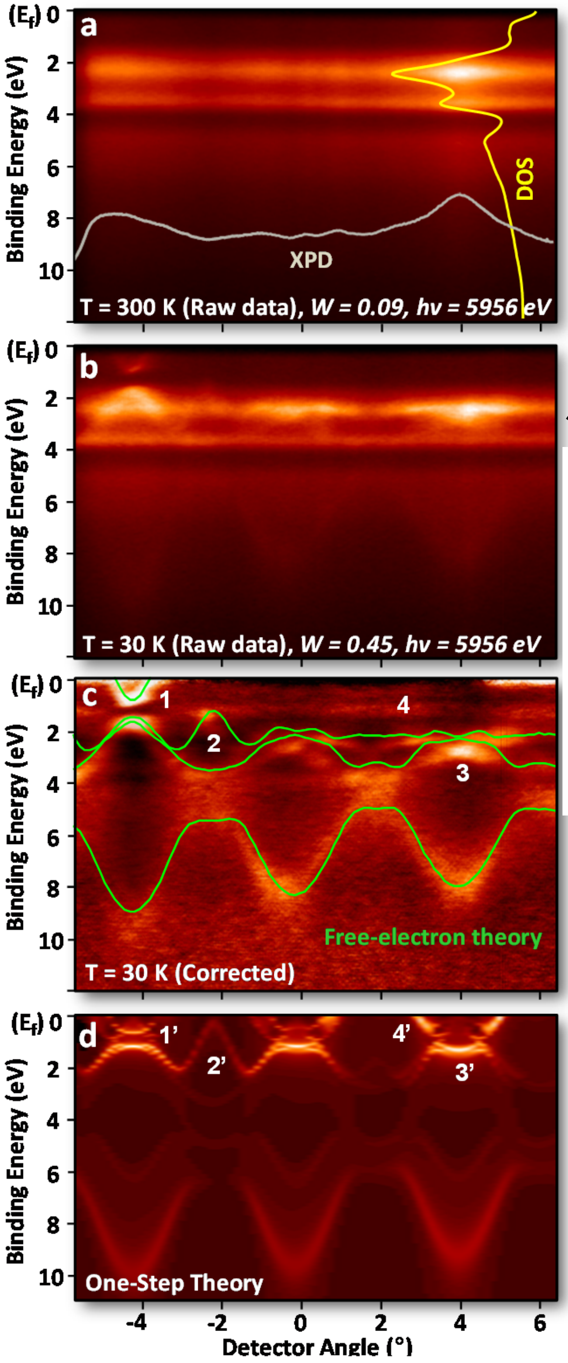

Bostwick-Rotenberg Correction: Divide by average over angle (~DOS) and energy (~XPD)

ARPES→HARPES-How high can we go? Photoemission Debye-Waller Factors and Recoil Energies

Photon energy for ~50% DTs = O.5 D-W @ 20K

Recoil energy for all atoms and different photon energies

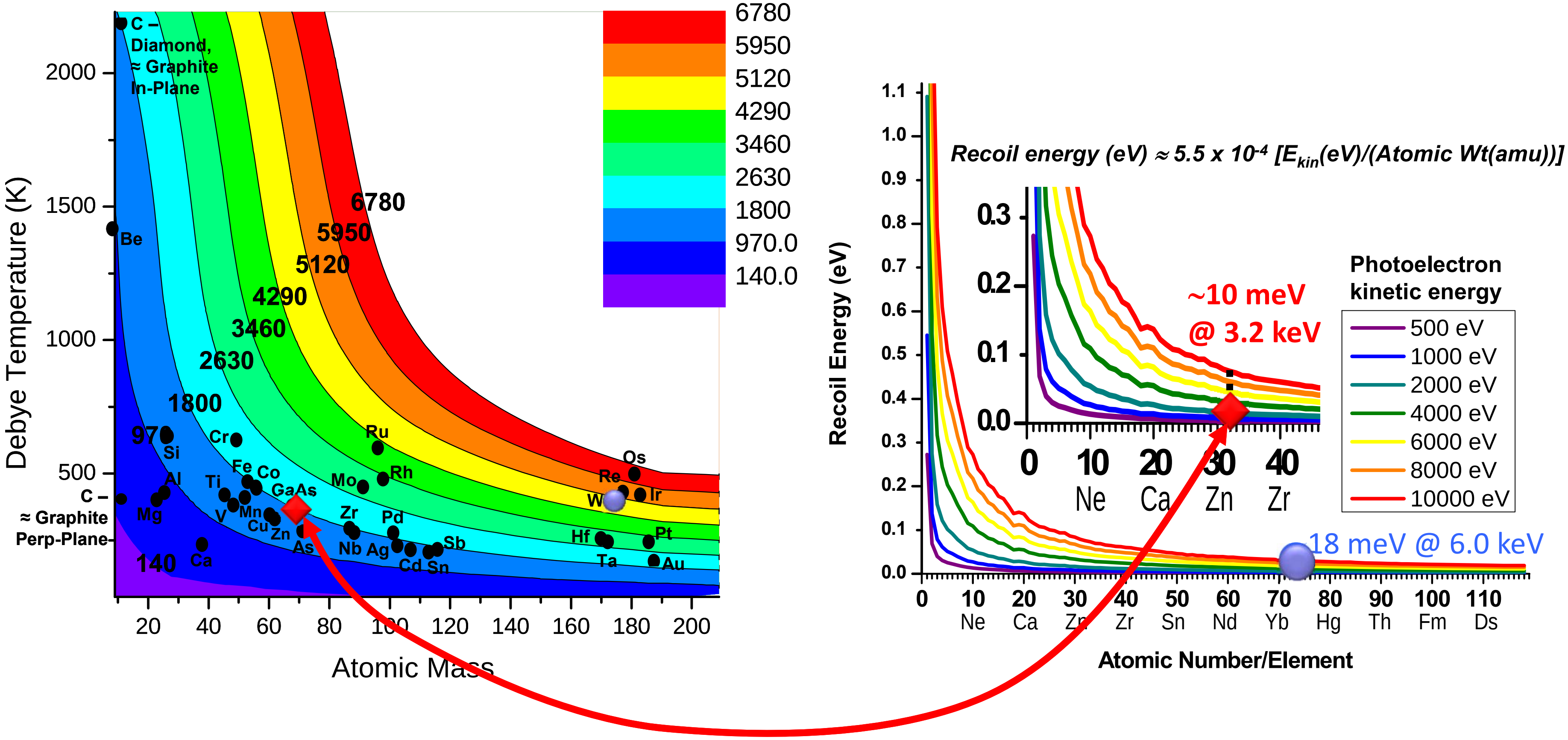

Recoil energy (eV) ≈ 5.5 x 10^{-4} [E_{kin}(eV)/(Atomic Wt(amu))]

~10 meV @ 3.2 keV

18 meV @ 6.0 keV

C. Papp. L. Plucinski, et al., Phys. Rev. B 84, 045433 (2011)

Hard x-ray ARPES for GaAs(001): 3.2 keV

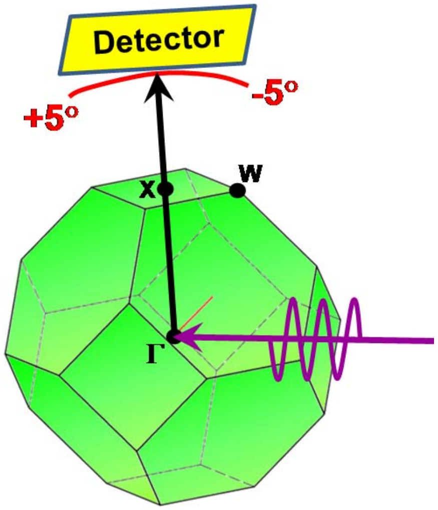

$h\nu$ = 3238 eV
SPring-8

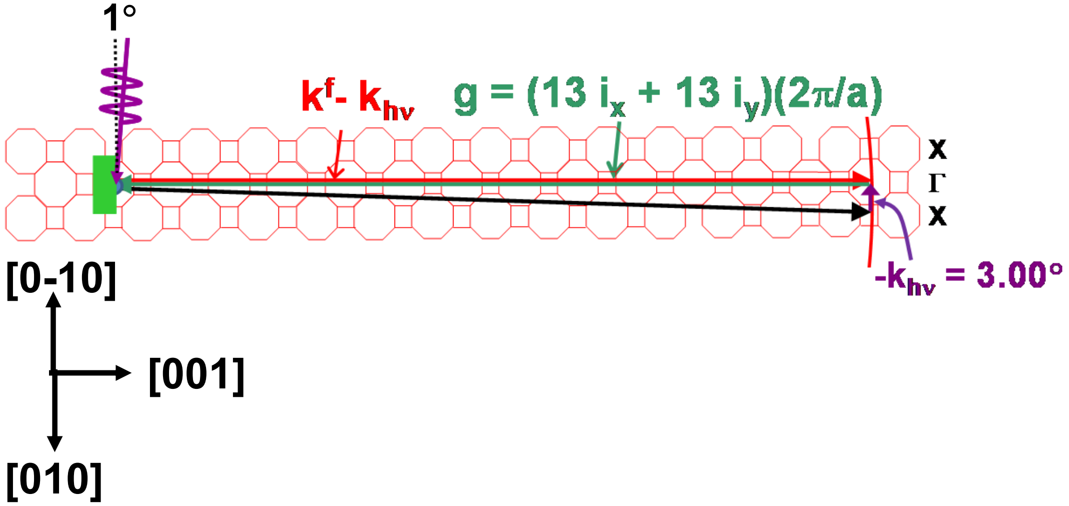

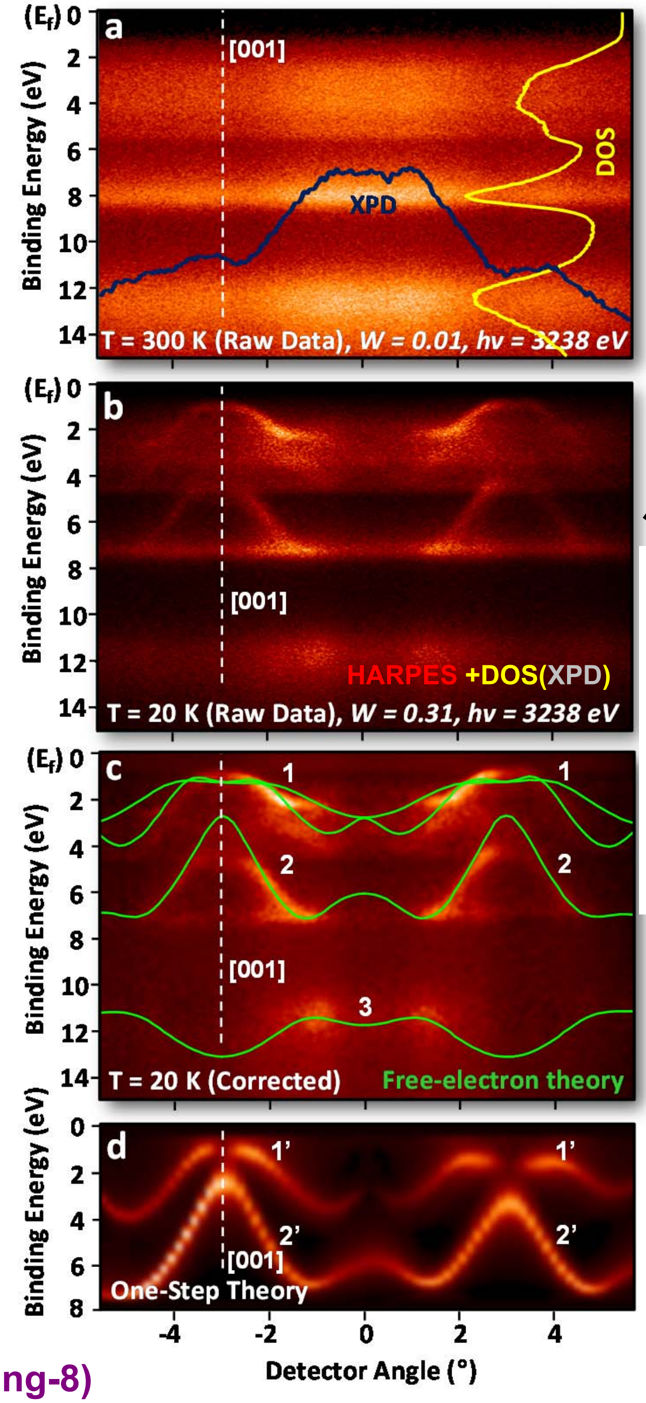

Bostwick-Rotenberg Correction: Divide by average over angle (~DOS) and energy (~XPD)

Gray, Minar et al., Nature Materials 10, 759 (2011-SPring-8)

Hard x-ray ARPES--GaAs and the dilute magnetic semiconductor $Ga_{0.97}Mn_{0.03}As$

How does Mn alter the GaAs electronic structure so as to produce ferromagnetic coupling?
Differing views: p-d exchange, double exchange?

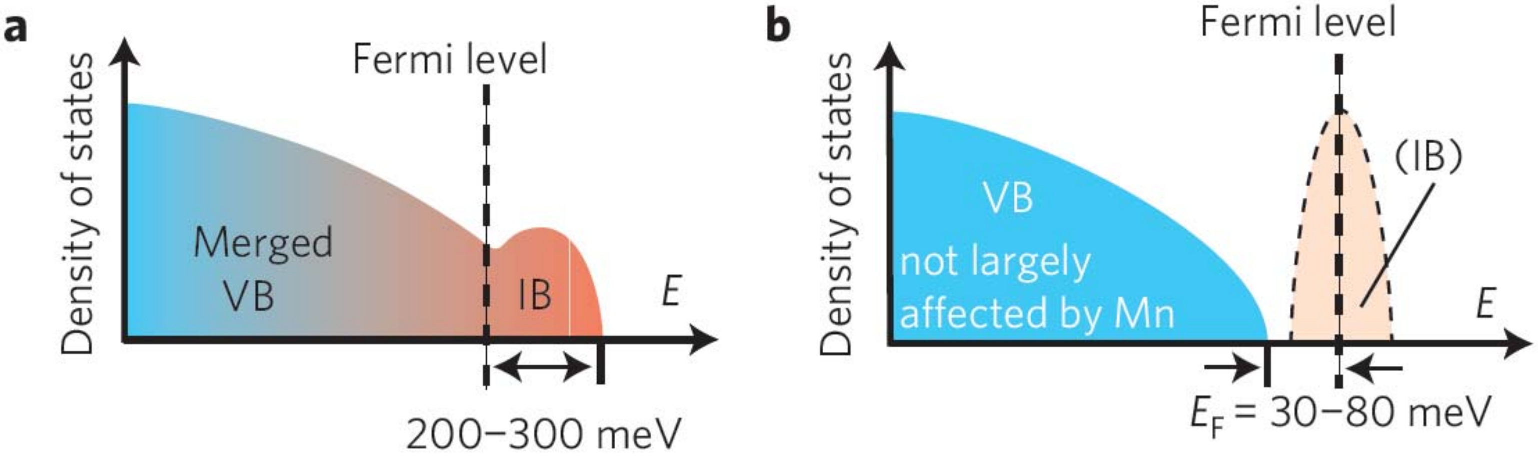

Ohya et al., Nature Physics 7, 342 (2011)

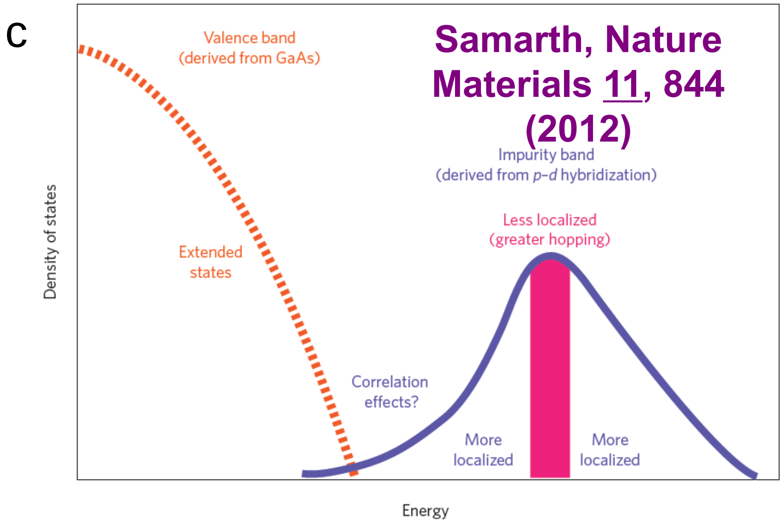

Samarth, Nature Materials 11, 844 (2012)

?

Hard x-ray ARPES--GaAs and DMS $Ga_{0.97}Mn_{0.03}As$
Comparing Experiment (3.2 keV, 30K) and One-Step KKR Theory

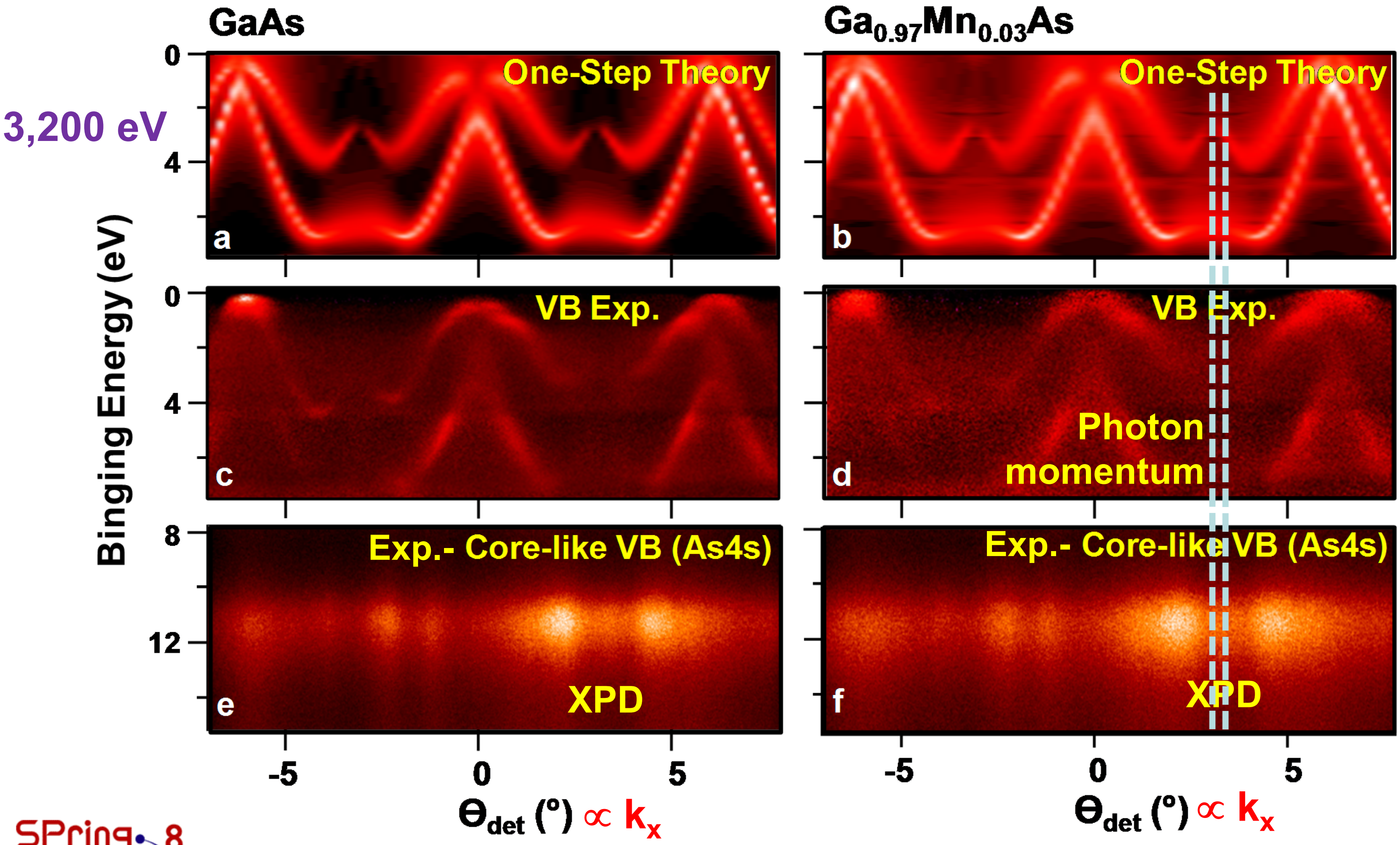

SPring-8

Gray, Minar et al., Nature Materials 11, 957 (2012)

GaAs and $Ga_{0.97}Mn_{0.03}As$
Angle-Integrated Hard X-Ray ARPES @ 3.2 keV
Experiment and One-Step KKR Theory

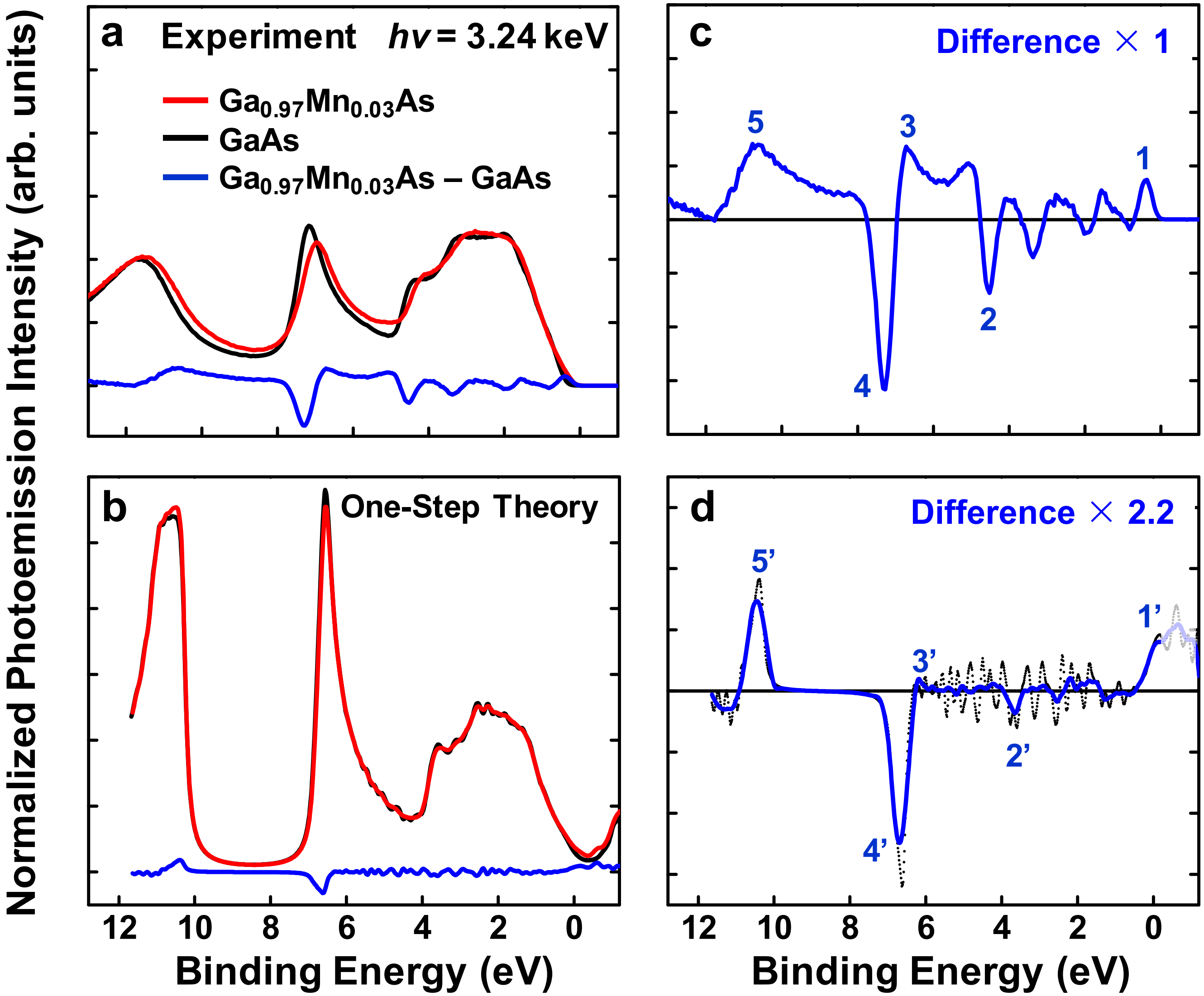

Gray et al., Nature Materials 11, 957 (2012)

Hard x-ray ARPES--GaAs and the dilute magnetic semiconductor $Ga_{0.97}Mn_{0.03}As$

How does Mn alter the electronic structure so as to produce ferromagnetic coupling? Differing views:

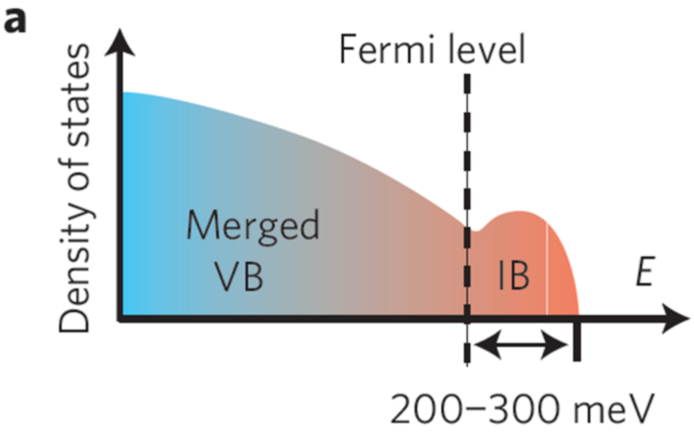

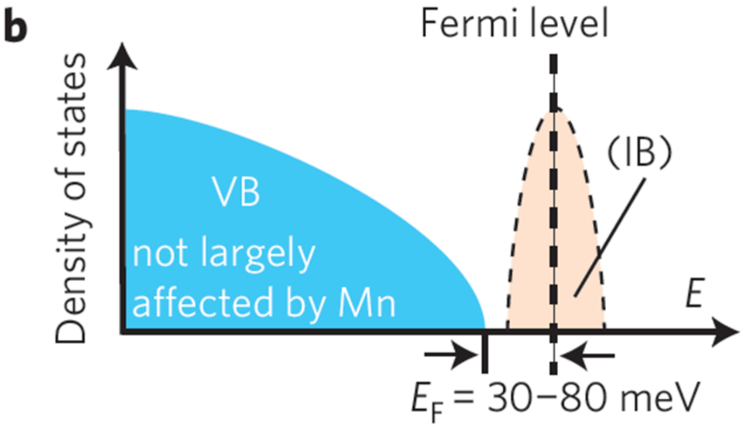

Ohya et al., Nature Physics 7, 342 (2011)

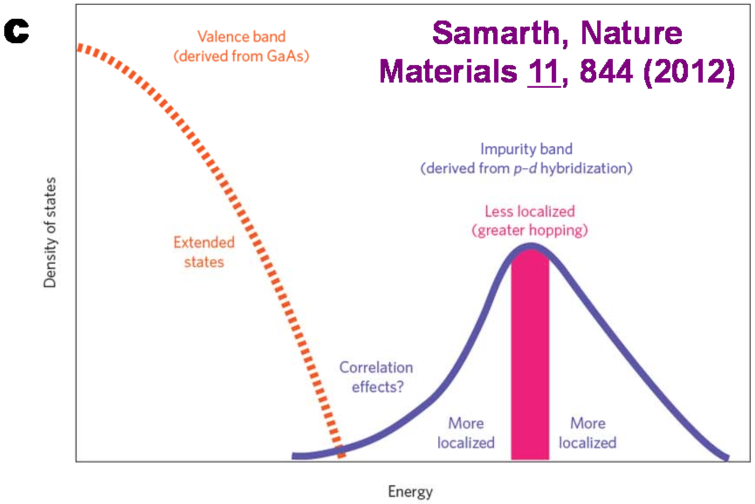

Samarth, Nature Materials 11, 844 (2012)

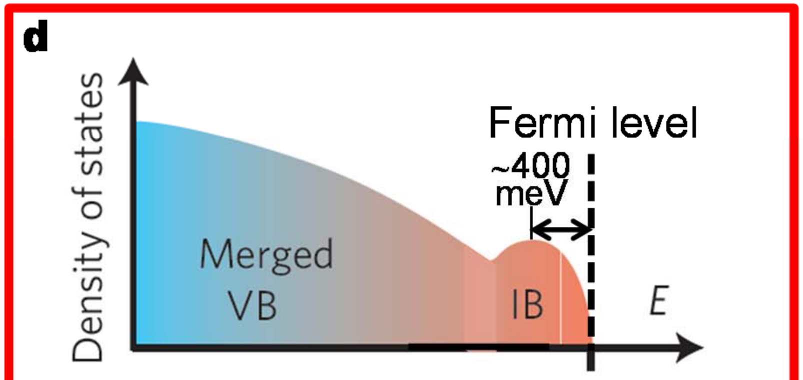

Gray et al., Nature Materials 11, 957 (2012)

$Ga_{0.975}Mn_{0.025}As$: Resonant soft x-ray ARPES

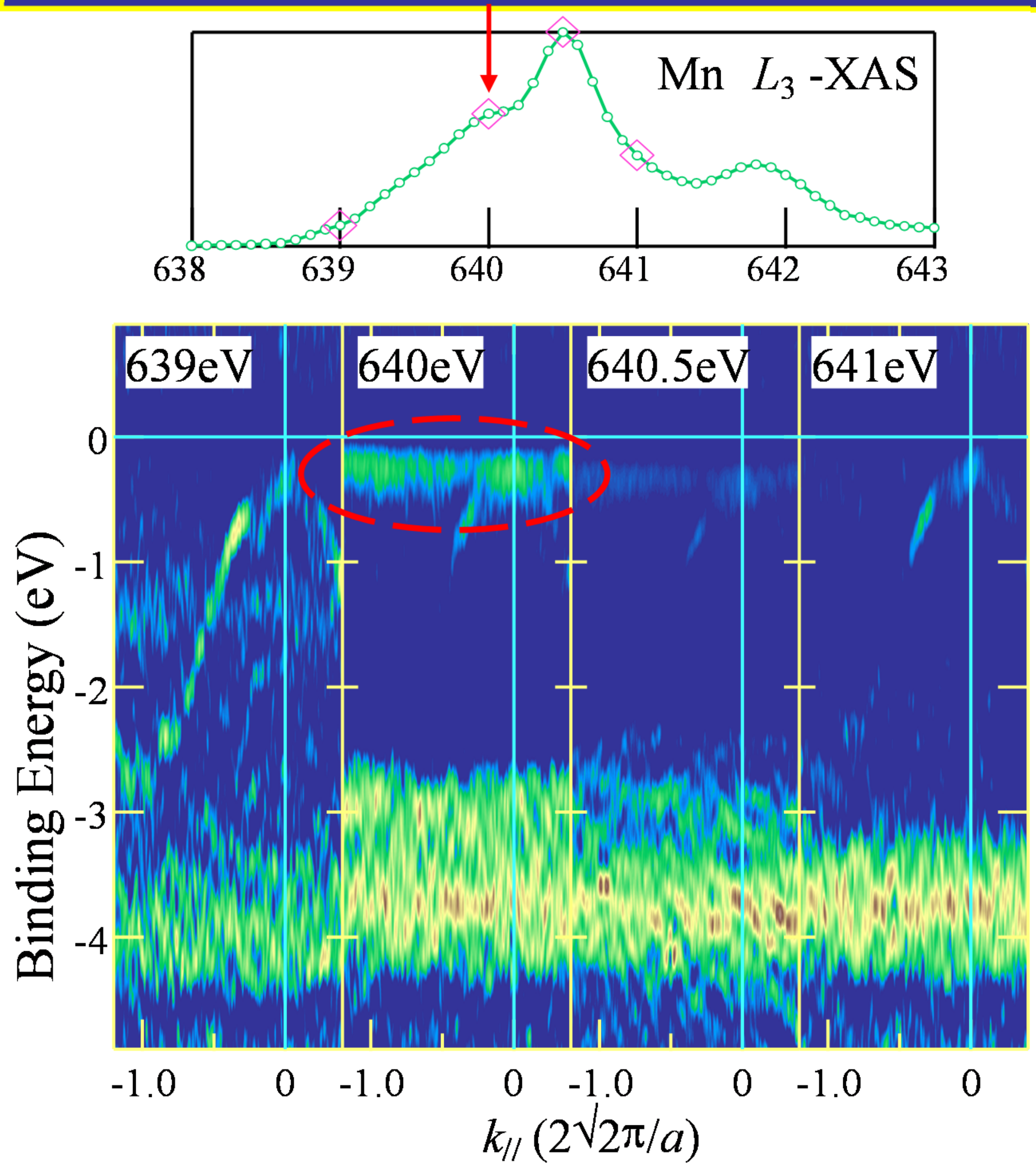

Kobayashi, Strocov, et al., Phys Rev B 89, 205204 (2014)

Hard x-ray photoemission @ 3.2 keV: GaAs doped with Mn-- $Ga_{0.96}Mn_{0.04}As$, a magnetic semiconductor: T = 20K, Broad Survey

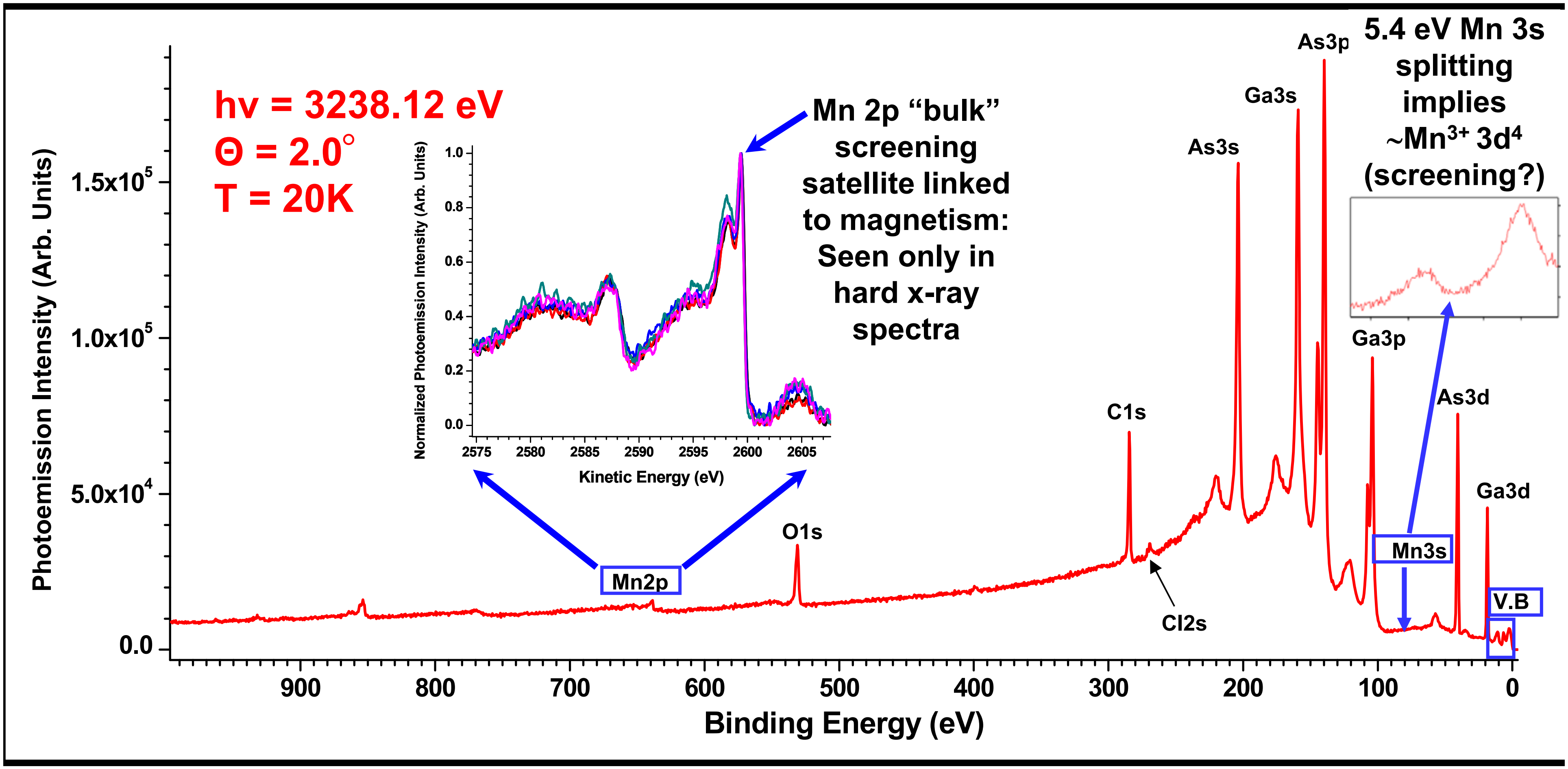

hν = 3238.12 eV
Θ = 2.0°
T = 20K

Mn 2p “bulk” screening satellite linked to magnetism: Seen only in hard x-ray spectra

5.4 eV Mn 3s splitting implies ~Mn^{3+} $3d^4$ (screening?)

SPring-8

Samples: Stone, Dubon
Expt.-Gray, Papp, Ueda, Yamashita, Kobayashi
Theory- Pickett, Ylvisaker, Minar, Braun, Ebert
Nature Materials, 11, 957 (2012)

$Ga_{0.96}Mn_{0.04}As$: Using MCD in screening satellites to determine covalency

MCD Experiment- Below T_C

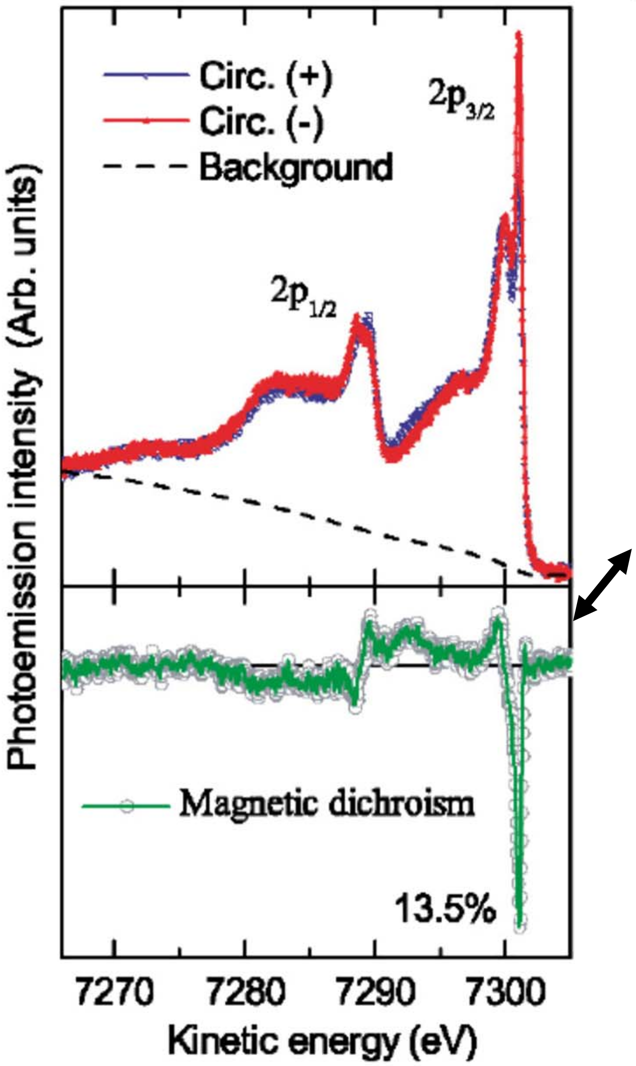

Anderson Impurity Model calcs. vs d hybridization V

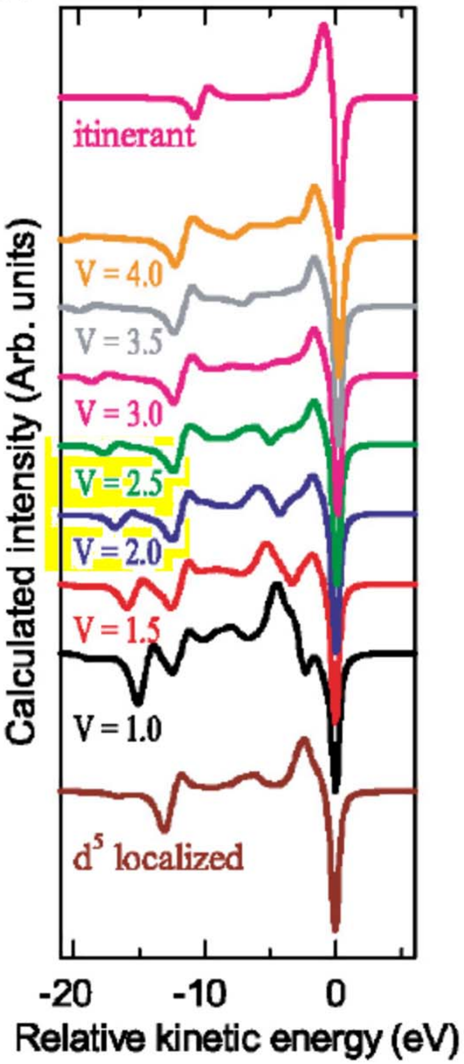

Plus detailed core-level and VB study: Fujii, Panaccione et al., Phys. Rev. Lett. 111, 097201 (2013)

Hard x-ray ARPES--GaAs and DMS $Ga_{0.97}Mn_{0.03}As$
Comparing Experiment (3.2 keV, 30K) and One-Step KKR Theory

3,200 eV

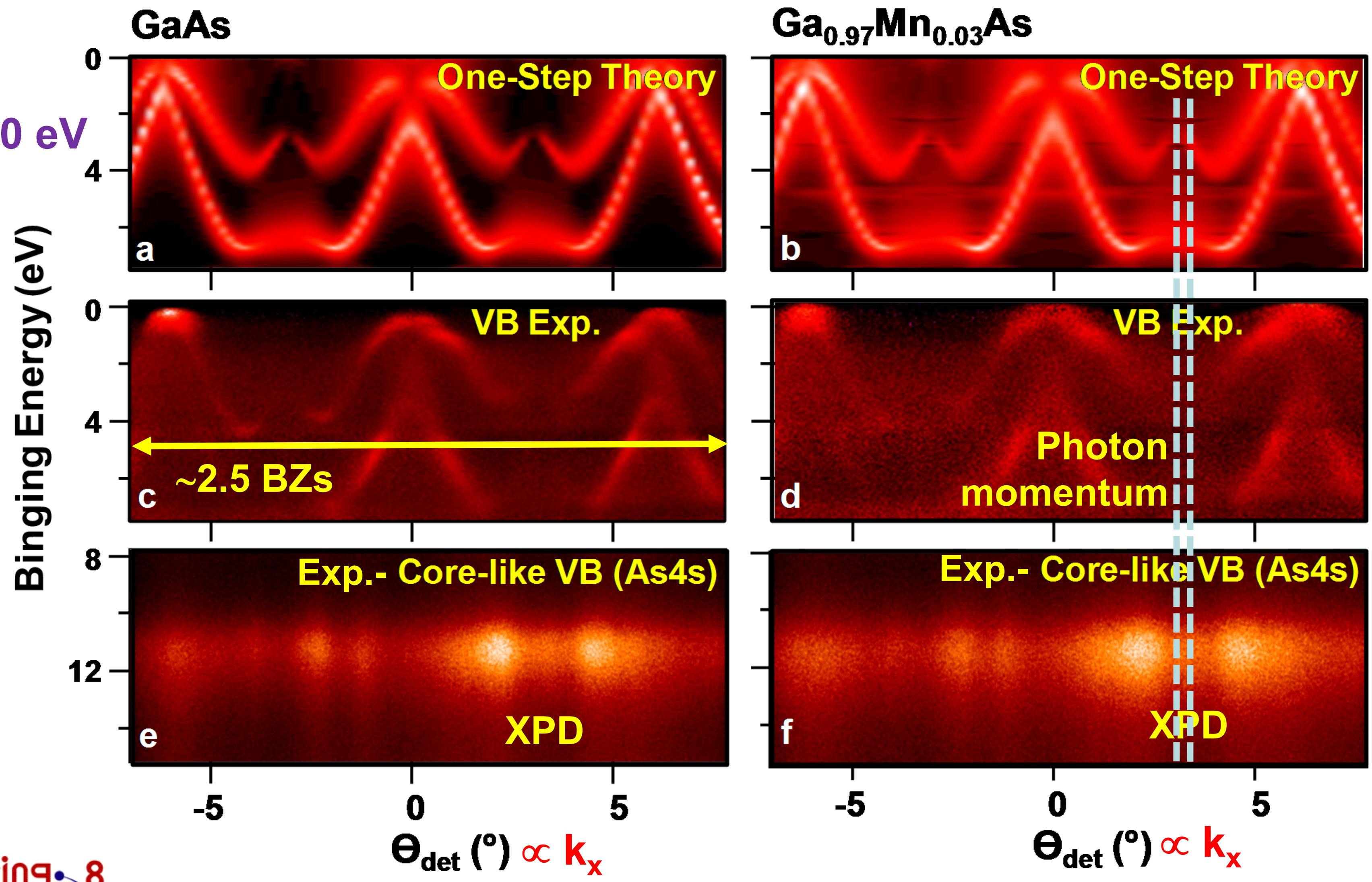

Gray, Minar et al., Nature Materials <u>11</u>, 957 (2012)

Looking to the future: Hard x-ray ARPES-- GaAs and Dilute Magnetic Semiconductor $Ga_{0.95}Mn_{0.05}As$ Experiment Diamond 3.2 keV

→Major differences throughout bands due to Mn!

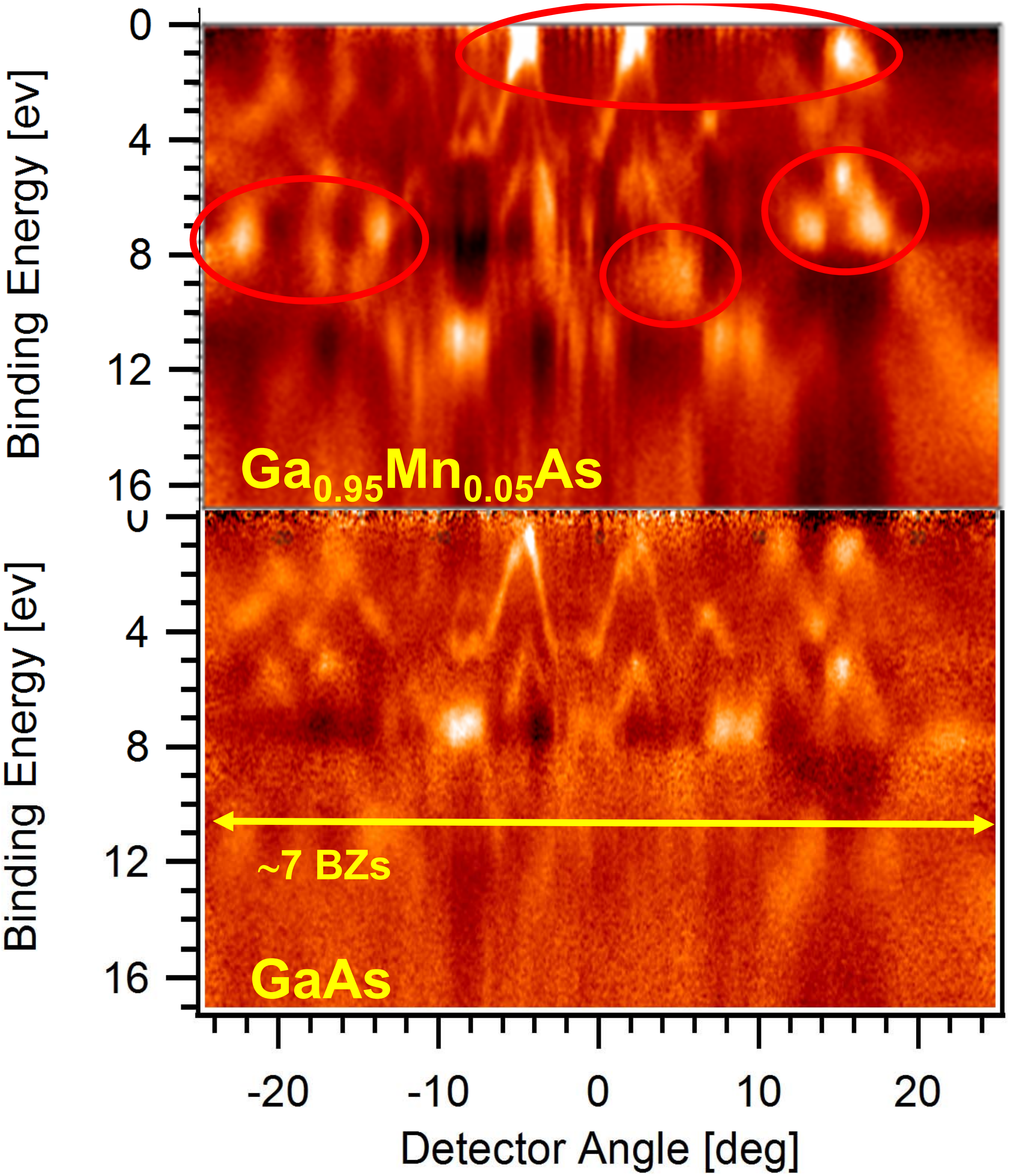

Nemšák, Lee,…CSF, samples H. Ohno, TBP

Varying photon energy: 3D band mapping of a “2D” material VSe_2

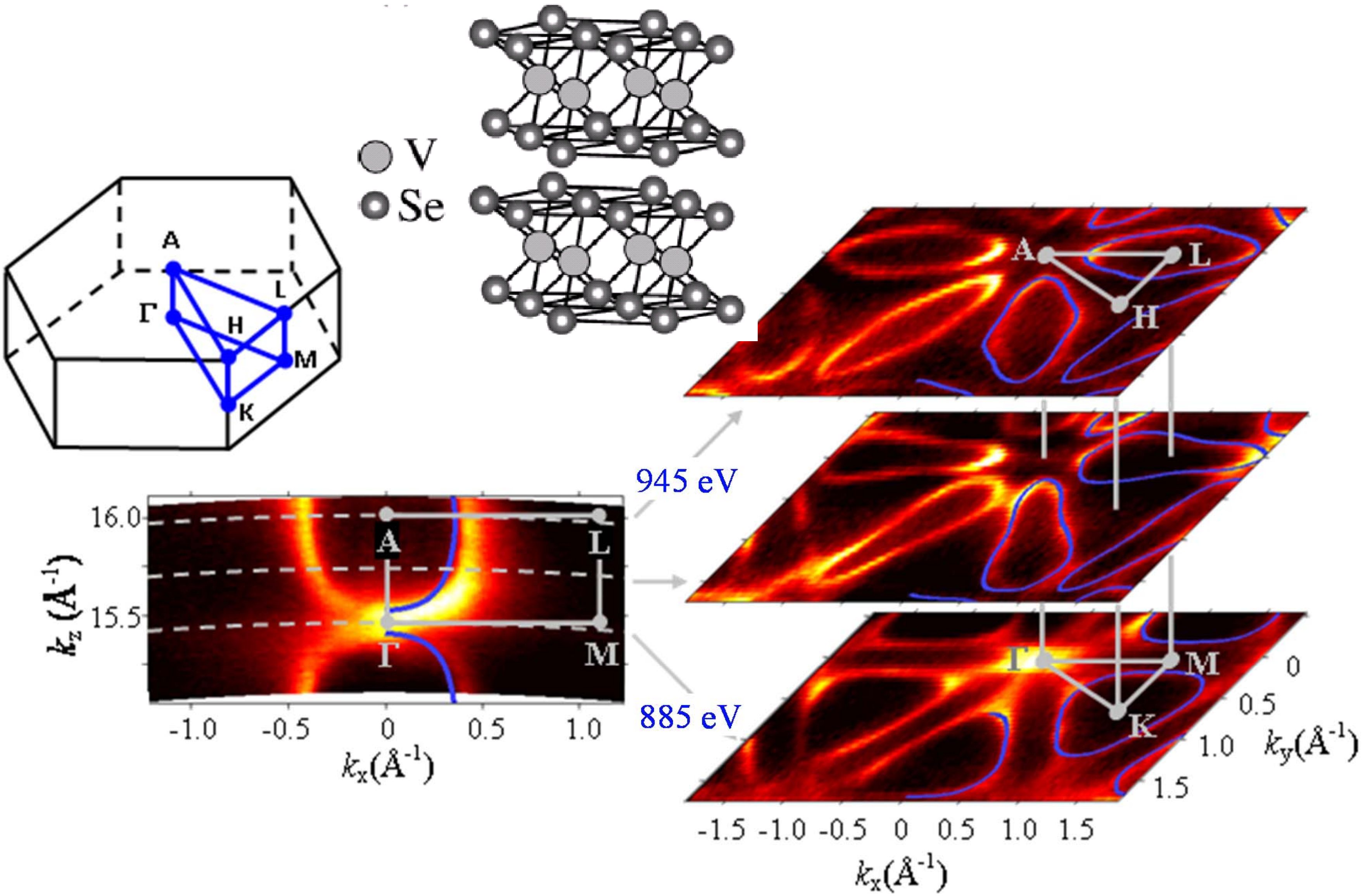

Strocov et al., PRL 109, 086401 (2012)

$\vec{k}_i = \vec{k}_f - \vec{k}_{h\nu} - \vec{g}_n$

Soft→Hard Angle-Resolved Photoemission: Basic Considerations

- + Deeper probing: "bulk" electronic structure, buried layers and interfaces, less surface sensitive
- + Free-electron final state: good approximation

$$E_f\,(\vec{k}_f\,) \approx \hbar^2 k_f^2\,/2m_e$$

- + Less $k_\perp$ broadening: $\Delta k_\perp \approx 1/\Lambda_e$*(inelastic)*
- + 3D band mapping: possible with photon energy variation
- + Resonant excitation: enhance a given atom's contribution, move standing wave in sample
- + Standing-wave excitation: possible, multilayers, epi-, single crystal- systems
- + Core-level spectra: provide complementary information on charge states, structure via XPD
- - Phonon smearing: need cryocooling, DW factor as criterion

$$DW\;(T) \approx\; exp[-g_n^2 \left\langle u^2\;(T)\right\rangle]$$

- - Angular resolution: need higher for $\Delta k_{||}$ resolution
- - Non-dipole effects: allowance for photon momentum, but easy

$$\vec{k}_i = \vec{k}_f - \vec{k}_{h\nu} - \vec{g}_n$$

- - Recoil effects: shift and smear energies

$$E_{recoil} \approx \frac{\hbar^2 k_f^2}{2M} \approx 5.5\times10^{-4}\left[\frac{E_{kin}\,(eV\,)}{M\,(amu\,)}\right]$$

CSF, Synch.Rad. News. 25, 26 (2012); V. Strocov et al., Appl. Phys. Lett. 101, 242103 (2012)

Standing Wave Behavior During a Rocking Curve or Photon-Energy Scan

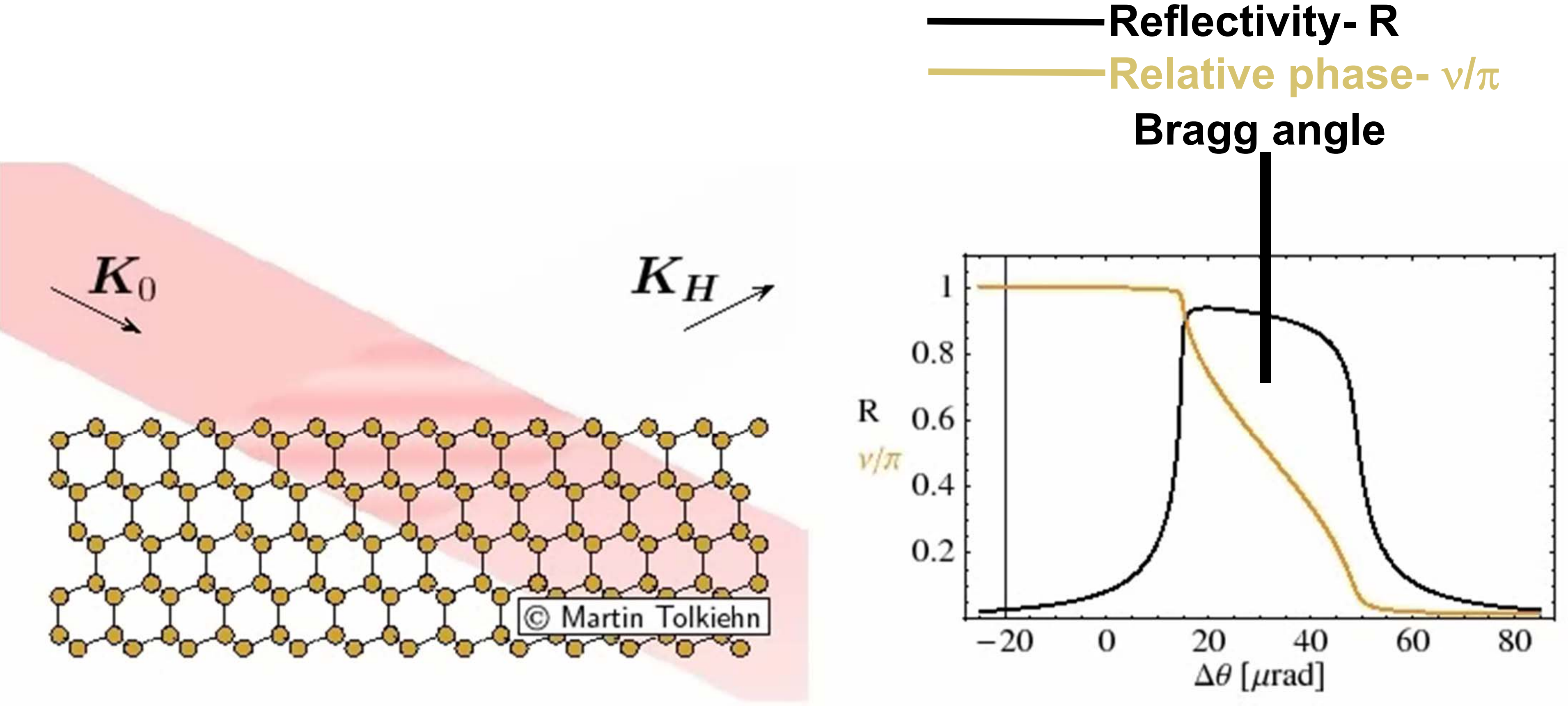

Reflectivity- R

Relative phase- ν/π

Bragg angle

+Same general forms if photon energy is scanned

With thanks to Martin Tolkiehn, Dimitri Novikov, DESY

Form of rocking curve is unique to position of emitter

Intensity vs
atomic position

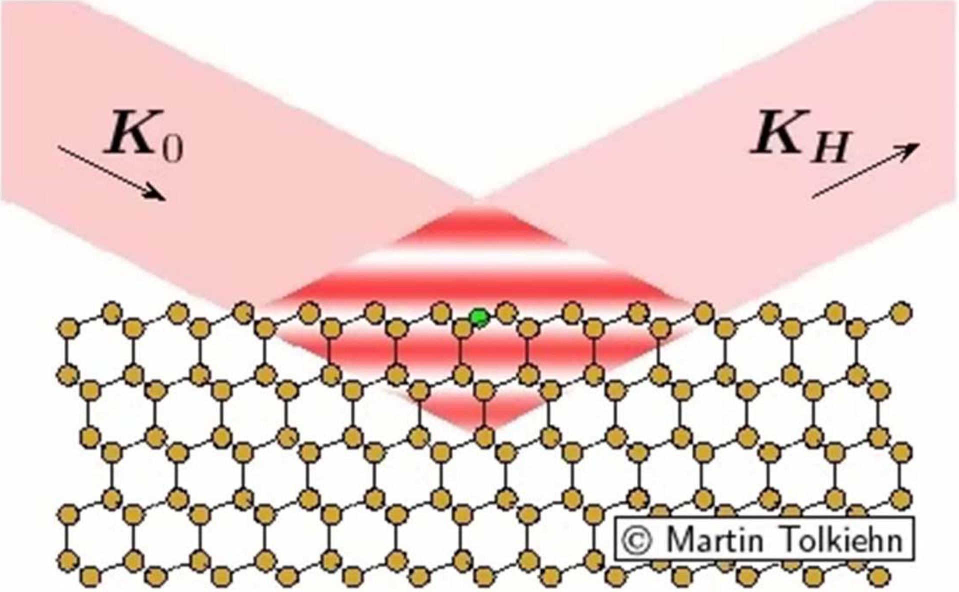

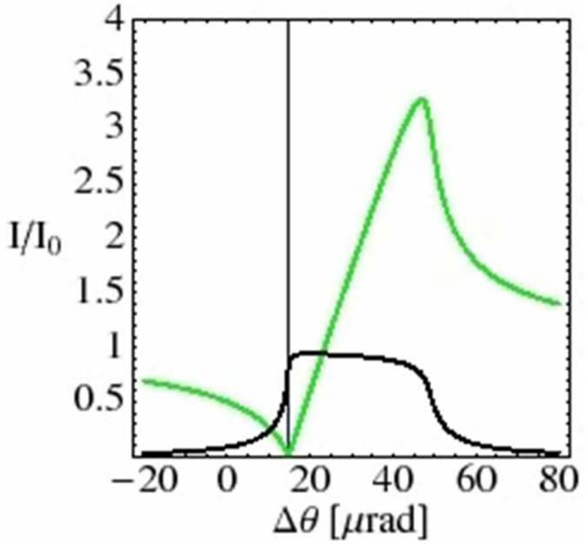

X-ray optical effects in photoelectron or x-ray emission from a multilayer structure

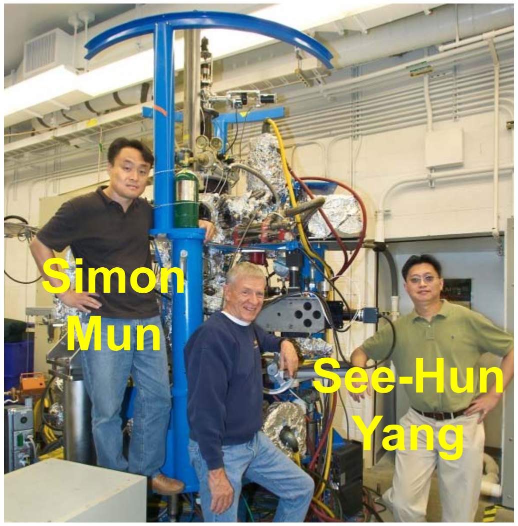

"Depth-resolved photoemission spectroscopy from surface and buried layers with soft X-ray standing waves", S.-H. Yang , B.S. Mun, A.W. Kay S.-K. Kim, J.B. Kortright, J.H. Underwood, Z. Hussain, C.S. Fadley, Surf. Sci. 461, L557 (2000).

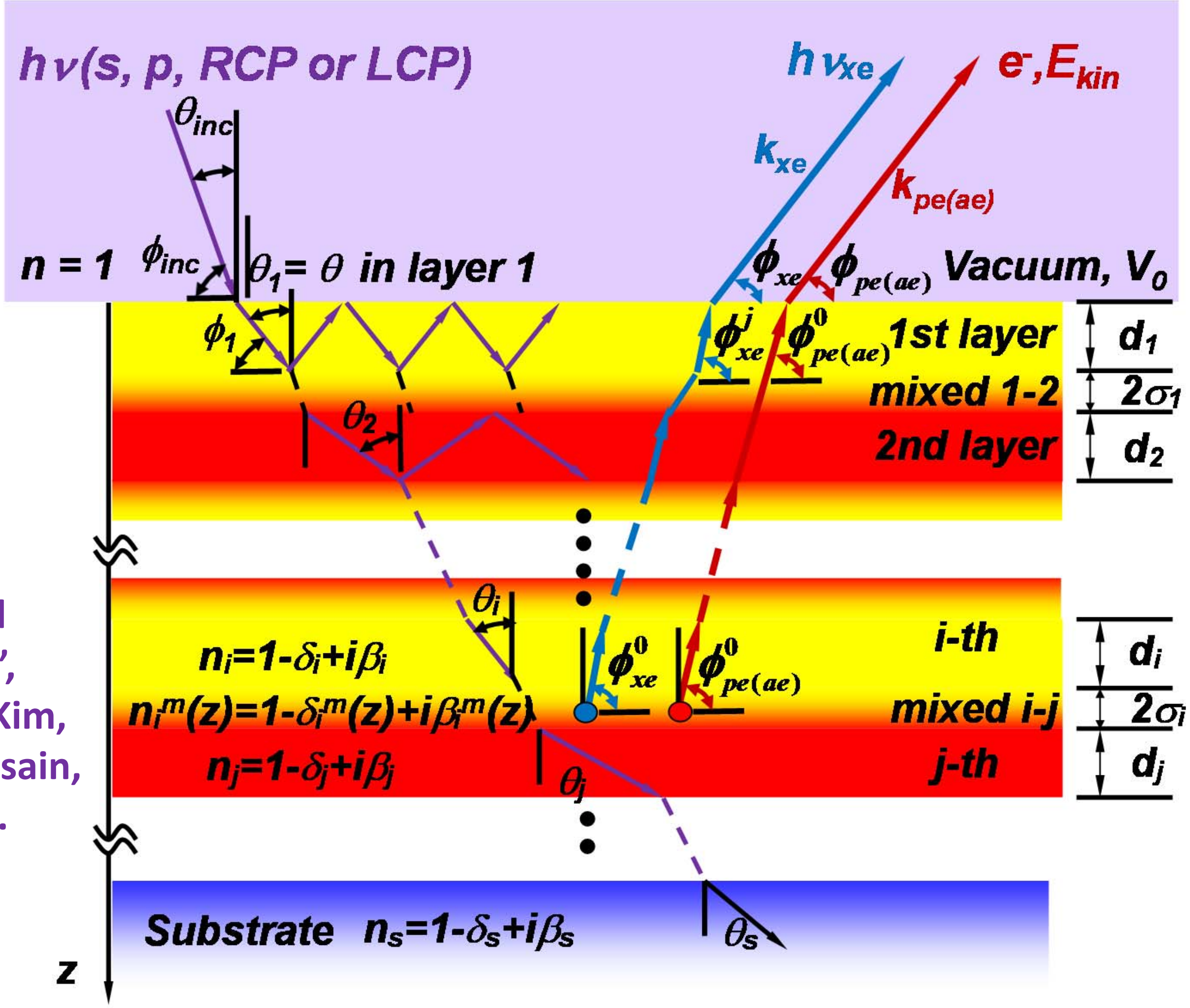

"Making use of x-ray optical effects in photoelectron-, Auger electron-, and x-ray emission spectroscopies: total reflection, standing-wave excitation and resonant effects", S.-H. Yang et al., J. Appl. Phys. 113, 073513 (2013); downloadable Yang XRO software package: https://sites.google.com/a/lbl.gov/yxro/home

X-ray optical effects in hard x-ray reflectivity from a multilayer structure

$h\nu$ = 5.9 keV

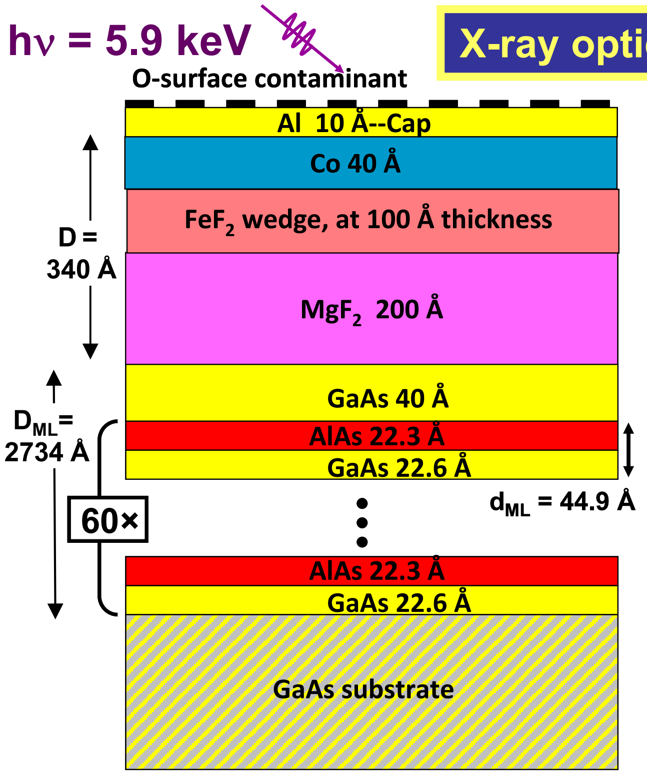

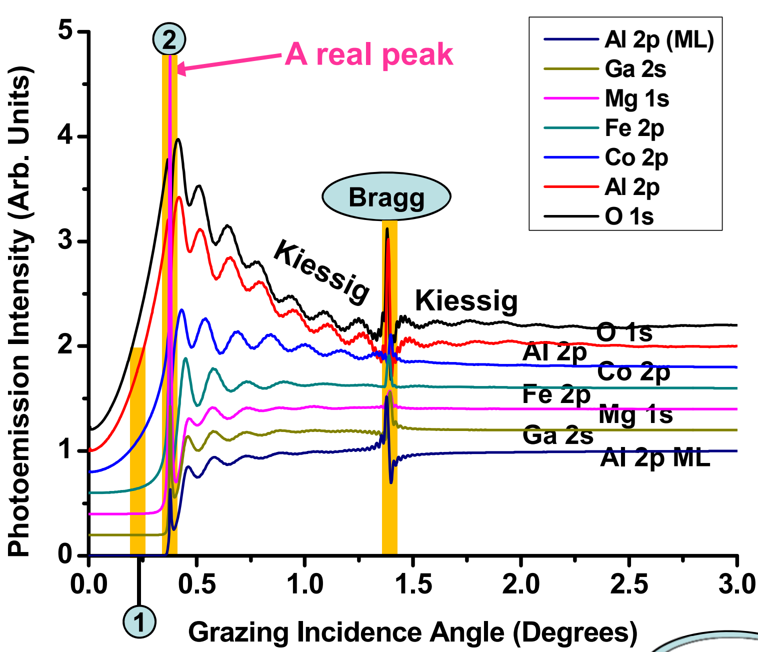

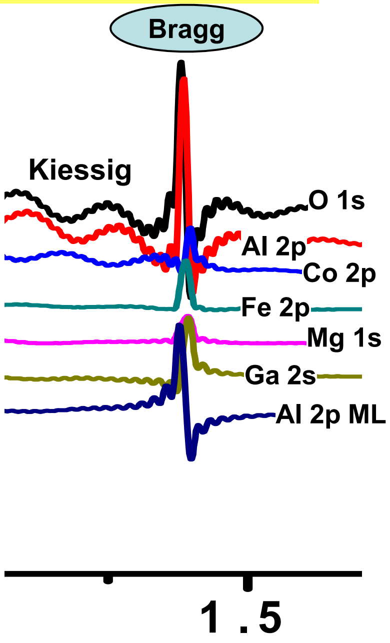

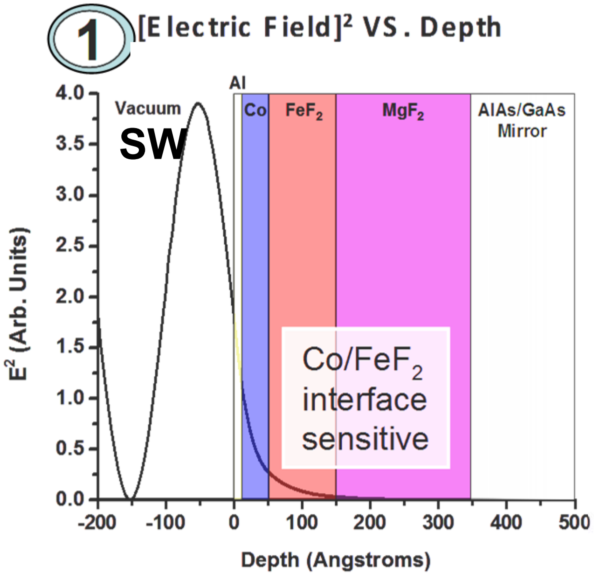

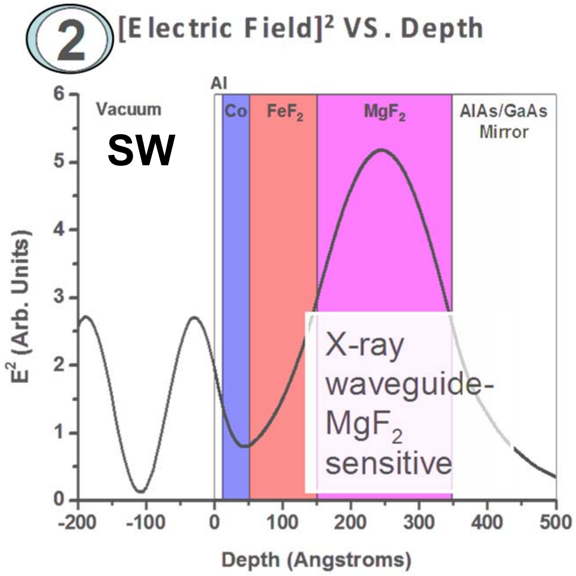

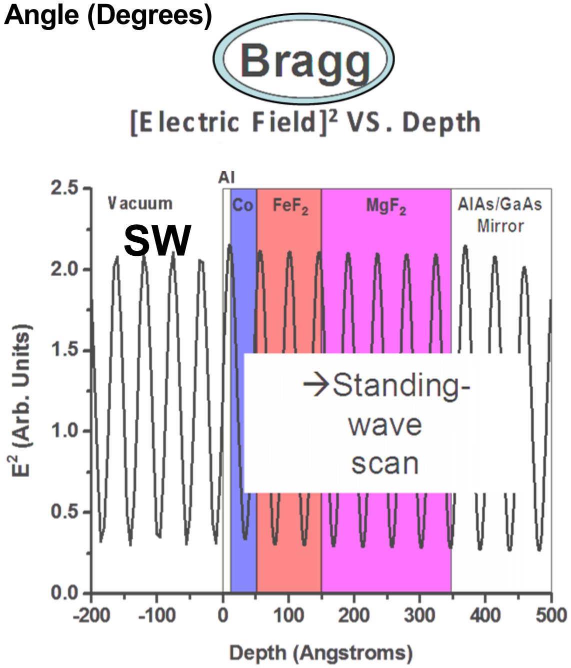

A.X. Gray, in C.F., J. Electron Spectrosc. 178–179, 2 (2010); S.-H. Yang et al., J. Appl. Phys. 113, 073513 (2013)

Depth-resolved composition of the $BiFeO_3$/(Ca,Ce)MnO_3 interface (Ferroelectric/Mott insulator)

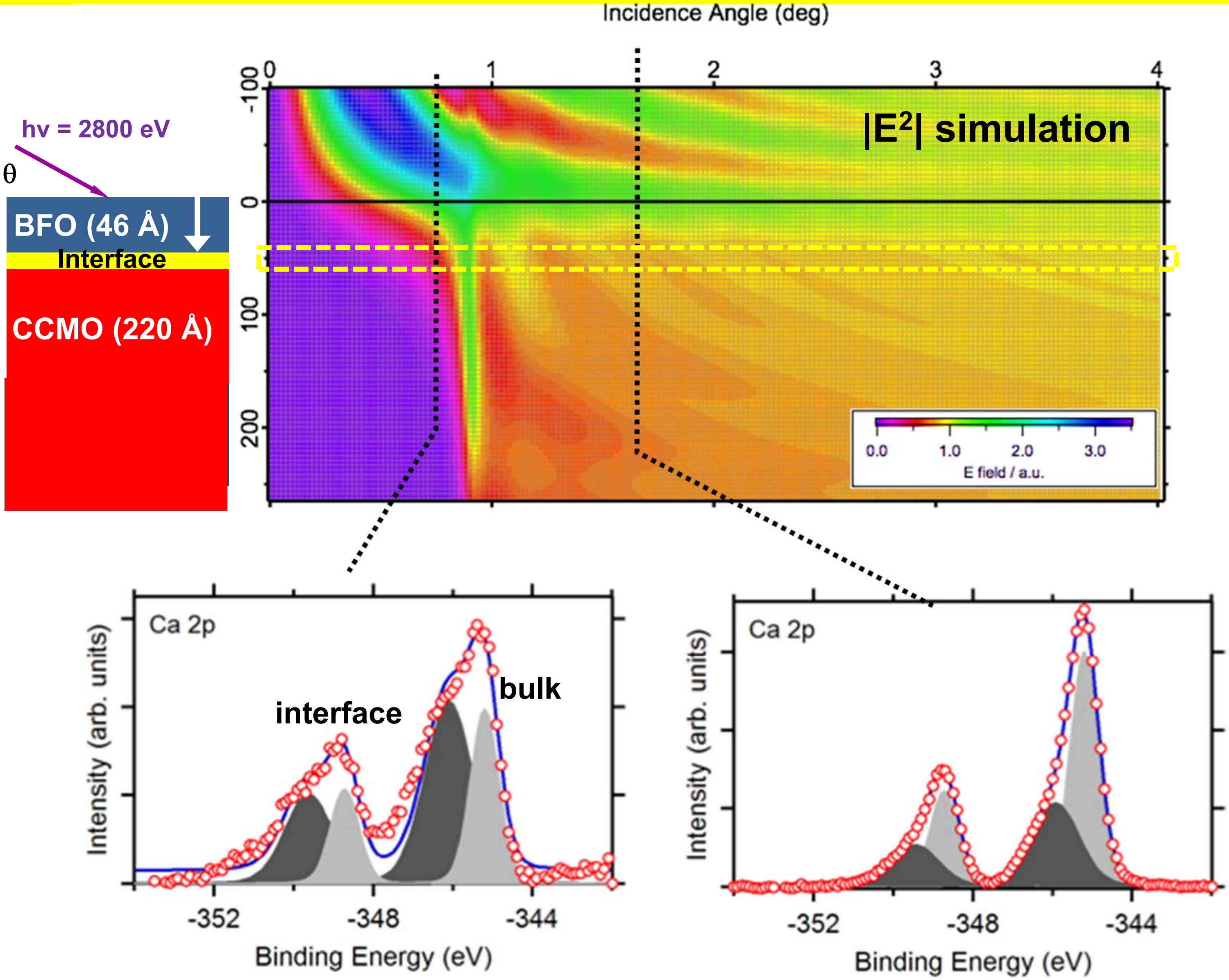

ALS, Galaxies

Rault, Rueff, Bibes et al.

Depth-resolved composition of the $BiFeO_3/(Ca,Ce)MnO_3$ interface (Ferroelectric/Mott insulator)

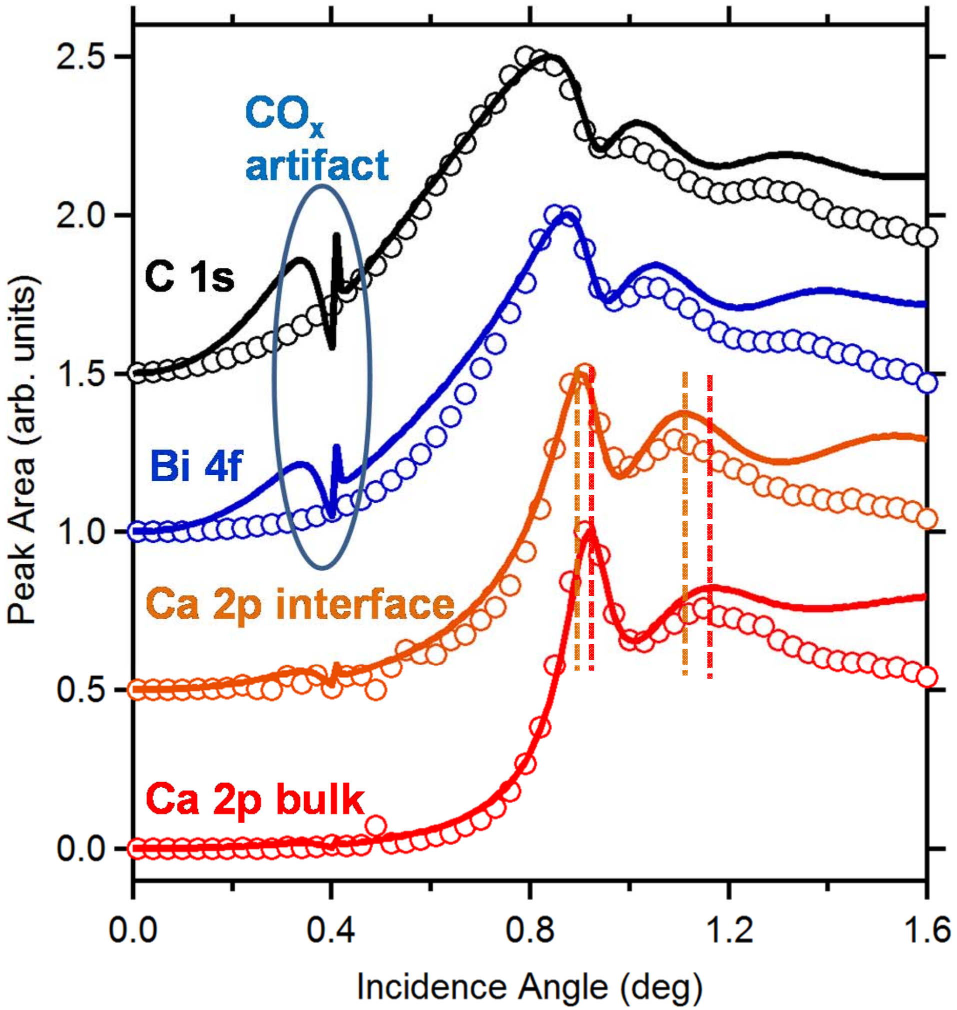

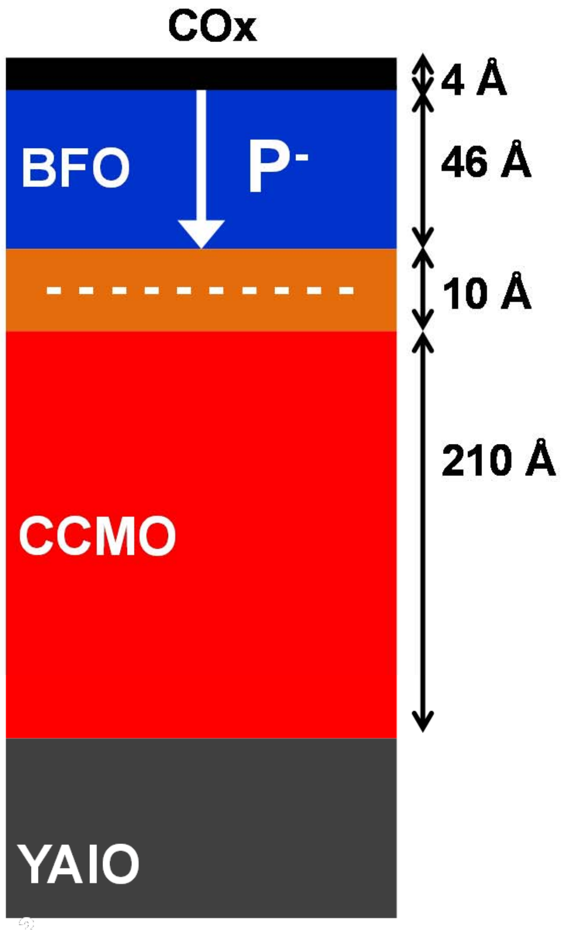

P-induced interface layer in CCMO

Rault, Rueff, Bibes et al.

Multilayer GTO/STO

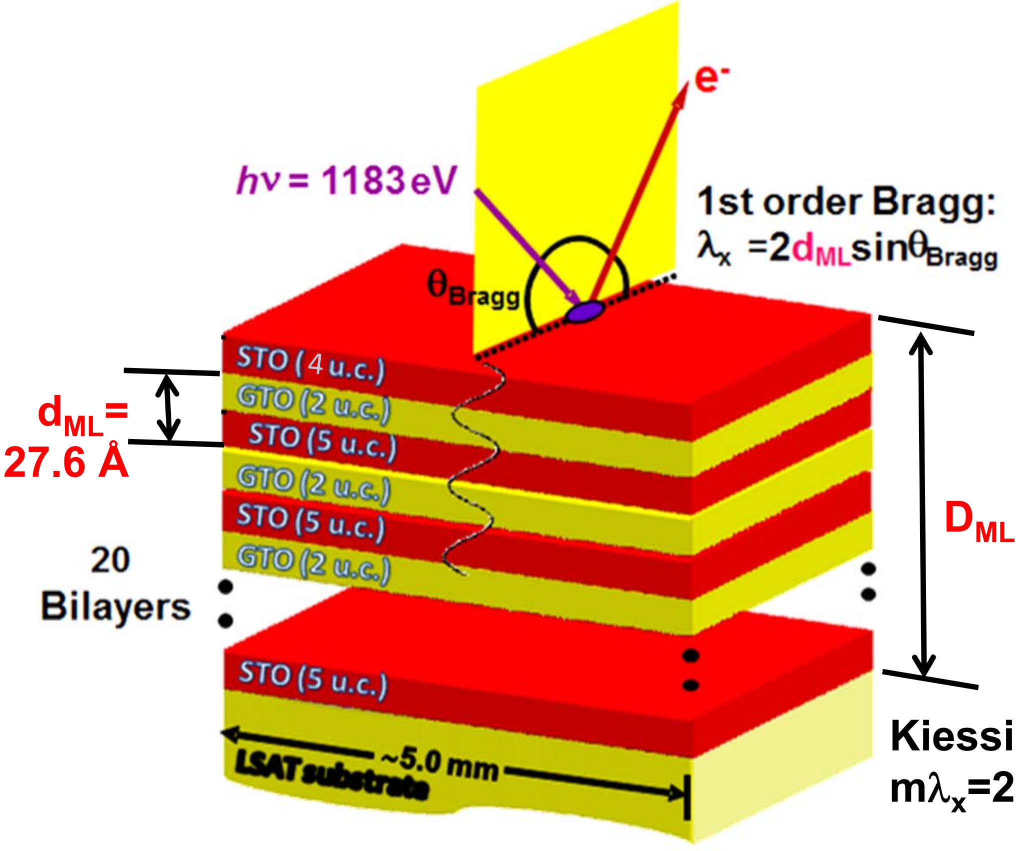

1st order Bragg: $\lambda_x = 2d_{ML}\sin\theta_{Bragg}$

Kiessig fringes: $m\lambda_x = 2D_{ML}\sin\theta_{inc}$

4 u.c. STO/[2 u.c. GTO/5 u.c. STO]$_{20}$
STO: c = 3.934 Å; GTO: c = 3.941 Å

Standing-Wave Excited Photoemission

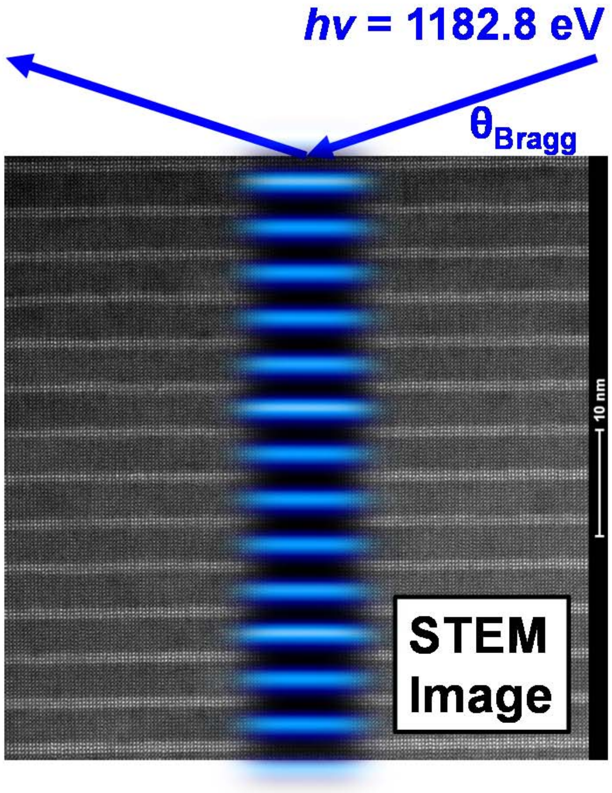

P. Moetakef, S. Stemmer,
UCSB

Resonant effects: $SrTiO_3/GdTiO_3$ multilayer
Sweeping the photon energy through the Gd M_5 resonance

Index of refraction: $n = 1 - \delta - i\beta$

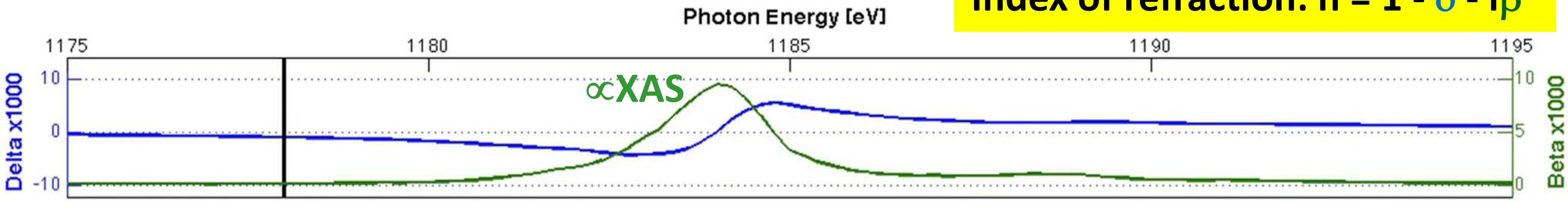

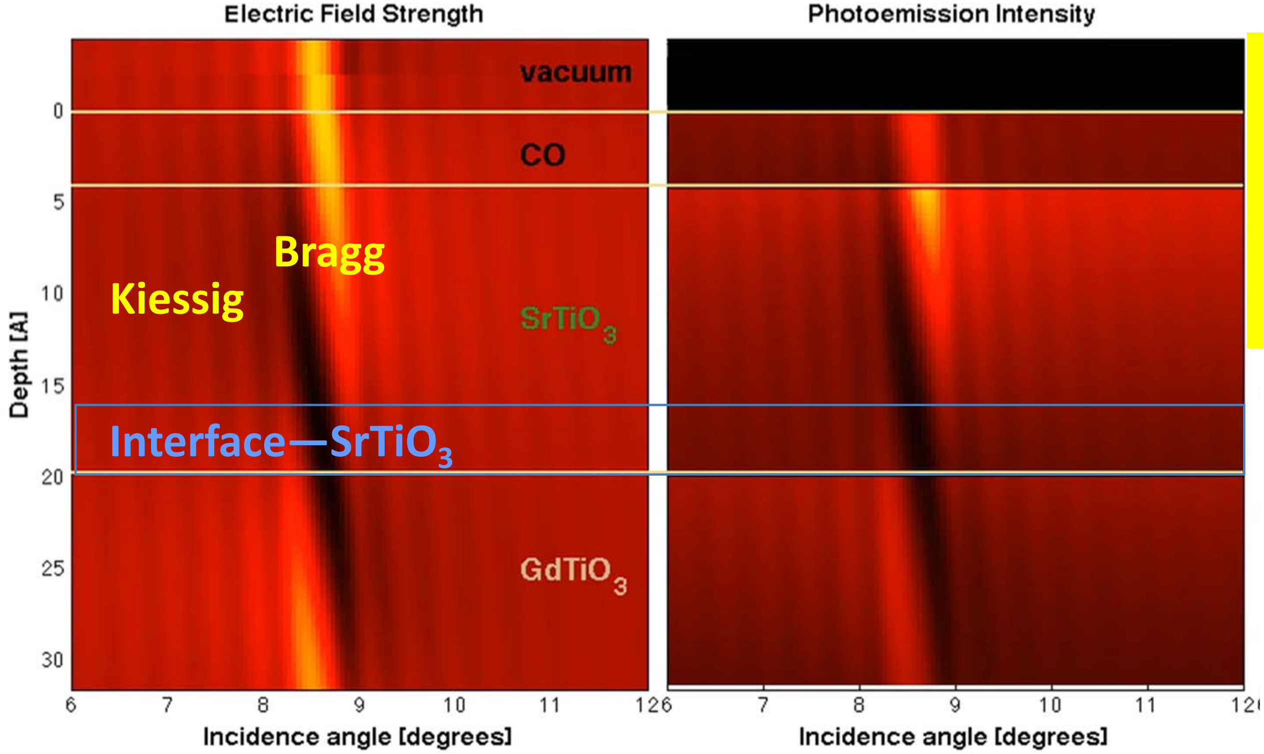

Electric field intensity, $|E^2|$
and Layer-resolved
photoemission intensity
versus Depth
and Incidence Angle

Nemšák, Palsson
et al. TBP

Going below and above an edge: A new trick to focus better on buried interfaces →
Observing a 2D electron gas at the STO/GTO interface

Photoemission with soft and hard x-rays: Some future perspectives

Chuck Fadley
Dept. of Physics, UC Davis
Materials Sciences Division
Lawrence Berkeley National Laboratory
Soleil Synchrotron

Supported by:
DOE: LBNL Materials Sciences Division
"Nanoscale Magnetic Materials"
ARO-Multi-University Research Initiative:
"Emergent Phenomena at Mott Oxide Interfaces"
Peter Grünberg Institute, PGI 6, Jülich Research Center
LABEX-PALM-APTCOM Project, Triangle de Physique, Paris

Soleil seminars: 21 July, 15 September, 22 September, 2014

Photoemission from complex materials, heterostructures, and interfaces

Three ways to address the limitations of traditional photoemission:

- **Use of harder x-ray excitation (SXPS→2 keV, HXPS, HAXPES→10 keV) for deeper probing: core levels and valence DOSs, incl. soft and hard x-ray ARPES**

- **Use of soft and hard x-ray standing waves, total reflection, other x-ray optical effects, resonant excitation, to selectively look below the surface, at buried interfaces, including ARPES**

- **Use of differentially-pumped systems to provide multi-Torr ambient pressure photoemission, more real-world conditions for studying surface chemical processes, catalysis, electrochemistry**

Three ways to scan a standing wave formed in reflection from single-crystal Bragg planes, or a multilayer mirror

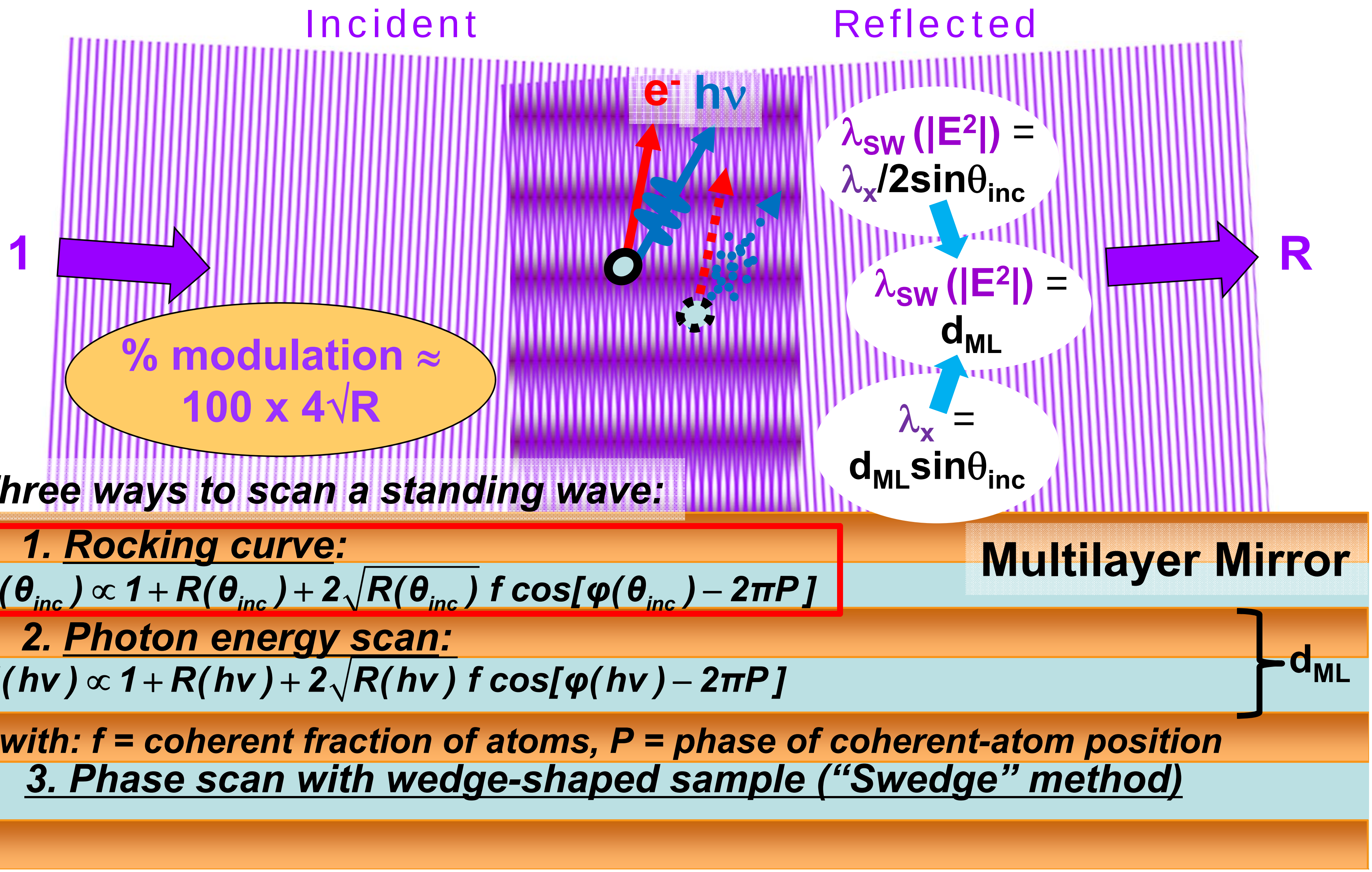

$\lambda_{SW}(|E^2|) = \lambda_x/2\sin\theta_{inc}$

$\lambda_{SW}(|E^2|) = d_{ML}$

$\lambda_x = d_{ML}\sin\theta_{inc}$

% modulation ≈ 100 x 4√R

Three ways to scan a standing wave:

1. ***Rocking curve:***

$$I(\theta_{inc}) \propto 1 + R(\theta_{inc}) + 2\sqrt{R(\theta_{inc})}\, f \cos[\varphi(\theta_{inc}) - 2\pi P]$$

2. ***Photon energy scan:***

$$I(h\nu) \propto 1 + R(h\nu) + 2\sqrt{R(h\nu)}\, f \cos[\varphi(h\nu) - 2\pi P]$$

with: f = coherent fraction of atoms, P = phase of coherent-atom position

3. ***Phase scan with wedge-shaped sample ("Swedge" method)***

Standing Wave Behavior During a Rocking Curve or Photon-Energy Scan

Reflectivity- R

Relative phase- ν/π

Bragg angle

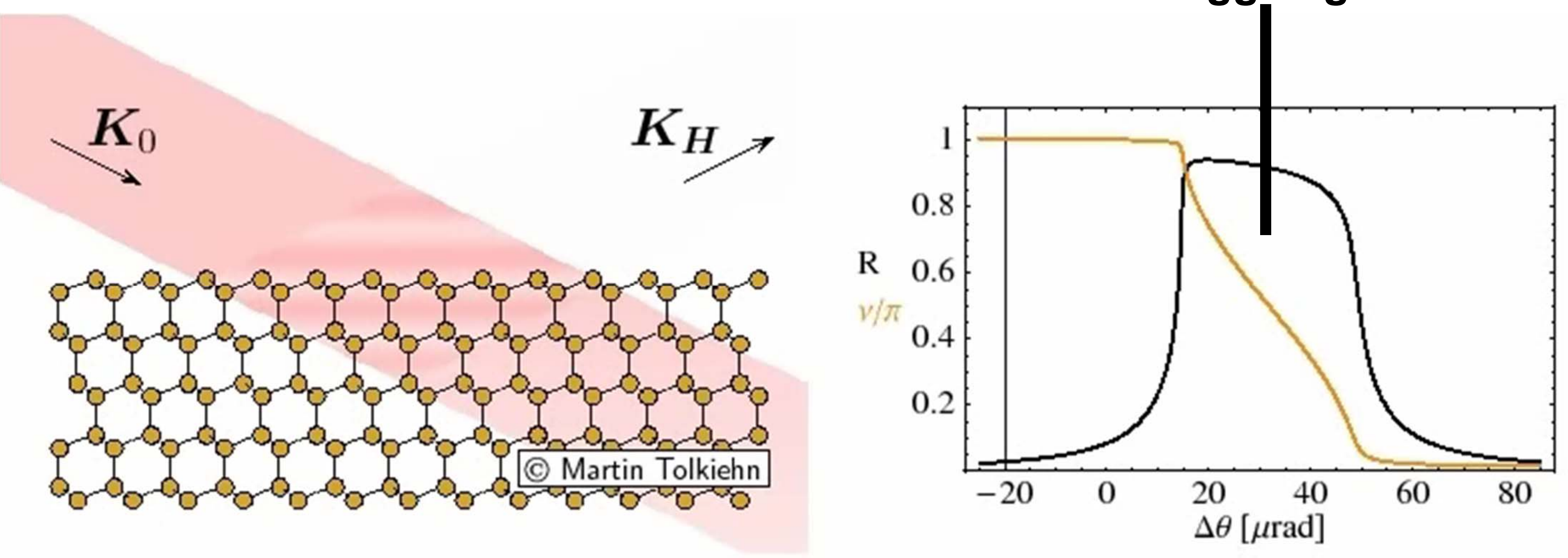

+Same general forms if photon energy is scanned

With thanks to Martin Tolkiehn, Dimitri Novikov, DESY

Form of rocking curve is unique to position of emitter

Intensity vs
atomic position

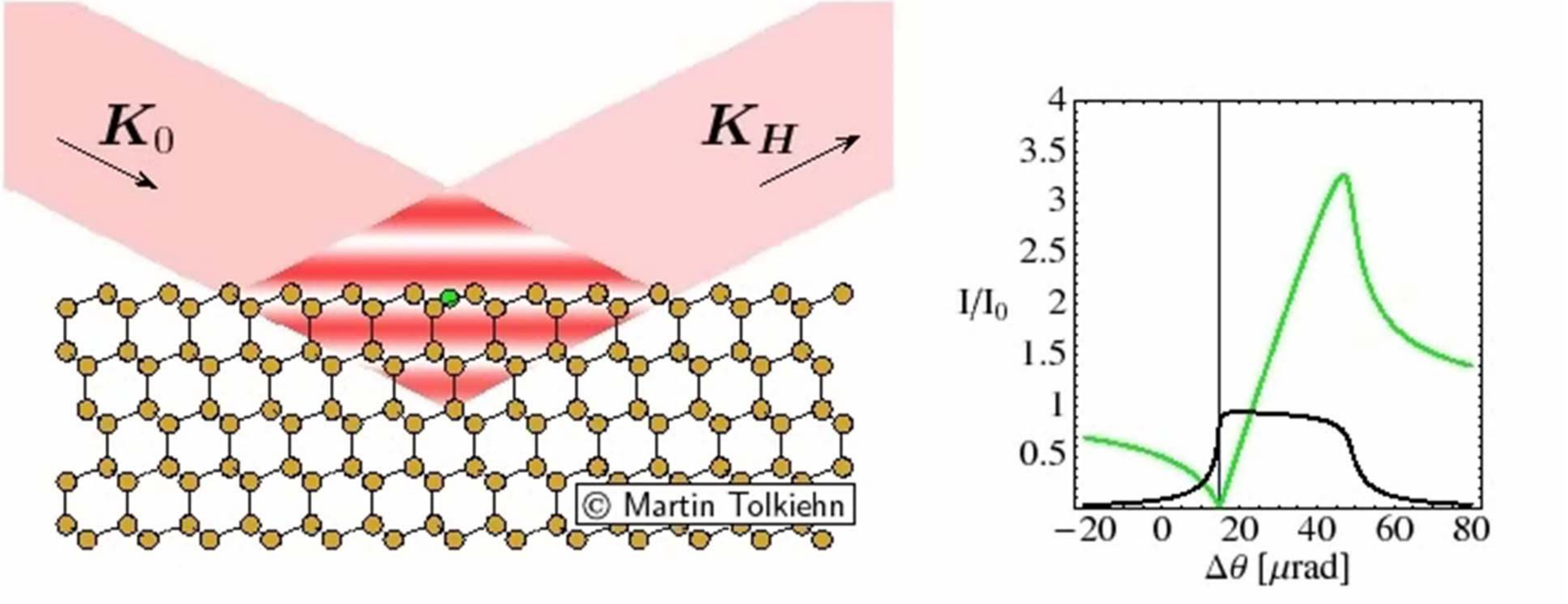

Standing wave/rocking curve analysis of an epitaxial $SrTiO_3/La_{0.67}Sr_{0.33}MnO_3$ interface: near-resonant soft x-ray excitation

The Advanced Light Source

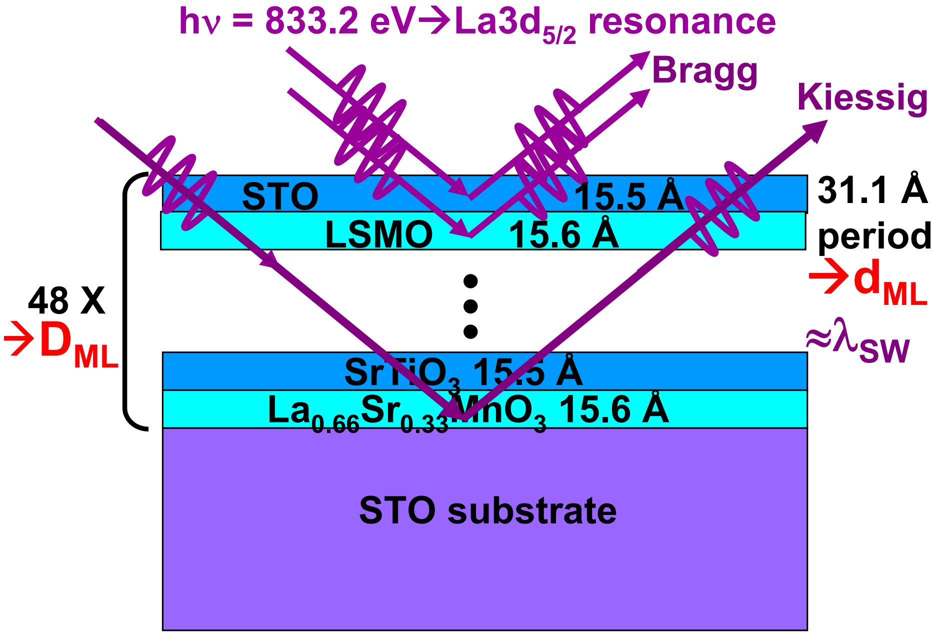

$$\lambda_x = 2d_{ML}\sin\theta_{Bragg}$$

$$m\lambda_x = 2D_{ML}\sin\theta_{Kiessig}$$

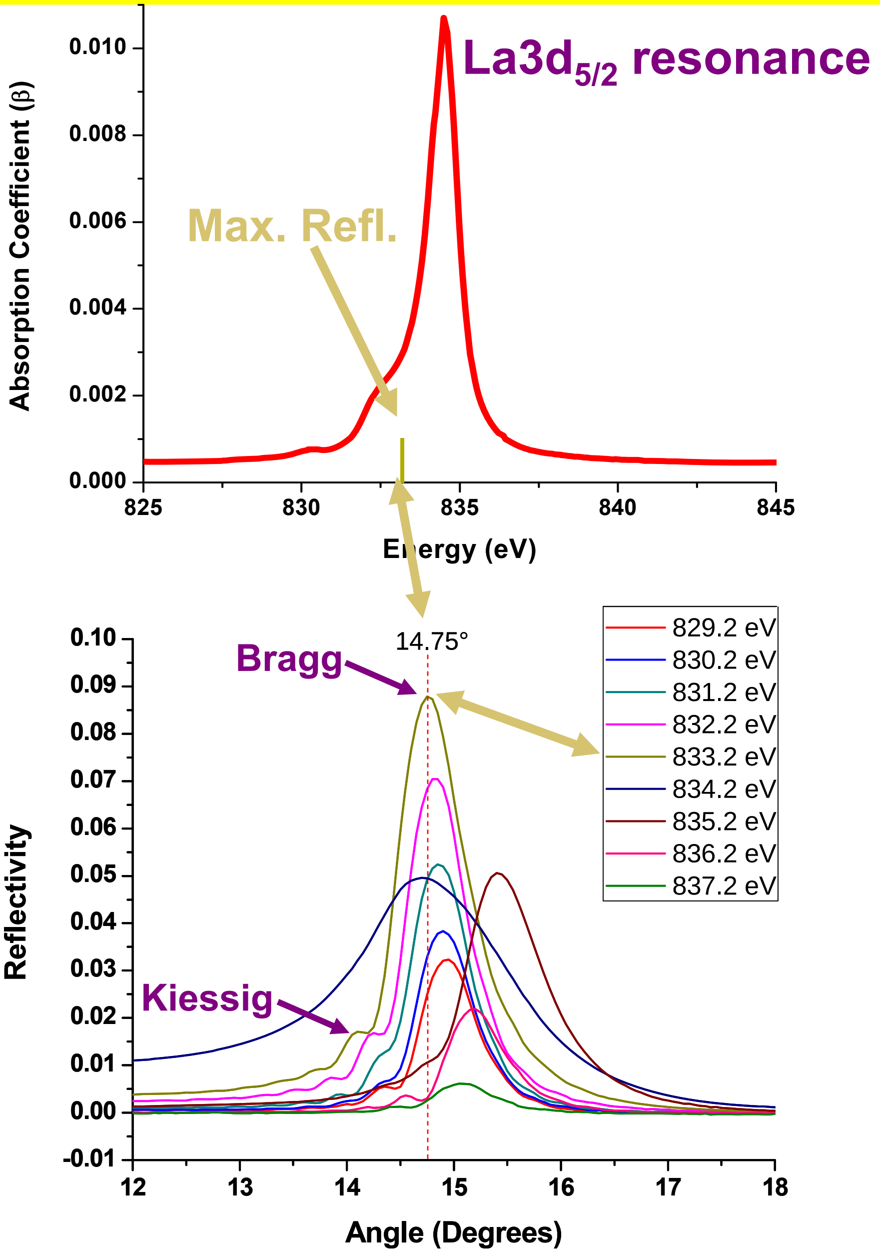

Gray et al., Phys. Rev. B 82, 205116 (2010);
Europhysics Letters 104, 17004 (2013)
Samples: Ramesh, Huijben

$SrTiO_3/La_{0.67}Sr_{0.33}MnO_3$ Multilayer

Analysis of Rocking Curves

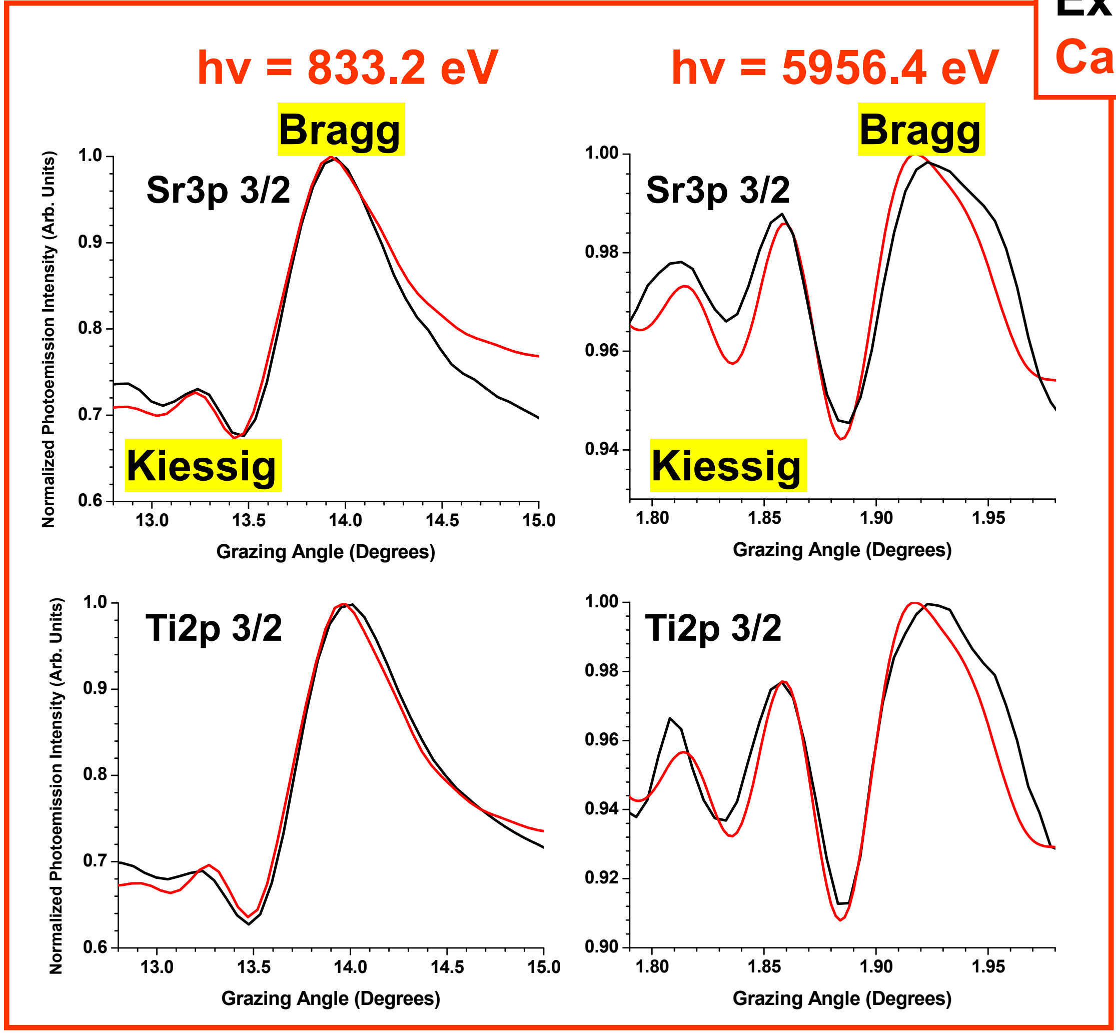

Exp.

Calc.

BEST FIT

Bilayer Thickness Gradient Profile

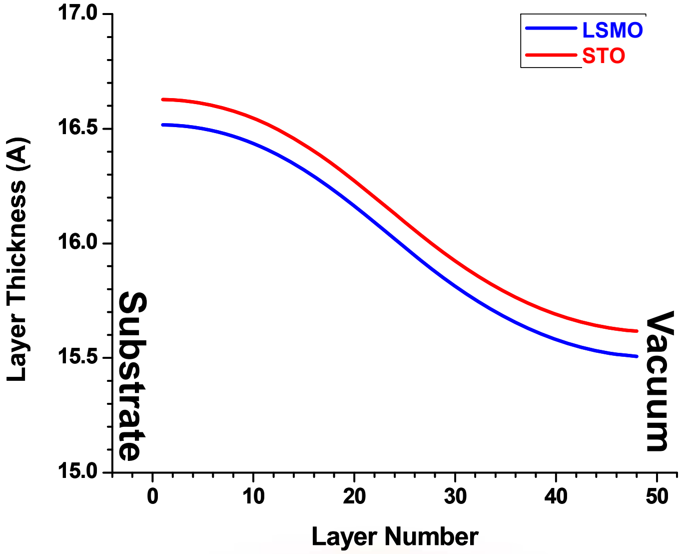

→Average multilayer d_{ML} changes by about -2 Å ≈ -6% from top to bottom

Gray et al., Phys. Rev. B 82, 205116 (2010)

Photoemission from complex materials, heterostructures, and interfaces

Three ways to address the limitations of traditional photoemission:

- **Use of harder x-ray excitation (SXPS→2 keV, HXPS, HAXPES→10 keV) for deeper probing: core levels and valence DOSs, incl. soft and hard x-ray ARPES**

- **Use of soft and hard x-ray standing waves, total reflection, other x-ray optical effects, resonant excitation, to selectively look below the surface, at buried interfaces, including ARPES**

- **Use of differentially-pumped systems to provide multi-Torr ambient pressure photoemission, more real-world conditions for studying surface chemical processes, catalysis, electrochemistry—previous seminar by Hendrik Bluhm**

Challenges for high-pressure photoemission: analyzer pressure and short electron mean free fath

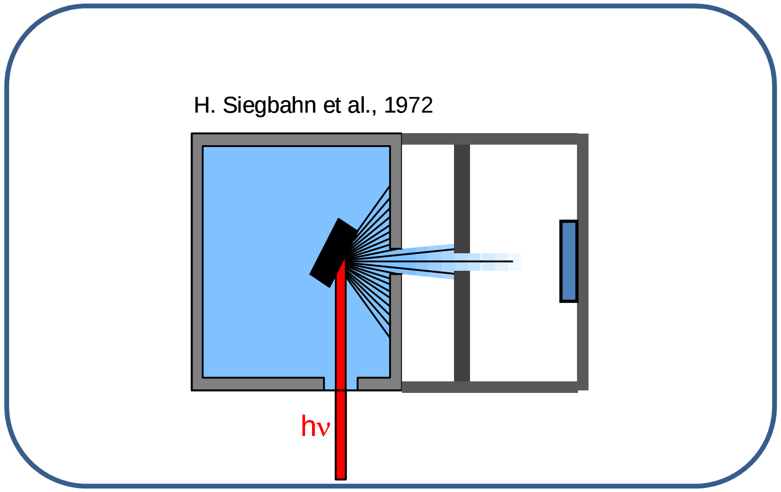

H. Siegbahn et al., 1972

Very low efficiency

IMFP: N_2 @ 500 eV

1 atm ~ 0.003 mm = 3 microns
20 torr ~ 0.1 mm = 100 microns
1 torr ~ 2 mm

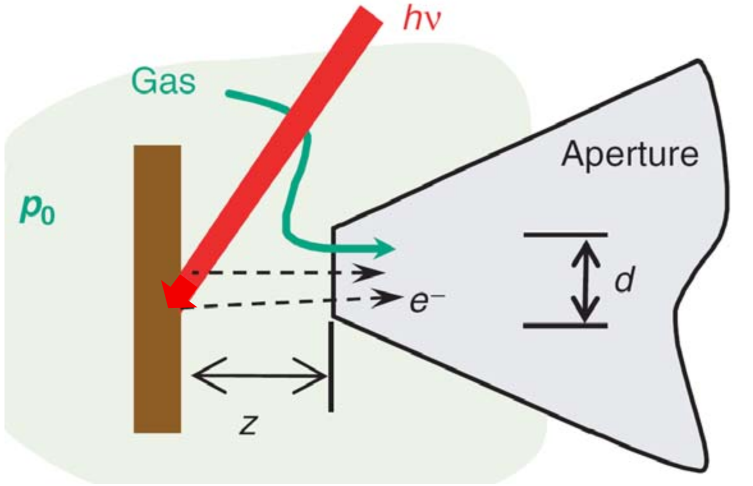

Smaller x-ray spot, z & d → Higher Pressure.

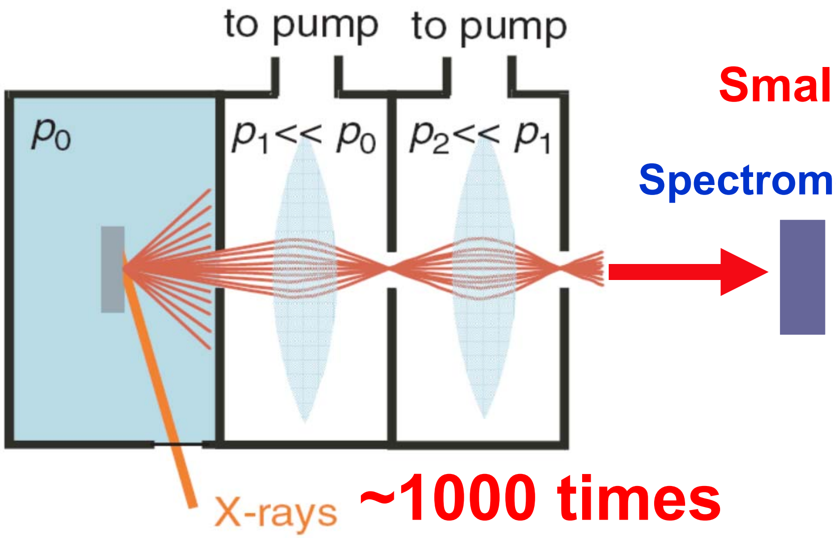

~1000 times

The first endstation at a SR facility (ALS, Beamlin 9.3.2):

- D.F. Ogletree, H. Bluhm, G. Lebedev, CSF, Z. Hussain, M. Salmeron, Rev. Sci. Instrum. 73 (2002) 3872.

Good review papers:

- M. Salmeron and R. Schlögl, Surf. Sci. Rep. 63, 169-199 (2008).
- A. Knop-Gericke et al., Adv. Catal. 52, 213-272 (2009).

From Zhi Liu, LBNL

Ambient Pressure XPS→HXPS Systems

1st Gen

2000: Differentially-pumped electrostatic transfer lens allows operation at p ~ 5 torr (equilibrium vapor pressure of water at 0 °C)

D.F. Ogletree, H. Bluhm, G. Lebedev, C.S. Fadley, Z. Hussain, M. Salmeron, Rev. Sci. Instrum. 73 (2002) 3872.

2nd Gen

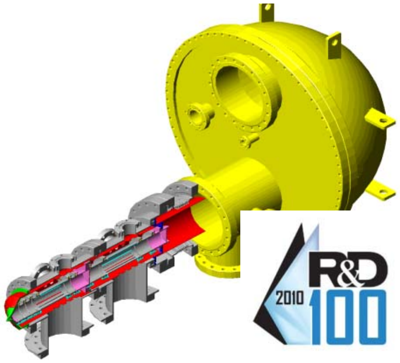

2005: The first commercial system from Specs. Installed at ALS and BESSY

3rd Gen

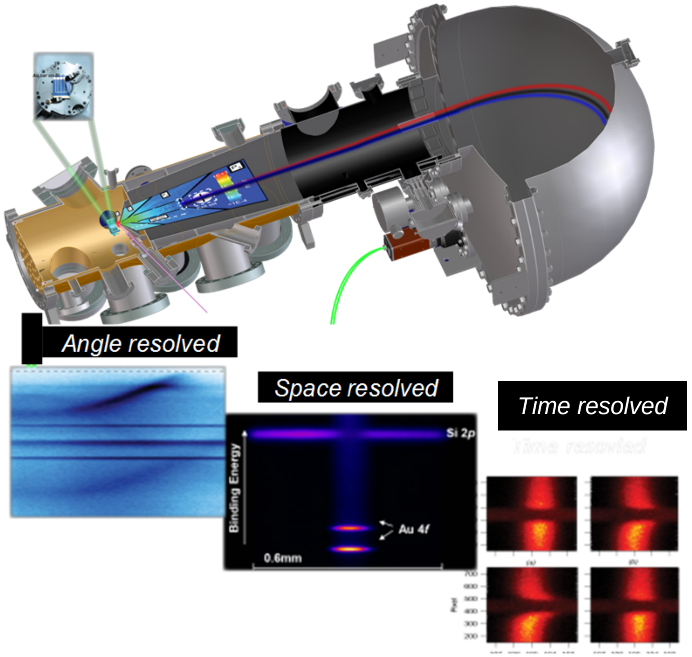

2009: Fast 2D detector and superior electron transmission from Scienta Hipp 4000 installed at ALS BL9.3.2.
New Specs at BL 11.0.2

M.E. Grass, P.G. Karlsson, F. Aksoy, M. Lundqvist, B. Wannberg, B.S. Mun, Z. Hussain, Z. Liu, Rev. Sci. Instrum. 81, 053106 (2010)

AP XPS/HXPS systems in use/ in commissioning or construction:
ALS, BESSY, Soleil, MAXLAB, SSRL, ALBA, NSLS, Photon Factory...
First hard x-ray endstation @ ALS BM, + soft/hard x-ray @ EMIL-BESSY
→100 Torr, even 1 atm (Nilsson, SSRL)

The NAP facility at TEMPO

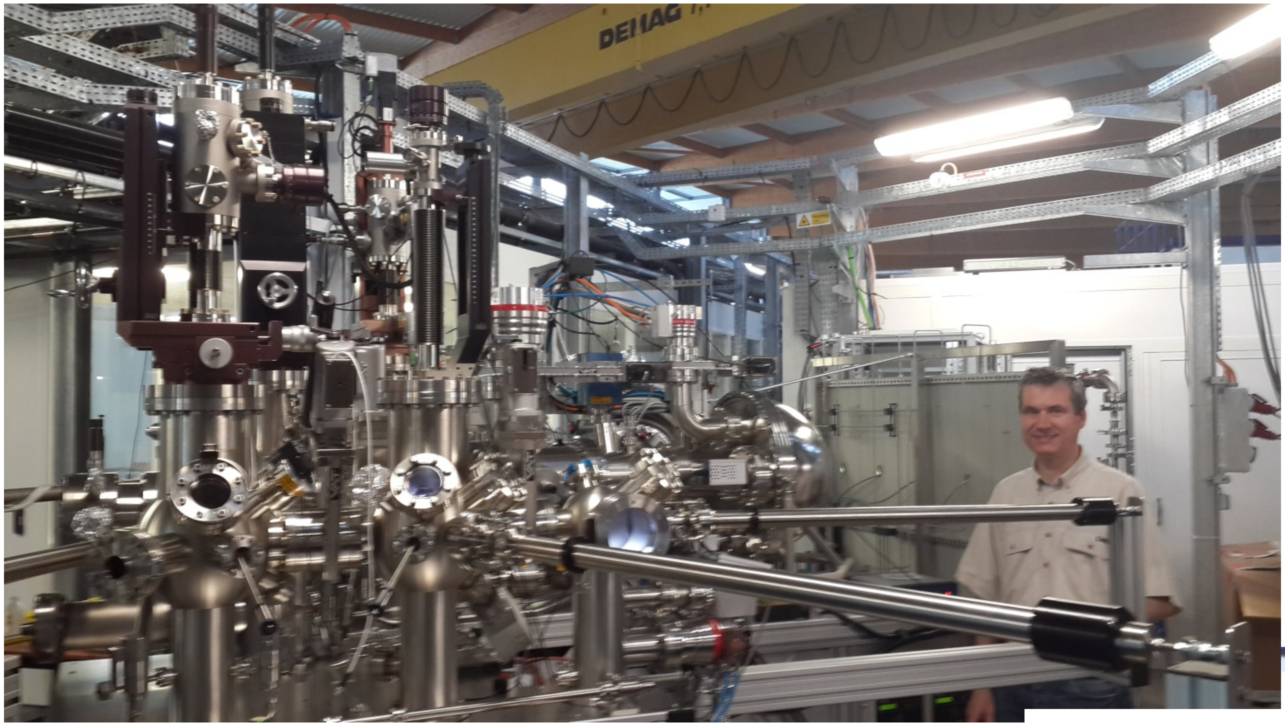

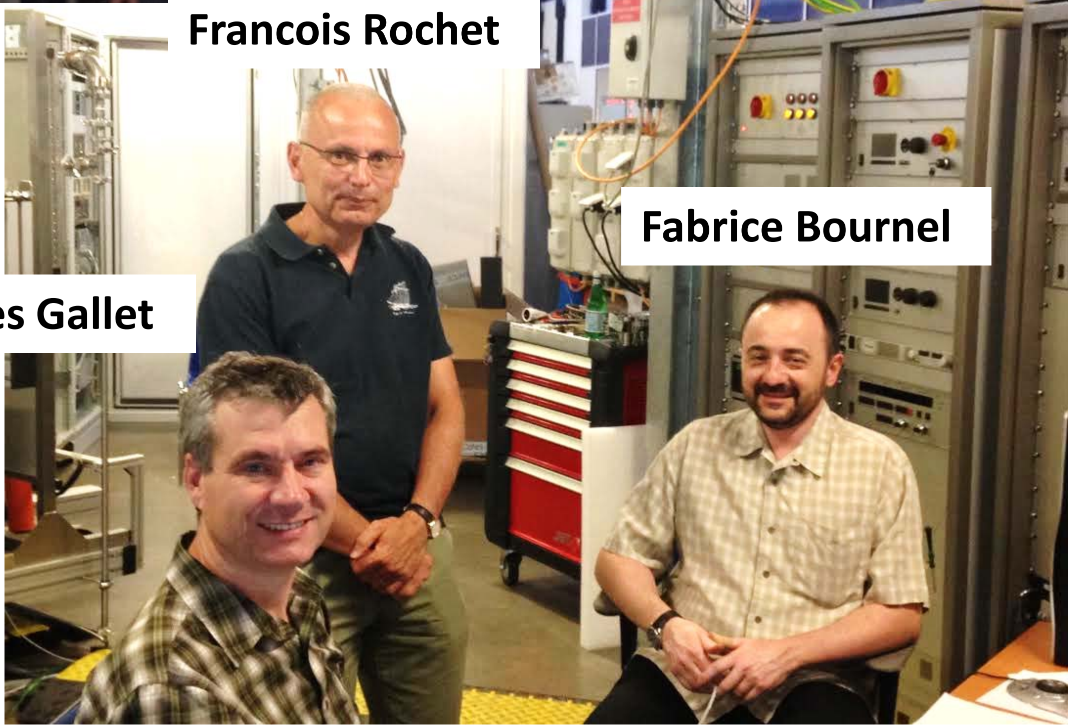

Francois Rochet

Fabrice Bournel

Jean-Jacques Gallet

Fausto Sirotti

Looking *in operando* at the solid-liquid interface of an electrode *The dip-stick method with hard x-rays→higher pressures*

20 Torr, Room Temperature: “Dipstick Method”

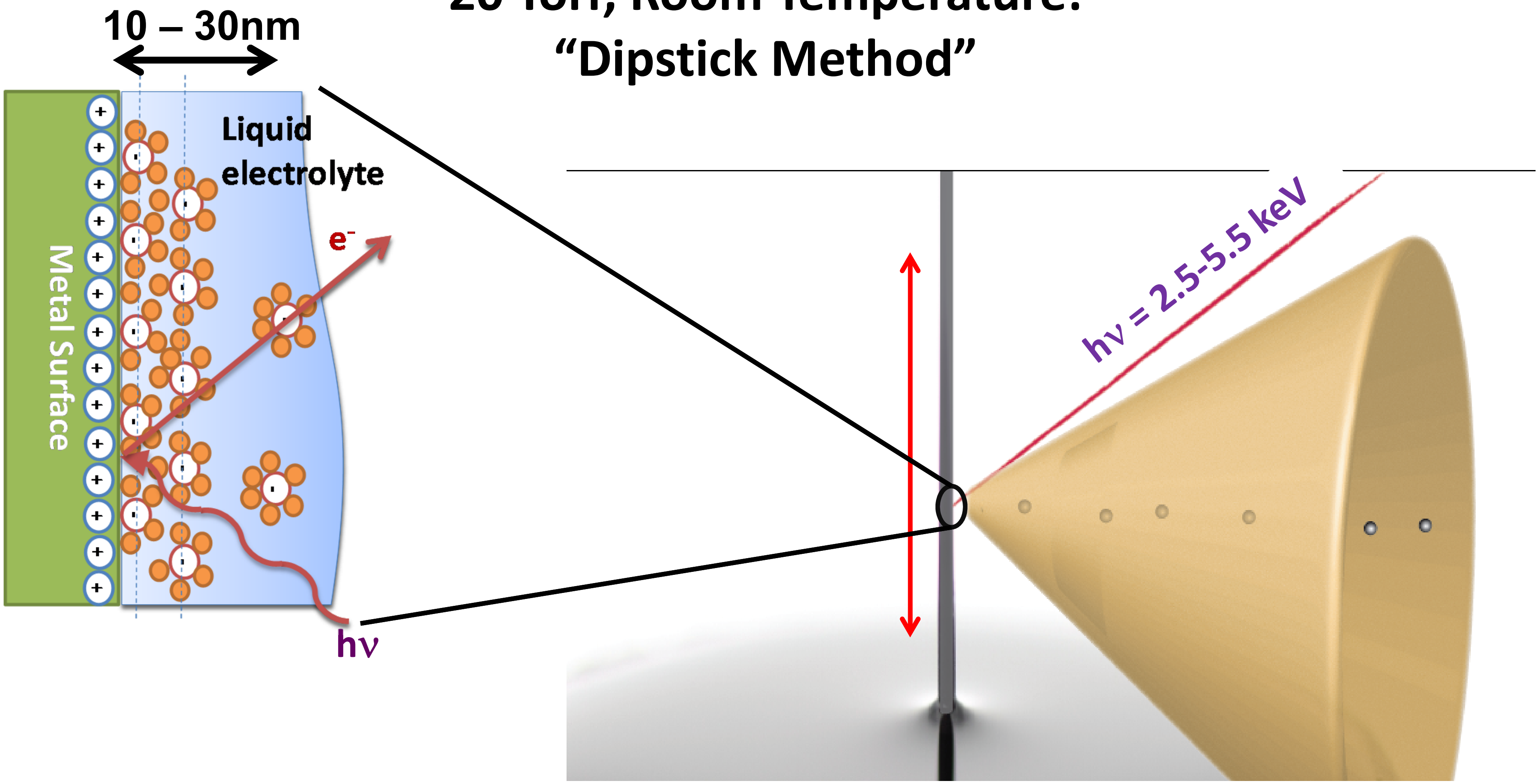

ALS

Axnanda, Crumlin, Mao, Rani, Chang, Shen, Stolte, Karlsson, Edwards, Lundqvist, Moberg, Ross, Husssain, Liu (ALS, to be submitted)

Looking *in operando* at the solid-liquid interface of an electrode *The dip-stick method with hard x-rays→higher pressures*

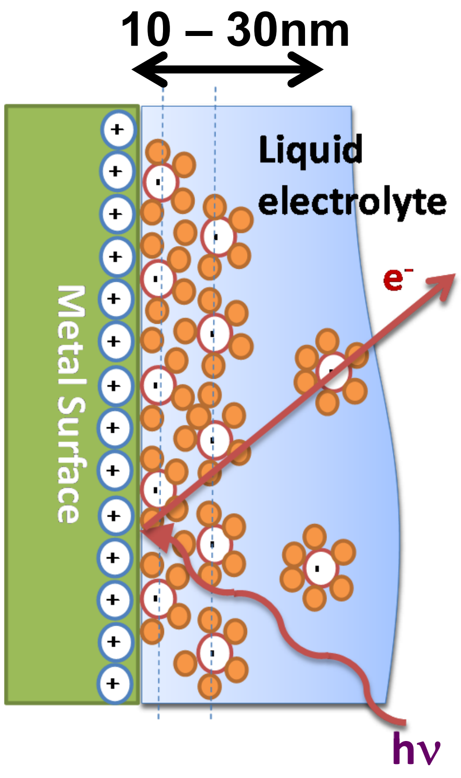

20 Torr, Room Temperature: "Dipstick Method"

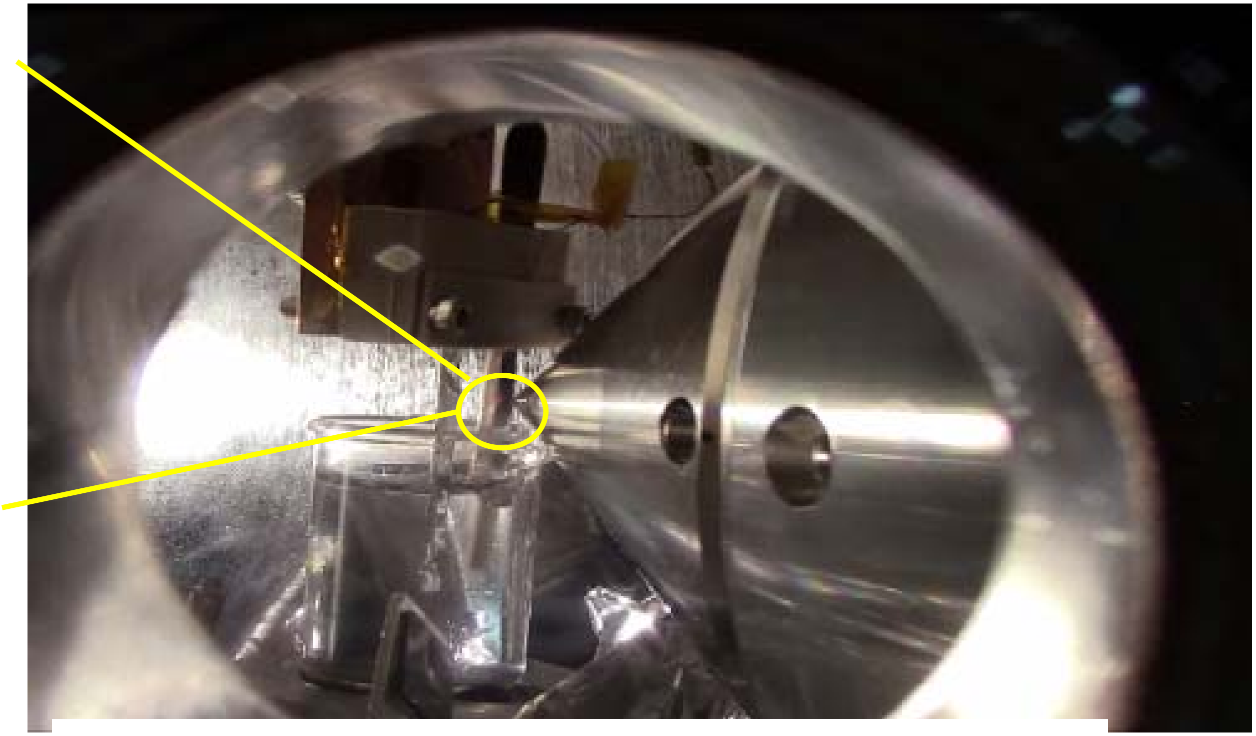

ALS

Axnanda, Crumlin, Mao, Rani, Chang, Shen, Stolte, Karlsson, Edwards, Lundqvist, Moberg, Ross, Husssain, Liu (ALS, to be submitted)

Soft →hard x-rays and standing waves: a few example studies

$SrTiO_3/La_{2/3}Sr_{1/3}MnO_3$-tunnel junction

Depth-resolved composition, dielectric properties, bonding, k-resolved electronic structure

$SrTiO_3/GdTiO_3$-2D electron gas

Depth-resolved composition, charge states, k-resolved electronic, structure

Fe/MgO-tunnel junction

Depth-resolved composition, chemical states, magnetization

$SrTiO_3$ and Ga(Mn)As

Single-crystal Bragg reflection→Projected densities of states

Fe_2O_3 reacting with NaOH, CsOH, and H_2O

Using standing wave XPS to probe the solid/gas and solid/liquid interface: some first ambient pressure results

Fe_2O_3 reacting with NaOH, CsOH, and H_2O

Using standing wave XPS to probe the solid/gas and solid/liquid interface: some first ambient pressure results

S. Nemšák, A. Shavorskiy, O. Karslioglu, I. Zegkinoglou, A. Rattanachata, C.S. Conlon, A. Keqi, P.K. Greene, E.C. Burks, K. Liu, F. Salmassi, E.M. Gullikson, S.-H. Yang, K. Liu, H. Bluhm, C.S.F., Nature Comm., to appear

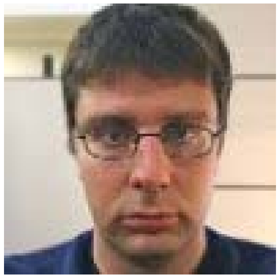

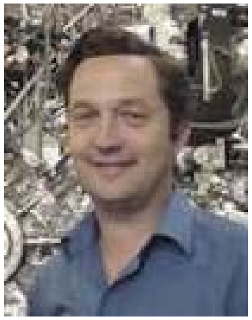

+Samples: Liu Group UCD

+Mirrors: CXRO LBNL

Standing-wave photoemission at the solid-liquid interface: some first experiments at ambient pressure

- Fe_2O_3 on Si/Mo multilayer mirror
- ~0.01M NaOH + ~0.01M CsOH, dried in air, into APS chamber

H_2O(g): P_{H2O} = 0.4 Torr, 2.5° C, ~8% rel. humidity

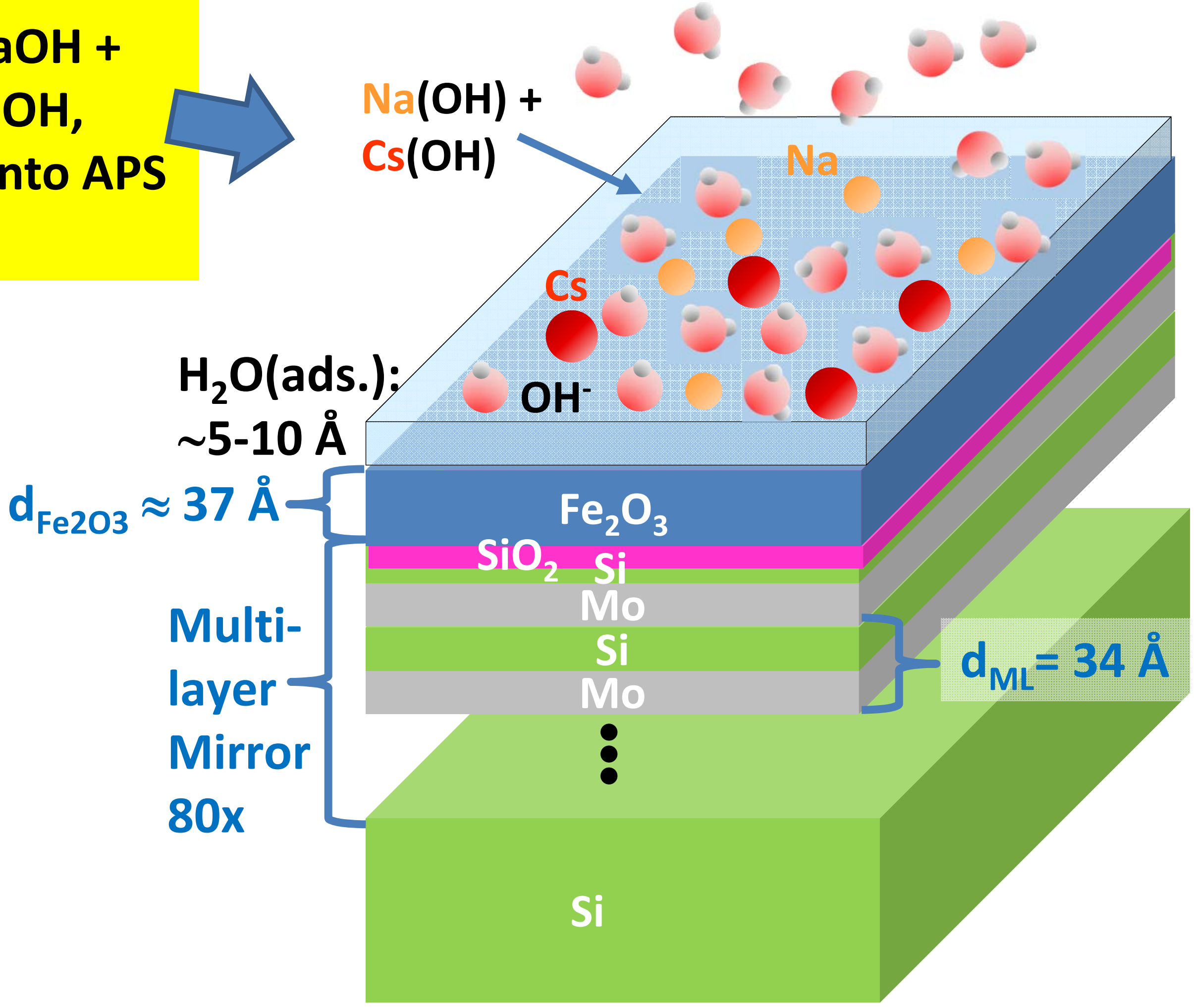

Standing-wave photoemission at the solid-liquid interface: some first experiments at ambient pressure

- Fe_2O_3 on Si/Mo multilayer mirror
- ~0.01M NaOH + ~0.01M CsOH, dried in air, into APS chamber

H_2O(g): P_{H2O} = 0.4 Torr, 2.5° C, ~8% rel. humidity

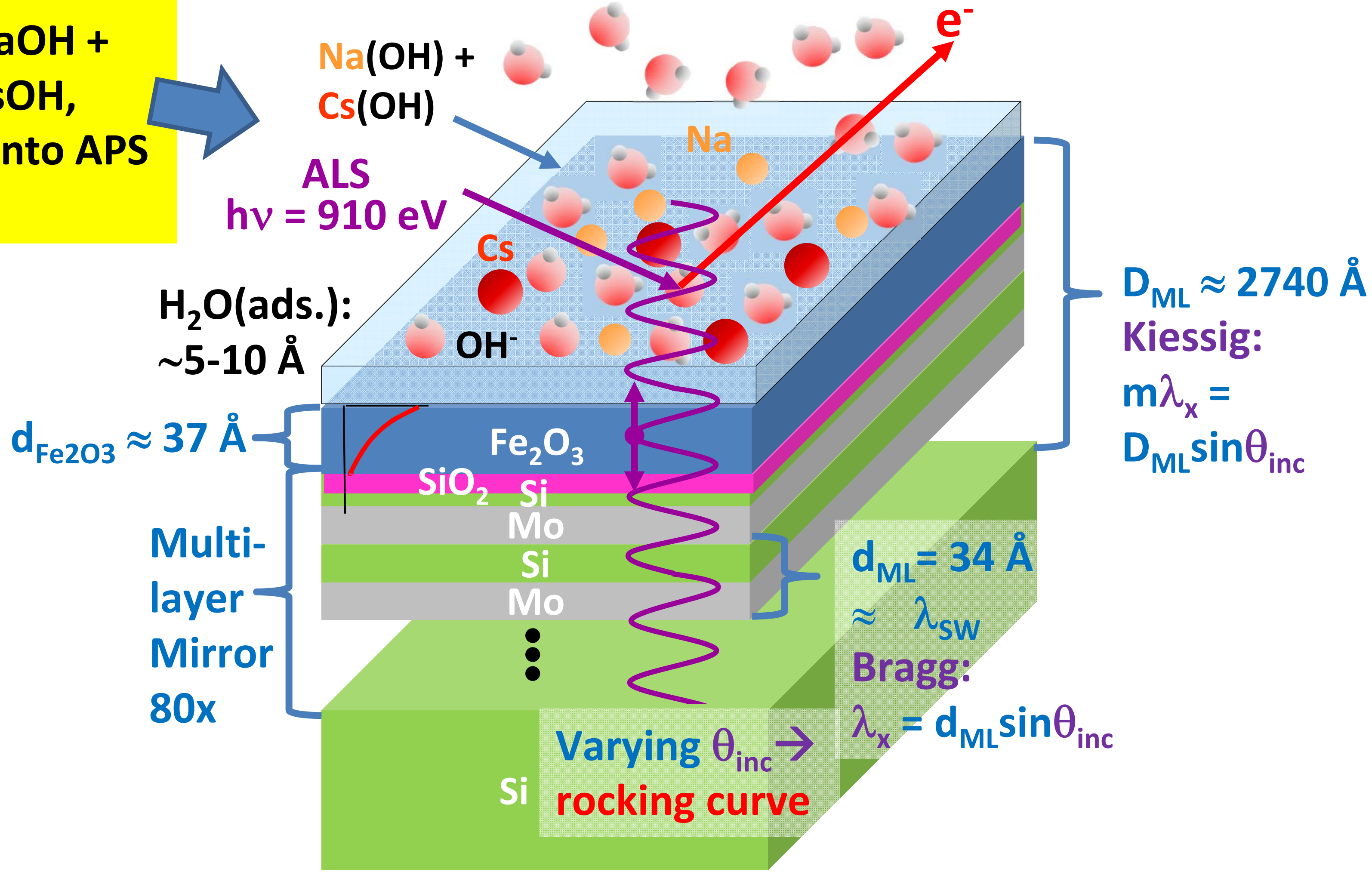

e^-

Na(OH) + Cs(OH)

Na

ALS

hν = 910 eV

Cs

H_2O(ads.): ~5-10 Å

OH^-

d_{Fe2O3} ≈ 37 Å

Fe_2O_3

SiO_2

Si

Mo

Si

Mo

Multi-layer Mirror 80x

D_{ML} ≈ 2740 Å

Kiessig: $m\lambda_x = D_{ML}\sin\theta_{inc}$

d_{ML}= 34 Å ≈ λ_{SW}

Bragg: $\lambda_x = d_{ML}\sin\theta_{inc}$

Varying θ_{inc} →

rocking curve

Si

Rocking curves from the O 1s spectrum

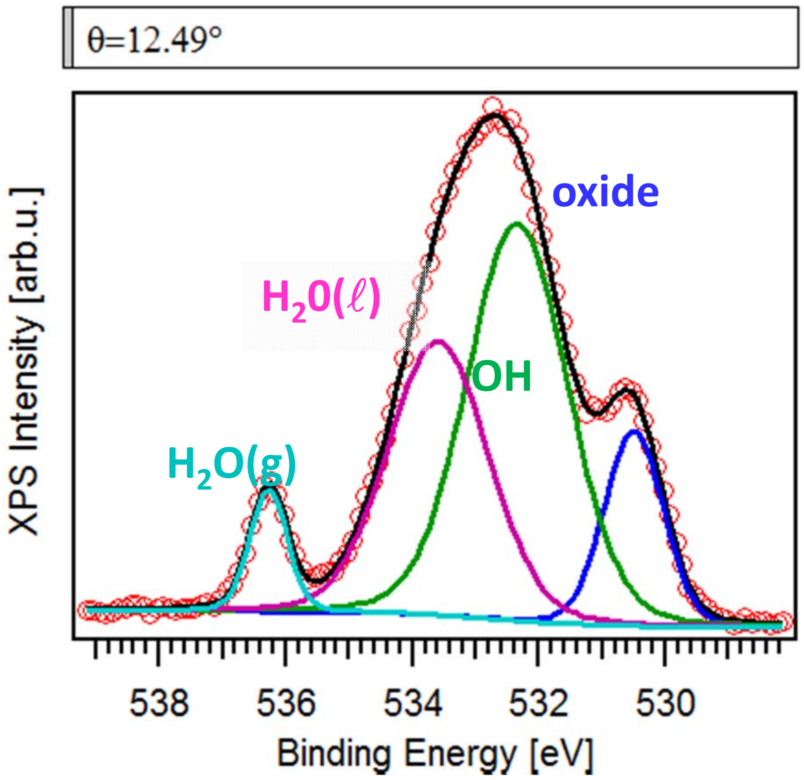

Rocking curves

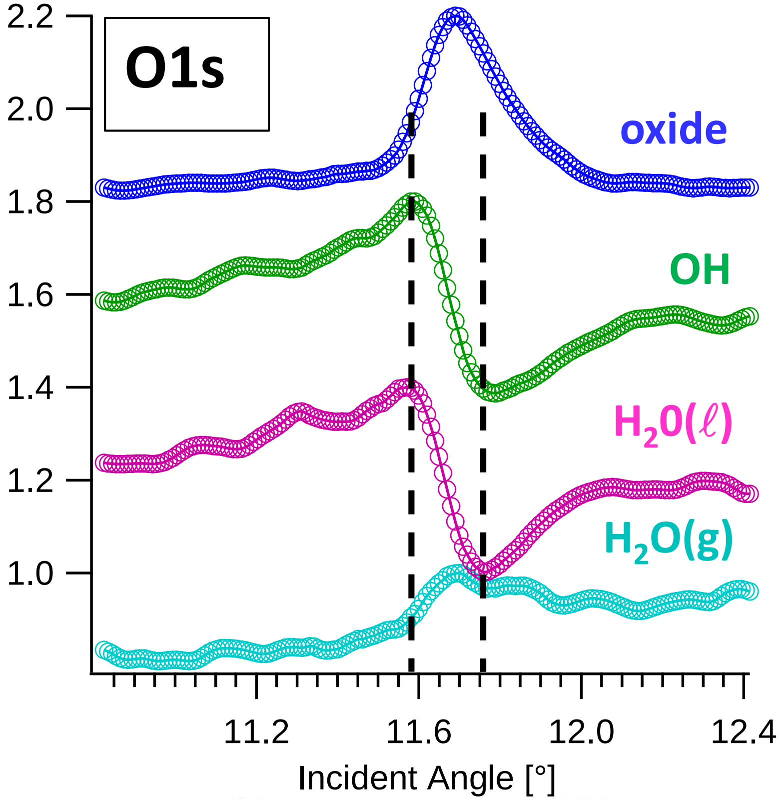

→ Clearly four components in O 1s from rocking curve data

Rocking curves for Na$^+$ and Cs+

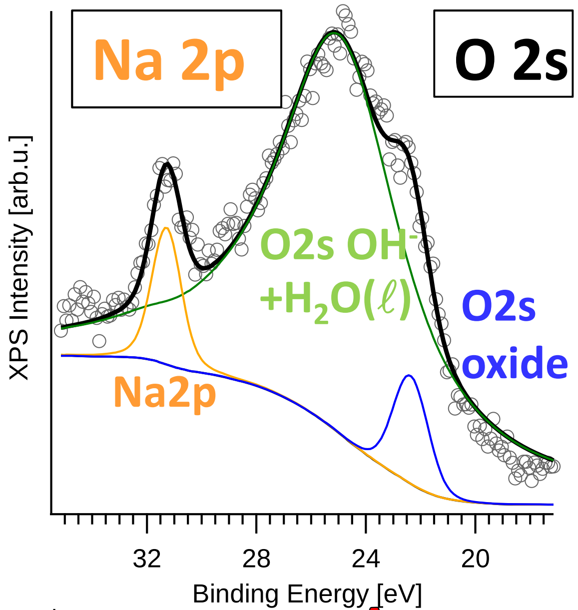

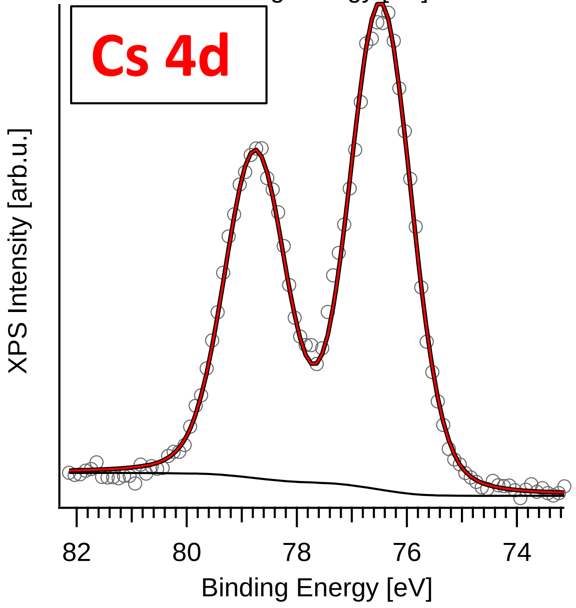

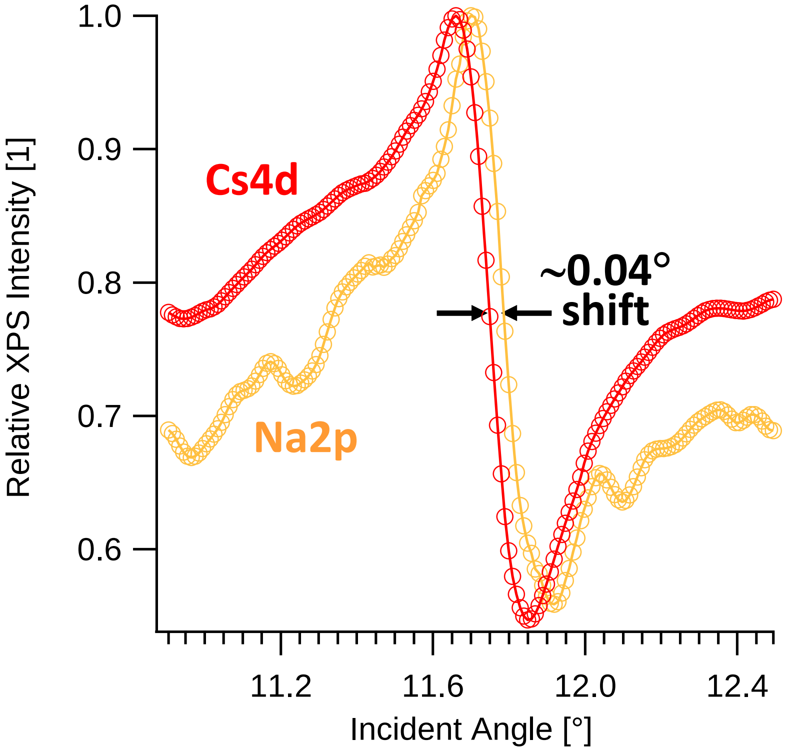

→ Clear differences in position and wings, indicating different depth distributions

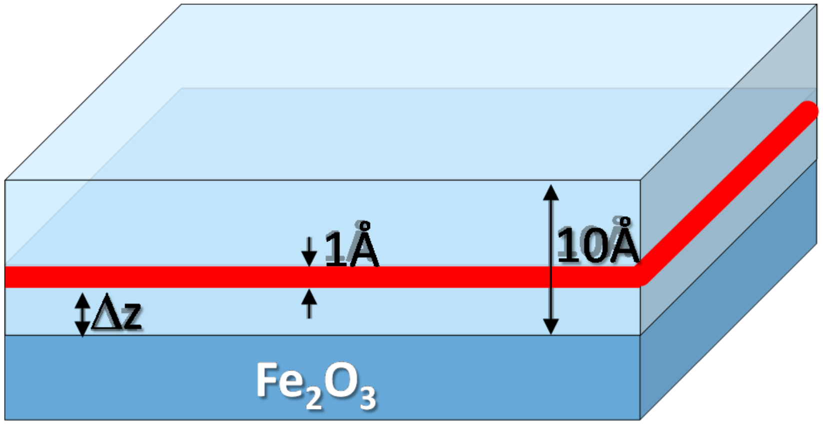

Delta-layer calculations for some more insight

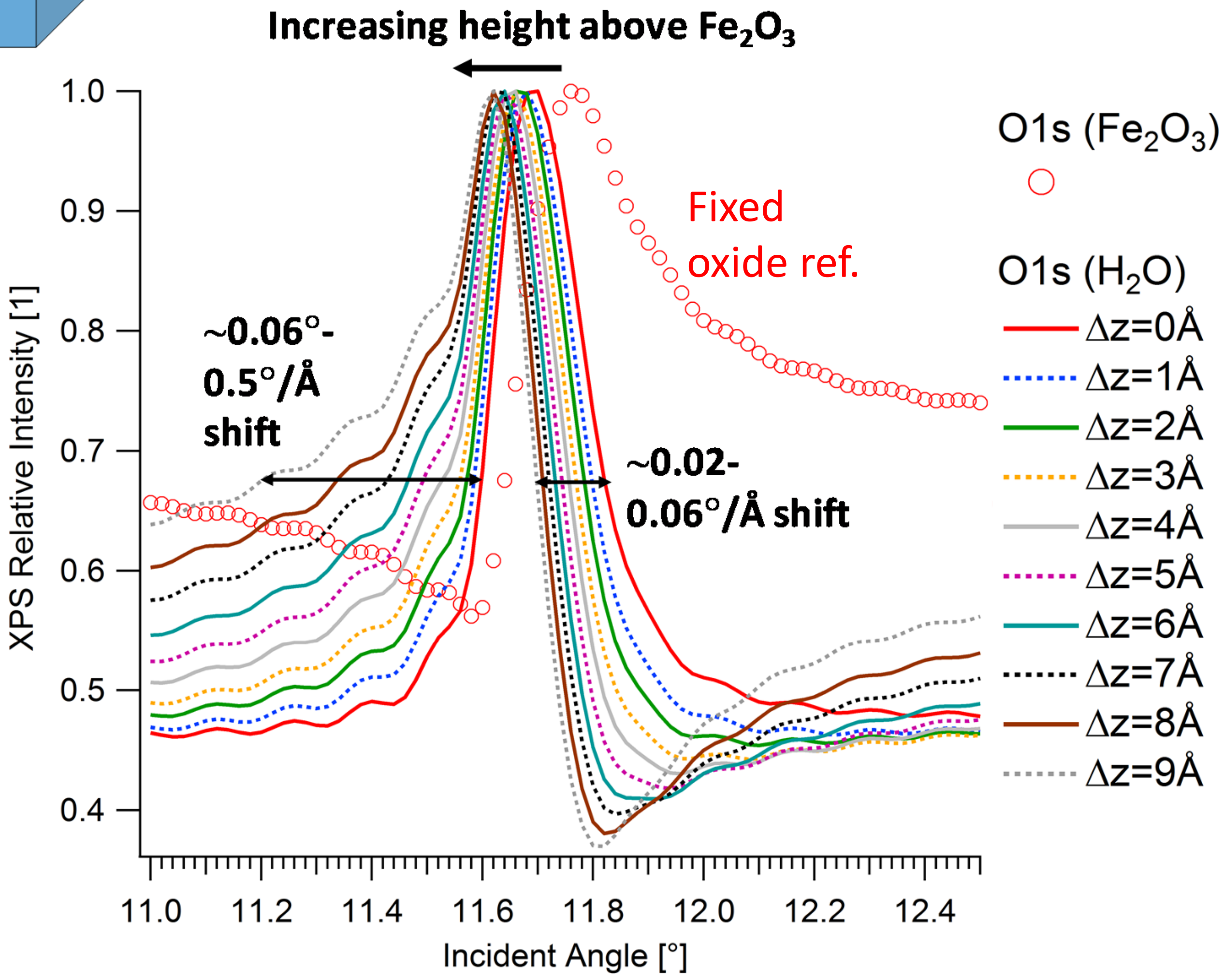

→ Suggests sensivity on ~ Å scale

Rocking curves for Na$^+$ and Cs+

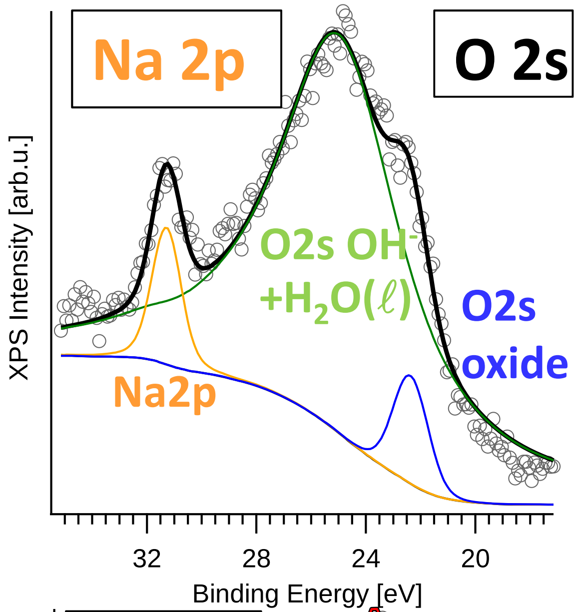

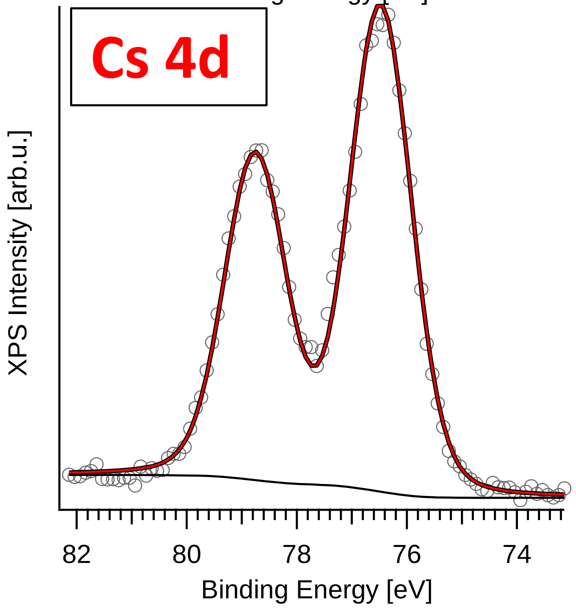

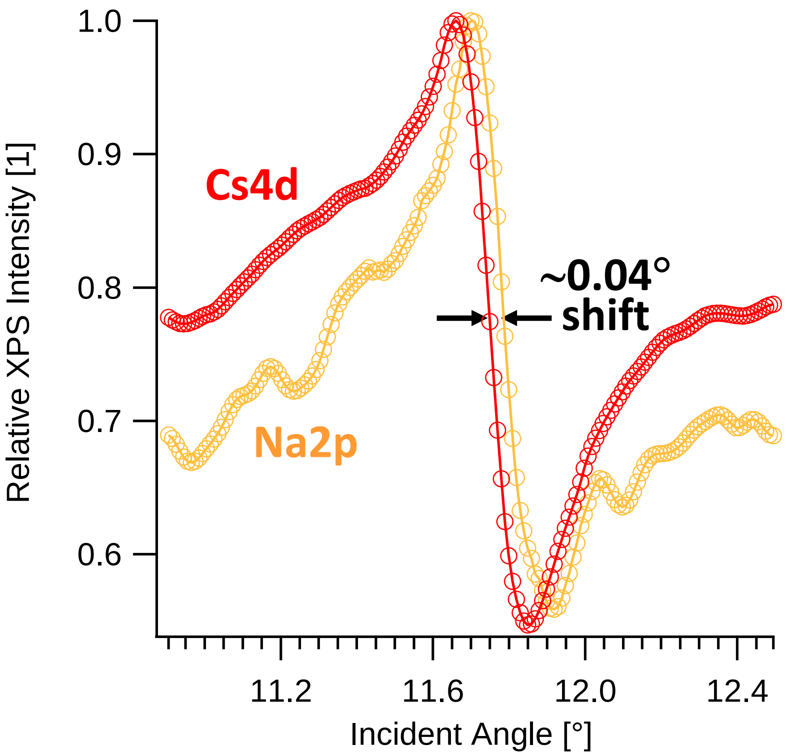

→ **Clear differences in position and wings, indicating different depth distributions**

Final structure optimization after fitting x-ray optical calculations to rocking curves

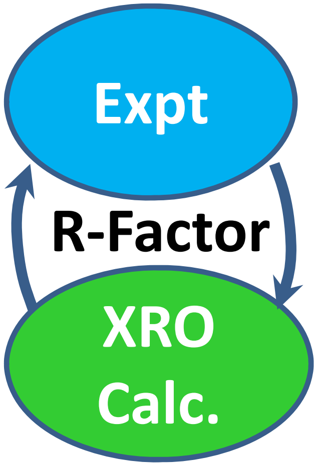

Expt

R-Factor

XRO Calc.

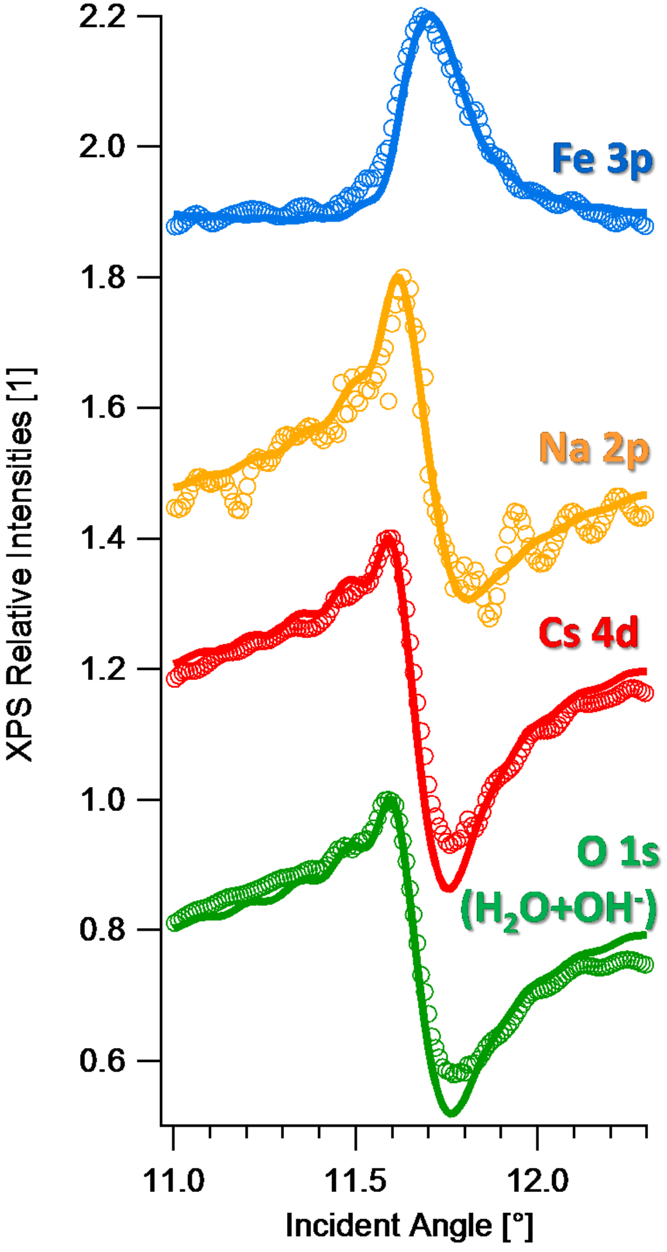

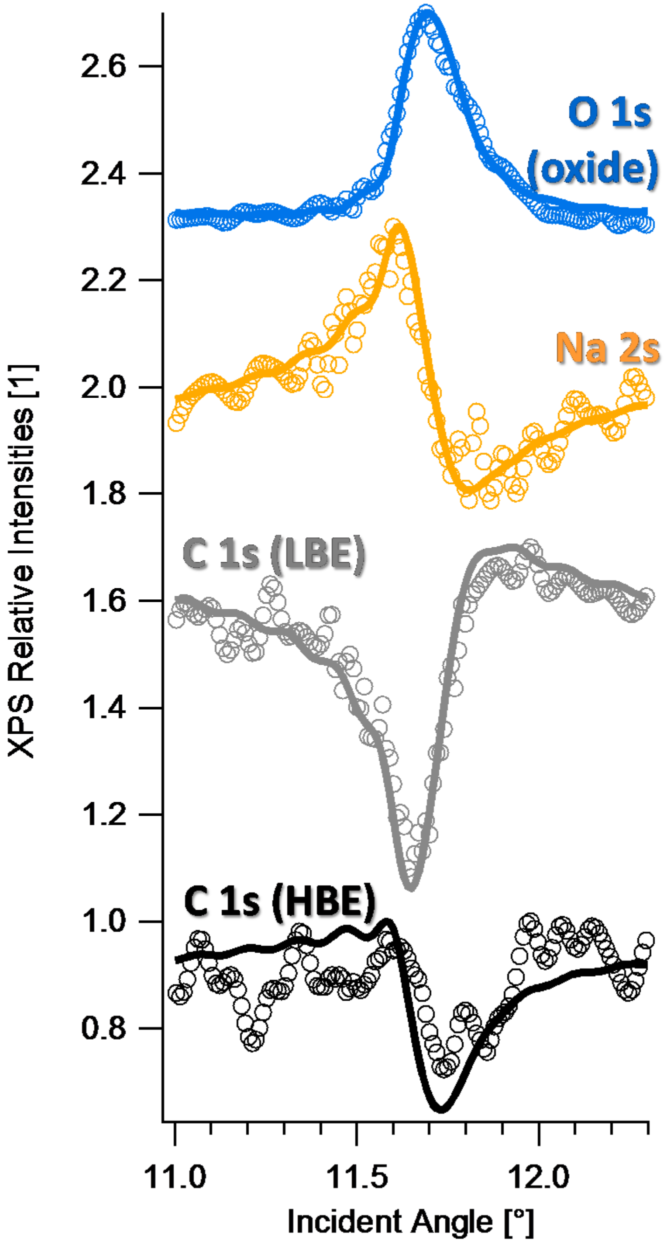

Nemšák

Final structure and the standing wave

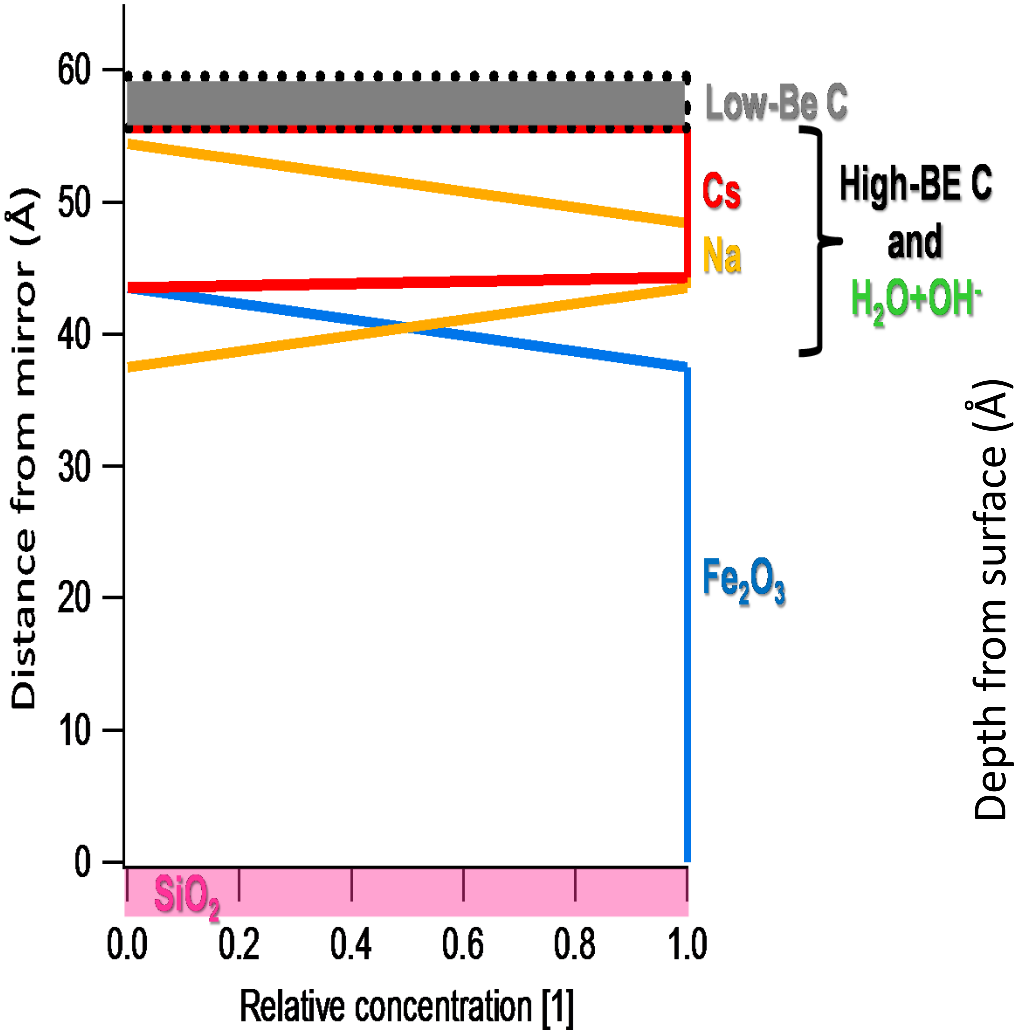

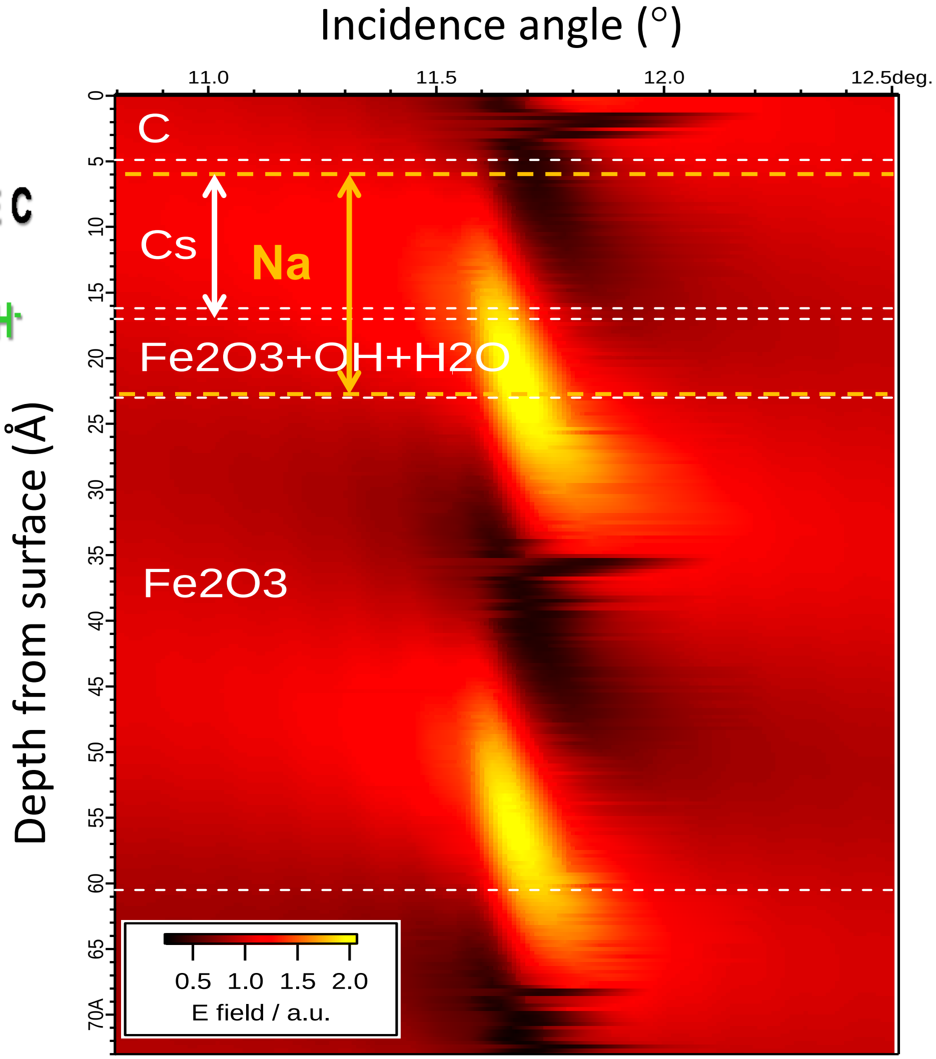

Final structure and atomic concentrations

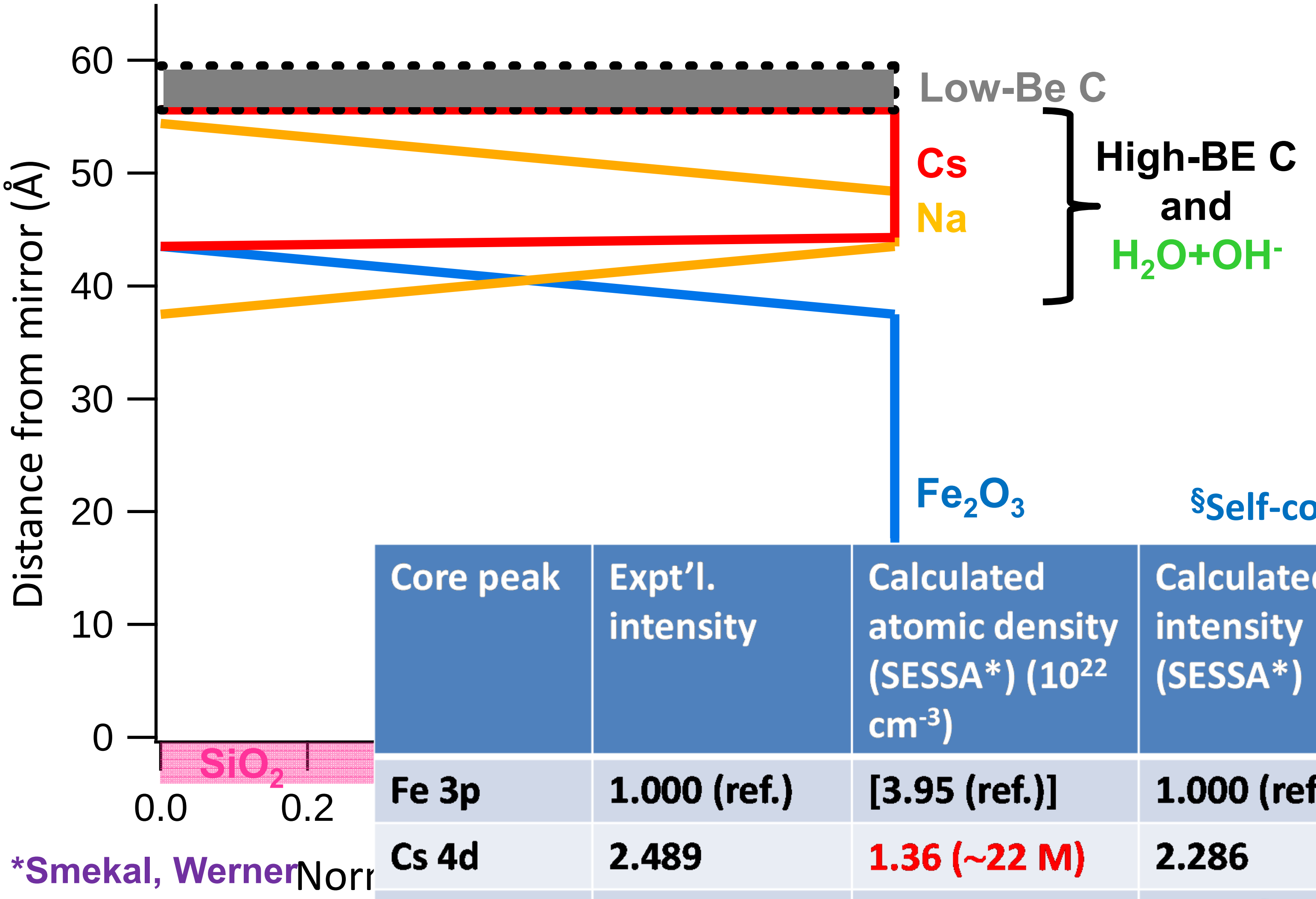

§Self-consistency checks

Core peak	Expt'l. intensity	Calculated atomic density (SESSA*) (10^{22} cm^{-3})	Calculated intensity (SESSA*)	Expt'l./ Calculated§
Fe 3p	1.000 (ref.)	[3.95 (ref.)]	1.000 (ref.)	1.000 (ref.)
Cs 4d	2.489	1.36 (~22 M)	2.286	1.043
Na 2p	0.0491 2p/2s	0.64 (~10 M)	0.0566 2p/2s	0.867
Na 2s	0.0731 0.671§	0.64 (~10 M)	0.0715 0.792§	1.022

*Smekal, Werner Powell, Surf. Interface Anal. 3, 1059 (2005)

Depth-dependent binding energies and the standing wave

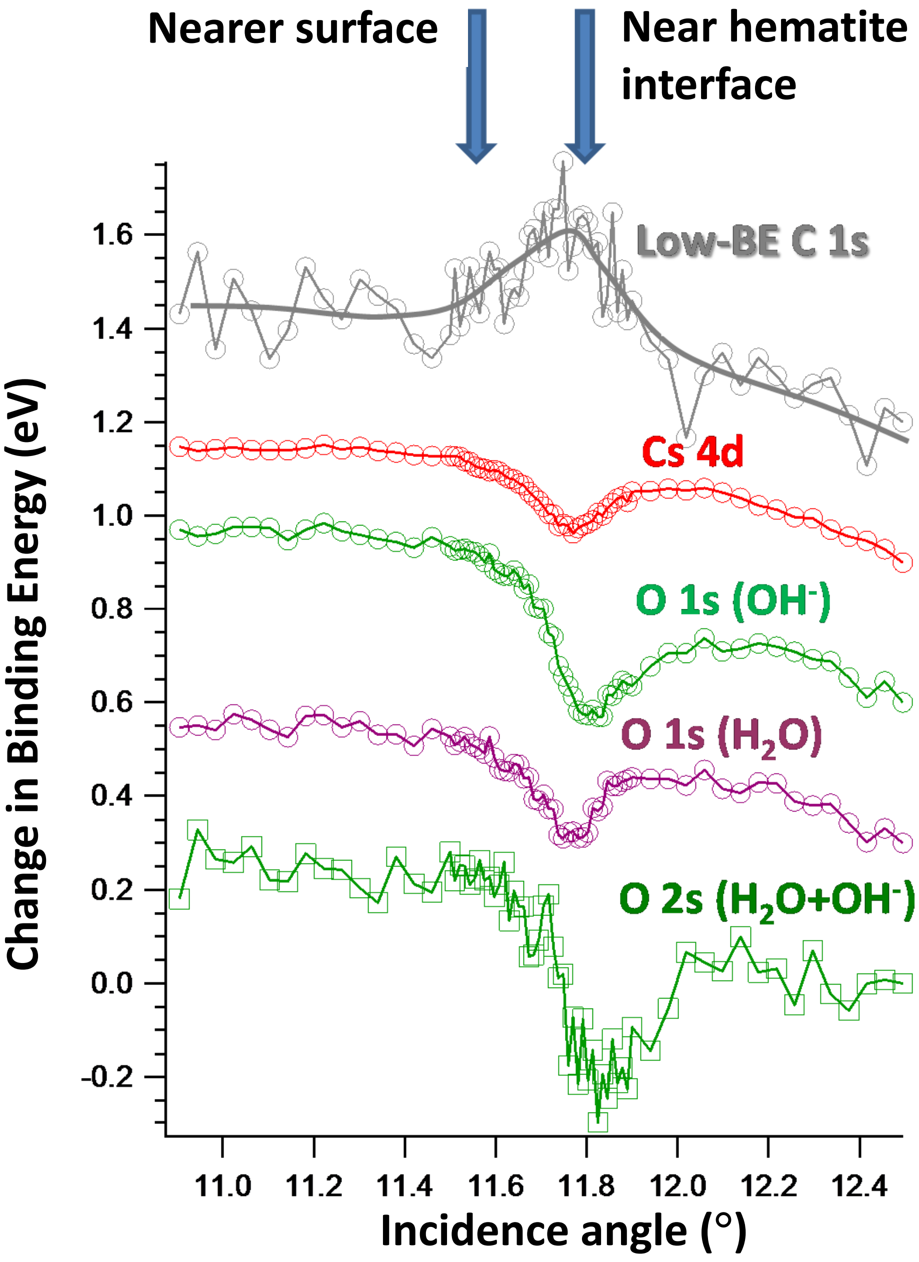

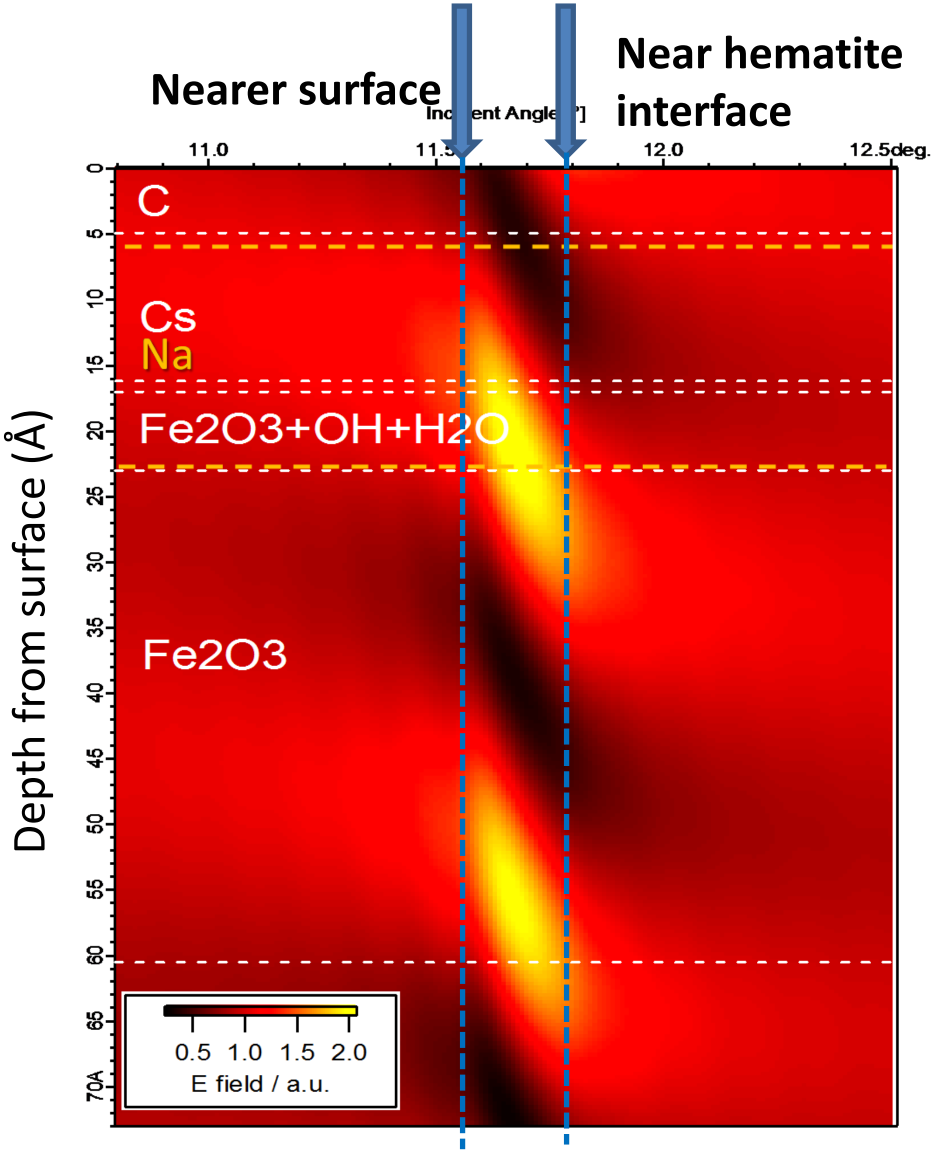

Conclusions: Standing Wave Ambient Pressure Photoemission (SWAPPS) of NaOH + CsOH + H_2O on Fe_2O_3

From standing-wave rocking curves of all elements present:

- **Fe_2O_3 surface--effective roughness of ~6 Å, agrees with AFM**
- **Na^+: average distance ~5.5 Å above Fe_2O_3, total distribution over ~11 Å**
- **Cs^+: larger average distance of ~9.5 Å above Fe_2O_3, total distribution over ~12 Å→ Cs^+ and Na^+ separated by ~ 5 Å.**
- **Low-binding-energy C: very thin ~5 Å layer on the surface of the sample →hydrocarbons?**
- **High-binding-energy C: spread over the entire depth range of the "wet" layer, H_2O+CO_2 → bicarbonate?**
- **OH^- + H_2O: Very nearly the same depth distribution**
- **Quantitative analysis for atomic concentrations possible**
- **Depth-dependent binding energies → depth dependent chemistry and potentials**
- **Provided that the sample can be grown on a multilayer mirror, SWAPPS a powerful new technique for looking at solid/solid and solid/liquid interaces, with resolution ~±2 Å**

S. Nemšák, et al., Nature Comm. to appear

Soft →hard x-rays and standing waves: a few example studies

$SrTiO_3/La_{2/3}Sr_{1/3}MnO_3$-tunnel junction

Depth-resolved composition, dielectric properties, bonding, k-resolved electronic structure

$SrTiO_3/GdTiO_3$-2D electron gas

Depth-resolved composition, charge states, k-resolved electronic, structure

Fe/MgO-tunnel junction

Depth-resolved composition, chemical states, magnetization

$SrTiO_3$ and Ga(Mn)As

Projected densities of states

Fe_2O_3 reacting with NaOH, CsOH, and H_2O

Using standing wave XPS to probe the solid/gas and solid/liquid interface: some first ambient pressure results

$SrTiO_3/GdTiO_3$-2D electron gas

Depth-resolved composition, charge states,
k-resolved electronic, structure, 2D electron gas

$SrTiO_3/GdTiO_3$-2D electron gas

Depth-resolved composition, charge states, k-resolved electronic, structure, 2D electron gas

S. Nemšák et al., TBP

$SrTiO_3$

- Band insulator (E_g=2.3 eV)
- Low temperature superconductor

$GdTiO_3$

- Mott-Hubbard insulator

$GdTiO_3/SrTiO_3$ interface

- Two-dimensional electron gas (2DEG) at the interface between two insulators (*Appl. Phys. Lett.* ***99****, 232116, 2011*)
- Sheet carrier density on the order of $3x10^{14}$ cm^{-2}
- Ferromagnetism in the 2DEG at the interface (*Phys. Rev. X* ***2****,021014, 2012*)

Stemmer et al., UCSB

The Advanced Light Source

Julich Res. Ctr.

The GTO/STO 2D Electron Gas

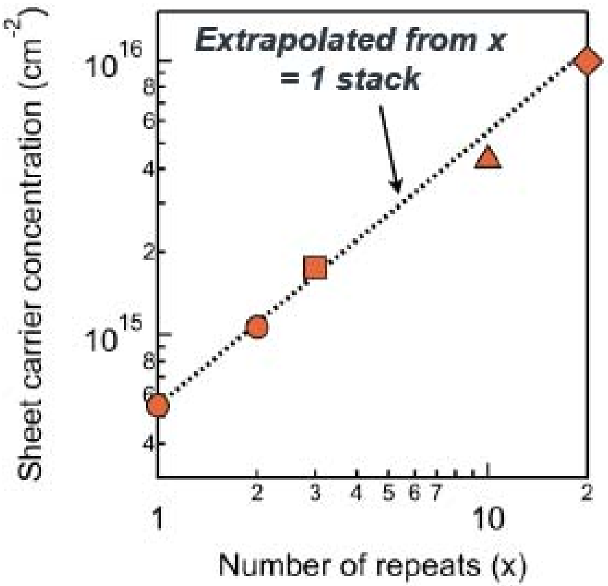

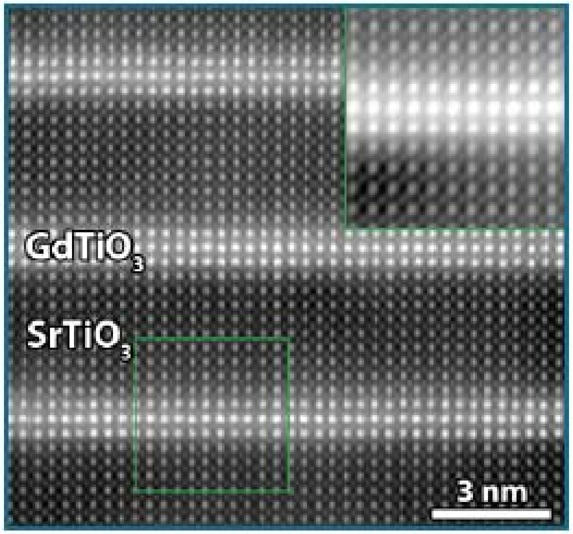

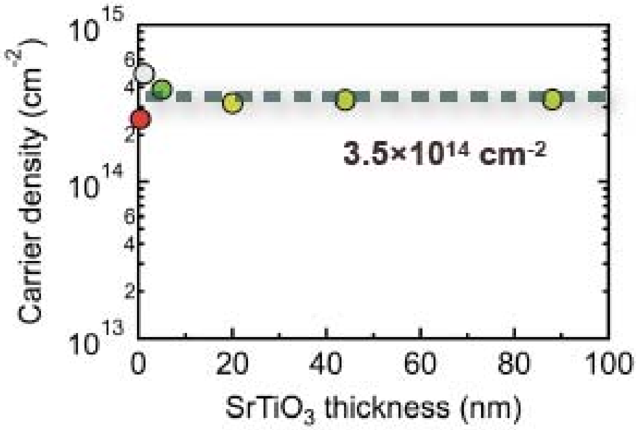

Appl. Phys. Lett. 99, 232116 (2011).

Stemmer, Allen groups

$SrTiO_3$ - prototype *d*-band perovskite oxide
$GdTiO_3$ - prototype Mott insulator

Can we see this 2DEG with standing wave ARPES, including its momentum dispersion and its depth distribution?

Multilayer GTO/STO

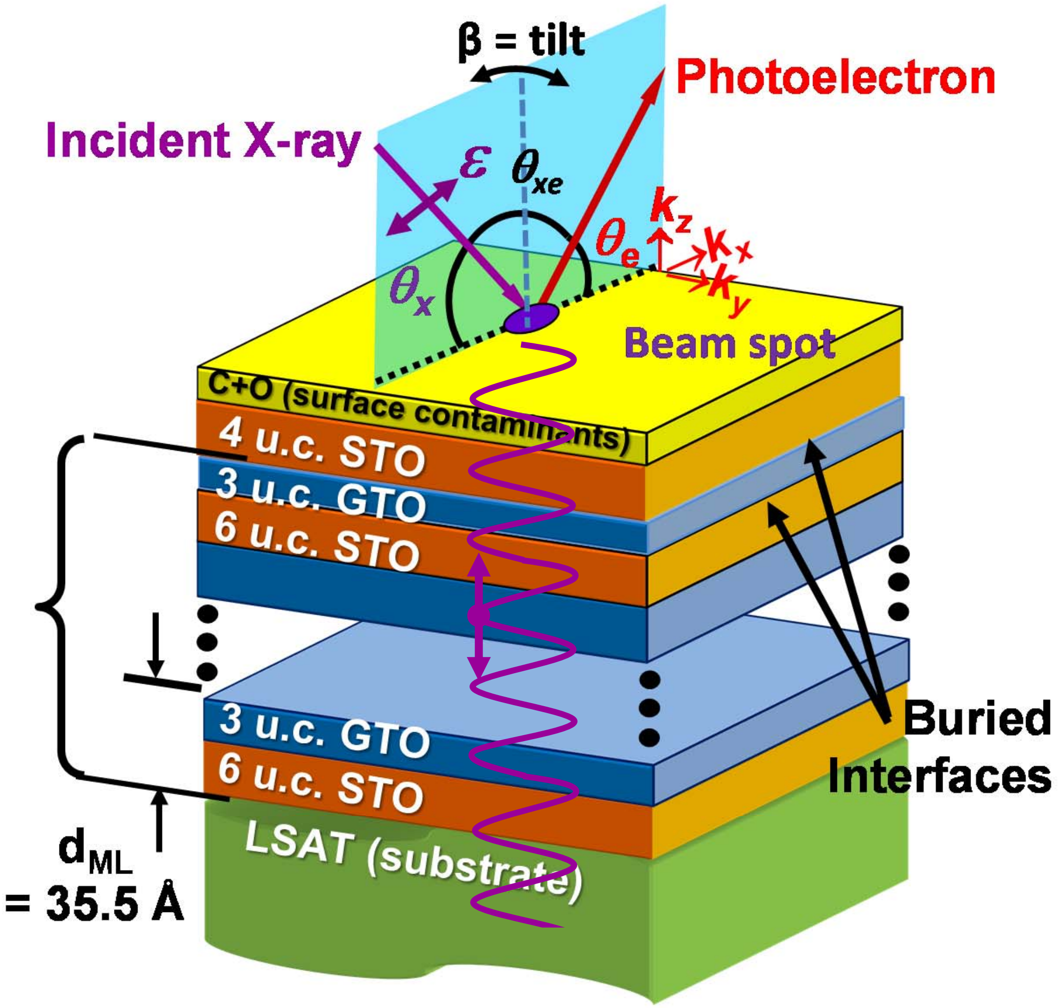

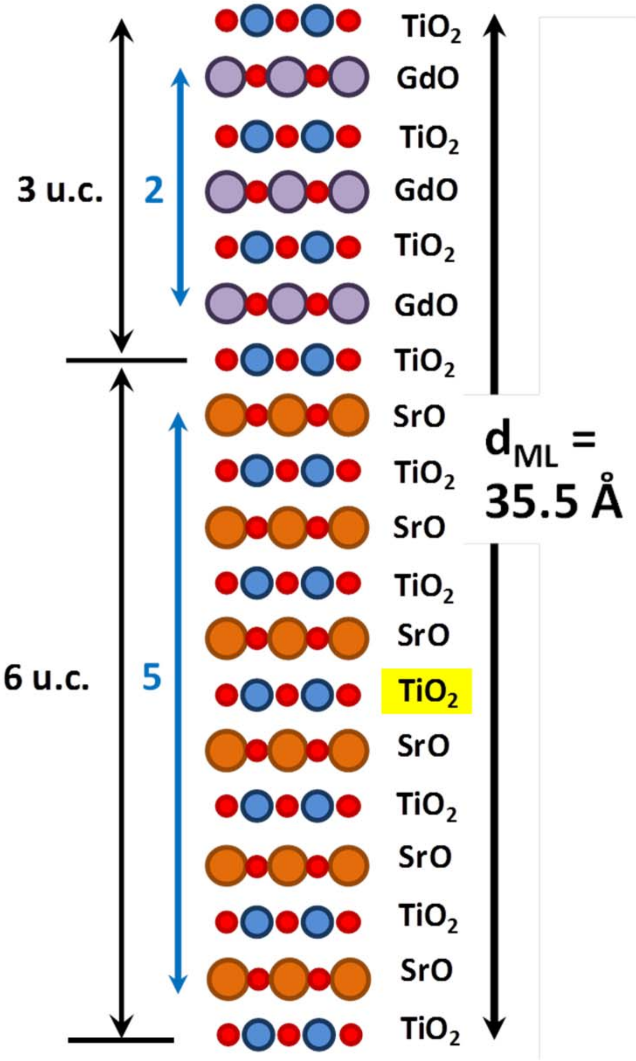

P. Moetakef, S. Stemmer, UCSB

Multilayer GTO/STO

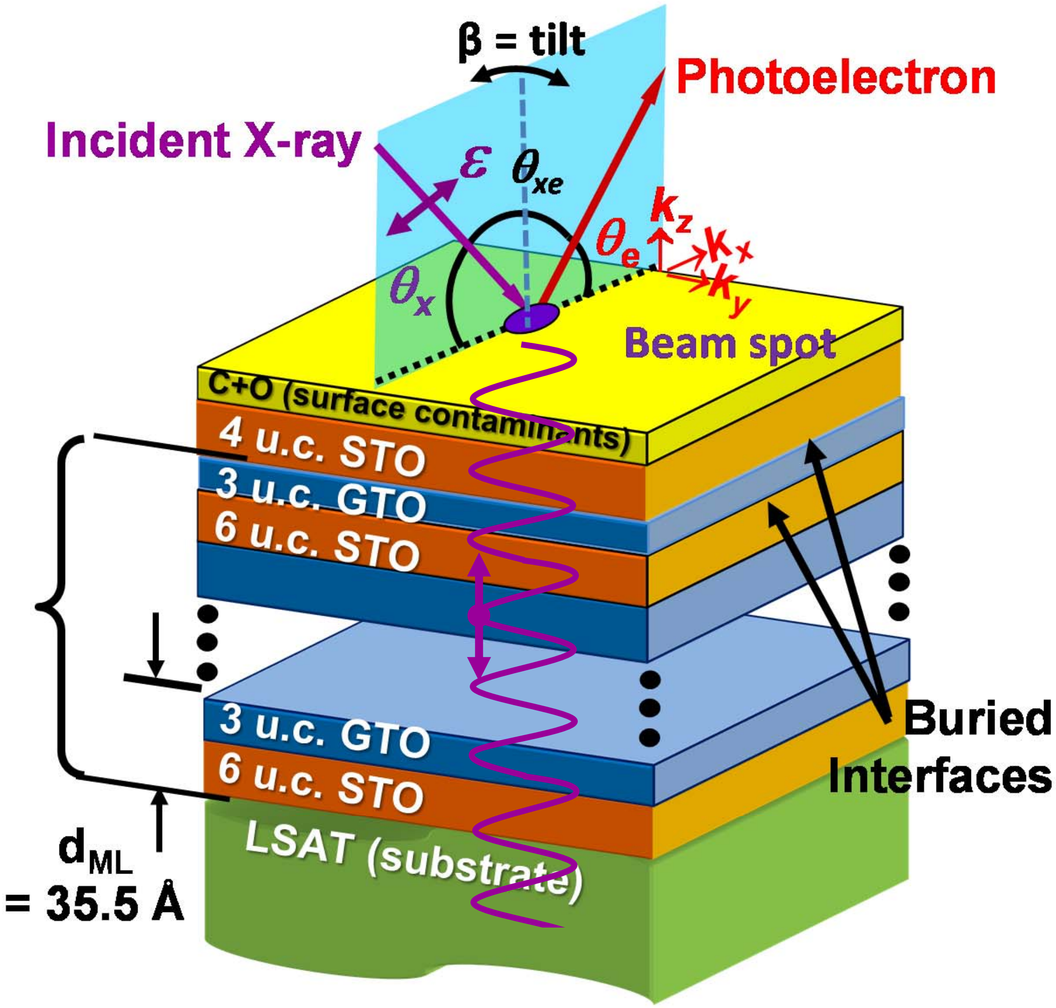

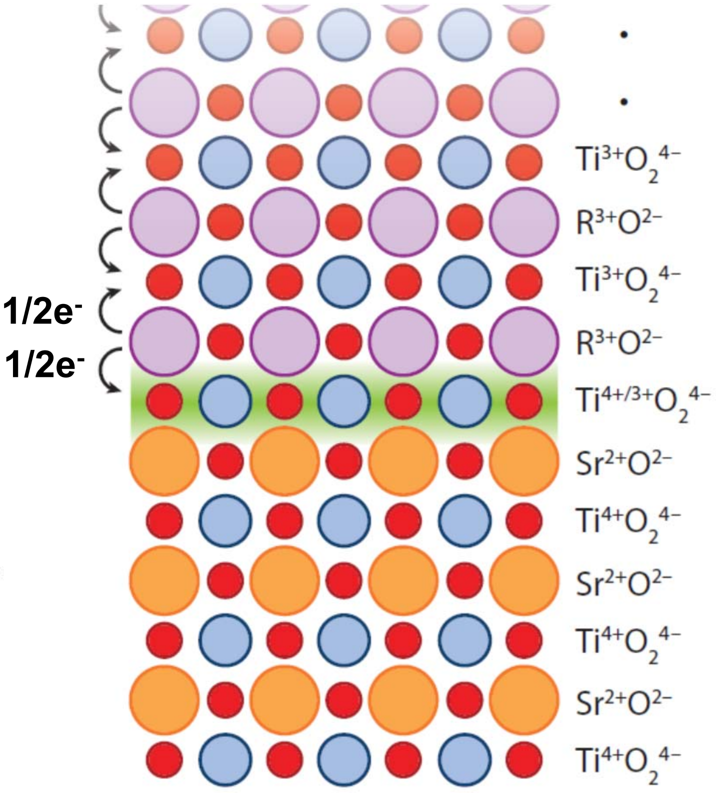

Stemmer, Allen
Annu. Rev. Mater. Res.
44:, 51–71 (2014)

P. Moetakef, S. Stemmer,
UCSB

Electronic structure of bulk $GdTiO_3$- LDA+hybrid functionals

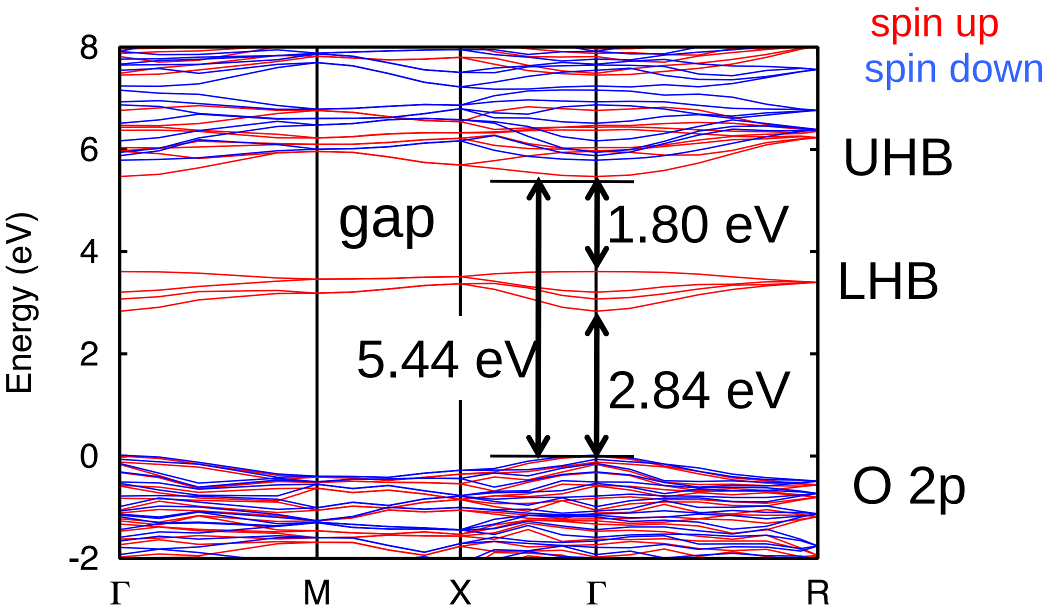

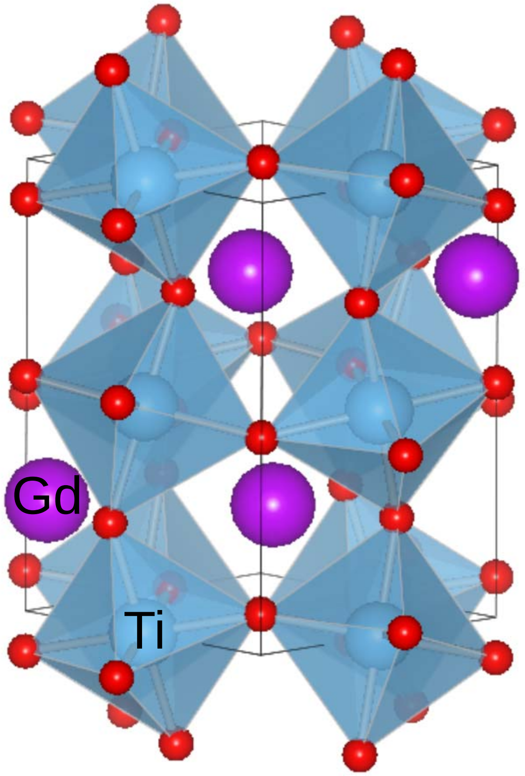

LHB width: 0.80 eV

4 bands compose LHB, one e^- for each Ti

A. Janotti, C. Van de Walle

Bulk $GdTiO_3$ and bulk $SrTiO_3$-
Densities of states aligned using calculated valence-band offset

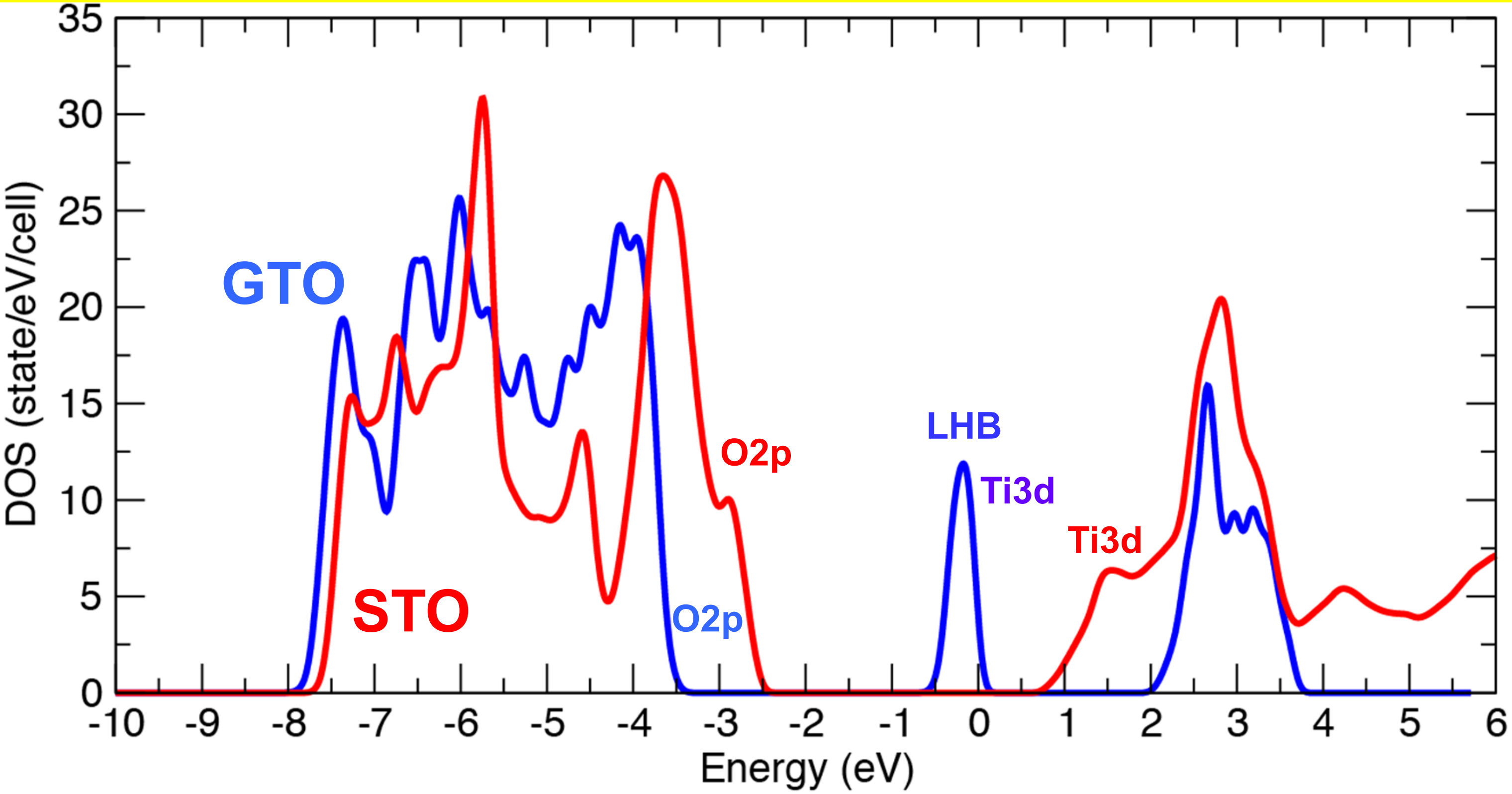

- Calculated valence band offset (between GTO-LHB and STO-O2p-band) of 2.56 eV

A. Janotti, C. Van de Walle

Valence band offsets for multilayer $SrTiO_3/GdTiO_3$ from core-level and VBM measurements

Standard XPS→HXPS method based on measurements of bulk STO and GTO, and the multilayer*:

$$\Delta E_{VBO}(A/B) = (E_{Core}^{ML,STO} - E_{Core}^{ML,GTO}) - (E_{Core}^{STO} - E_{VBM}^{STO}) + (E_{Core}^{GTO} - E_{VBM}^{GTO})$$

*Chambers et al., Appl. Phys. Lett. 77, 1662 (2000); J. Vac. Sci. Technol. B 22, 2205 (2004)

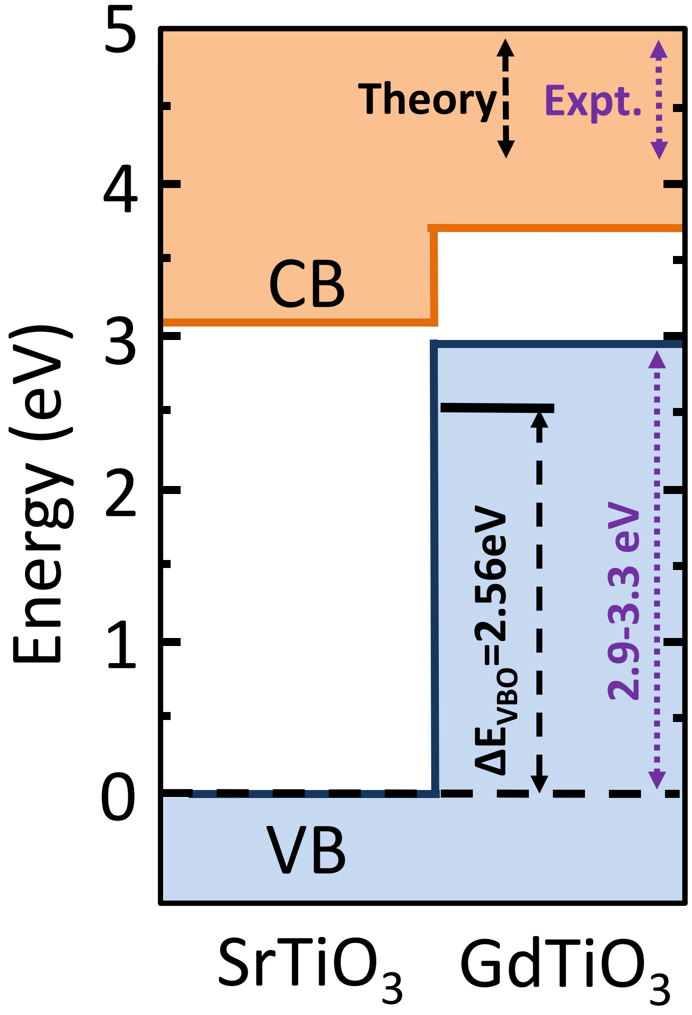

Conti et al., J. Appl. Phys. 113 143704 (2013)- theory: Janotti, van de Walle

Bulk $GdTiO_3$ and bulk $SrTiO_3$- Densities of states aligned using calculated valence-band offset

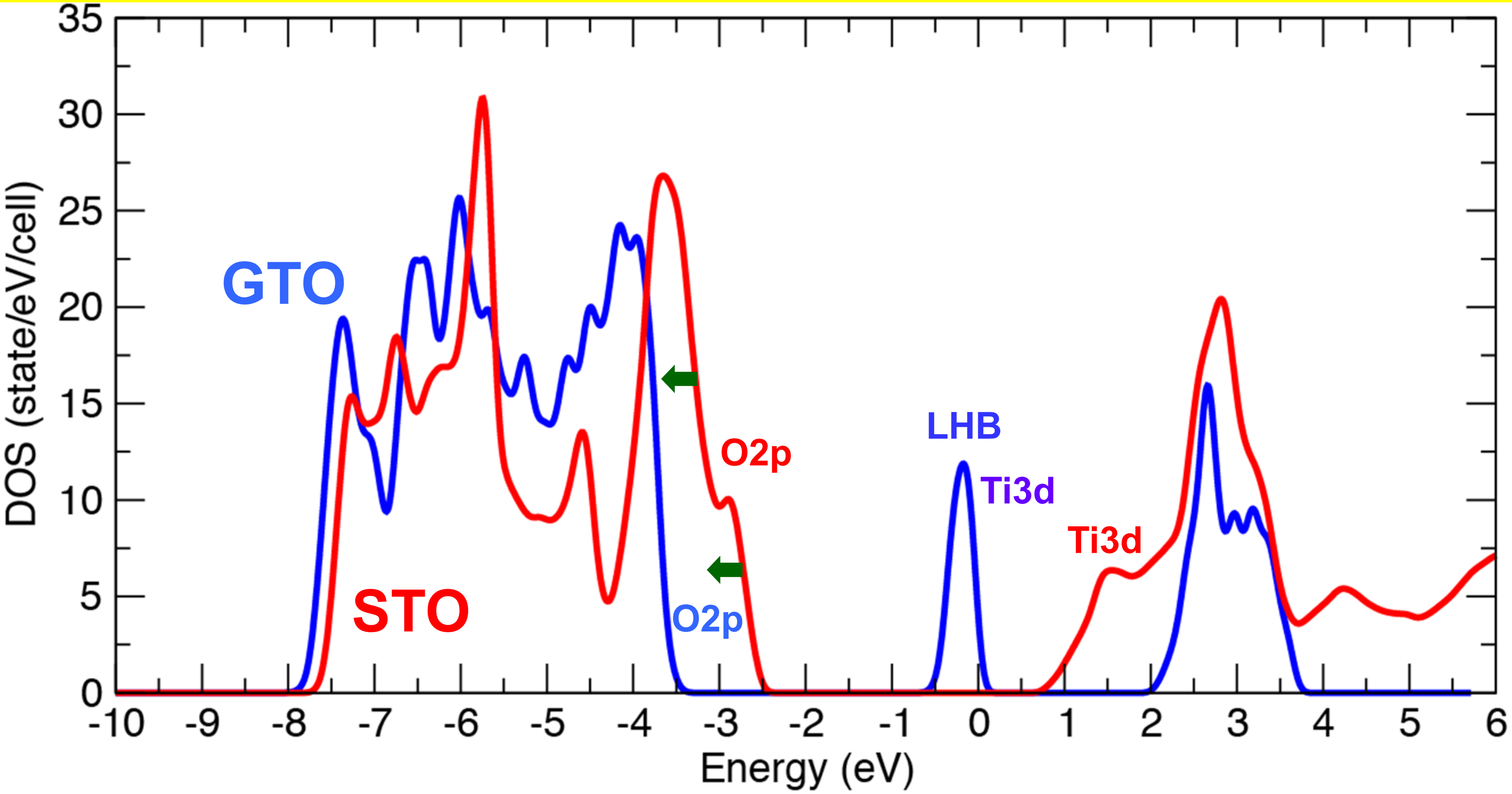

- **Calculated valence band offset (between GTO-LHB and STO-O2p-band) of 2.56 eV**

Compared to 2.9-3.3 ± 0.3 eV from XPS experiment

A. Janotti, C. Van de Walle
Band offsets: Conti et al.,
J. Appl. Phys. 113 143704 (2013).

GTO/STO multilayer:
Soft x-ray photoemission in the XPS limit @ 833 eV@ 298K
→Matrix-element-weighted densities of states

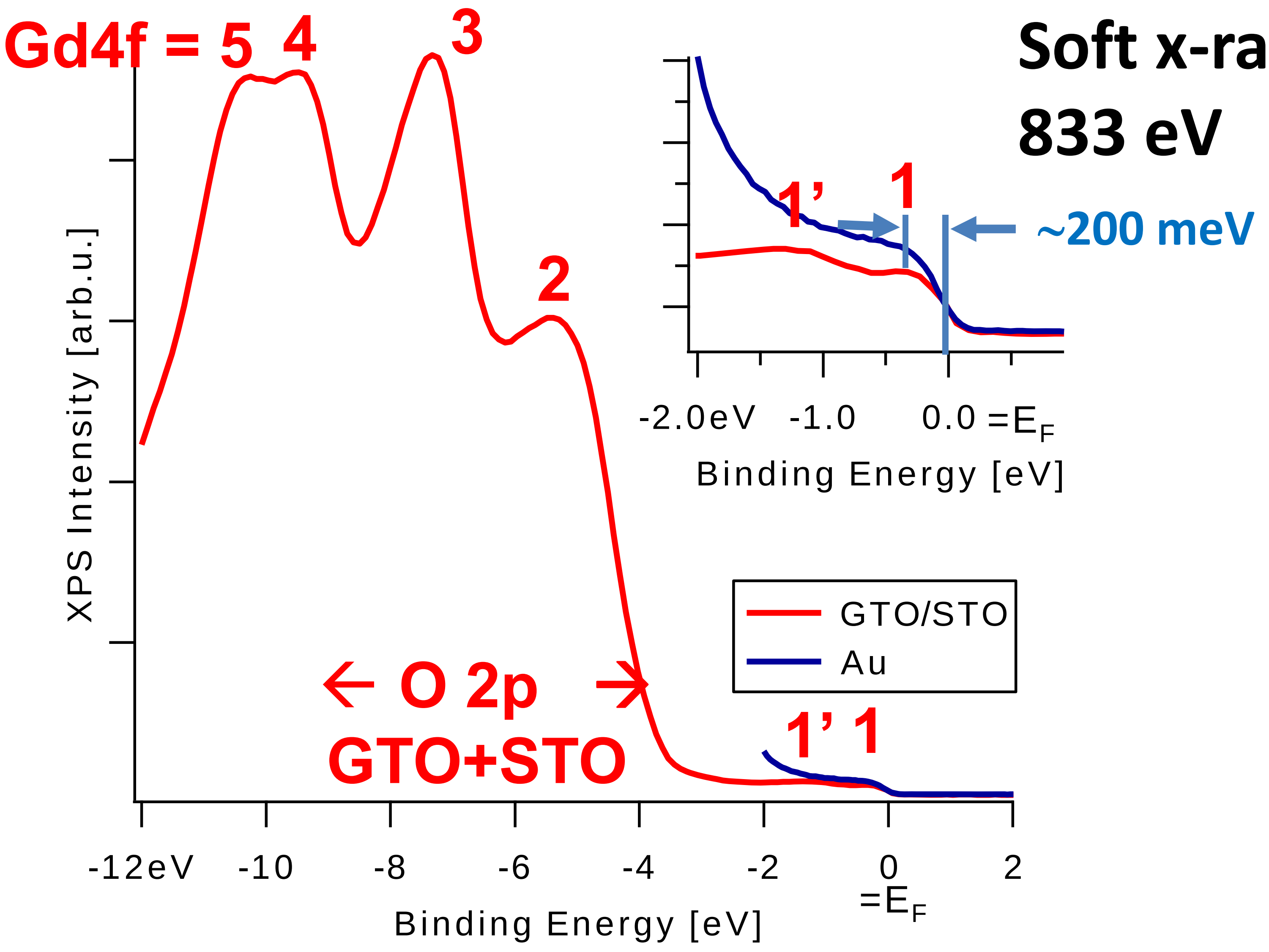

Soft x-ray

833 eV

Standing-wave rocking curves: Ti 2p spectra, 1182 eV

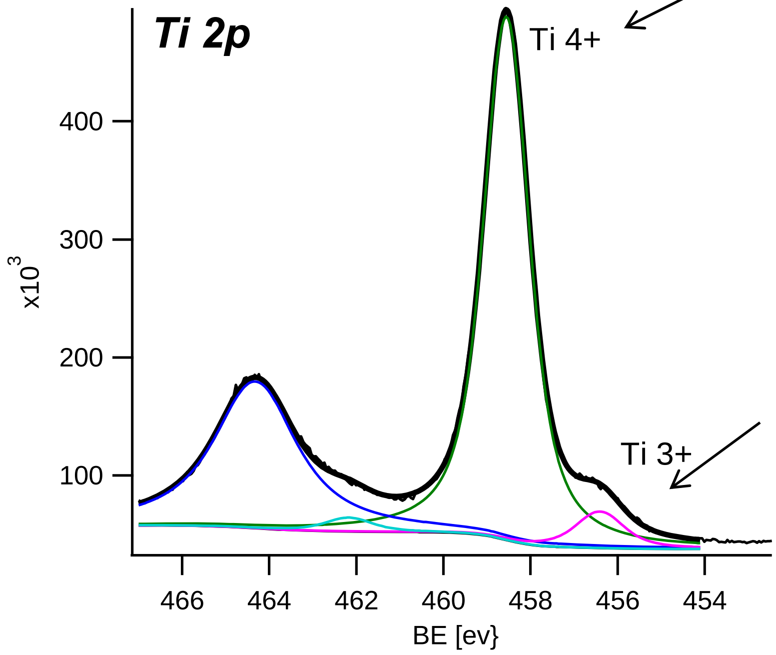

$SrTiO_3$

$GdTiO_3$

Ti^{4+} 2p rocking curve

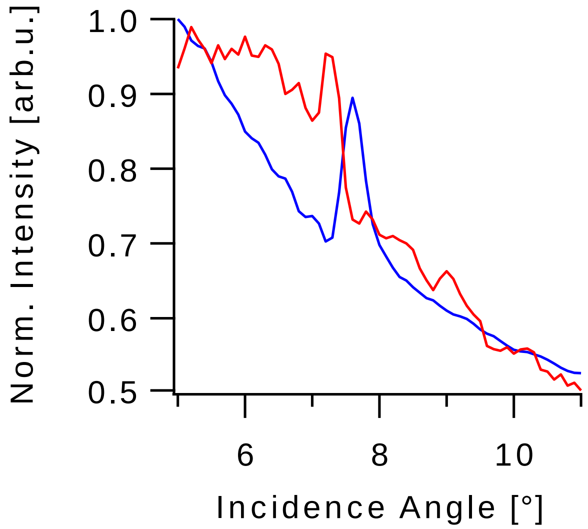

Ti^{3+} 2p rocking curve

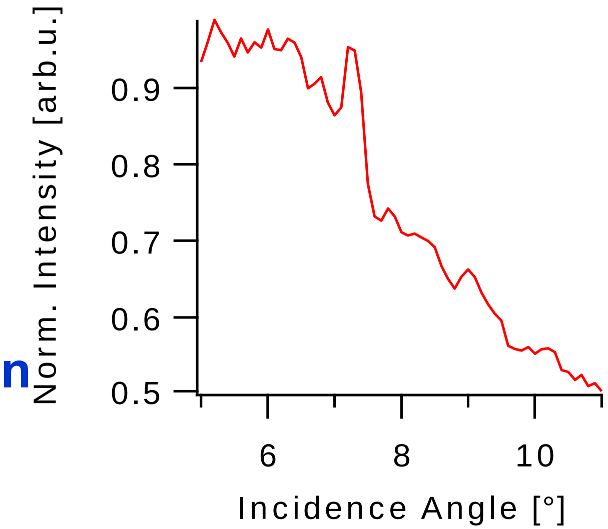

→ Rocking curves provide direct depth information on different Ti states

Swiss Light Source

Nemšák et al.

STO 4u.c./[GTO 2u.c./STO 5u.c.]$_{20x}$/LSAT
ARPES at 1182 eV in $\vec{k}$-space

$$\vec{k}_f = \vec{k}_i + \vec{g}_{bulk} (+\cancel{\vec{g}_{surf}}) + \vec{k}_{h\nu} + \cancel{\vec{k}_{phonon}}$$

$$\vec{k}_i = \vec{k}_f - \vec{k}_{h\nu} - \vec{g}_{bulk}$$

With cryocooling

Peak 1

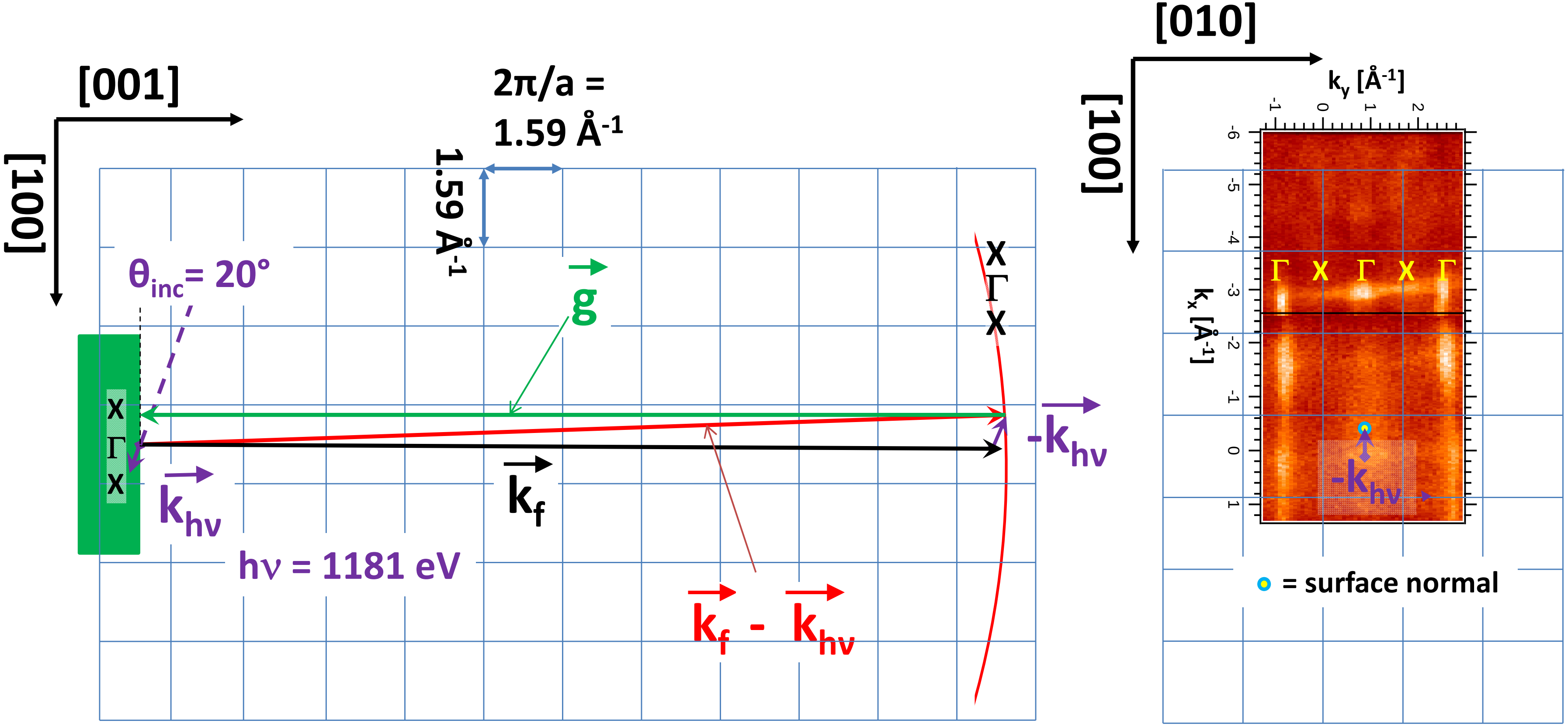

$|k_f|$ = 17.61 Å^{-1} $|k_{h\nu}|$=0.60 Å^{-1} Γ-X-Γ = 1.59 Å^{-1}

Swiss Light Source

STO/GTO multilayer – Standing-wave ARPES, 1182 eV

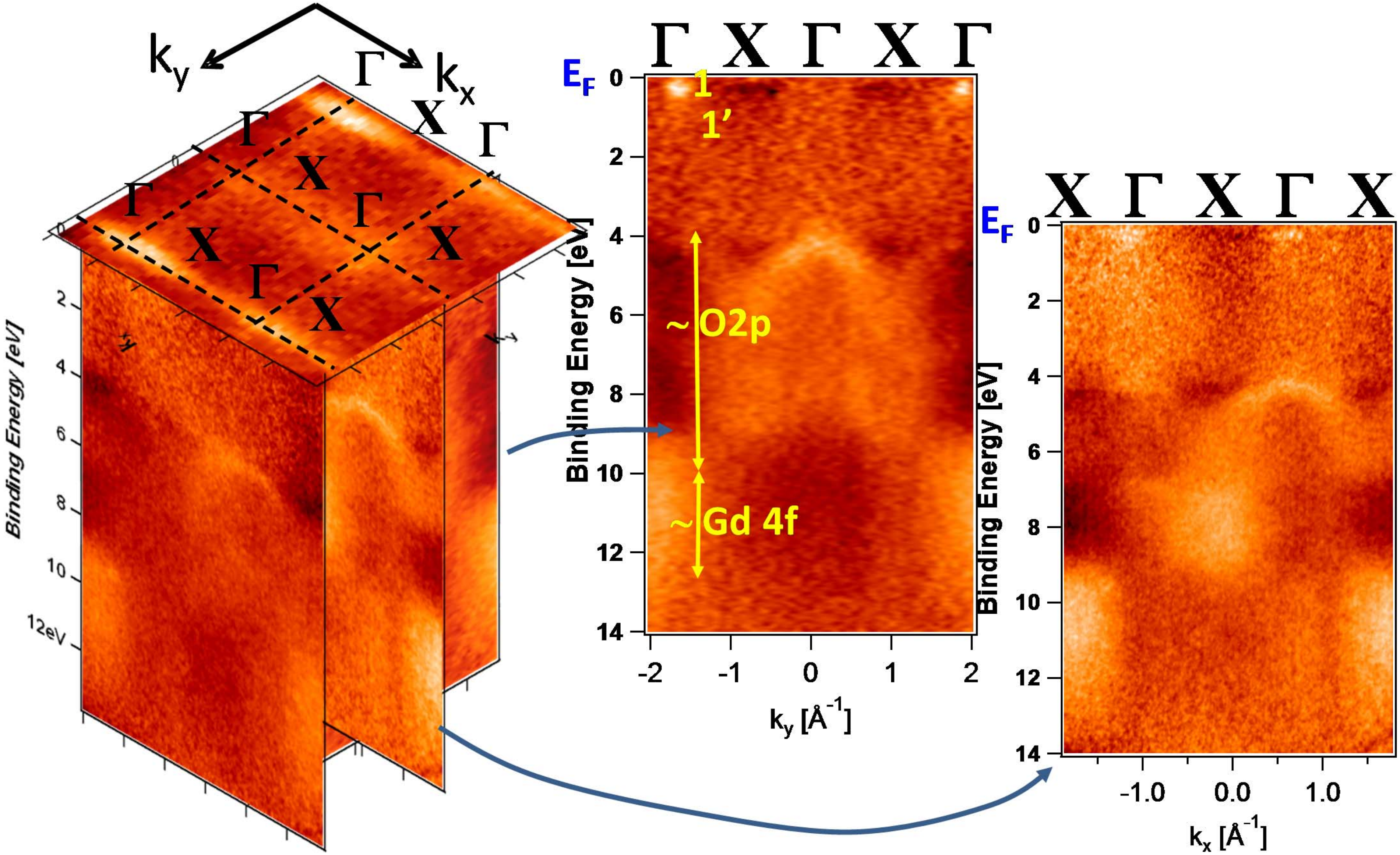

Swiss Light Source

STO/GTO Standing-Wave ARPES
ARPES at 833 eV in $\vec{k}$-space

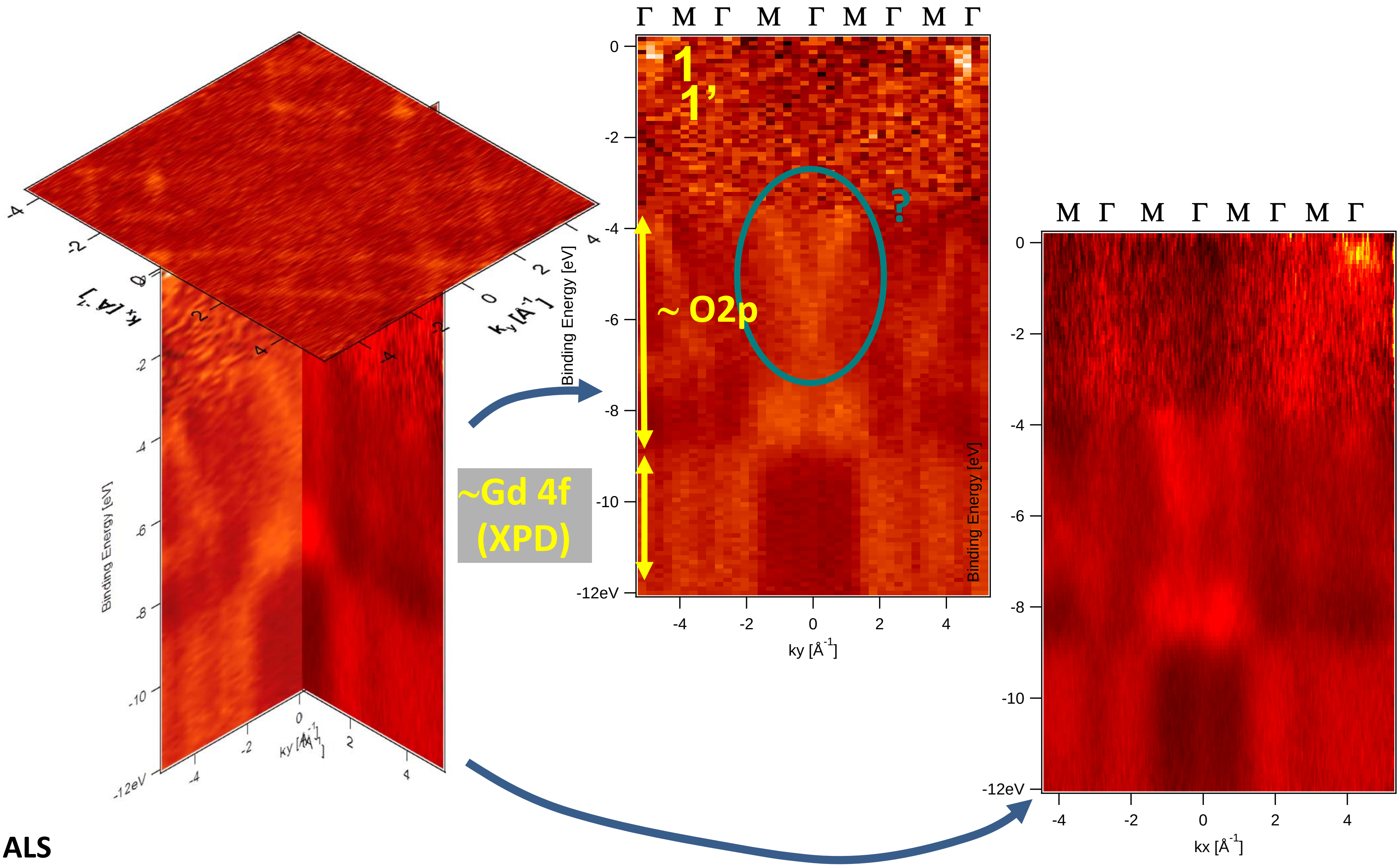

ALS

STO/GTO multilayer – Peak 1, 1’ compared to 2DEG on STO

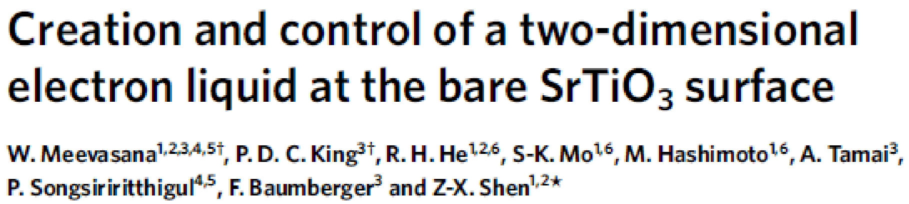

Creation and control of a two-dimensional electron liquid at the bare $SrTiO_3$ surface

W. Meevasana[1,2,3,4,5†], P. D. C. King[3†], R. H. He[1,2,6], S-K. Mo[1,6], M. Hashimoto[1,6], A. Tamai[3], P. Songsiriritthigul[4,5], F. Baumberger[3] and Z-X. Shen[1,2★]

Blowup of our data

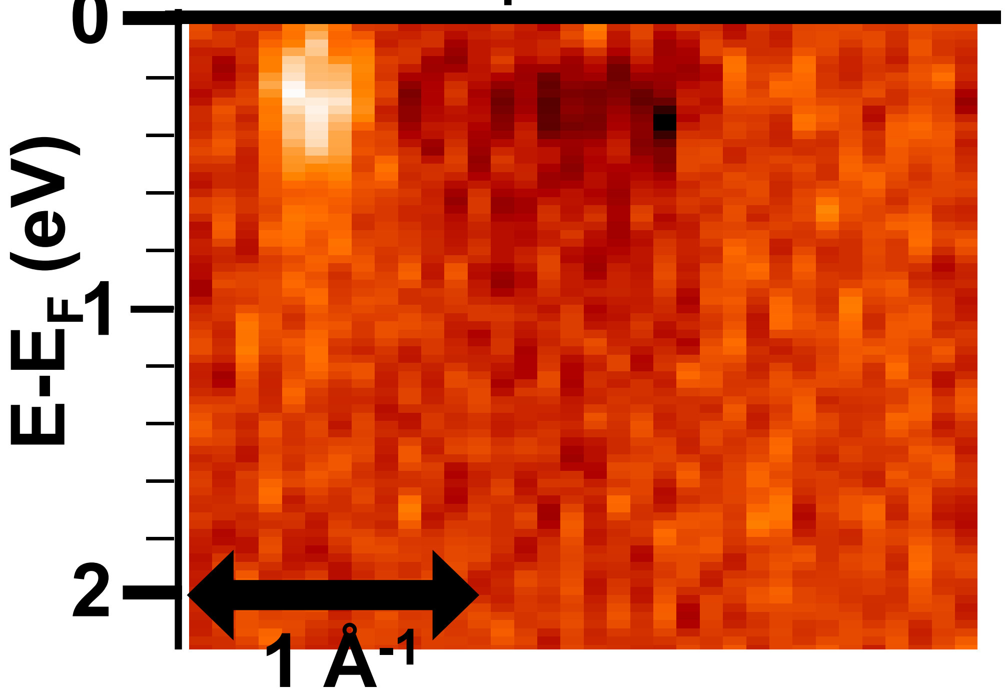

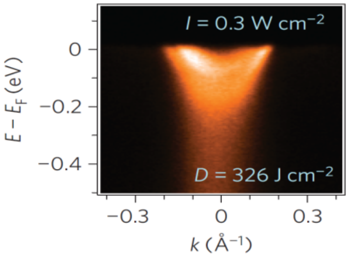

Same scales

Nature Materials <u>10</u> , 114 (2011)

→1 looks like interface 2DEG,
but where is LHB?

Swiss Light Source

GdTiO$_3$—Total & Projected DOSs

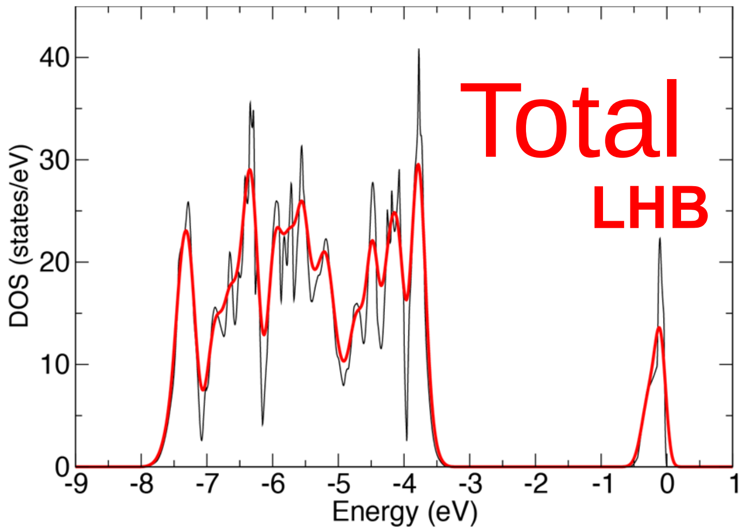

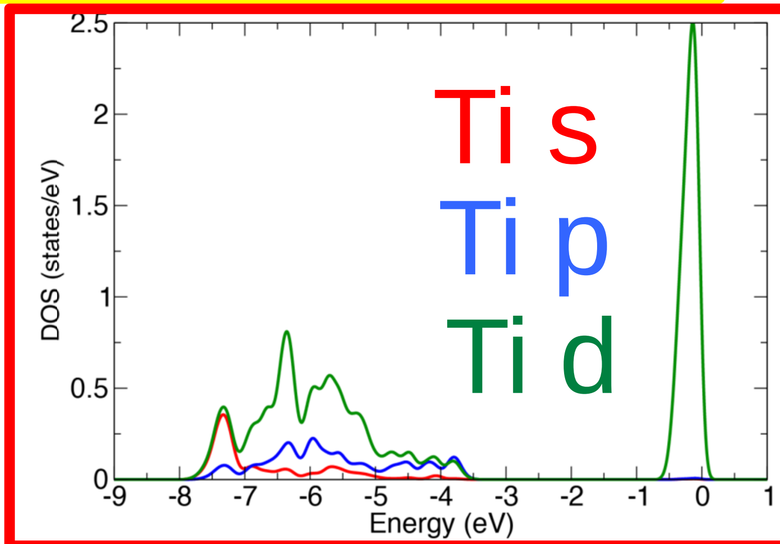

On Res.

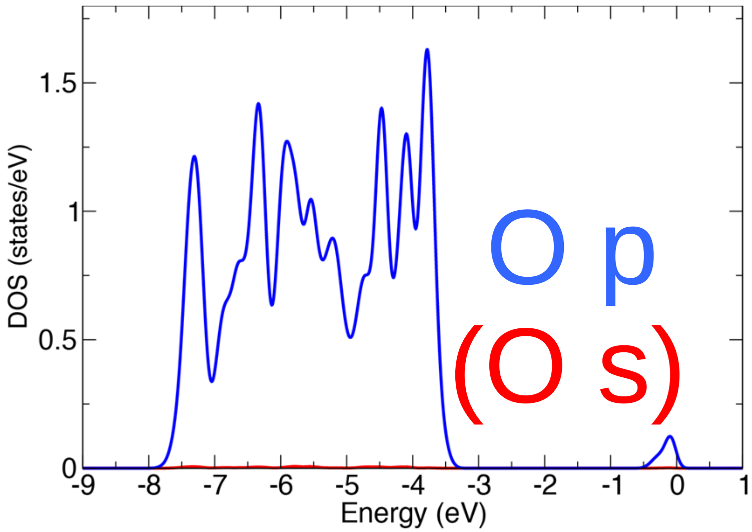

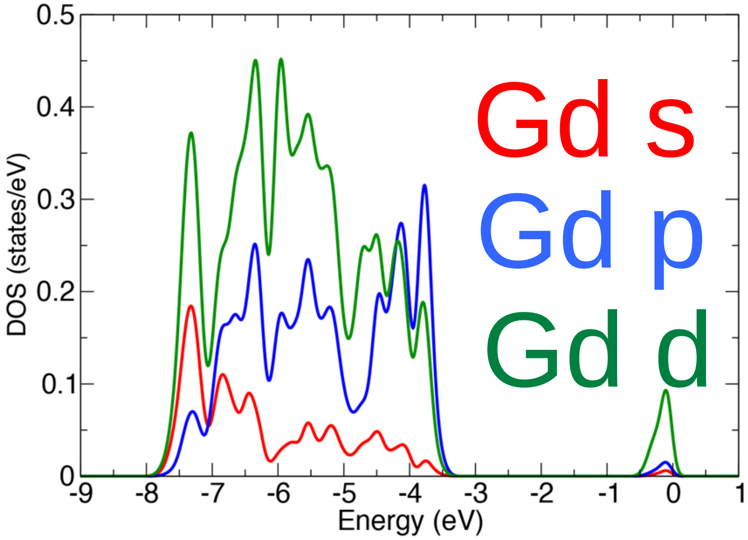

A. Janotti, C. Van de Walle

STO/GTO multilayer-Resonant photoemission
X-ray absorption scan over Ti 2p edge

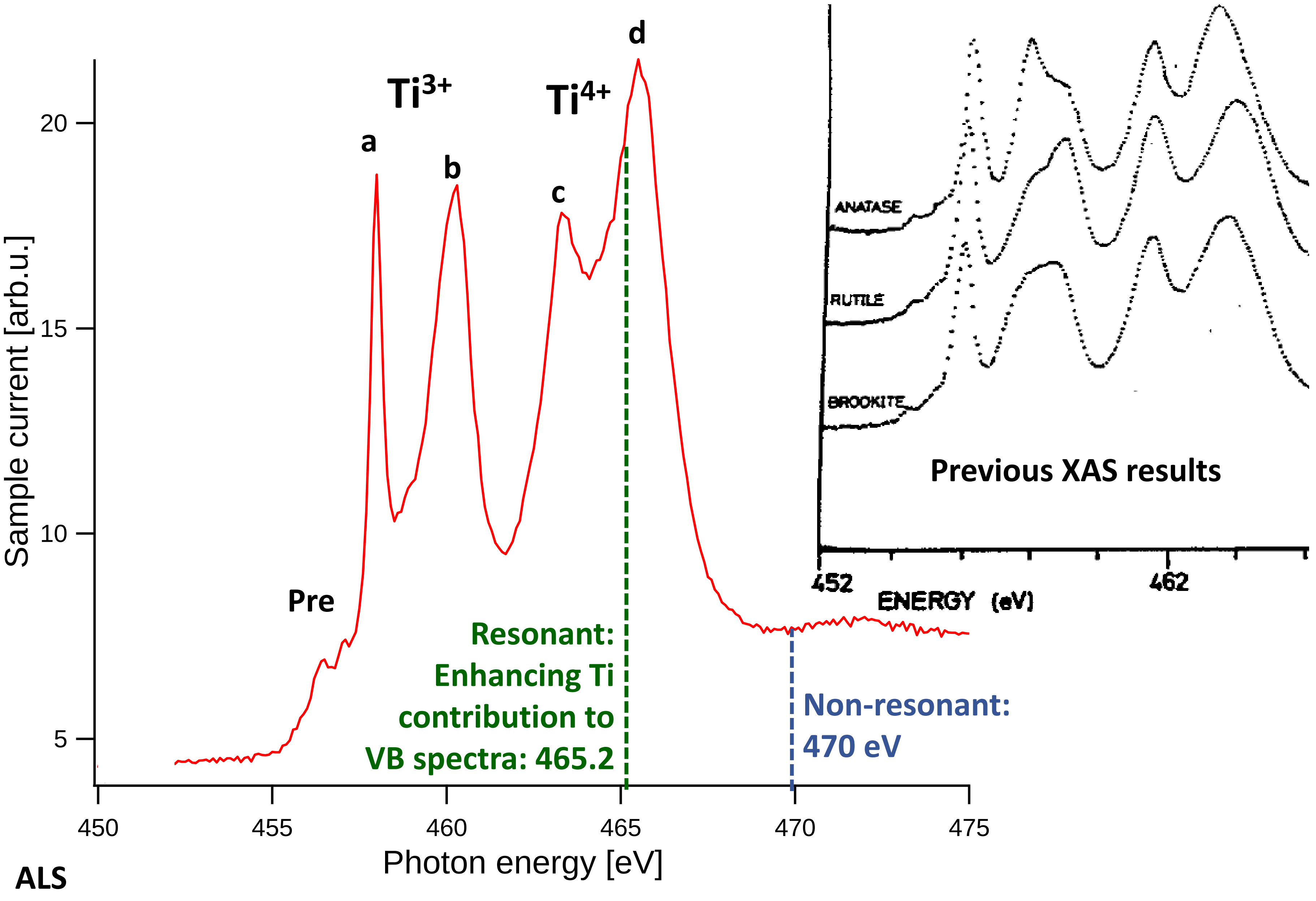

Resonant: Enhancing Ti contribution to VB spectra: 465.2

Non-resonant: 470 eV

Previous XAS results

ALS

STO/GTO--Resonant valence-band photoemission
Ti 2p edge → enhanced Ti contributions for peak 1

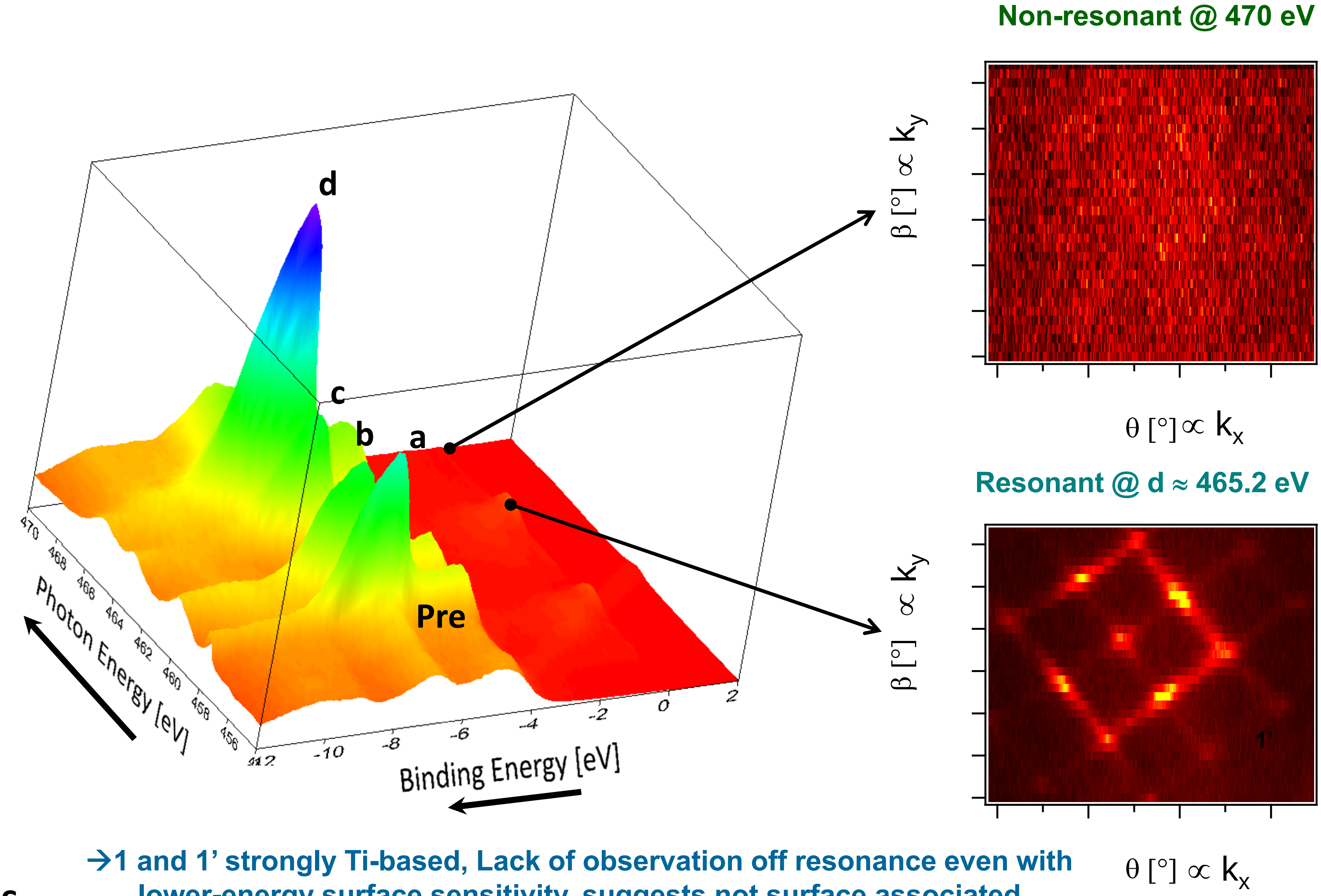
Non-resonant @ 470 eV

Resonant @ d ≈ 465.2 eV

→1 and 1' strongly Ti-based, Lack of observation off resonance even with lower-energy surface sensitivity, suggests not surface associated

ALS

STO/GTO multilayer-Dispersion of Peaks 1 and 1’ : ARPES @ 833.0 eV (non-resonant)

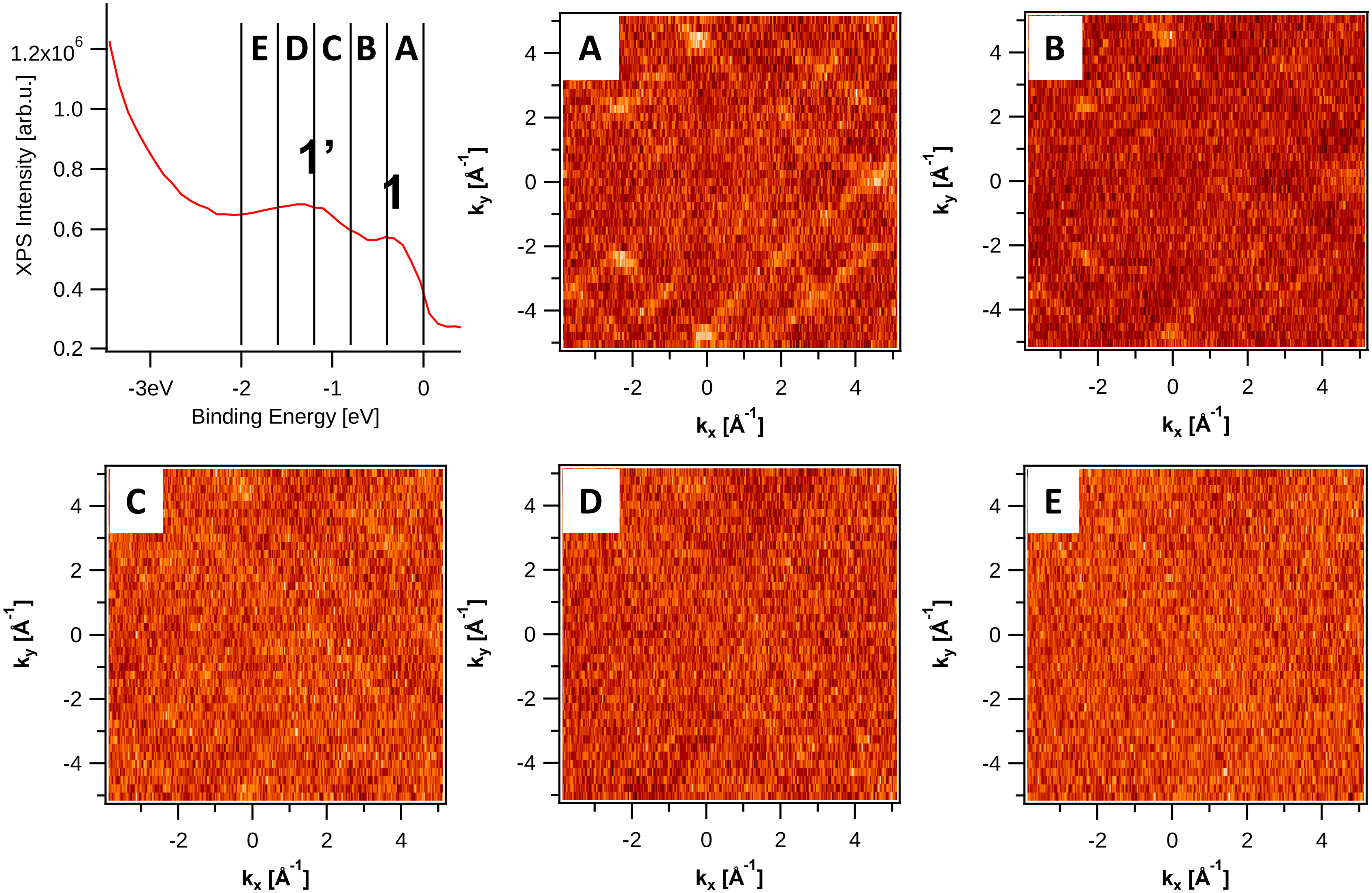

ALS

STO/GTO multilayer-Dispersion of Peaks 1 and 1’ : ARPES @ 465.2 eV (Ti resonant)

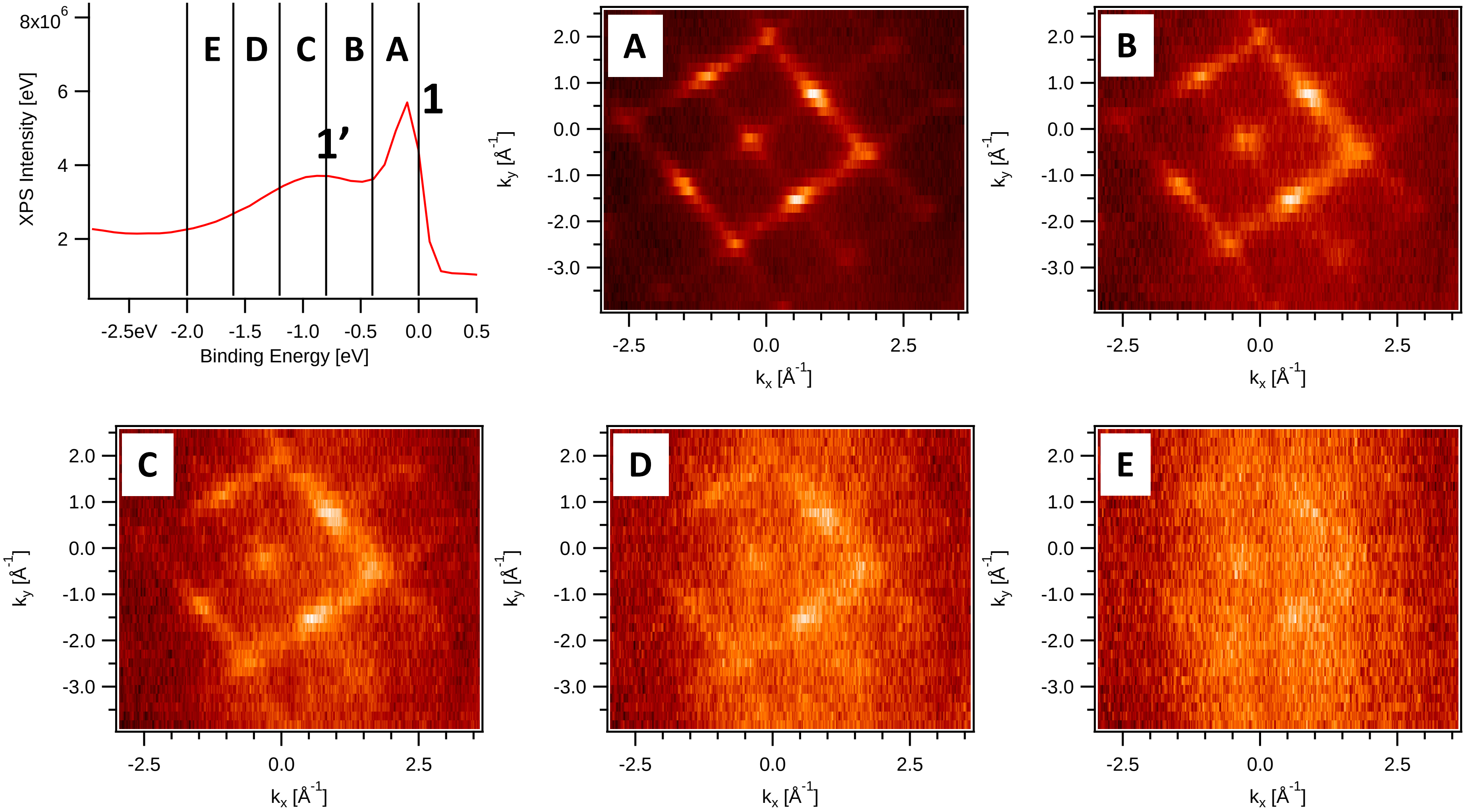

- 1, 1’ dispersions identical, states strongly mixed
- 1 has greater or different Ti character

ALS

Resonant effects: $SrTiO_3/GdTiO_3$ multilayer
Sweeping the photon energy through the Gd M_5 resonance

Index of refraction: $n = 1 - \delta - i\beta$

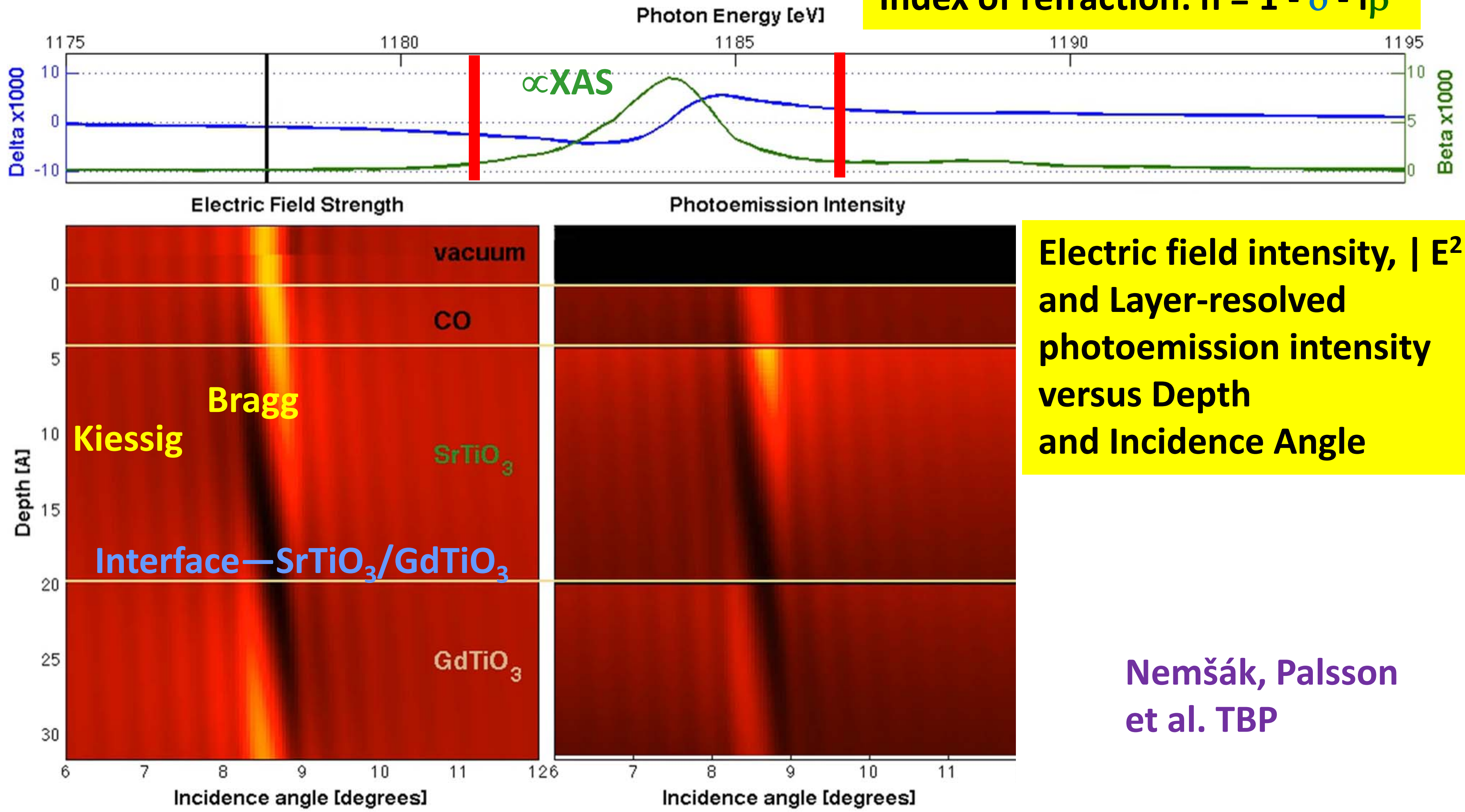

Electric field intensity, $|E^2|$ and Layer-resolved photoemission intensity versus Depth and Incidence Angle

Nemšák, Palsson et al. TBP

Going below and above the edge: A new trick to focus better on buried interfaces

Theoretical simulations vs. expt.—1182-just below Gd M_5 edge SW emphasizng STO

Rocking curves

Theory E^2 -field strength

Theory

Experiment

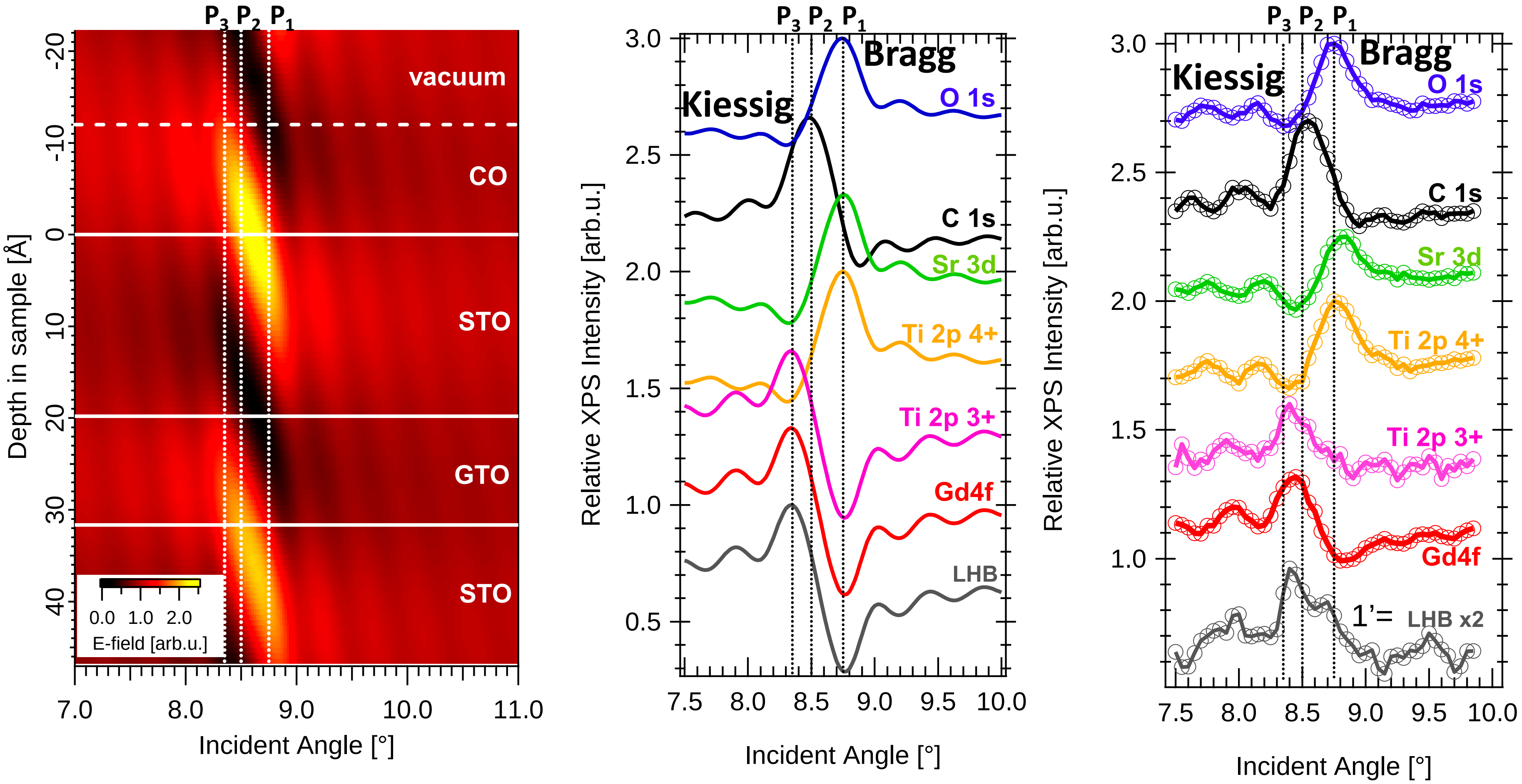

→Ti 4+ in STO, Ti 3+ in GTO, 1' = LHB in GTO

Swiss Light Source

Theoretical simulations vs. expt.—1187-just above Gd M_5 edge SW emphasizng STO/GTO interface

Theory: E^2 -field strength

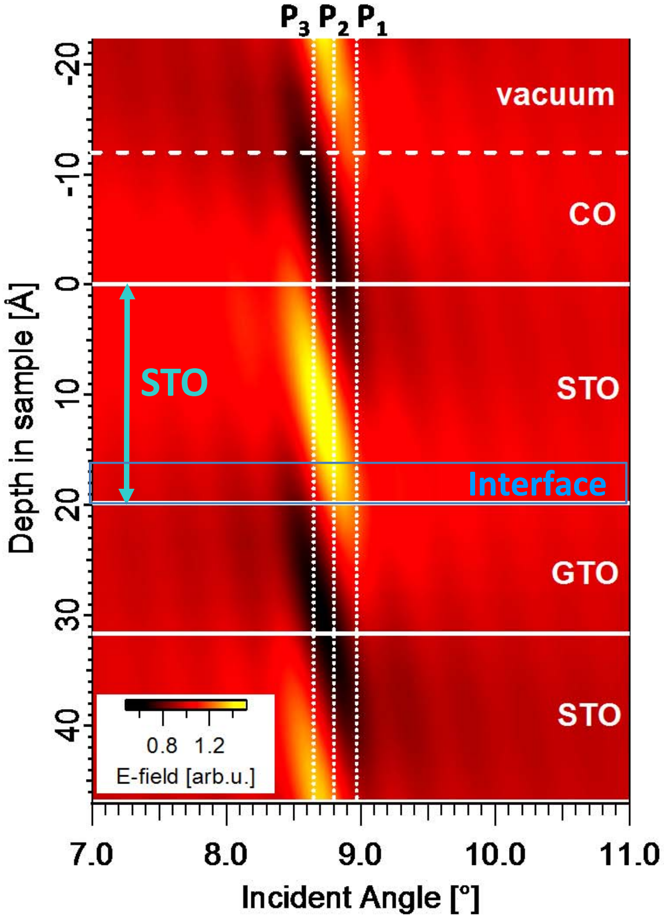

Rocking curves

Theory

Experiment

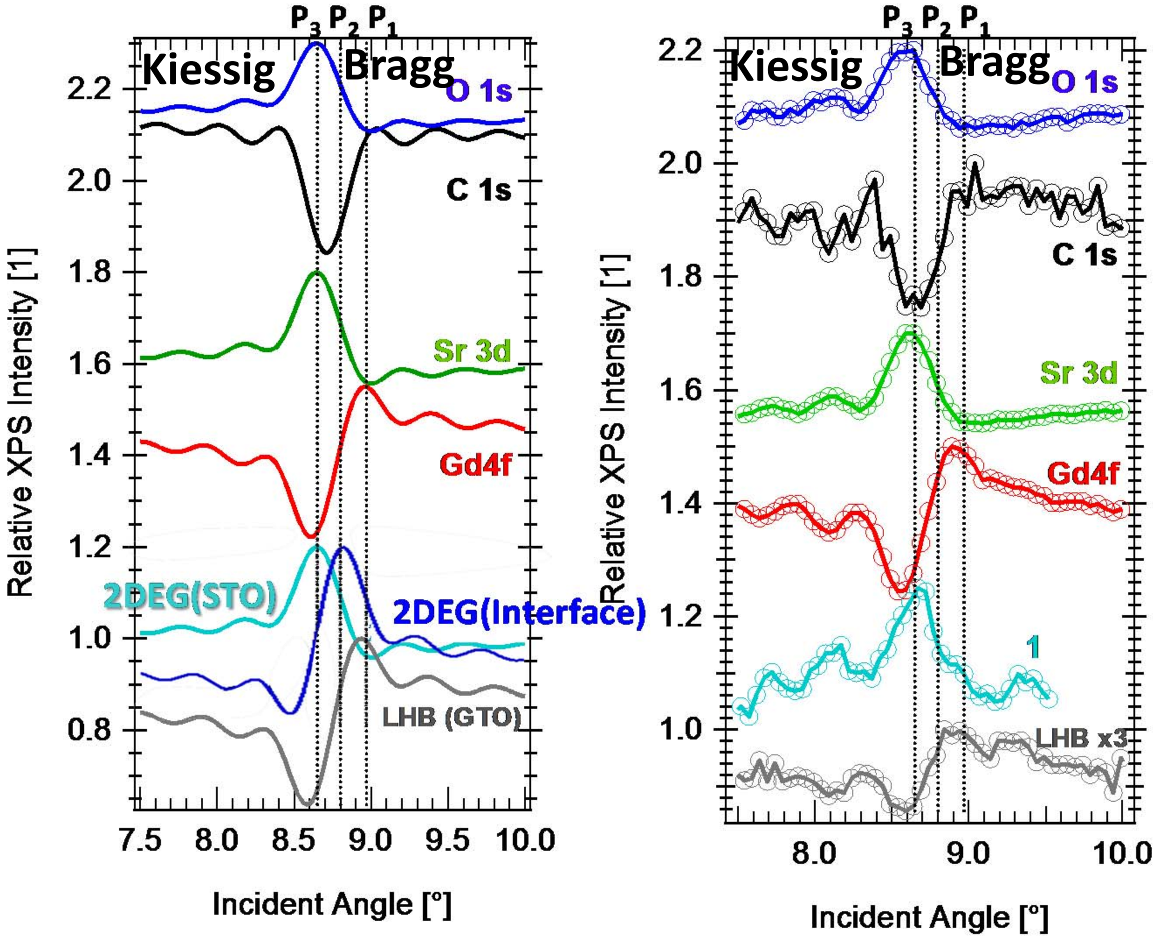

Swiss Light Source

Peak 1 = 2DEG→2DEG occupies the full STO layer

Theory/expt. comparison: $(STO)_5(GTO)_2$ superlattice

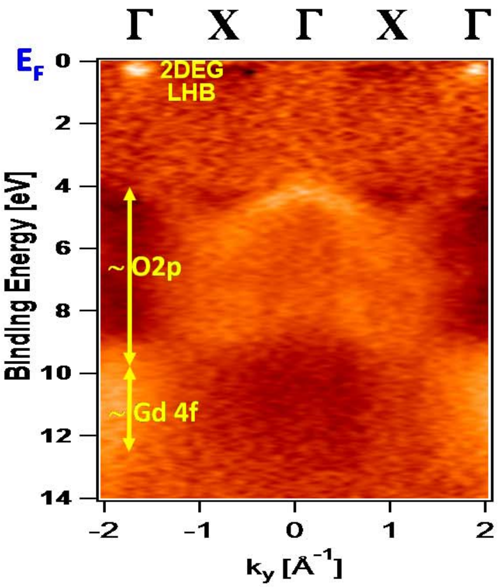

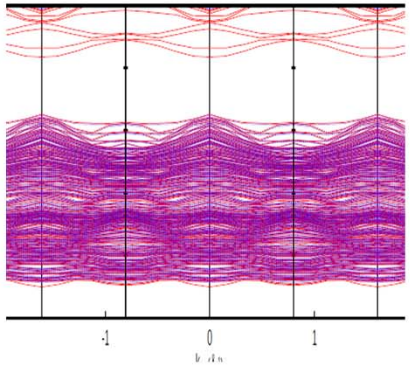

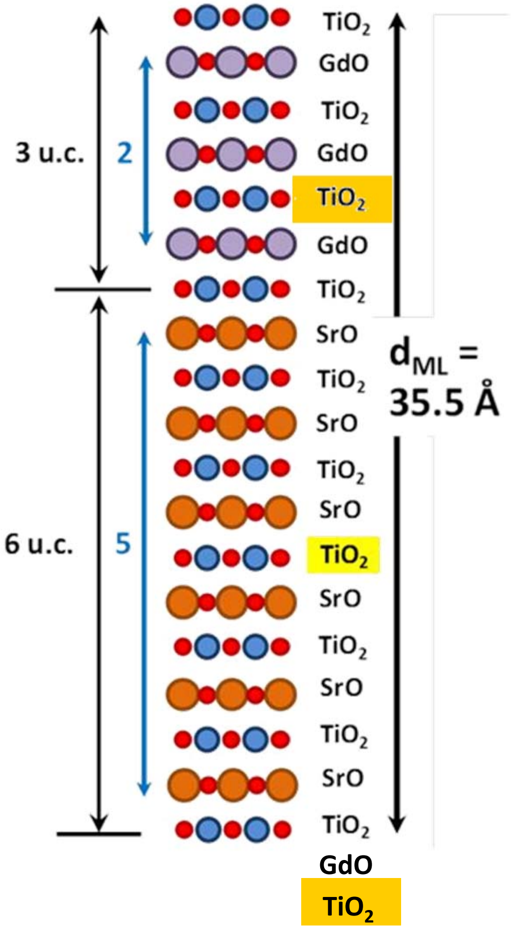

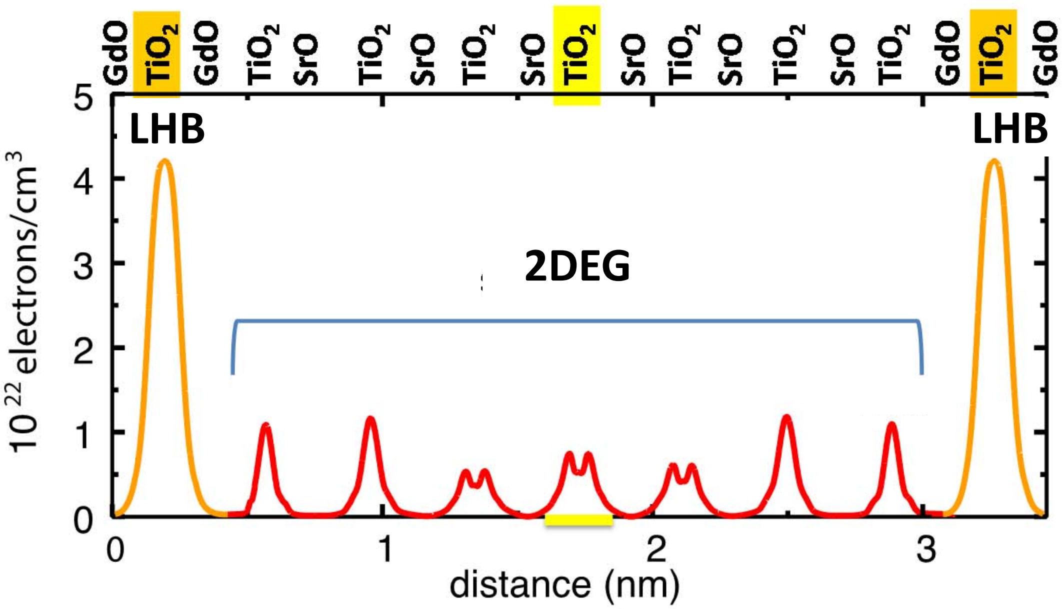

LDA+hybrid functional theory agrees: 2DEG occupies full STO layer

A. Janotti, L. Bjaalie,
C. Van de Walle

STO_5/GTO_2 (001): cross-section weighted superlattice density of states without 4f, comp. to expt.

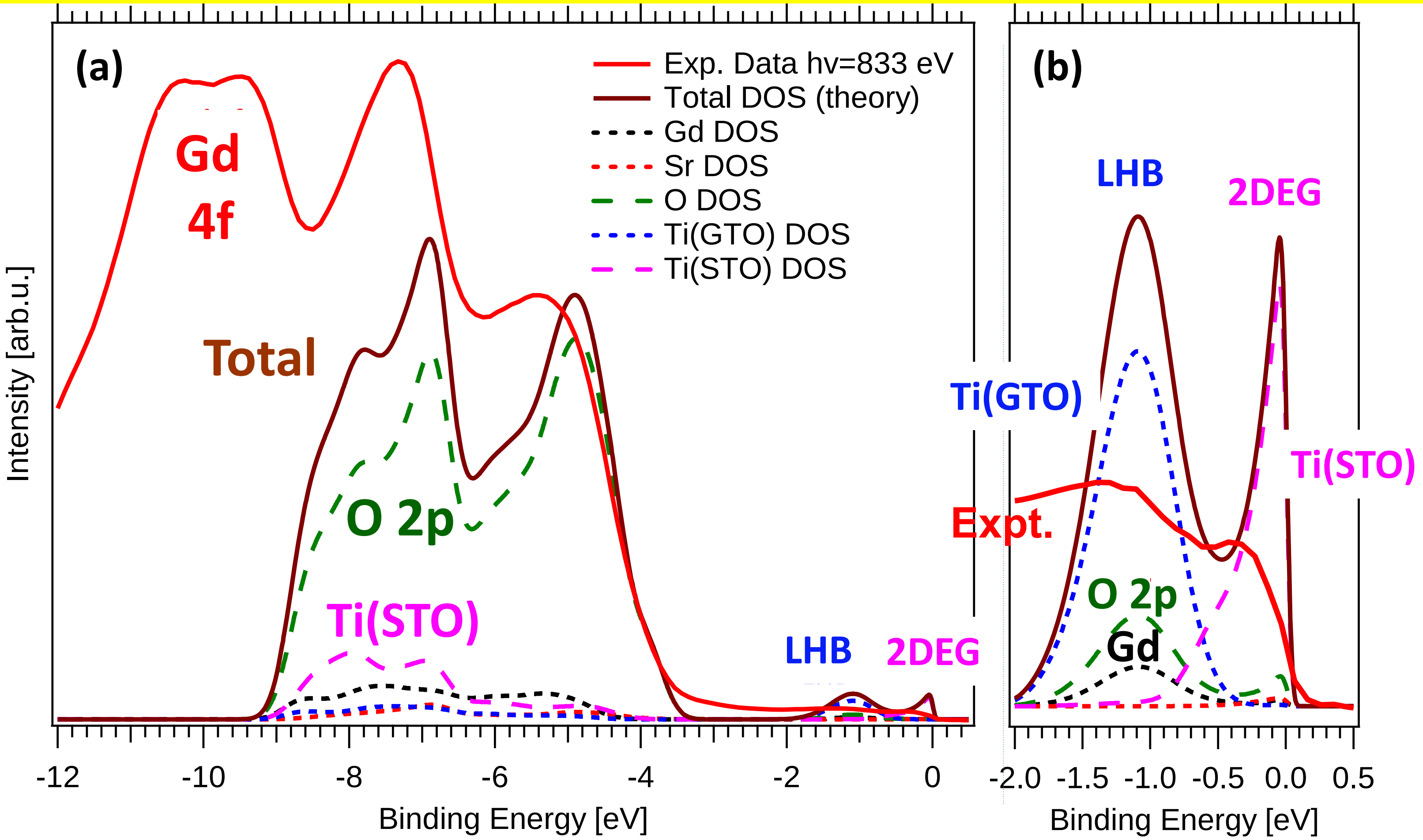

A. Janotti, L. Bjaalie, C. Van de Walle

Conclusions: Standing-Wave and Resonant PS and ARPES of $SrTiO_3/GdTiO_3$

- Determined the LHB and 2DEG in energy
- Measured the k-resolved bands of both, evidence for intermixing of LHB and 2DEG
- Determined the spatial localization of the 2DEG as throughout the entire STO layer from standing-wave rocking curve analysis
- Results consistent with 2DEG tunneling subband spacing measurements and tight binding, LDA + hybrid functional calculations

CSF and S. Nemšák,, J. Electron Spect. ,
195, 409–422 (2014):
S. Nemšák, et al., TBP

Soft →hard x-rays and standing waves: a few example studies

$SrTiO_3/La_{2/3}Sr_{1/3}MnO_3$-tunnel junction

Depth-resolved composition, dielectric properties, bonding,
k-resolved electronic structure

$SrTiO_3/GdTiO_3$-2D electron gas

Depth-resolved composition, charge states,
k-resolved electronic, structure

Fe/MgO-tunnel junction

Depth-resolved composition, chemical states,
magnetization

$SrTiO_3$ and Ga(Mn)As

Projected densities of states

Fe_2O_3 reacting with NaOH, CsOH, and H_2O

Using standing wave XPS to probe the solid/gas and solid/liquid interface: some first ambient pressure results

Three ways to scan a standing wave formed in reflection from single-crystal Bragg planes, or a multilayer mirror

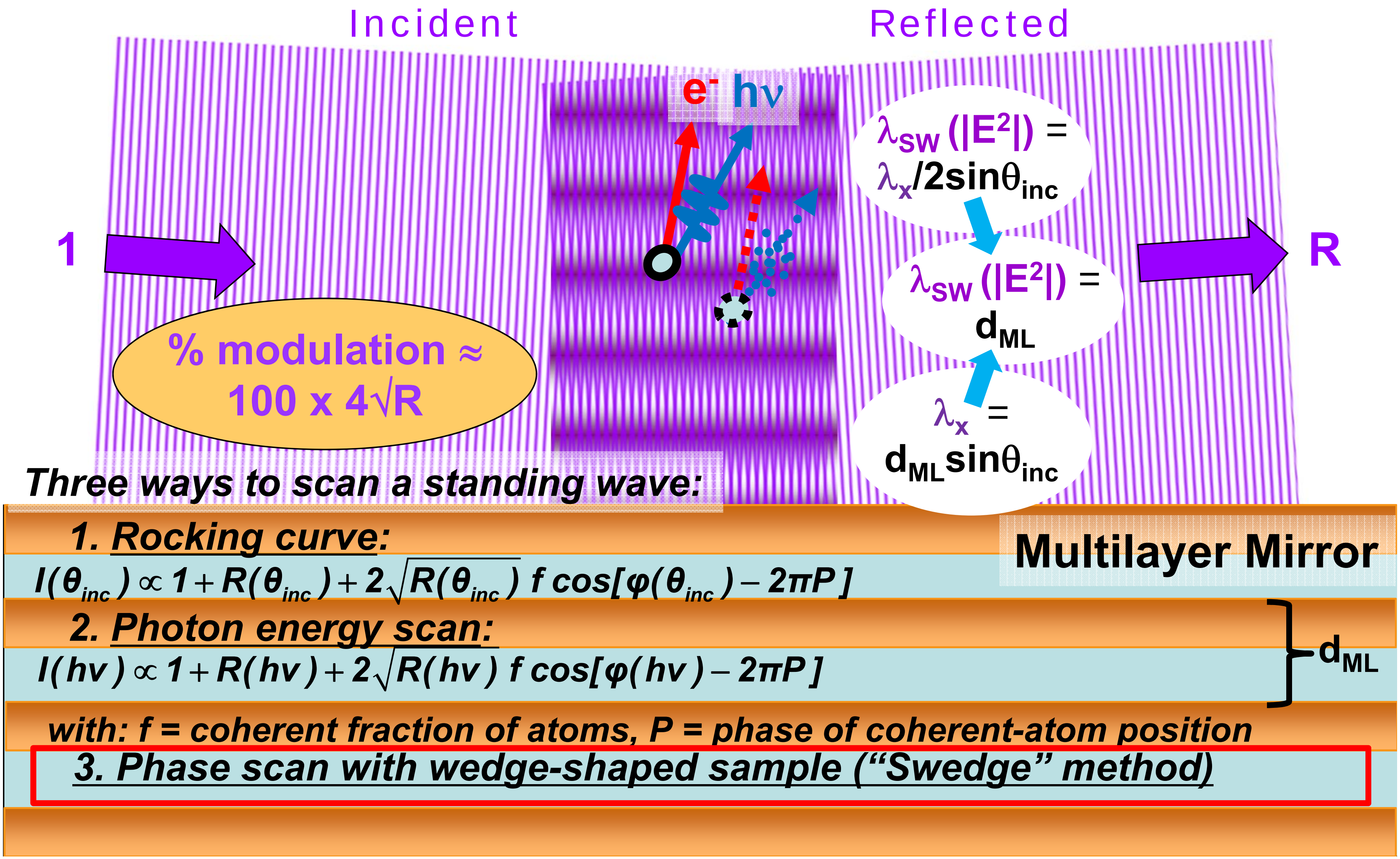

$\lambda_{SW}(|E^2|) = \lambda_x/2\sin\theta_{inc}$

$\lambda_{SW}(|E^2|) = d_{ML}$

$\lambda_x = d_{ML}\sin\theta_{inc}$

% modulation ≈ 100 x 4√R

Three ways to scan a standing wave:

1. Rocking curve:

$$I(\theta_{inc}) \propto 1 + R(\theta_{inc}) + 2\sqrt{R(\theta_{inc})}\, f \cos[\varphi(\theta_{inc}) - 2\pi P]$$

2. Photon energy scan:

$$I(h\nu) \propto 1 + R(h\nu) + 2\sqrt{R(h\nu)}\, f \cos[\varphi(h\nu) - 2\pi P]$$

with: f = coherent fraction of atoms, P = phase of coherent-atom position

3. Phase scan with wedge-shaped sample ("Swedge" method)

Probing Buried Interfaces: The Standing Wave-Wedge ("Swedge") Method

Example: The MgO/Fe magnetic tunnel junction interface

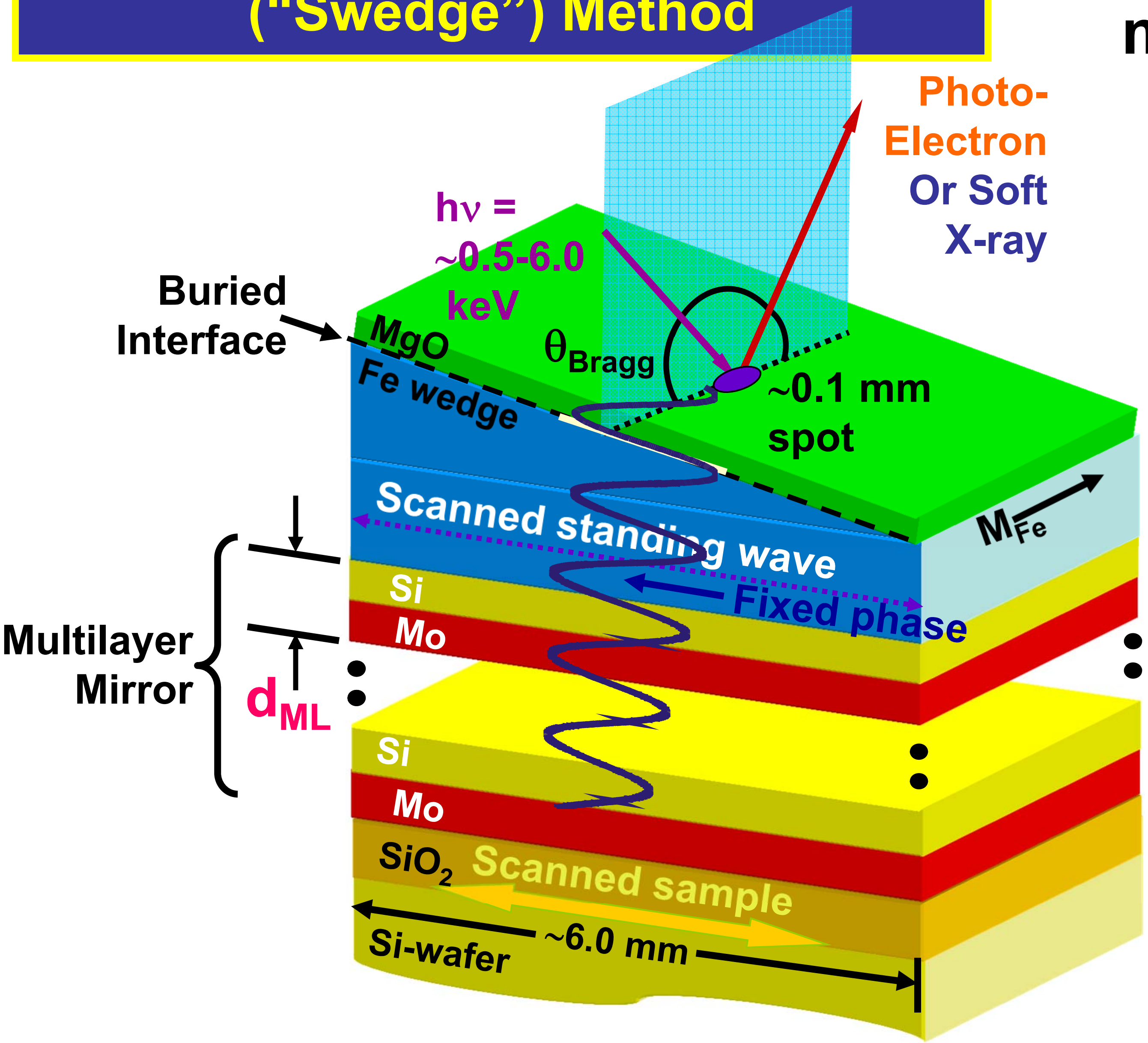

λ_{SW} ($|E^2|$) = $\lambda_x/2\sin\theta_{inc}$ $\approx d_{ML}$

1st order Bragg: $\lambda_x\ =2d_{ML}\sin\theta_{Bragg}$

MgO/Fe tunnel junction- the real interface

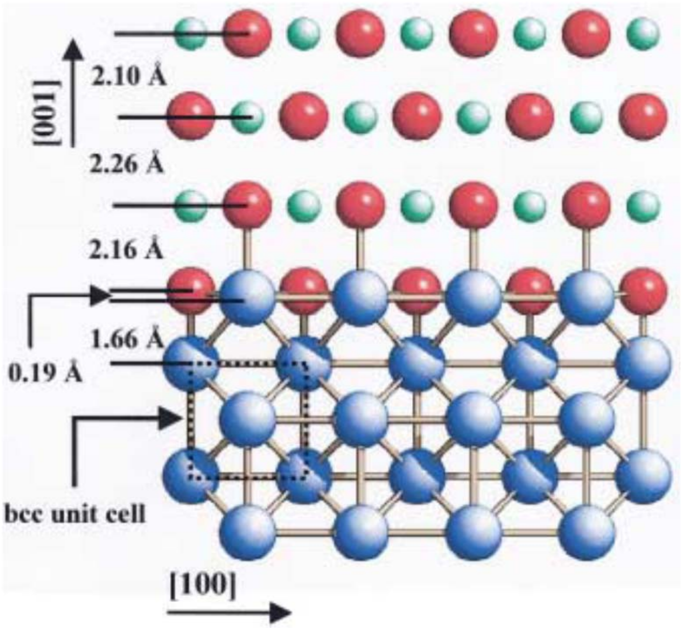

Meyerheim PRL 87, 076102 (2001).

- ***Is there FeO at the interface?***
- ***What is the density of states at the interface?***
- ***Δ_1 band controls tunneling? Can we see bands at epitaxial interfaces? (Soleil-June, 2014!)***

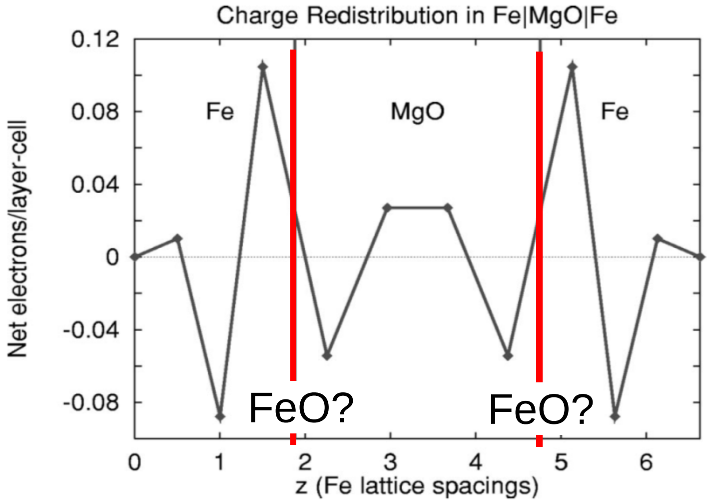

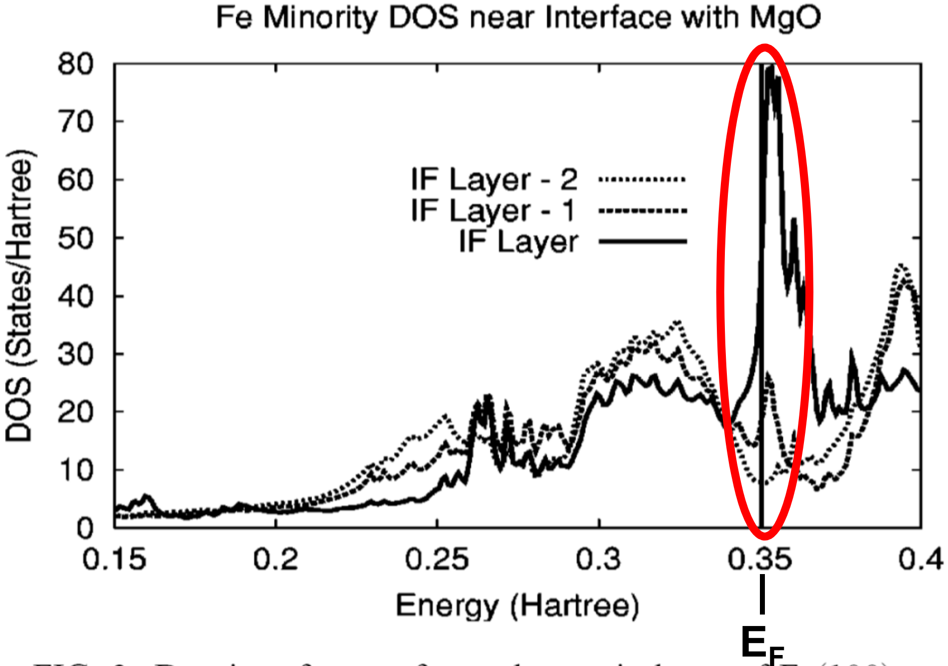

FIG. 3. Density of states for each atomic layer of Fe(100) near an interface with MgO. One hartree equals 27.2 eV.

Butler et al.,PRB 63, 054416 (2001);
Mathon & Umerski, PRB 63, 220403 (2001);
Mertig et al., PRB 73, 214441 (2006)

MgO/Fe tunnel junction-Δ_1 states dominant in tunneling for ideal interface

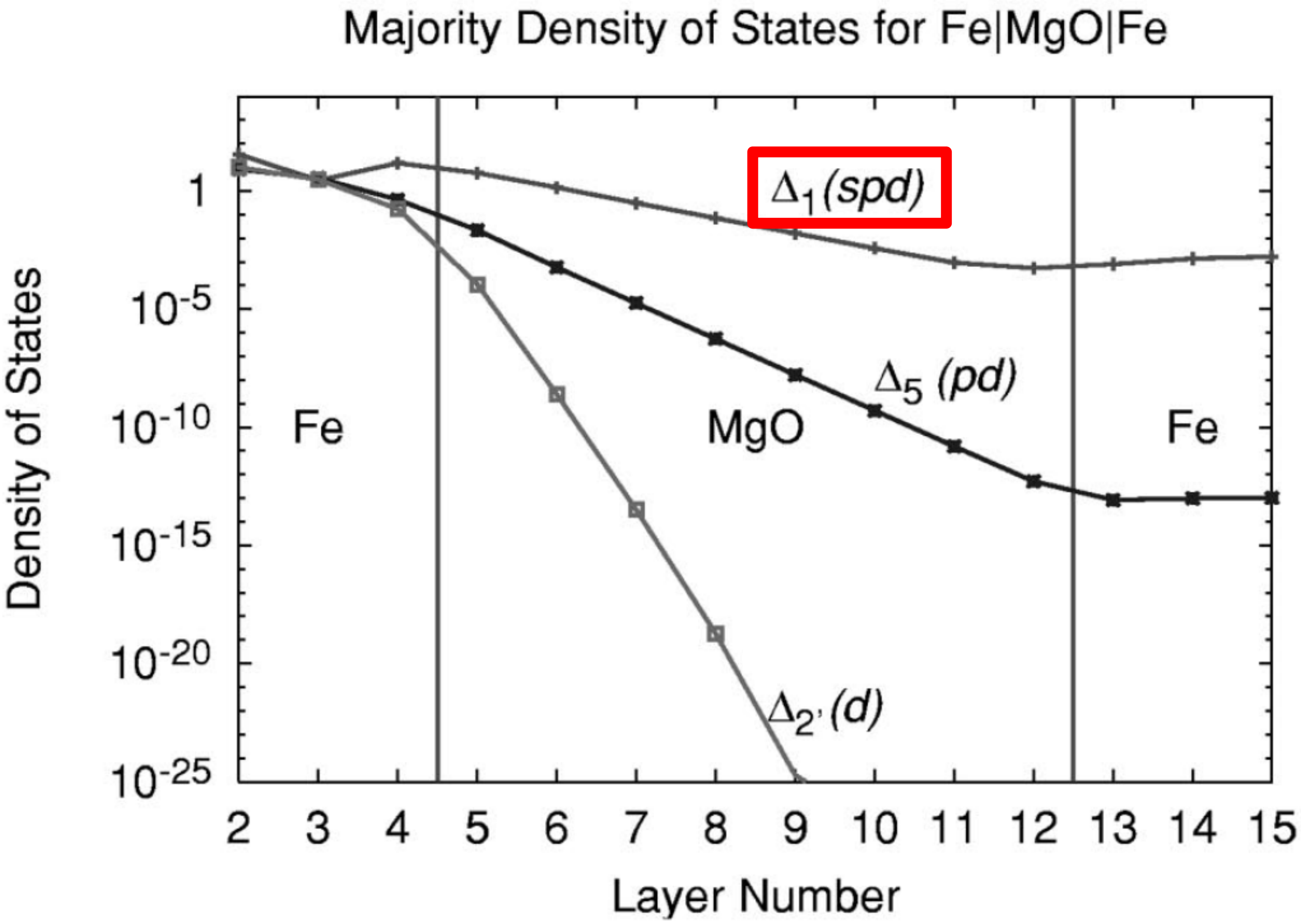

Butler et al.,PRB 63, 054416 (2001)

Soft x-ray standing-wave wedge scans through a magnetic tunnel junction

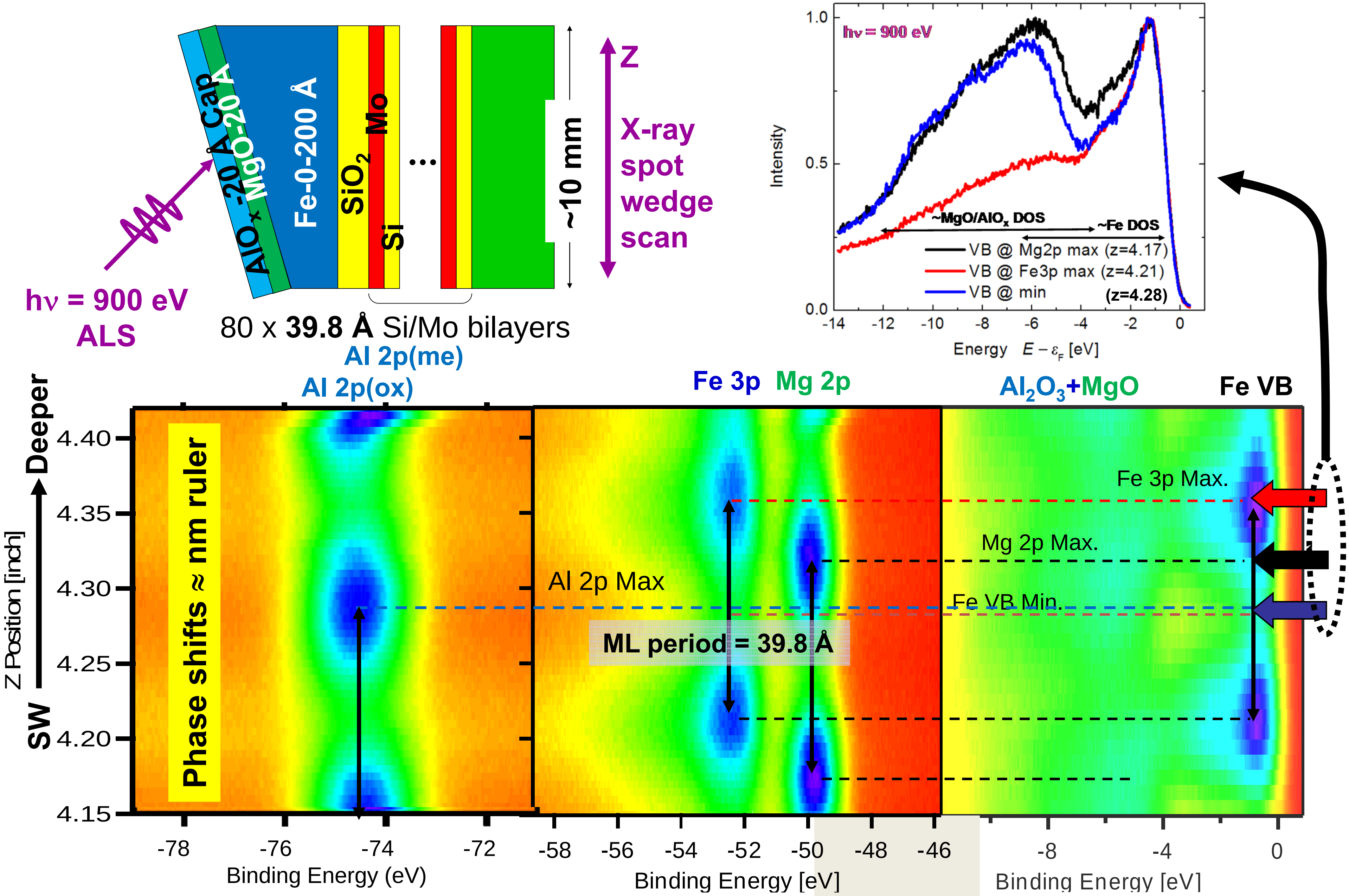

Balke, Yang et al., Phys. Rev. B 84, 184410 (2011)

Magnetic Circular Dichroism with Standing Wave Excitation- MgO/Fe, hν = 900 eV

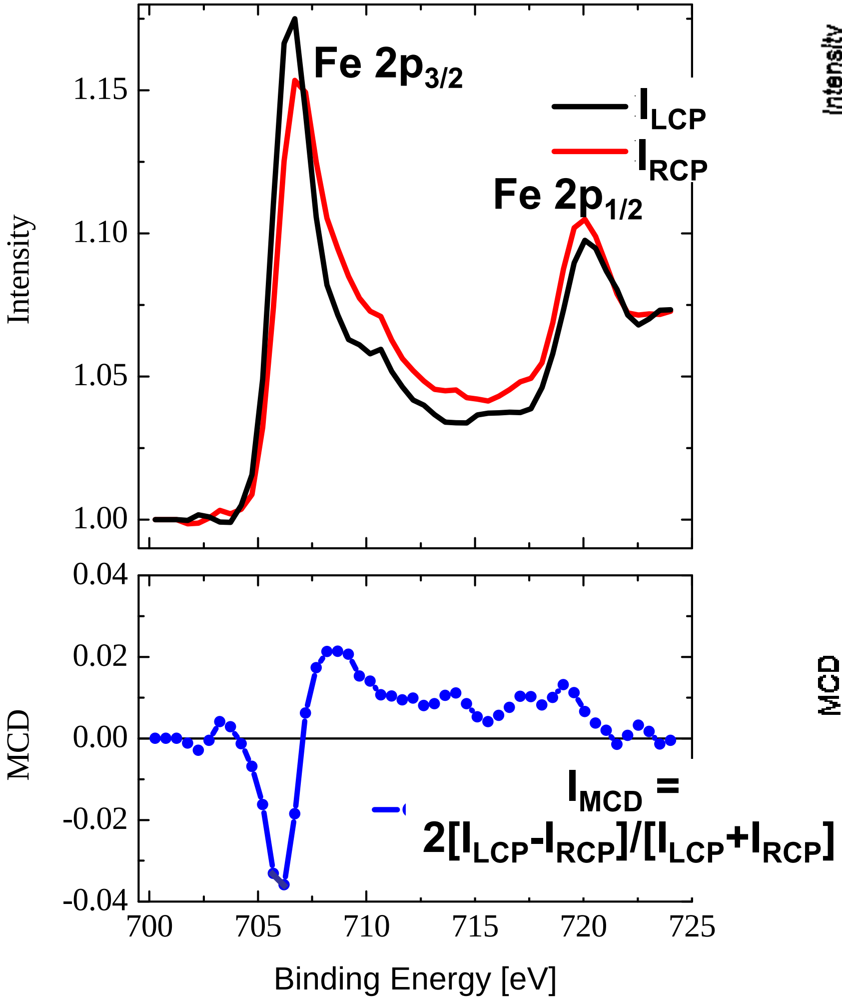

I_{MCD} = $2[I_{LCP}-I_{RCP}]/[I_{LCP}+I_{RCP}]$

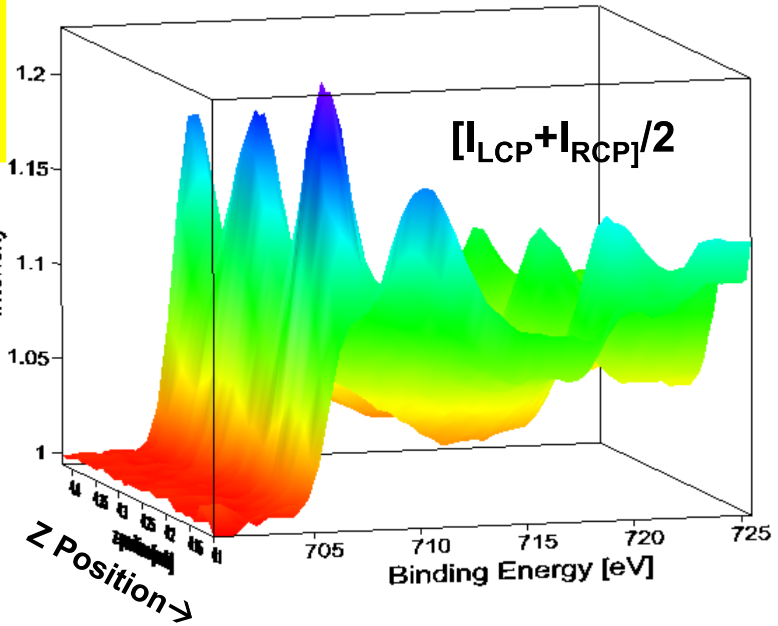

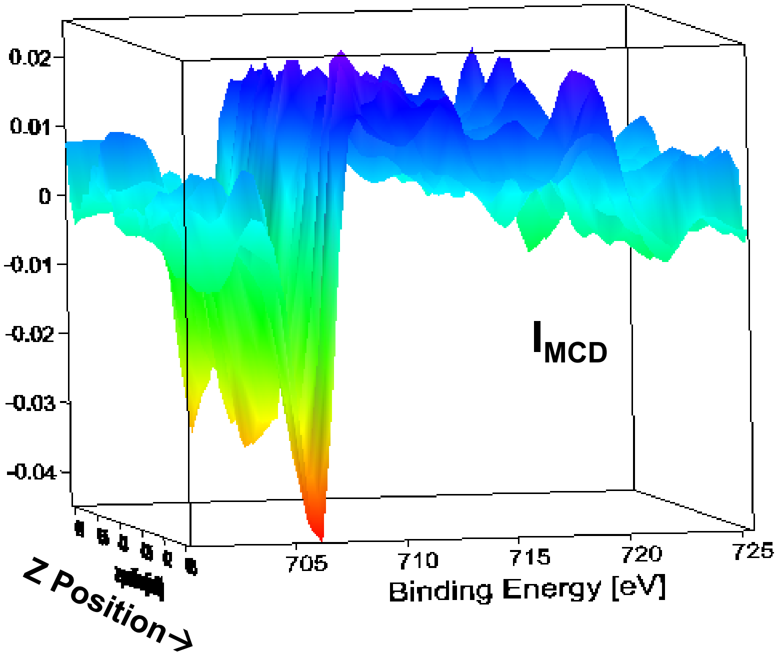

Yang, Balke et al., Phys. Rev. B 84, 184410 (2011)

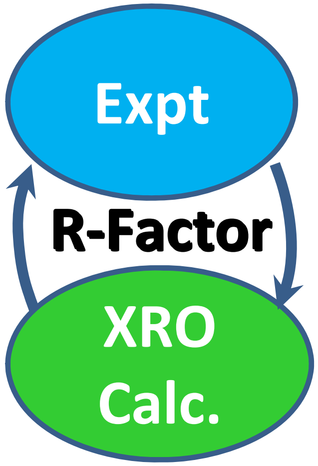

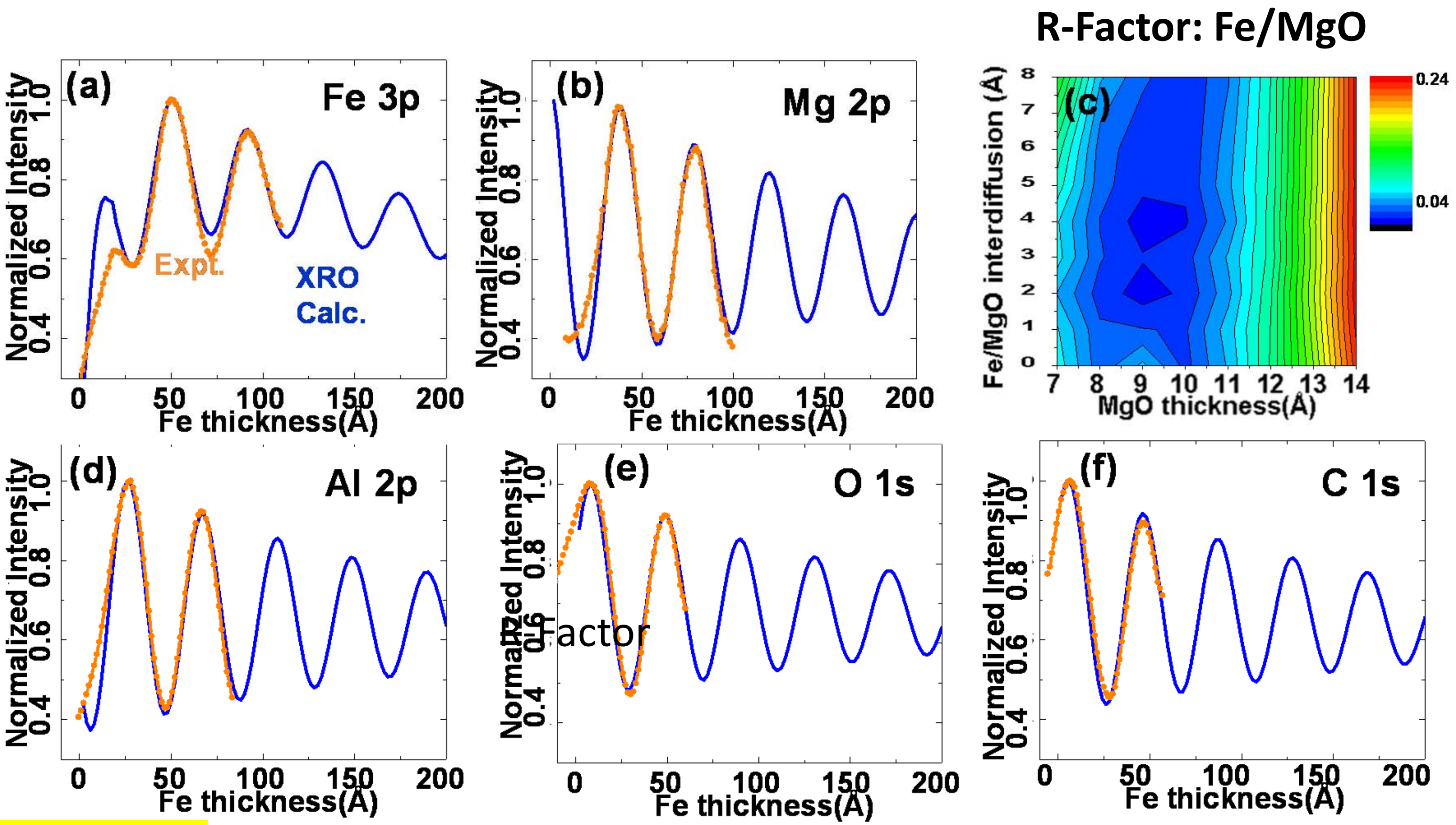

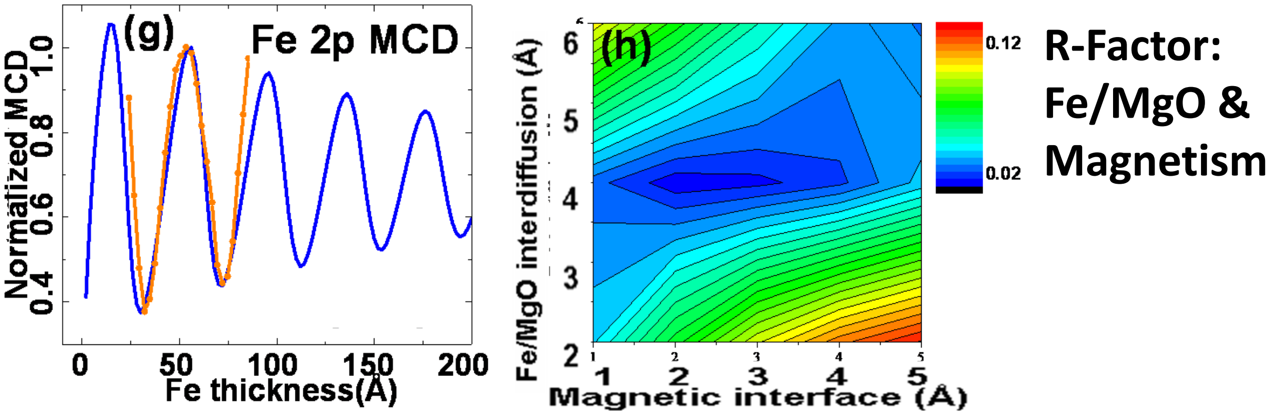

Standing wave/wedge analysis of an Fe/MgO tunnel junction multilayer:
final fits of expt. to x-ray optical calcs.

Balke, Yang et al., Phys. Rev. B 84, 184410 (2011)

Final profiles of concentration and magnetization

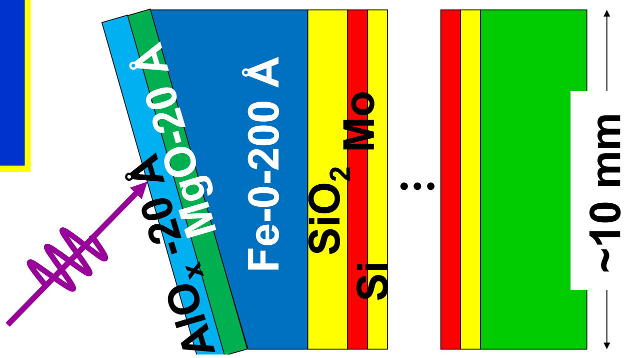

Concentration

Magnetization

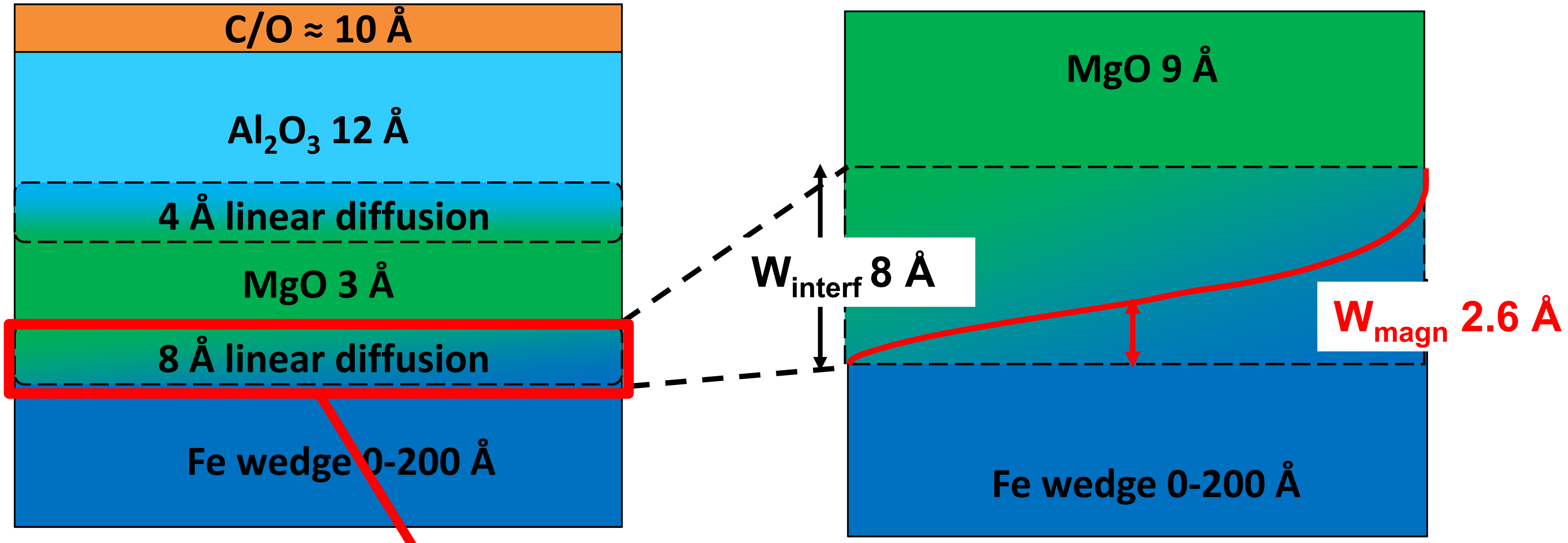

And what is the density of states in this interface region?

Yang, Balke et al., Phys. Rev. B 84, 184410 (2011)

Standing wave/wedge derivation of depth-dependent densities of states: Fe/MgO tunnel junction

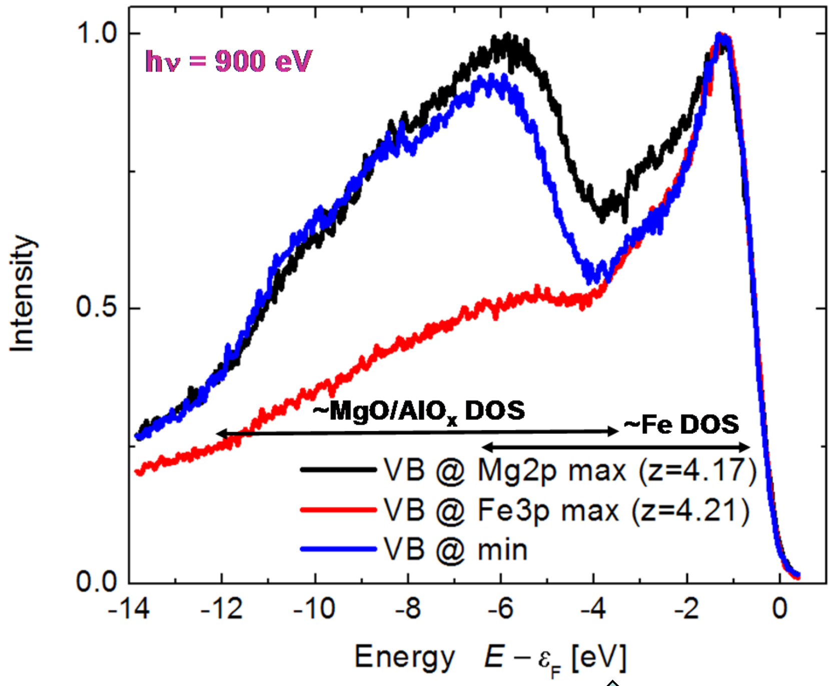

→Oxidation at the Fe/MgO interface

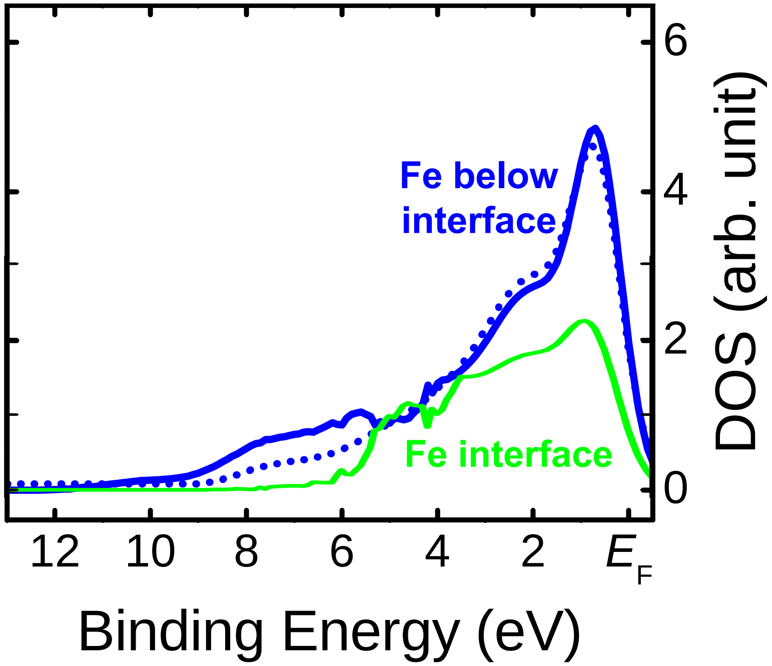

Self-consistent X-ray optical modeling of layer-resolved densities of states

Yang, Balke et al., Phys. Rev. B 84, 184410 (2011)

Conclusions: Standing-Wave Soft X-Ray Photoemission of the Fe/MgO Interface

- Measured the depth distribution of concentration and magnetization (via core-level PMCD) through the interface with ca. ±2 Å resolution
- Resolved the density of states into interface and bulk Fe components, indicating Fe oxidation at the interface

Yang, Balke et al., Phys. Rev. B 84, 184410 (2011)

Soft →hard x-rays and standing waves: a few example studies

$SrTiO_3/La_{2/3}Sr_{1/3}MnO_3$-tunnel junction

Depth-resolved composition, dielectric properties, bonding, k-resolved electronic structure

$SrTiO_3/GdTiO_3$-2D electron gas

Depth-resolved composition, charge states, k-resolved electronic, structure

Fe/MgO-tunnel junction

Depth-resolved composition, chemical states, magnetization

$SrTiO_3$ and Ga(Mn)As

Single crystal Bragg standing wave→Projected densities of states

Fe_2O_3 reacting with NaOH, CsOH, and H_2O

Using standing wave XPS to probe the solid/gas and solid/liquid interface: some first ambient pressure results

Three ways to scan a standing wave formed in reflection from single-crystal Bragg planes, or a multilayer mirror

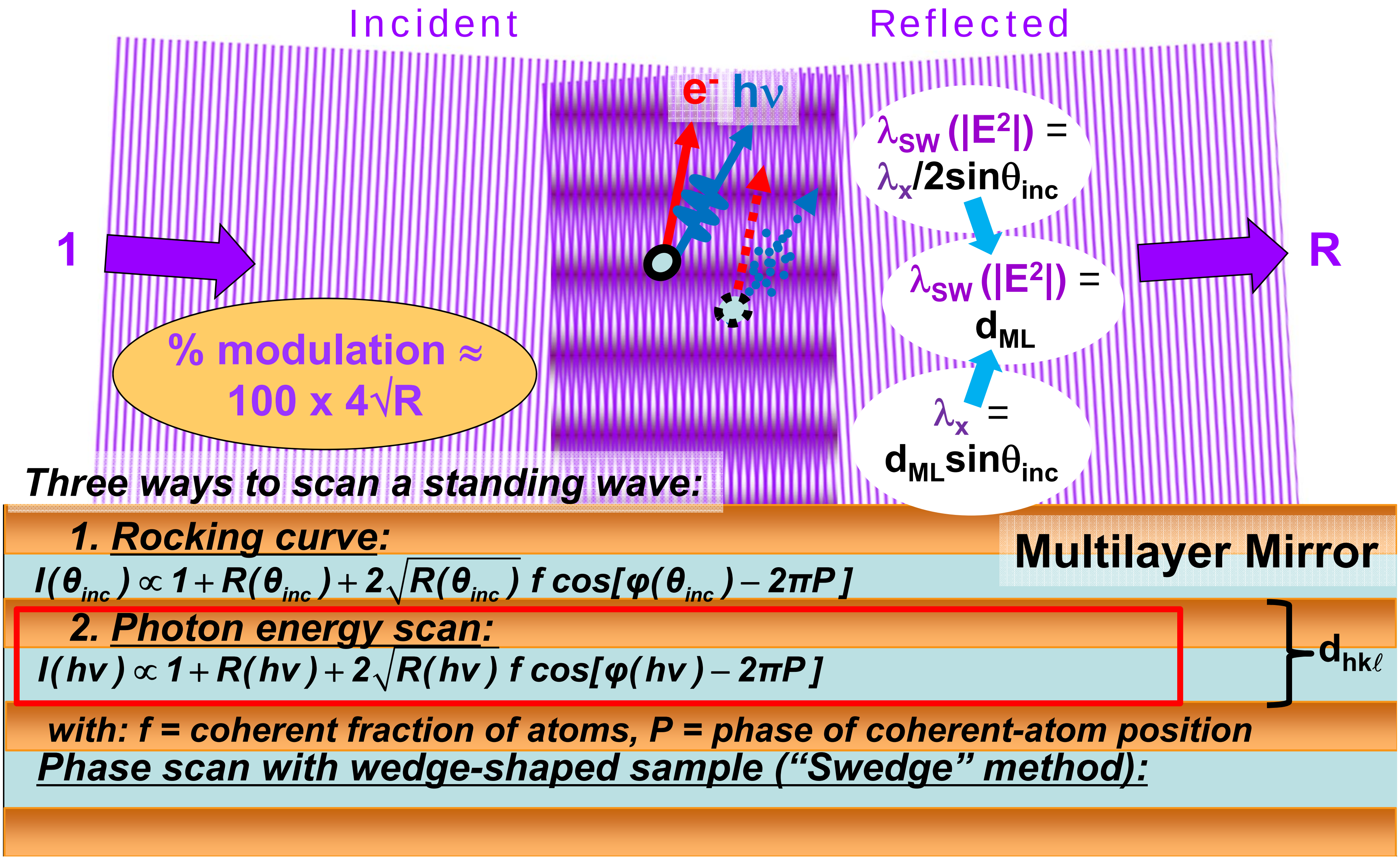

$\lambda_{SW}(|E^2|) = \lambda_x/2\sin\theta_{inc}$

$\lambda_{SW}(|E^2|) = d_{ML}$

$\lambda_x = d_{ML}\sin\theta_{inc}$

% modulation ≈ 100 x 4√R

Three ways to scan a standing wave:

1. <u>Rocking curve:</u>

$$I(\theta_{inc}) \propto 1 + R(\theta_{inc}) + 2\sqrt{R(\theta_{inc})}\, f \cos[\varphi(\theta_{inc}) - 2\pi P]$$

2. <u>Photon energy scan:</u>

$$I(h\nu) \propto 1 + R(h\nu) + 2\sqrt{R(h\nu)}\, f \cos[\varphi(h\nu) - 2\pi P]$$

with: f = coherent fraction of atoms, P = phase of coherent-atom position

<u>Phase scan with wedge-shaped sample ("Swedge" method):</u>

Bragg reflection from crystal planes:
Site-specific valence electronic structure of SrTiO3

hν = 2.75 keV

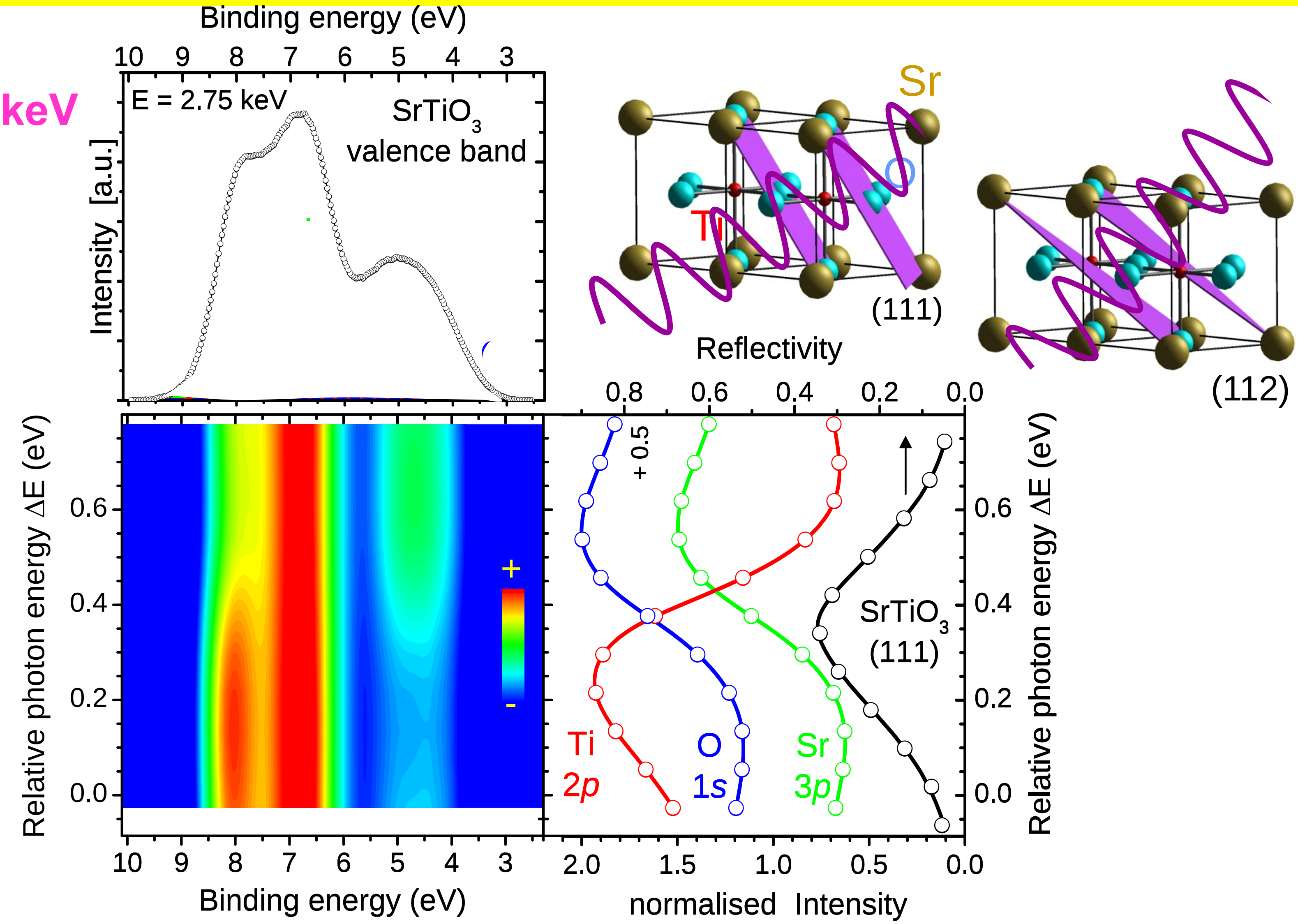

Valence band XSW *Core-level XSW*

T.-L. Lee et al., Solid State Communications 150 (2010) 553-ESRF,
also J. C. Woicik et al., Phys. Rev. B 64, 125115 (2001)-SSRL

Bragg reflection from crystal planes: Site-specific valence electronic structure of SrTiO3

hν = 2.75 keV

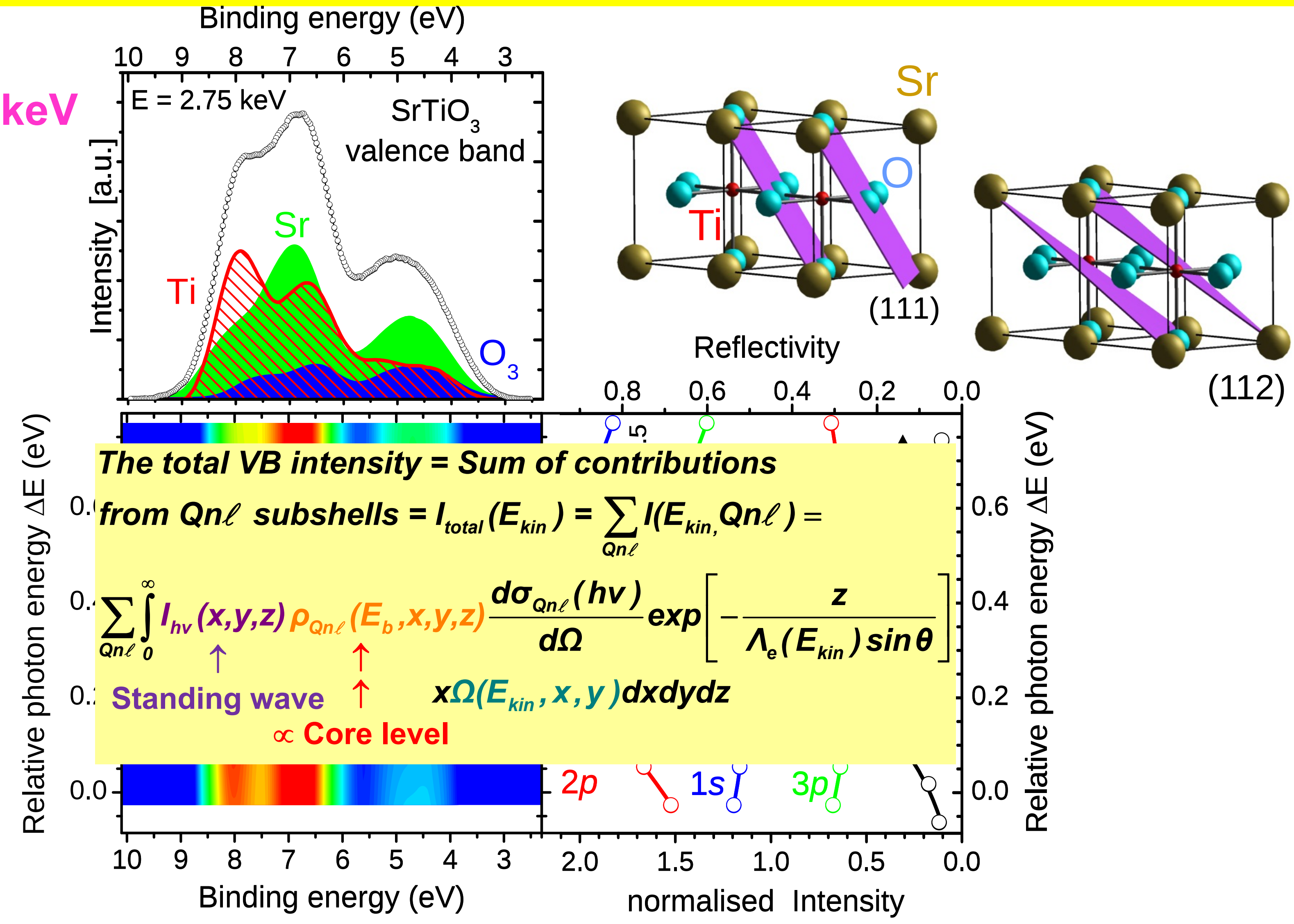

The total VB intensity = Sum of contributions from Qnℓ subshells = $I_{total}(E_{kin}) = \sum_{Qn\ell} I(E_{kin,}Qn\ell) =$

$$\sum_{Qn\ell}\int_0^\infty I_{h\nu}(x,y,z)\,\rho_{Qn\ell}(E_b,x,y,z)\,\frac{d\sigma_{Qn\ell}(h\nu)}{d\Omega}\exp\left[-\frac{z}{\Lambda_e(E_{kin})\sin\theta}\right]$$

$$\uparrow \qquad\qquad \uparrow$$

Standing wave $\uparrow$ $x\Omega(E_{kin},x,y)dxdydz$

∝ Core level

Valence band XSW *Core-level XSW*

T.-L. Lee et al., Solid State Communications 150 (2010) 553-ESRF, also J. C. Woicik et al., Phys. Rev. B 64, 125115 (2001)-SSRL

Looking to the future: Hard x-ray ARPES--GaAs and Dilute Magnetic Semiconductor $Ga_{0.95}Mn_{0.05}As$ Experiment Diamond 3.2 keV

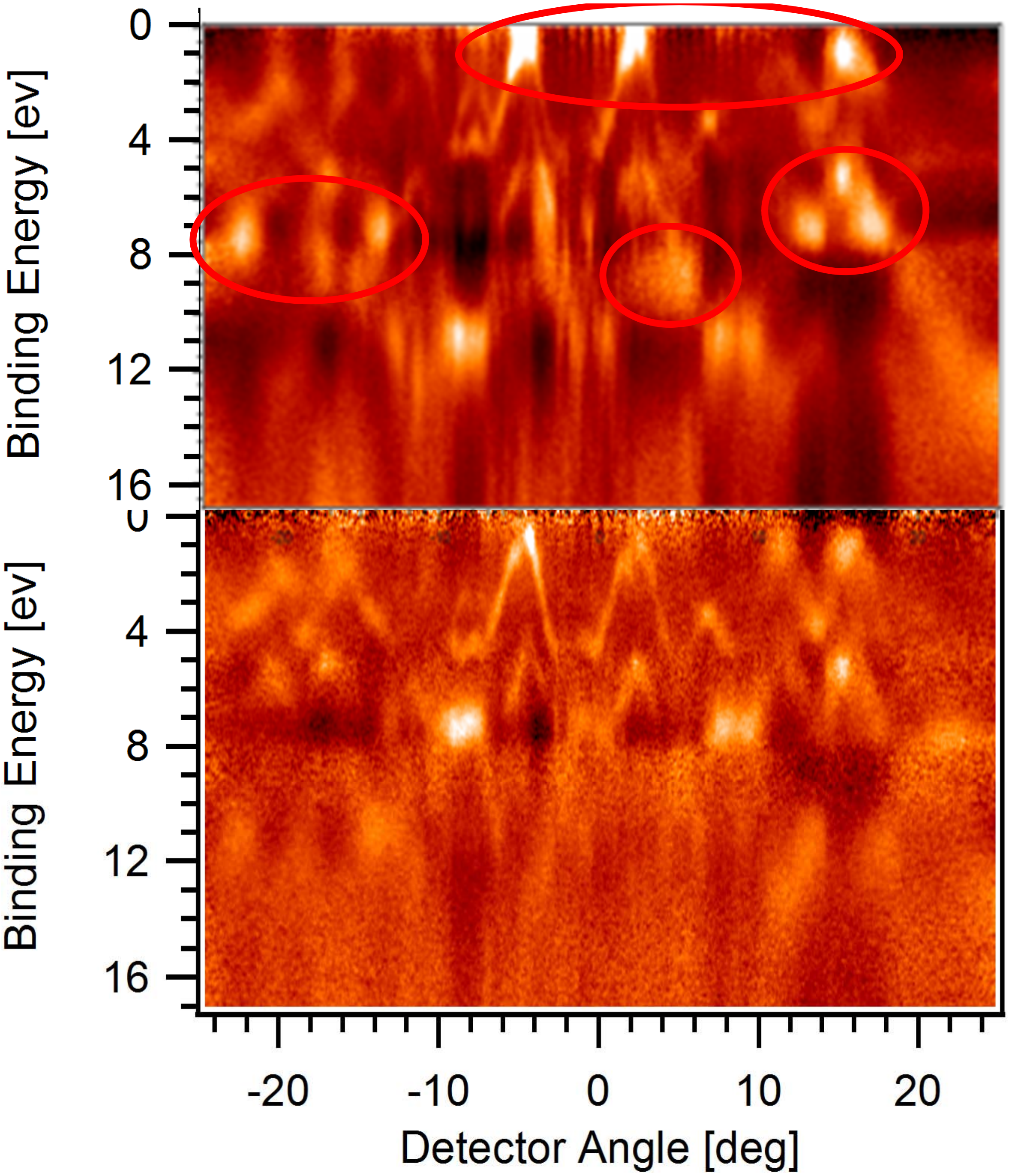

→ Major differences throughout bands due to Mn!

Nemšák, Lee,…CSF, samples H. Ohno, TBP

Bragg reflection from crystal planes:
Photon-energy scans and Site-specific HARPES from GaAs/Ga(Mn)As

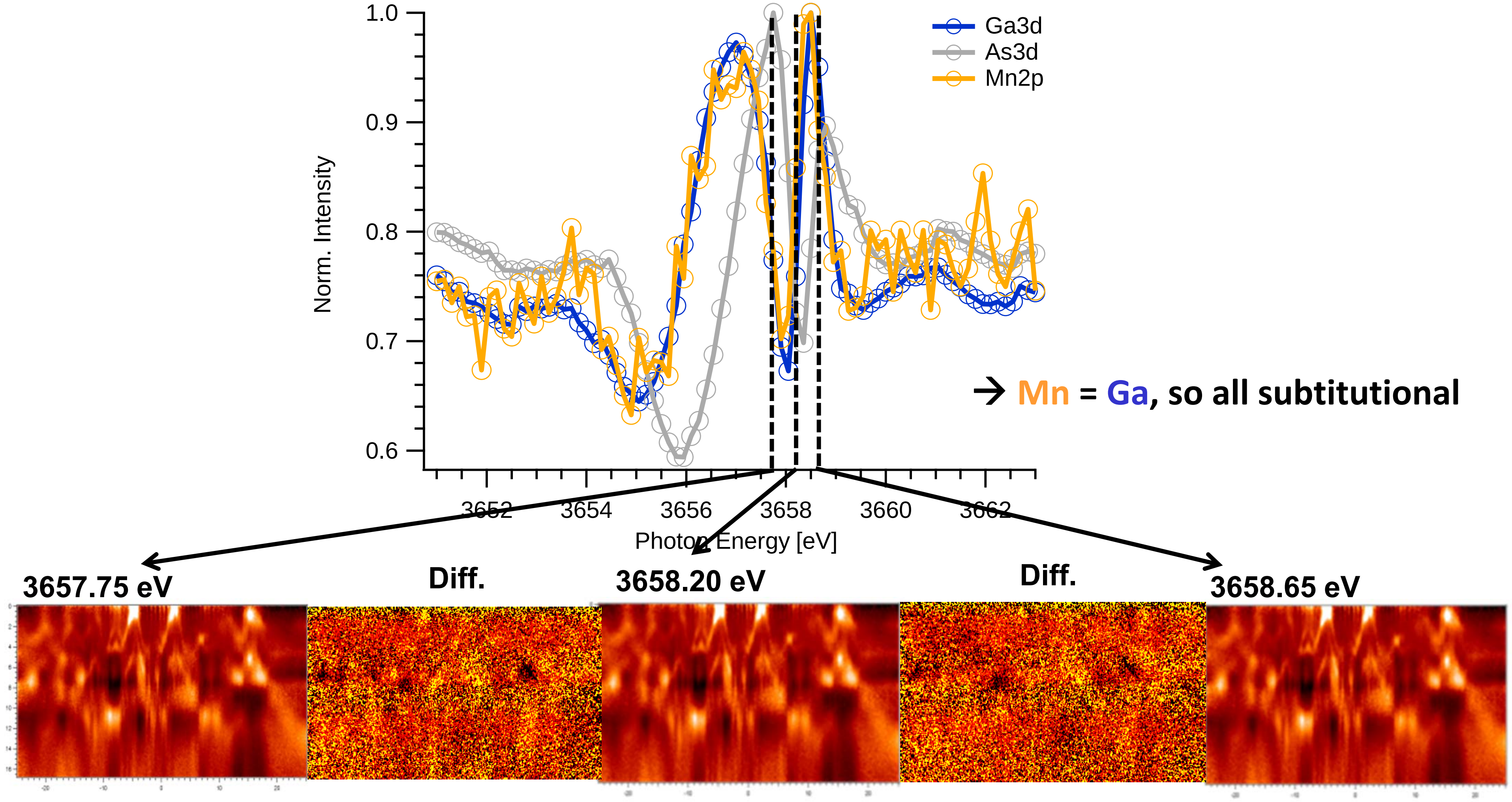

→ Mn = Ga, so all subtitutional

Increasing Ga(Mn) influence +
Decreasing As influence→

Diamond

→ Element- and k-resolved changes in electronic structure?

Conclusions: Single-crystal Bragg Standing-Wave Hard X-Ray Photoemission of $SrTiO_3$

- Using triangulation with two Bragg reflections, and core-level data, determined the projected density of states experimentally

Lee, Zegenhagen et al., Solid State Communications 150, 553 (2010)

- Future: Using Bragg standing waves to probe HARPES within the unit cell and with elemental resolution

Nemšák, Lee, et al., TBP

Soft →hard x-rays and standing waves: a few example studies

$SrTiO_3/La_{2/3}Sr_{1/3}MnO_3$-tunnel junction

Depth-resolved composition, dielectric properties, bonding,
k-resolved electronic structure

$SrTiO_3/GdTiO_3$-2D electron gas

Depth-resolved composition, charge states,
k-resolved electronic, structure

Fe/MgO-tunnel junction

Depth-resolved composition, chemical states,
magnetization

$SrTiO_3$ and Ga(Mn)As

Single-crystal Bragg reflection→Projected densities of states

Fe_2O_3 reacting with NaOH, CsOH, and H_2O

Using standing wave XPS to probe the solid/gas and solid/liquid interface: some first ambient pressure results

$SrTiO_3/La_{0.7}Sr_{0.3}MnO_3$
A classic magnetic tunnel junction

$SrTiO_3$

- Band insulator (E_g=3.4 eV)
- Low temperature superconductor

$La_{0.7}Sr_{0.3}MnO_3$

- Half-metallic ferromagnet
- Colossal magnetoresistive material

Alex Gray
→Stanford
→Temple U.

$SrTiO_3/La_{0.7}Sr_{0.3}MnO_3$ interface

- What does the interface look like?
- How are bonding and atomic/electronic structure at the interface different?

A. X. Gray, C. Papp, B. Balke, S.-H. Yang, M. Huijben, E. Rotenberg, A. Bostwick, S. Ueda, Y. Yamashita, K. Kobayashi, E. M. Gullikson, J. B. Kortright, F. M. F. de Groot, G. Rijnders, D. H. A. Blank, R. Ramesh, CSF, PRB 82, 205116 (2010); EPL 104, 17004 (2013)

Standing wave/rocking curve analysis of an epitaxial $SrTiO_3/La_{0.67}Sr_{0.33}MnO_3$ interface: near-resonant soft x-ray excitation

The Advanced Light Source

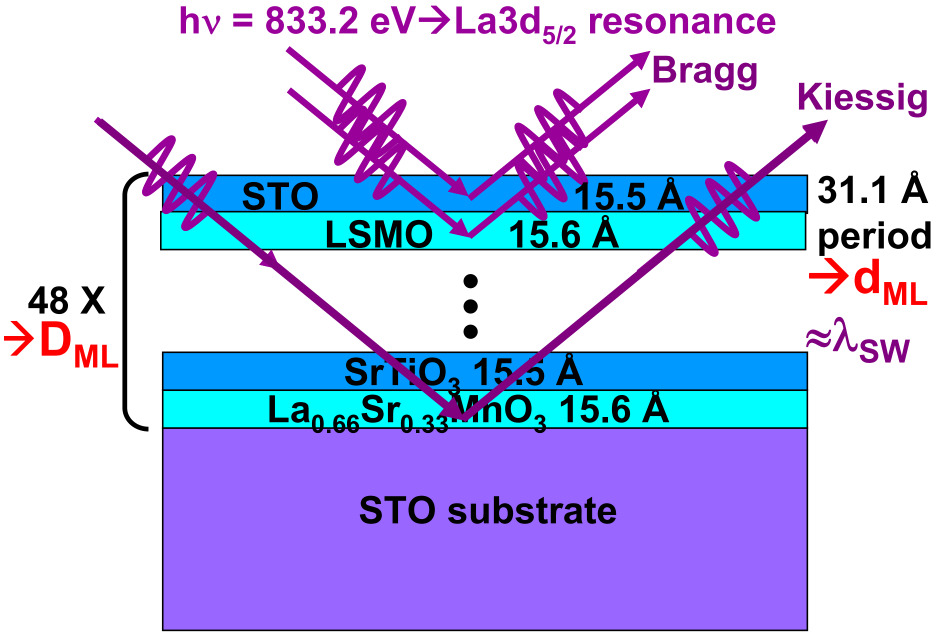

$$\lambda_x = 2d_{ML}\sin\theta_{Bragg}$$

$$m\lambda_x = 2D_{ML}\sin\theta_{Kiessig}$$

Gray et al., Phys. Rev. B 82, 205116 (2010);
Europhysics Letters 104, 17004 (2013)
Samples: Ramesh, Huijben

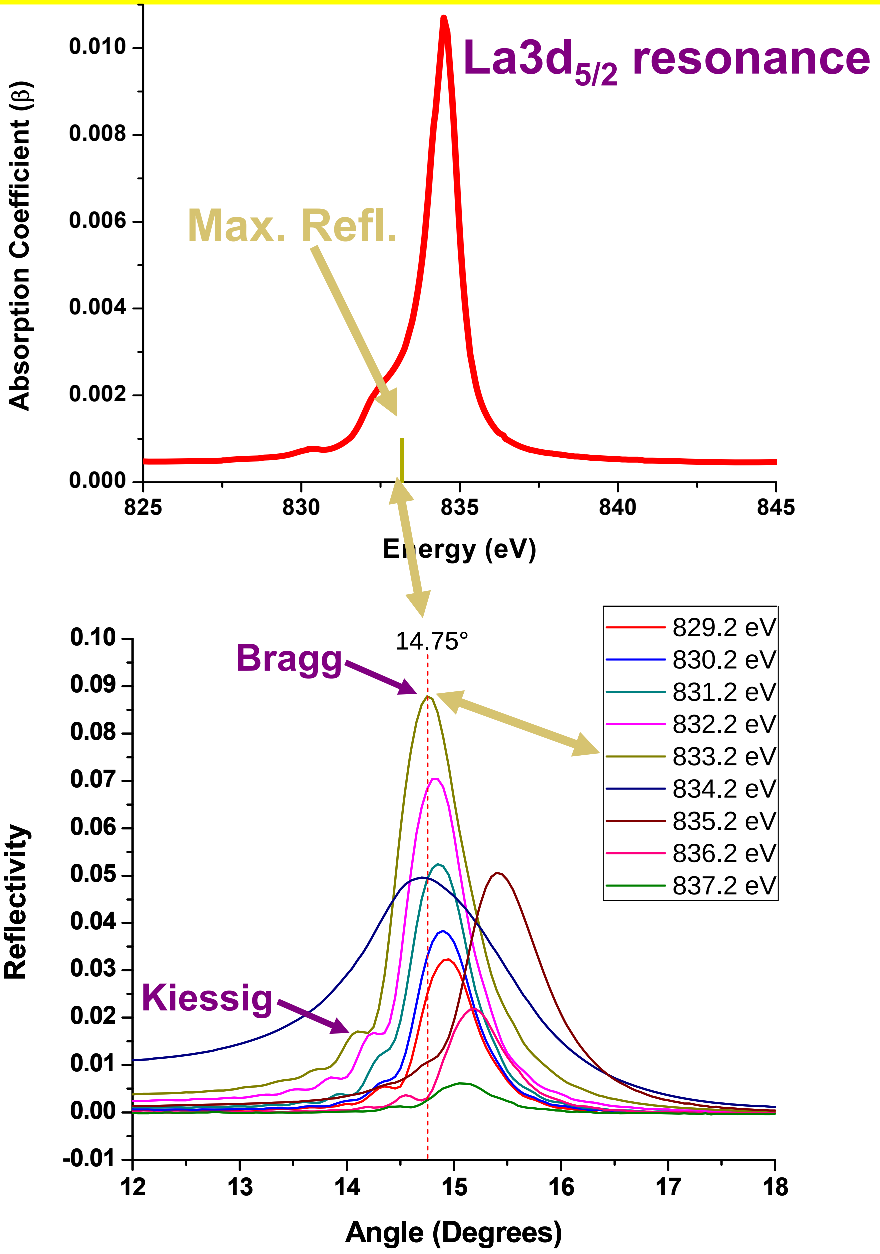

Standing wave/rocking curve analysis of an epitaxial $SrTiO_3/La_{0.67}Sr_{0.33}MnO_3$ interface: hard x-ray excitation

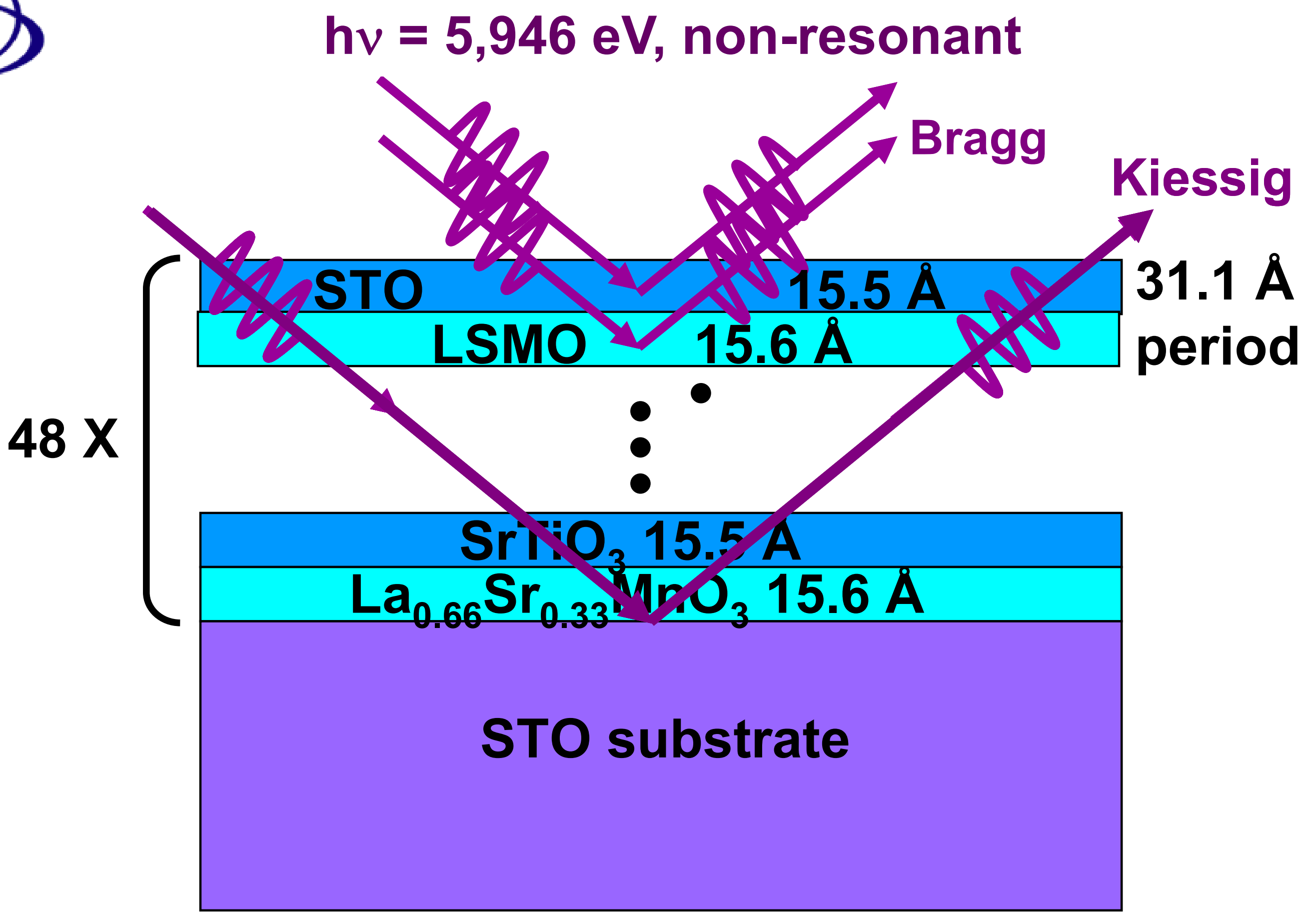

Gray et al., Phys. Rev. B 82, 205116 (2010)
Samples: Ramesh, Huijben

$SrTiO_3/La_{0.67}Sr_{0.33}MnO_3$ Multilayer
Analysis of Rocking Curves

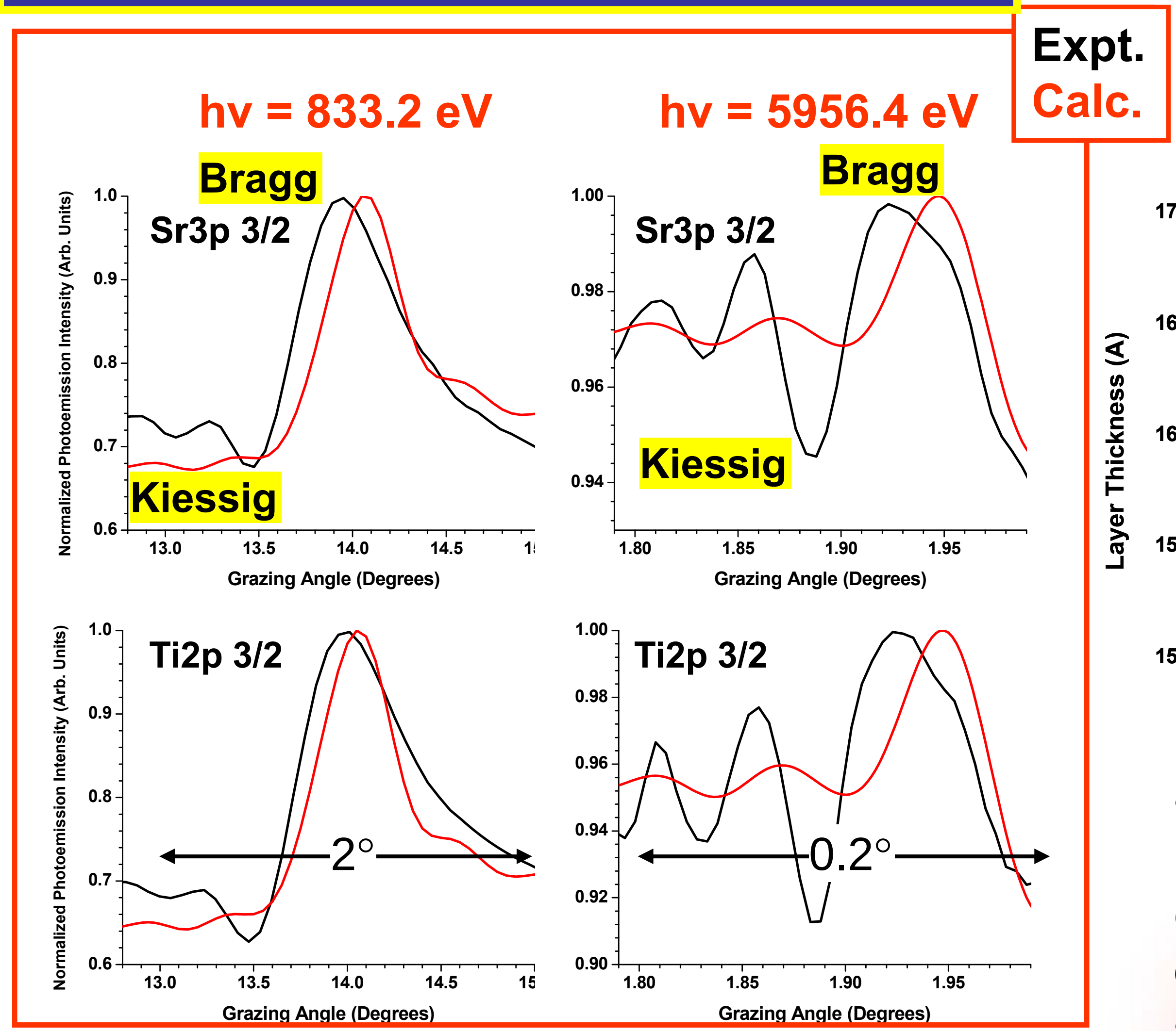

Ideal Bilayer Thickness Gradient Profile

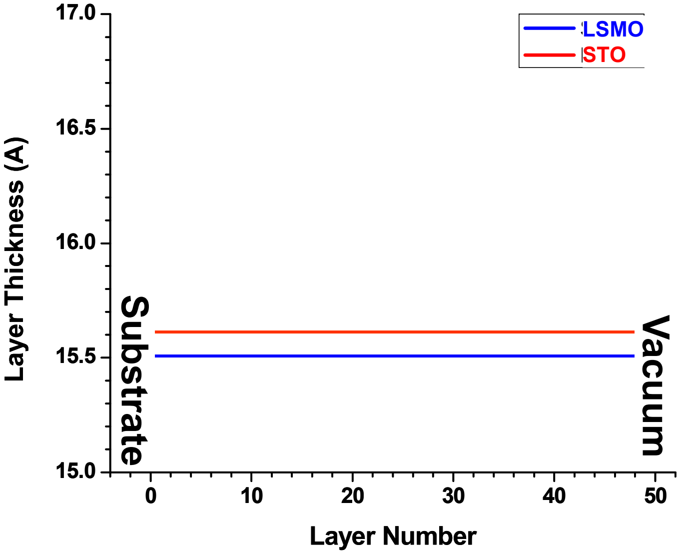

- Relative amplitude of the predicted Kiessig fringes does not agree with experiment
- Strong Kiessig fringes predicted on both sides of the rocking curves, esp. 5.9 keV

The Advanced Light Source

SPring-8

$SrTiO_3/La_{0.67}Sr_{0.33}MnO_3$ Multilayer
Analysis of Rocking Curves

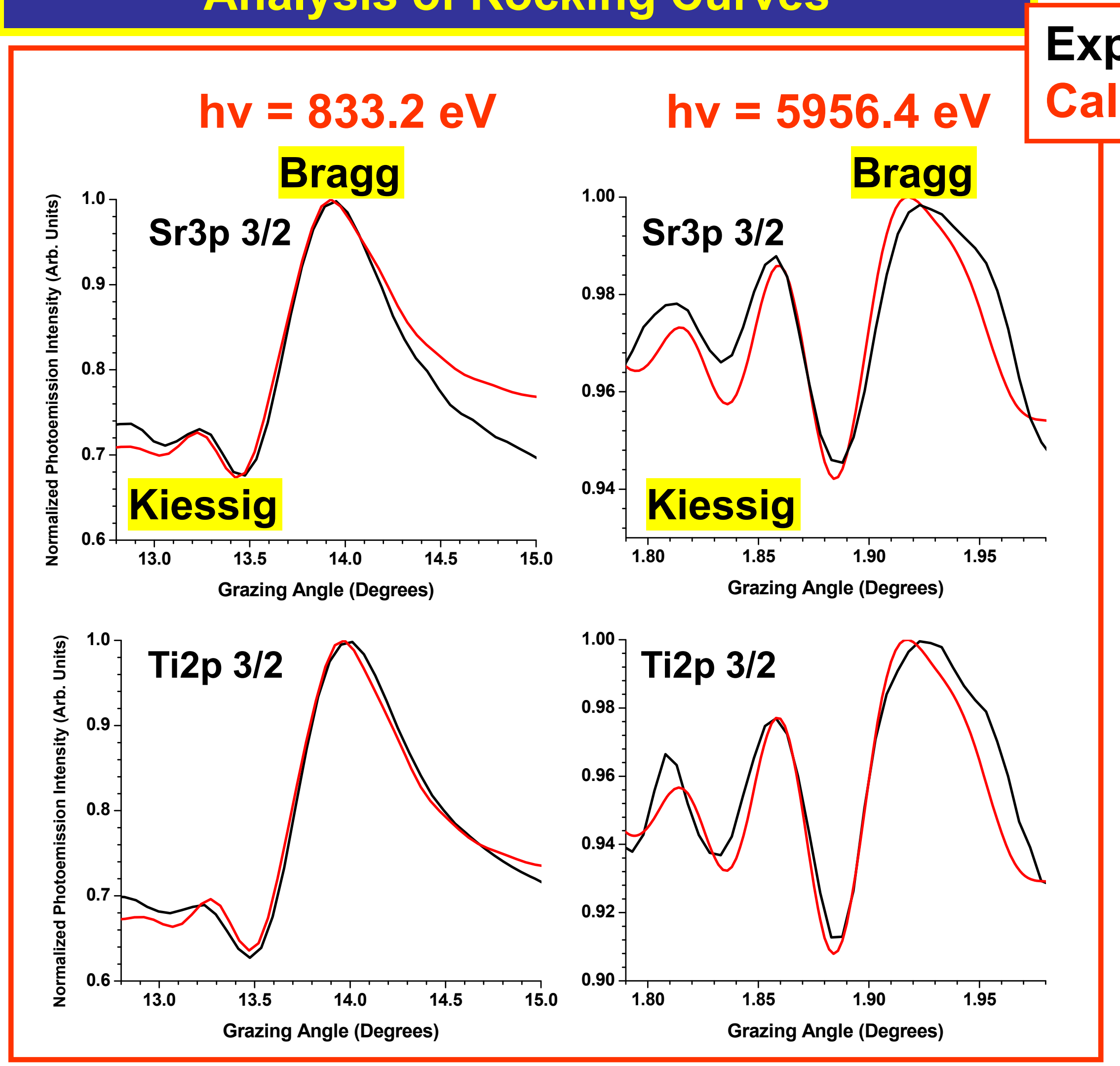

Bilayer Thickness Gradient Profile

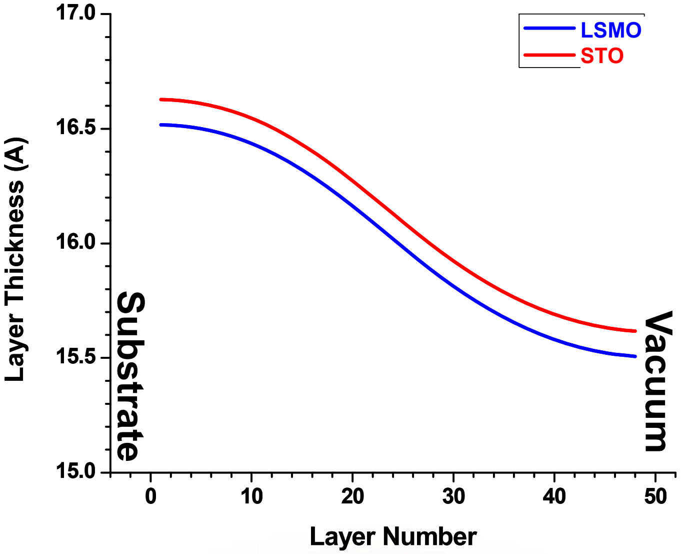

BEST FIT

→Average multilayer d_{ML} changes by about -2 Å ≈ -6% from top to bottom

Gray et al., Phys. Rev. B 82, 205116 (2010)

Fitting of Rocking Curves—All Elements Present, Soft and Hard X-rays

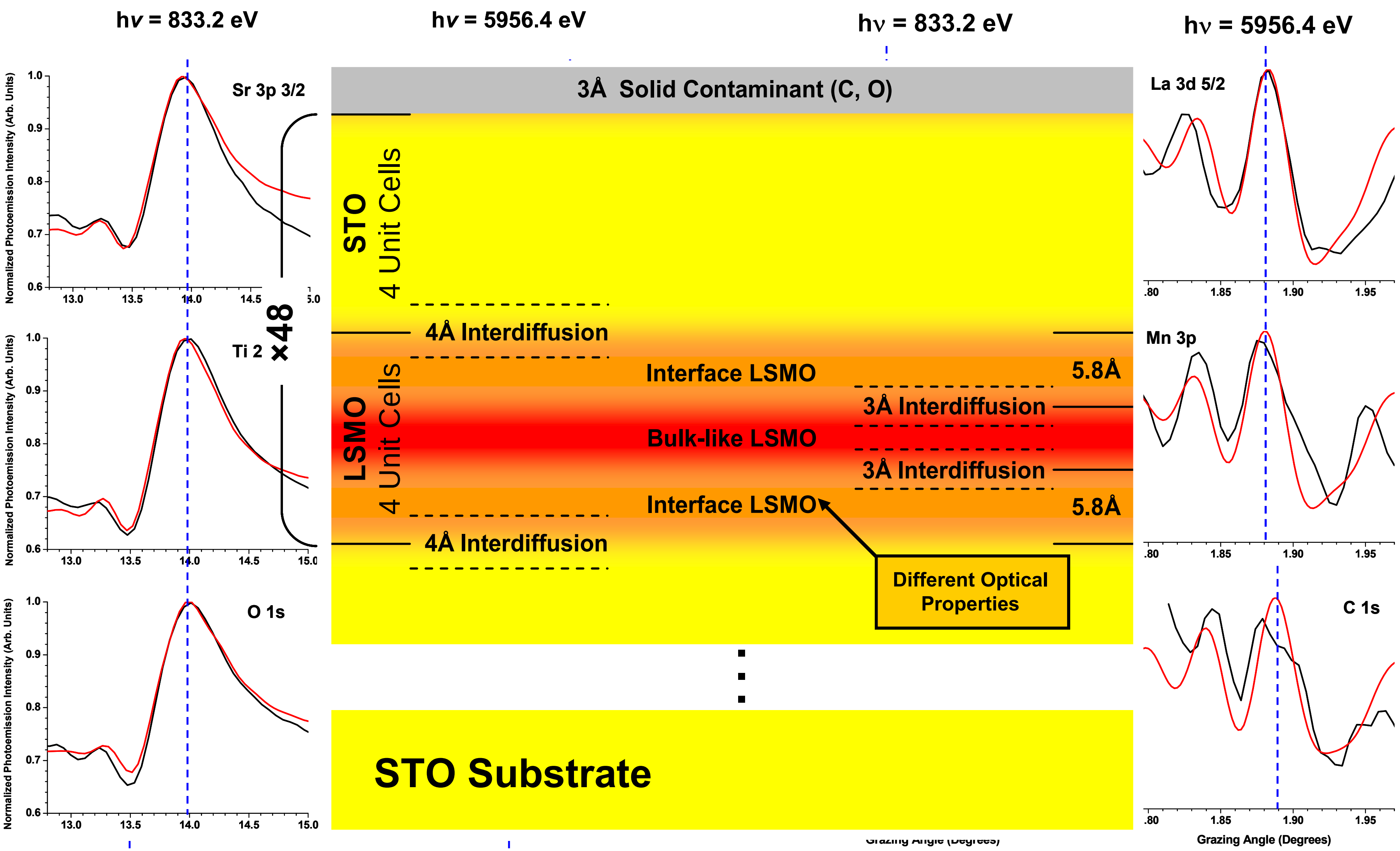

3Å Solid Contaminant (C, O)

STO 4 Unit Cells

4Å Interdiffusion

LSMO 4 Unit Cells

Interface LSMO

5.8Å

3Å Interdiffusion

Bulk-like LSMO

3Å Interdiffusion

Interface LSMO

5.8Å

4Å Interdiffusion

Different Optical Properties

STO Substrate

Gray et al., Phys. Rev. B 82, 205116 (2010)

TEM with EELS+HAADF-Confirms Conclusions of Standing-Wave Photoemission

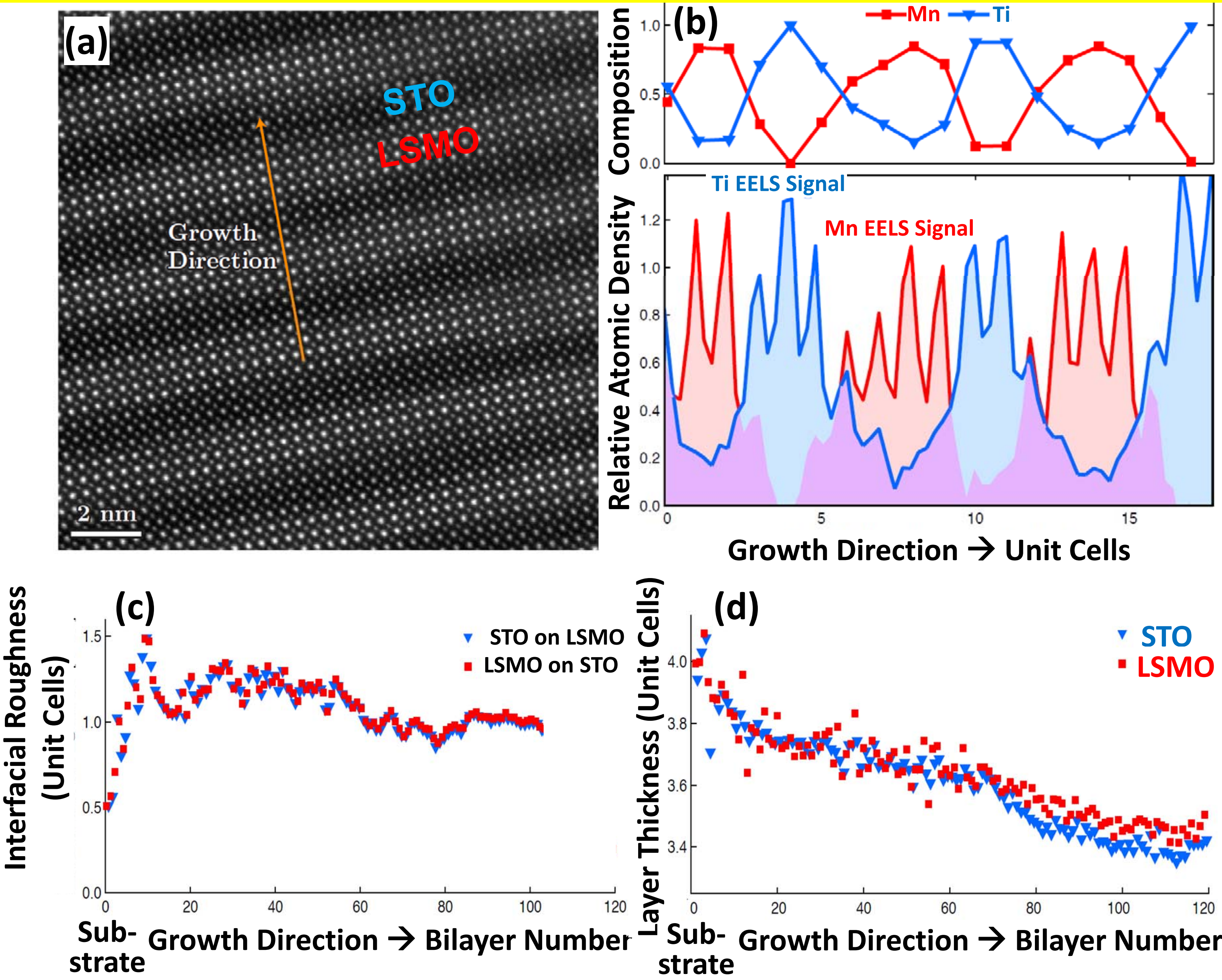

J. Ciston, NCEM, LBNL

STO/LSMO-Resonant soft x-ray standing wave/rocking curves at 833 eV: core photoelectron peaks compared to calculated standing-wave field

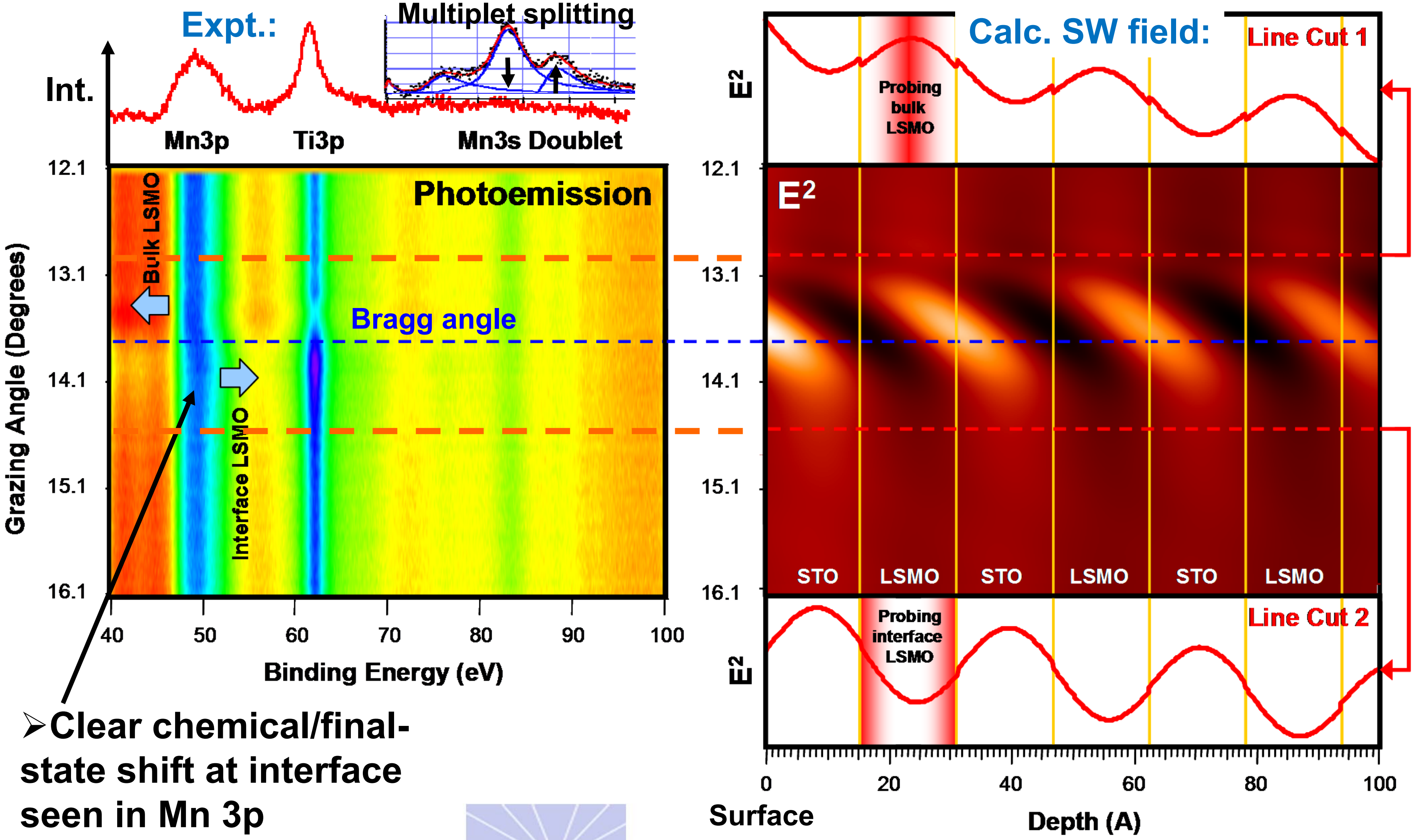

- Clear chemical/final-state shift at interface seen in Mn 3p
- No change in Mn 3s
- No change in Ti 3p—near surface

The Advanced Light Source

Gray, Yang et al., Phys. Rev. B 82, 205116 (2010)

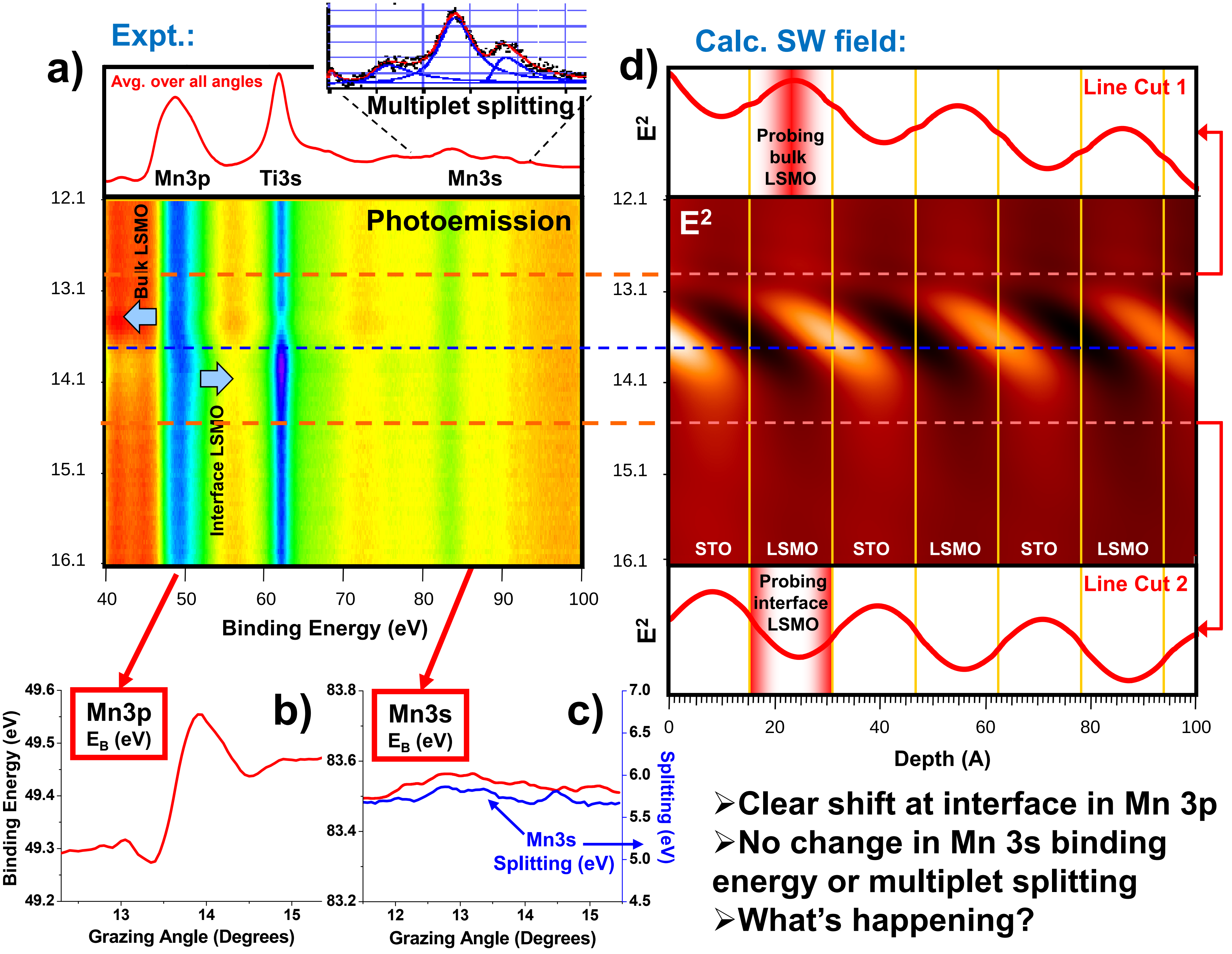

- ➢Clear shift at interface in Mn 3p
- ➢No change in Mn 3s binding energy or multiplet splitting
- ➢What's happening?

STO/LSMO-Explaining the Difference Between Mn 3p and Mn 3s behavior

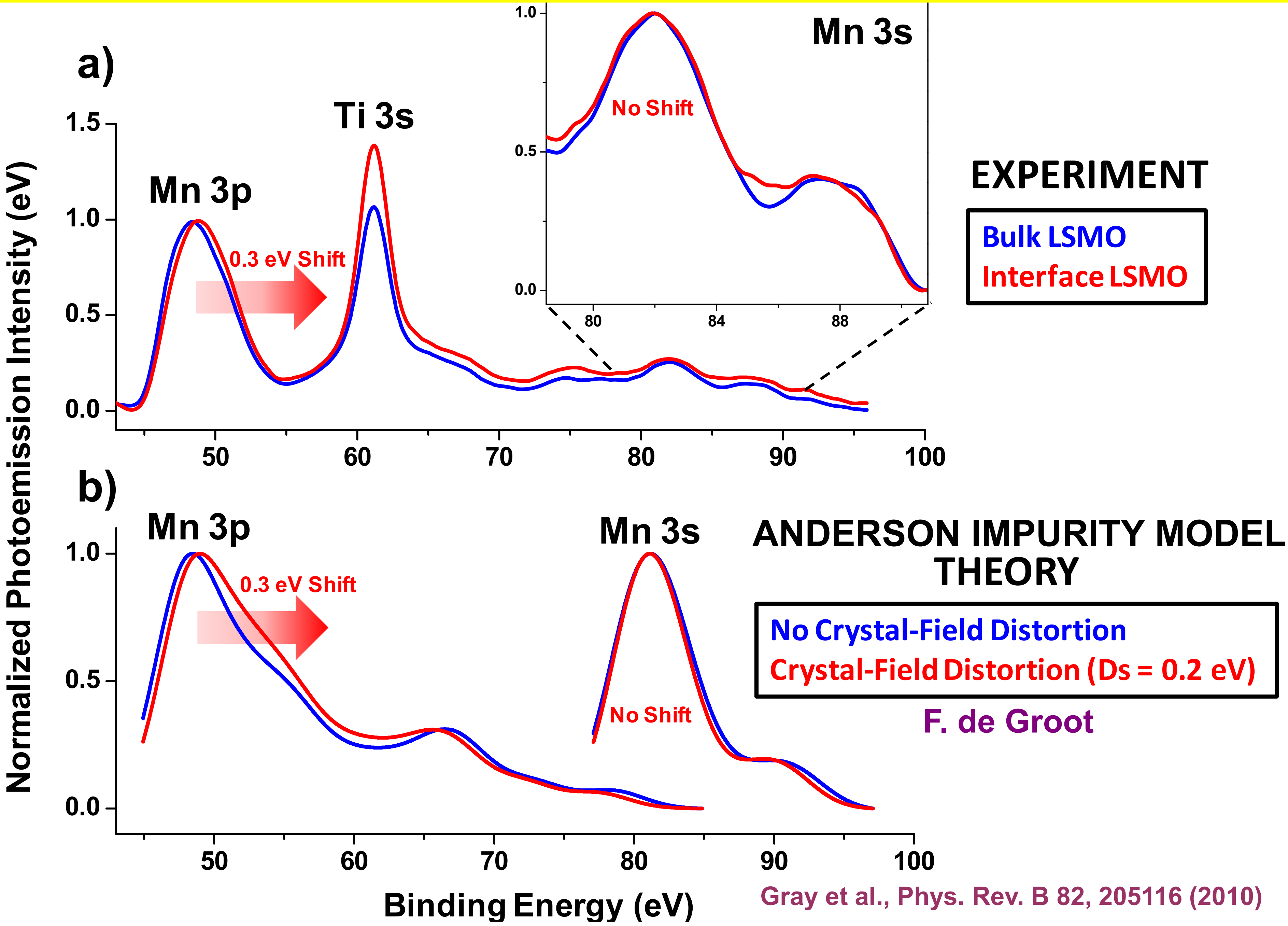

F. de Groot

Gray et al., Phys. Rev. B 82, 205116 (2010)

$SrTiO_3$ and $La_{0.67}Sr_{0.33}MnO_3$ band structures and DOS

$SrTiO_3$-band insulator

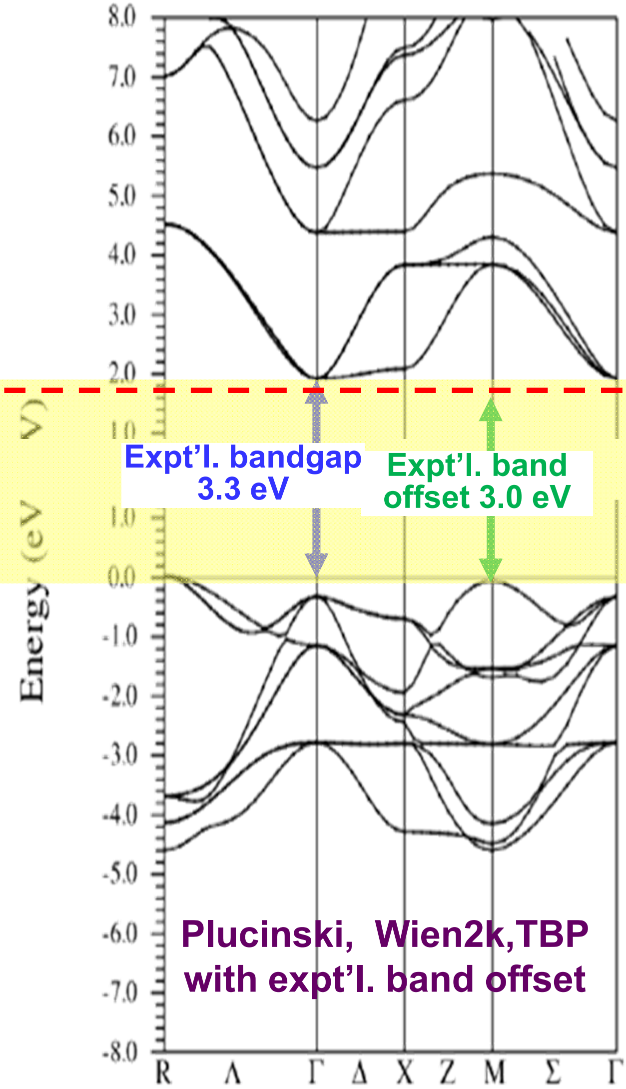

Expt'l. bandgap 3.3 eV

Expt'l. band offset 3.0 eV

Plucinski, Wien2k,TBP with expt'l. band offset

$La_{0.67}Sr_{0.33}MnO_3$- Half-Metallic Ferromagnet

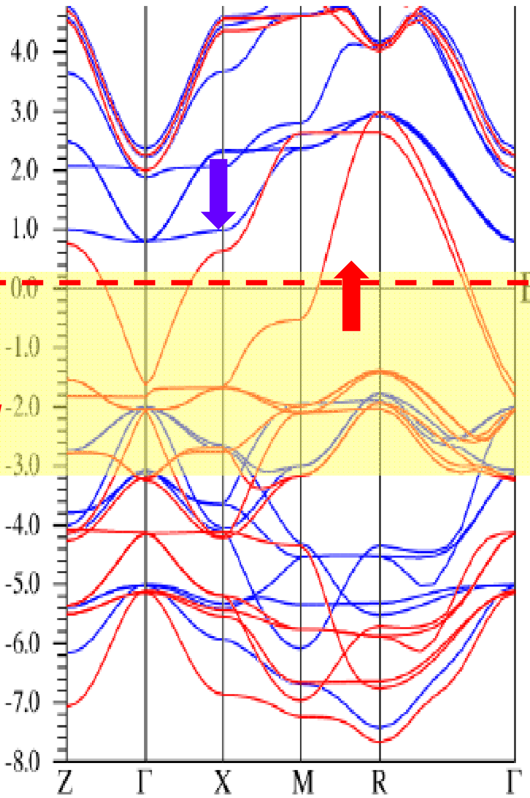

Mn e_g

Mn t_{2g}

Spin-up

Spin-down

Chikamatsu et al., PRB 73, 195105 (2006); Plucinski, TBP

Projected DOSs

Spin-up Spin-down

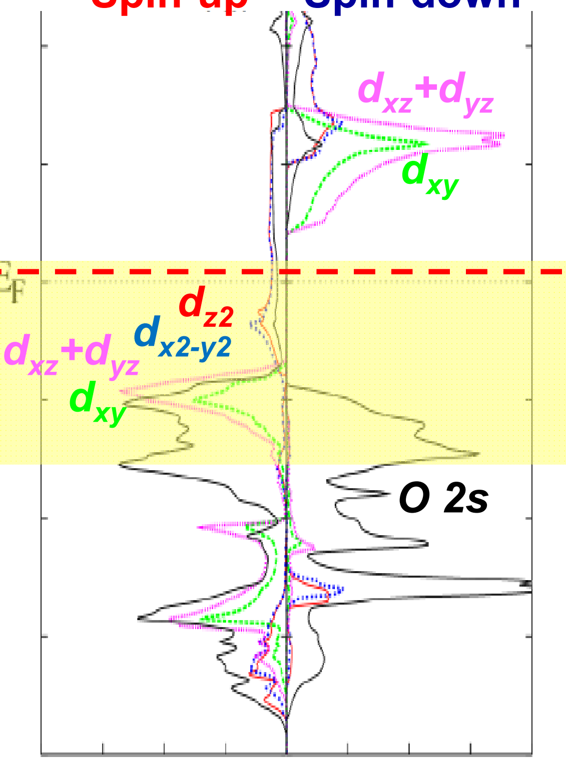

Zheng, Binggeli, J. Phys. Cond. Matt. 21, 115602 (2009) Plucinski, TBP

STO/LSMO-Standing wave/rocking curves of valence region: 833 eV, 300K
Depth- and layer- resolved DOSs

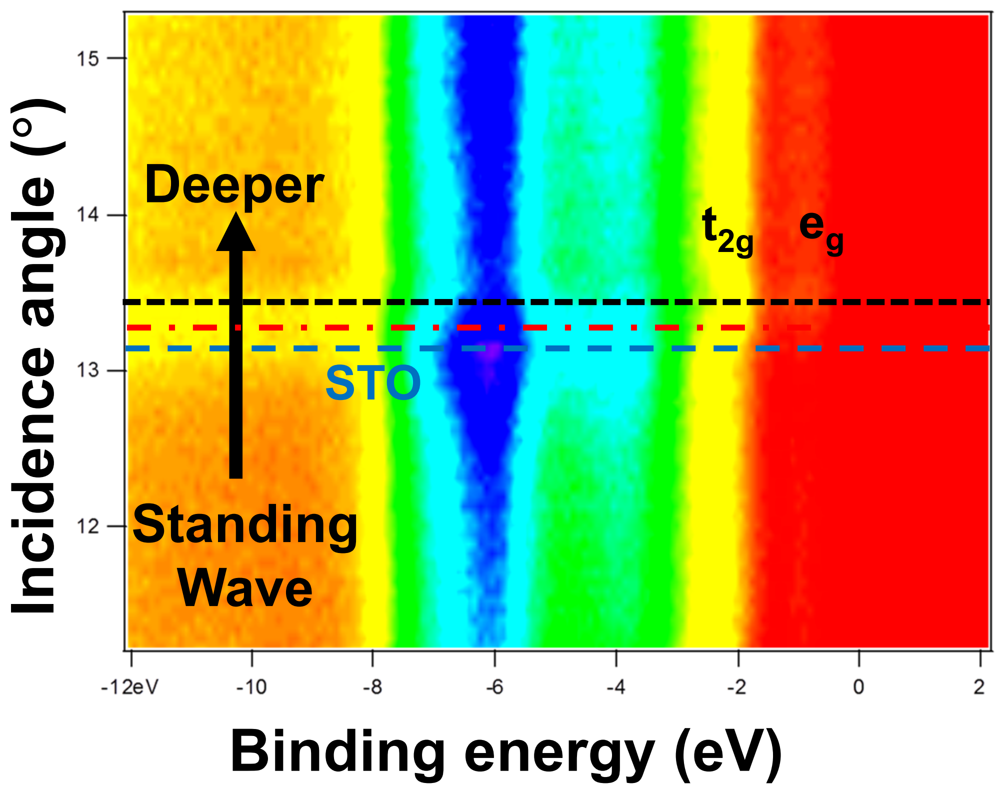

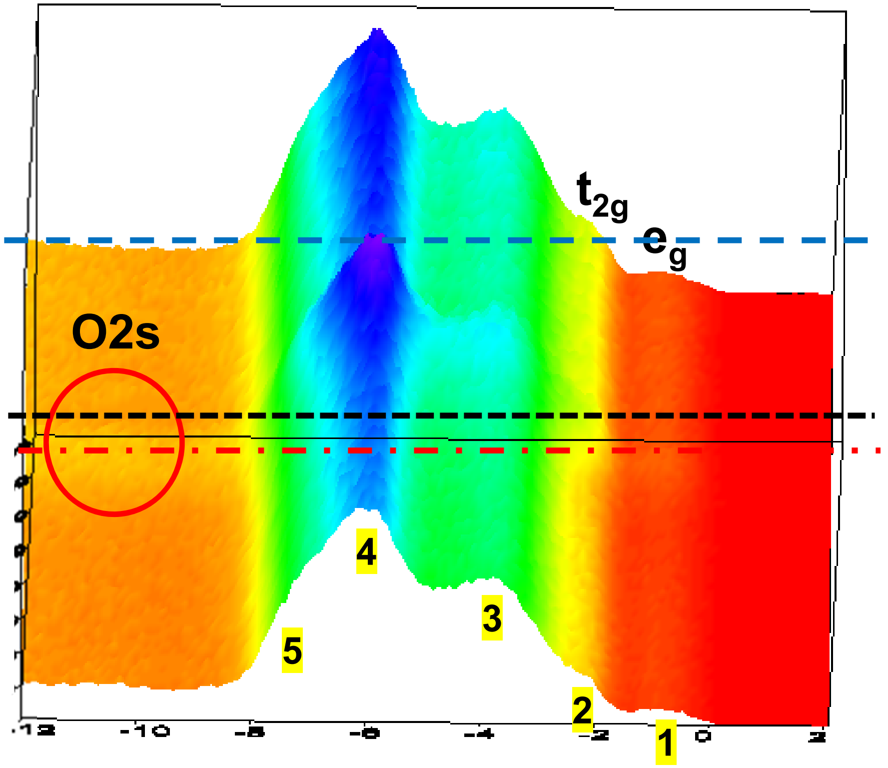

A. Gray et al., PRB 82, 205116 (2010); plus standing-wave ARPES in Gray et al., EPL 104, 17004 (2013)

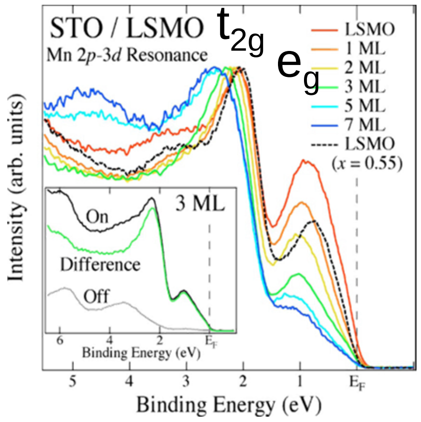

Prior resonant PS: Fujimori et al., J.A.P 99, 08S903 (2006)

The Advanced Light Source

Standing-wave angle-resolved photoemission

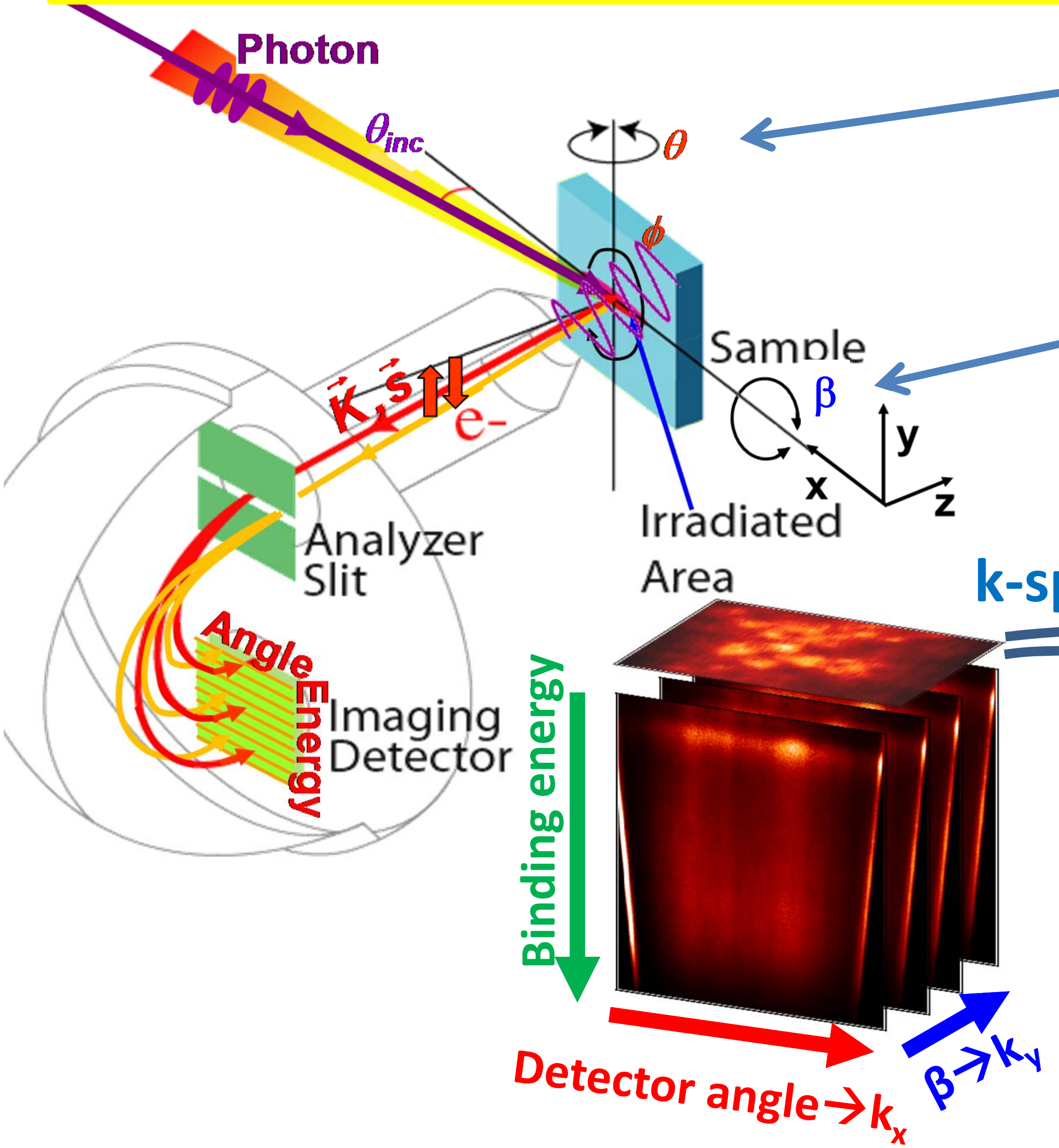

Variation of Θ_{inc}:
Change of incidence angle
⇨Standing wave sweeps

Variation of β:
Change of takeoff angle
⇨ Electron energies for different $\mathbf{k}_y$ vectors

k-space mapping

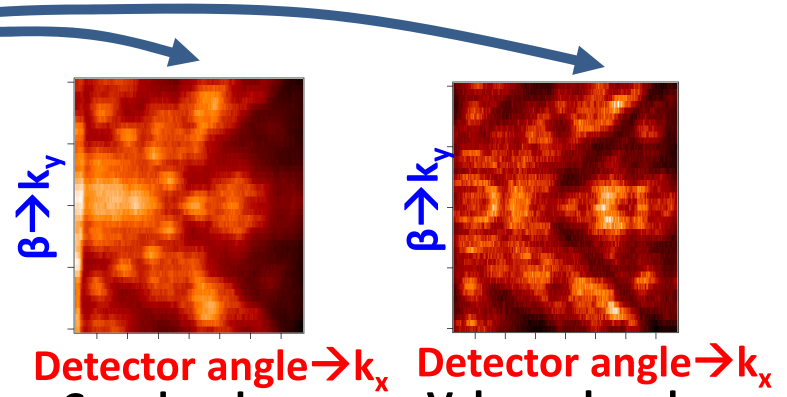

Core levels:
XPD

Valence bands:
ARPES

Photoelectron Diffraction with soft and hard x-ray excitation: expt. vs. Kikuchi-band theory at ~0.8 keV

Experiment

STO/LSMO Multilayer
Mn 3p emission
E = 793eV
hv = 833.2 eV

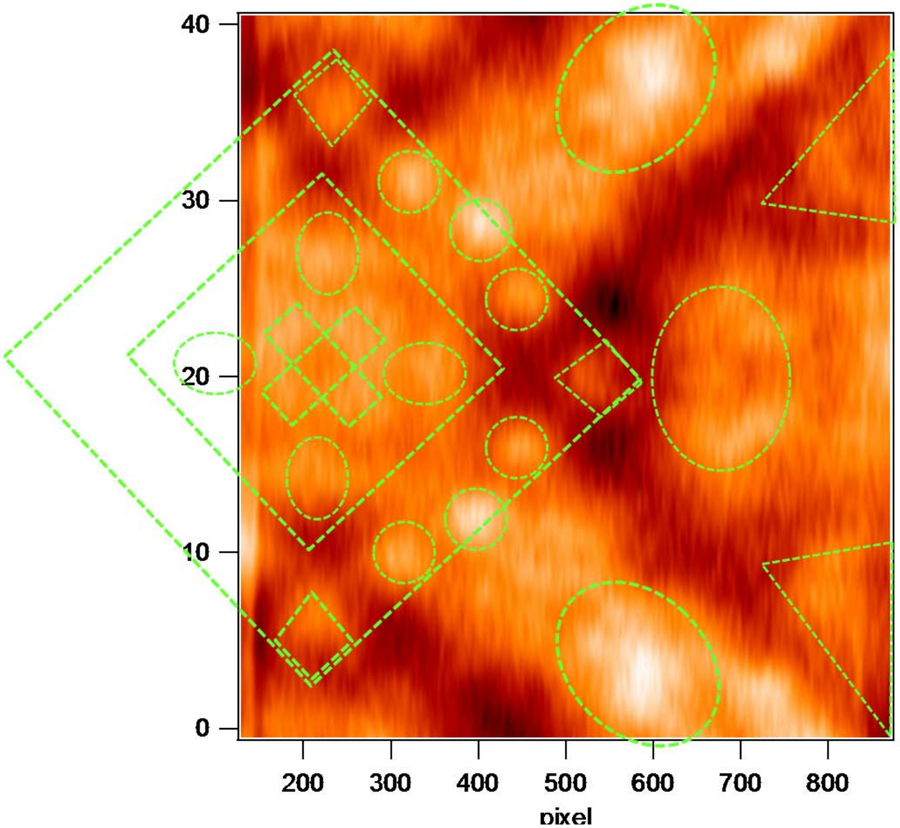

Experiment: Fadley Group

XPD Kikuchi-Band Theory

LSMO 5nm Film „bulk“
Mn emission
E = 793eV
hv = 833.2 eV

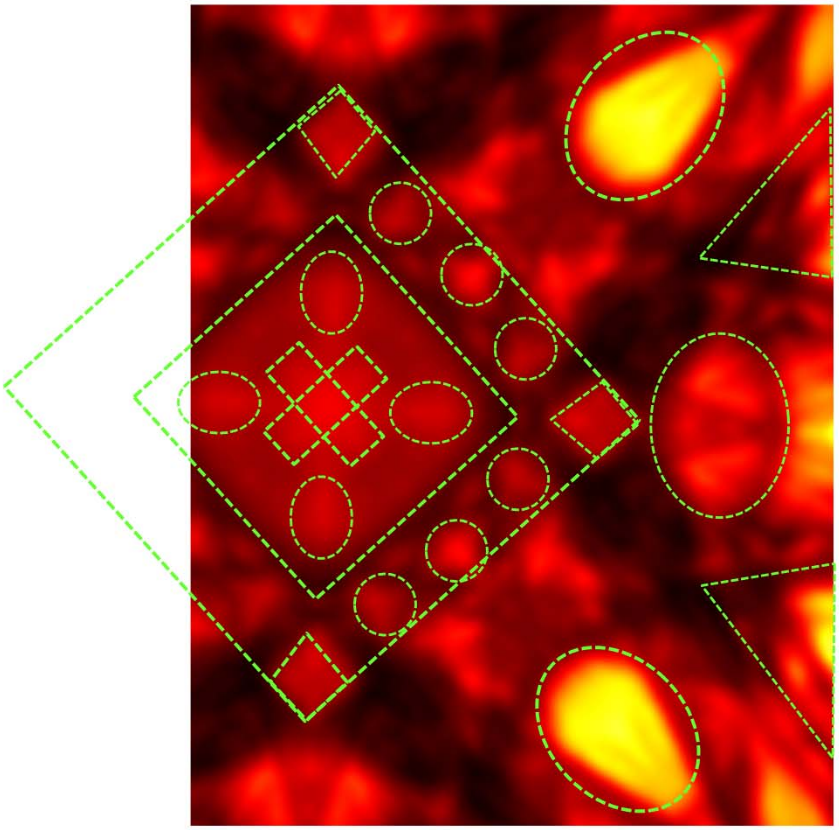

Theory: A. Winkelmann

Depth-Resolved Soft X-Ray ARPES? Cryocooling to supress phonon smearing: DW factor

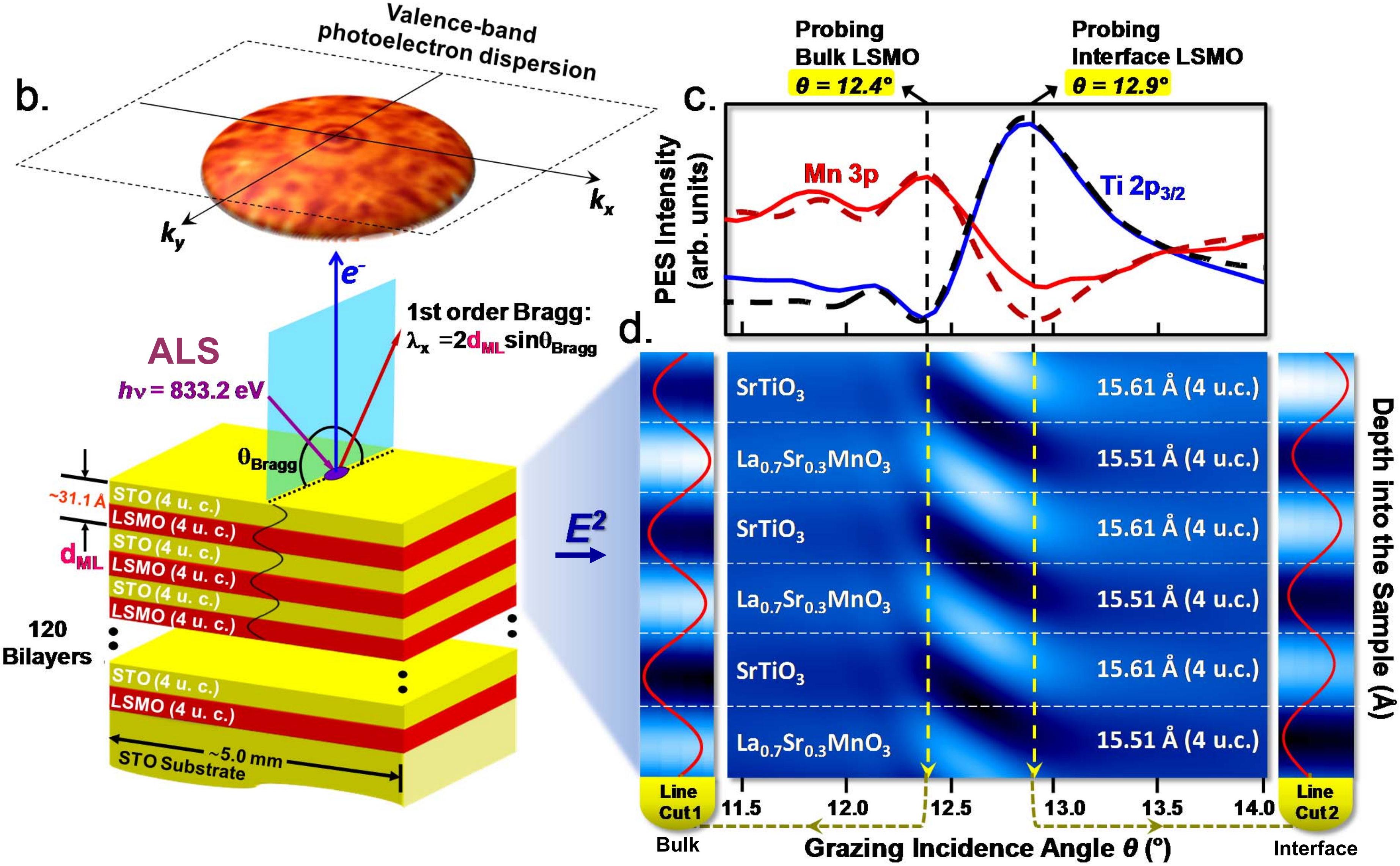

STO/LSMO Depth-resolved ARPES: hν=833 eV, RT (DW = 0.13) and 30K (DW = 0.75)

Room-Temperature DOS Spectrum, Standing-wave LSMO emphasis:

30 K ARPES:

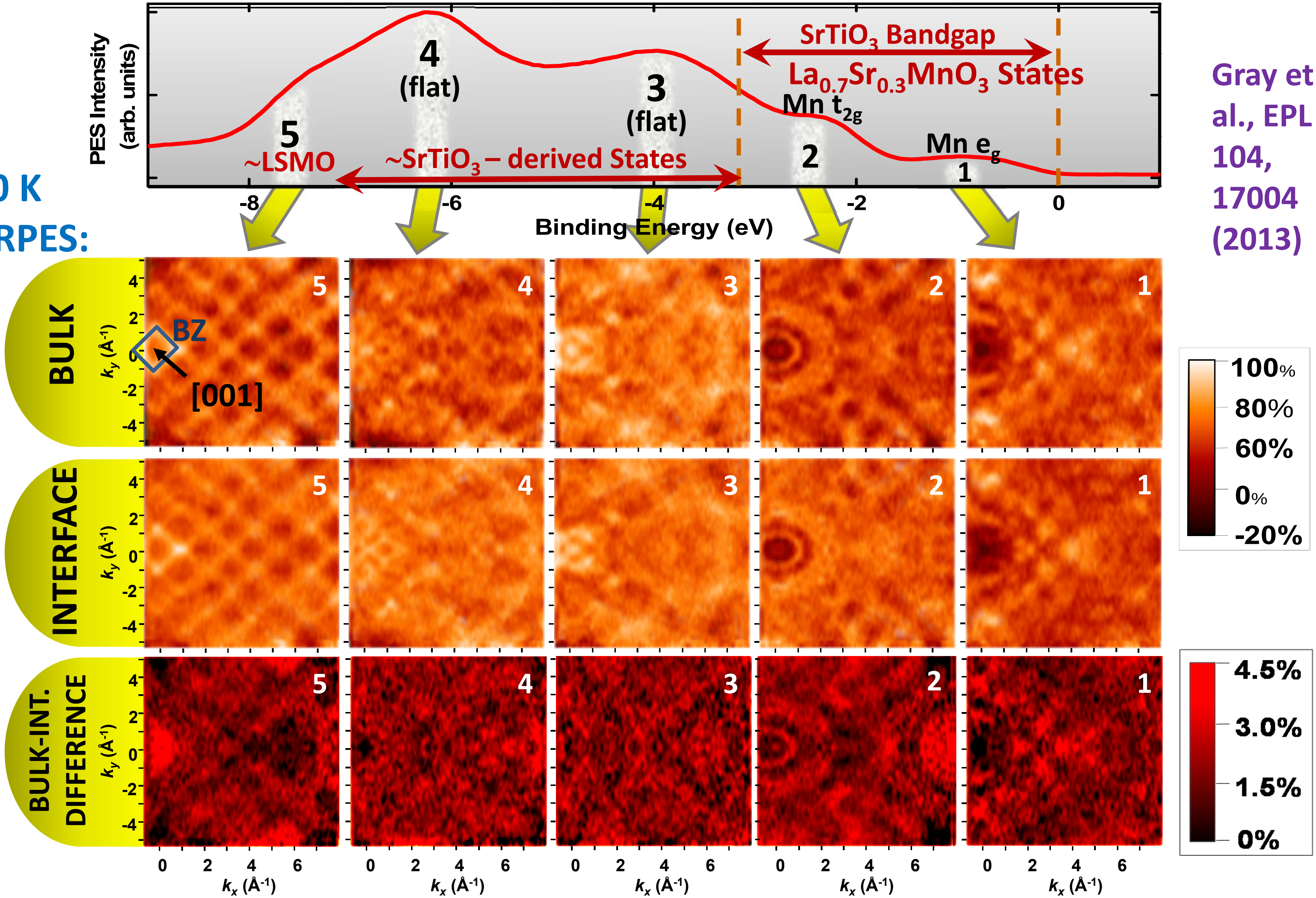

Gray et al., EPL 104, 17004 (2013)

First test case: STO/LSMO Depth-resolved ARPES: hν=833 eV, 20K- Expt. vs Theory

Theory:
Ground-state band structure→k-conserving free-e$^-$ final state
Plucinski

Theory:
One-step, t-reversed LEED, spin-polarized relativistic KKR, alloy CPA
Minar, Braun, Ebert

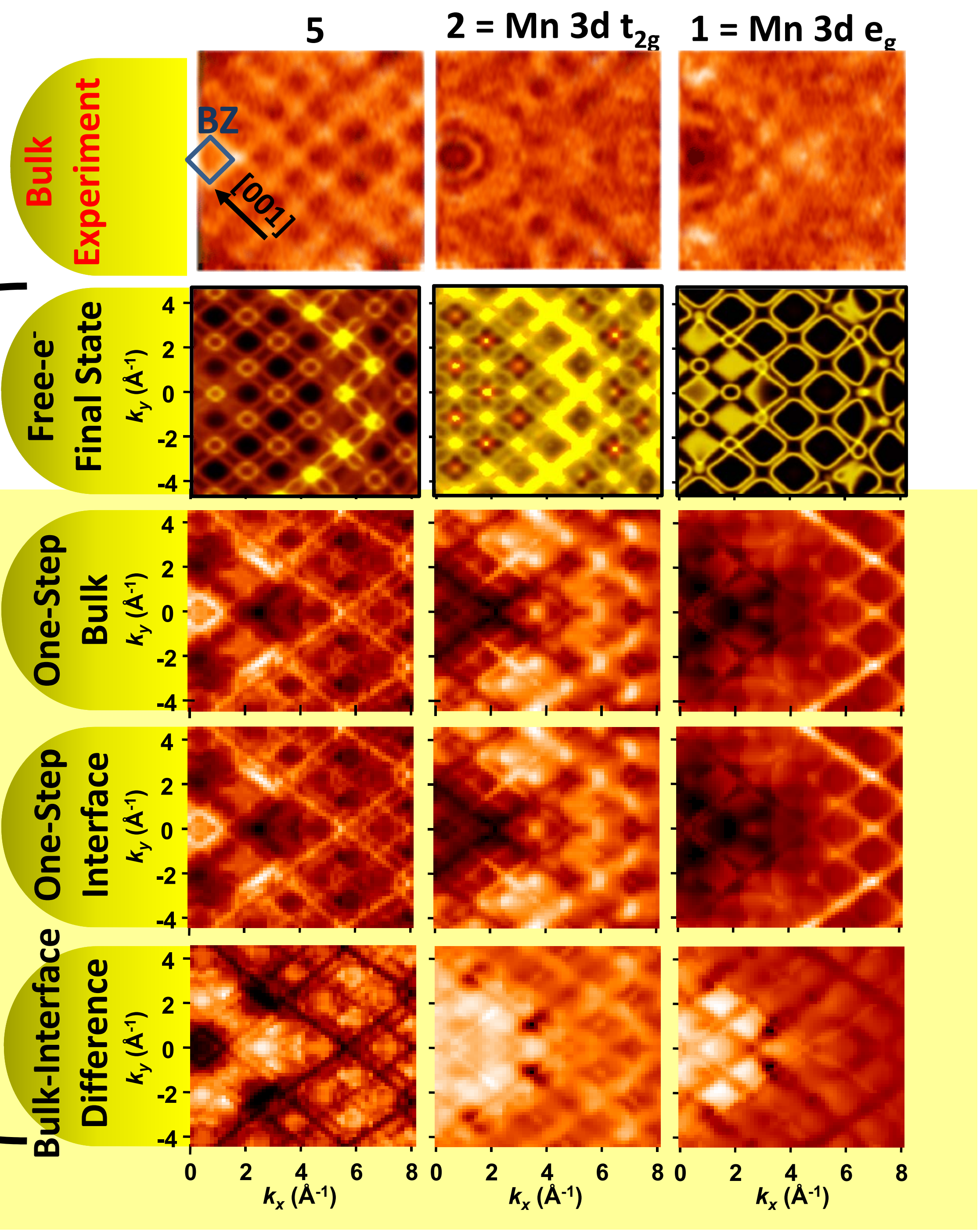

Gray et al., Phys. Rev. B 82, 205116 (2010); Europhysics Letters 104, 17004 (2013)

First measurement of k-resolved interface elec. structure: STO/LSMO hν=833 eV, 20K-Expt. vs Theory

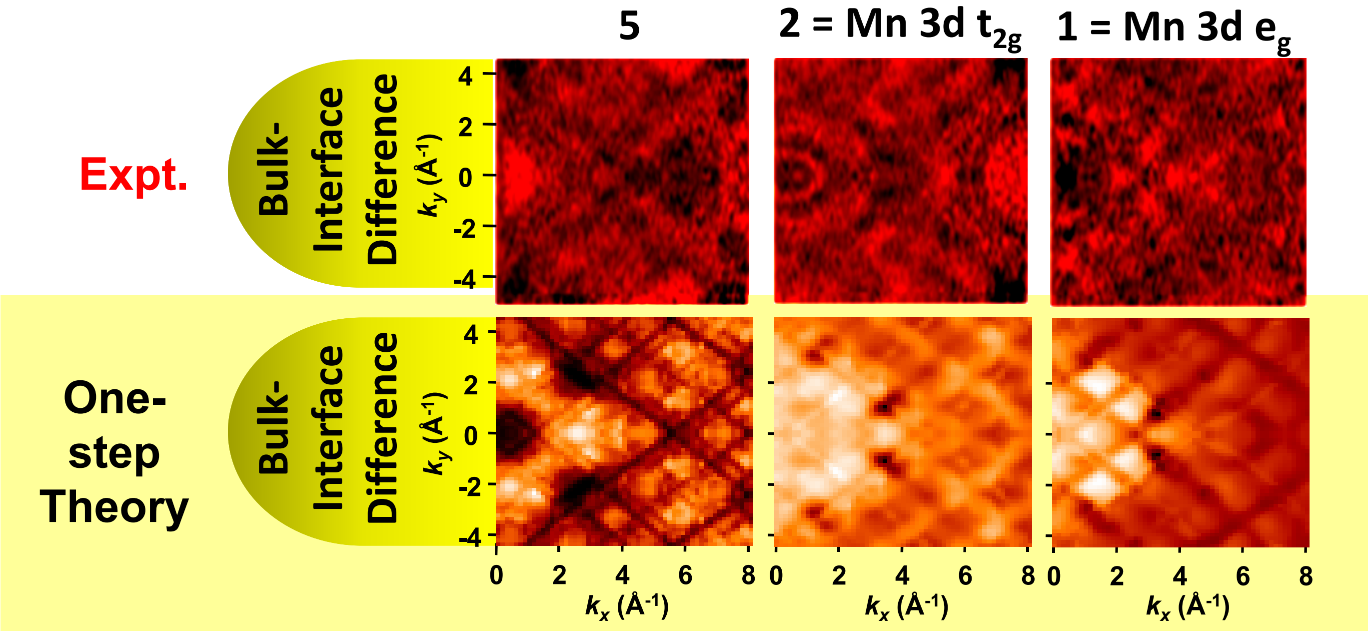

Further calculations in progress with relaxed atomic positions and multilayer roughness at interface (Pentcheva)
Gray et al., Phys. Rev. B 82, 205116 (2010);
Europhysics Letters 104, 17004 (2013)

Looking ahead: $[SrTiO_3/La_{0.7}Sr_{0.3}MnO_3]_{120}$ Variable-Polarization SWARPES

hv = 833.2 eV

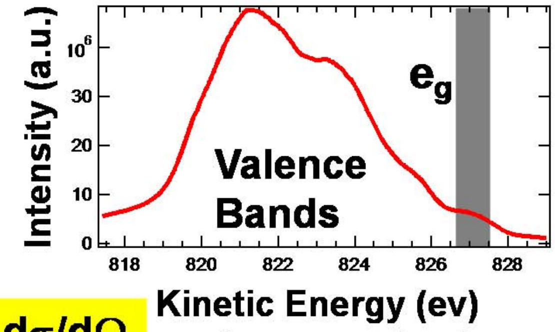

Bulk LSMO Geometry

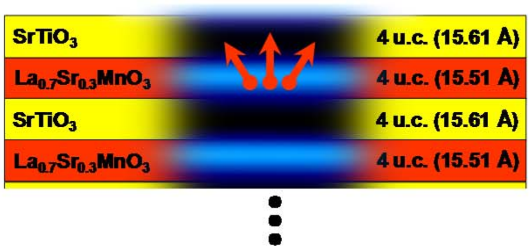

Interface LSMO Geometry

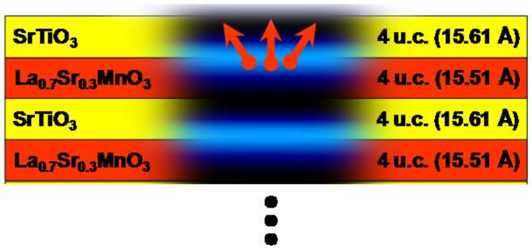

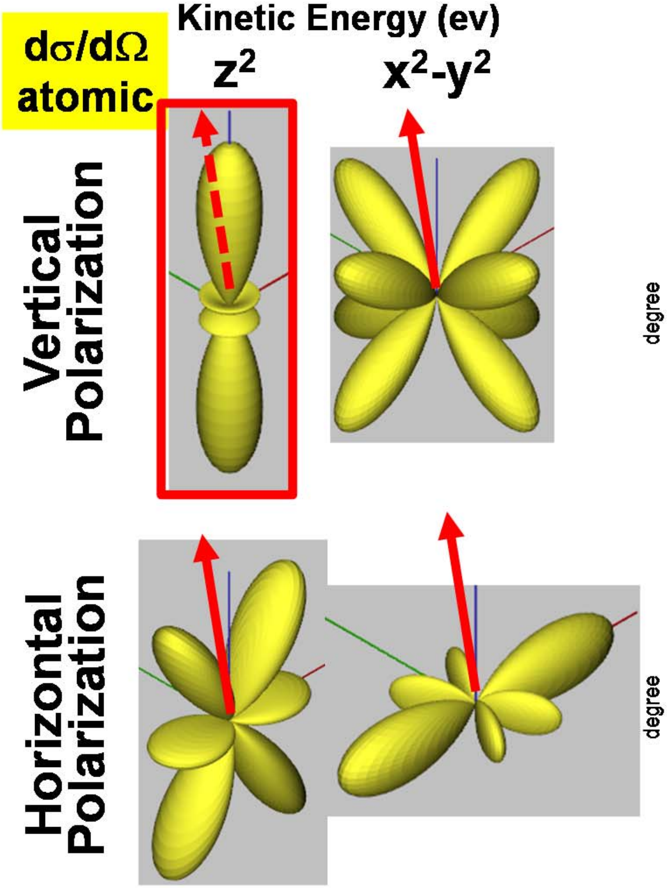

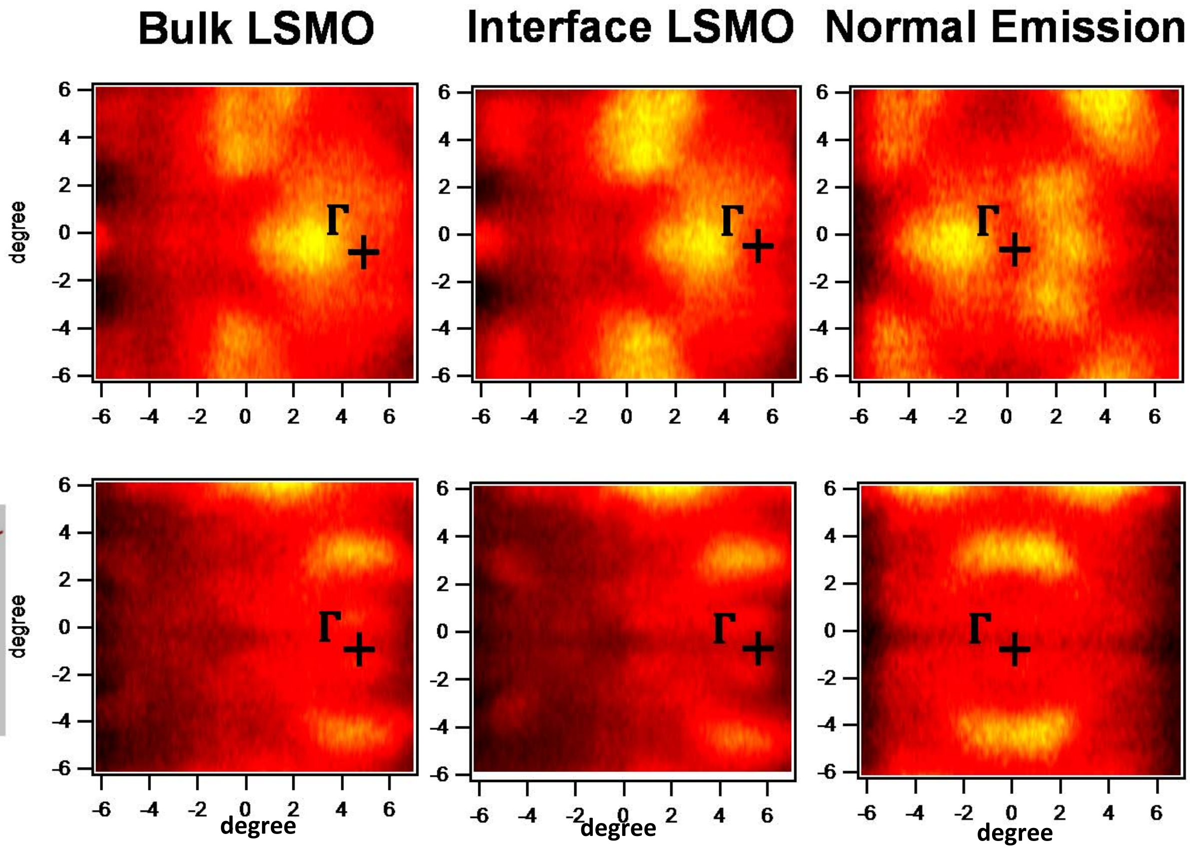

Gray, Nemšák et al., TBP

Looking ahead: $[SrTiO_3/La_{0.7}Sr_{0.3}MnO_3]_{120}$ Variable-Polarization SWARPES

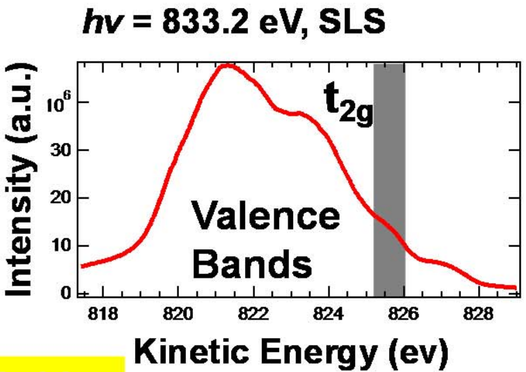

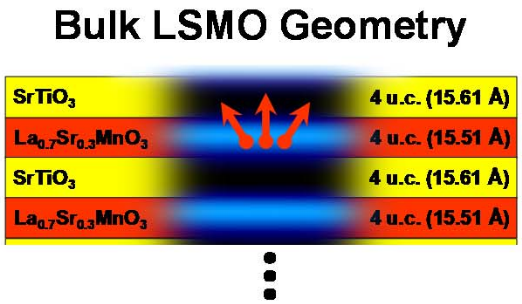

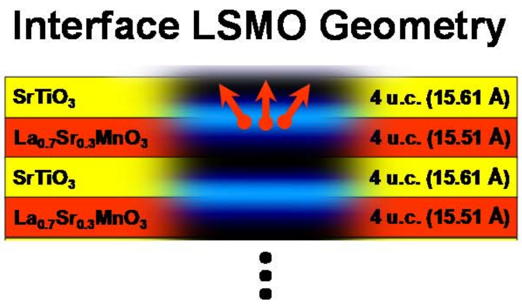

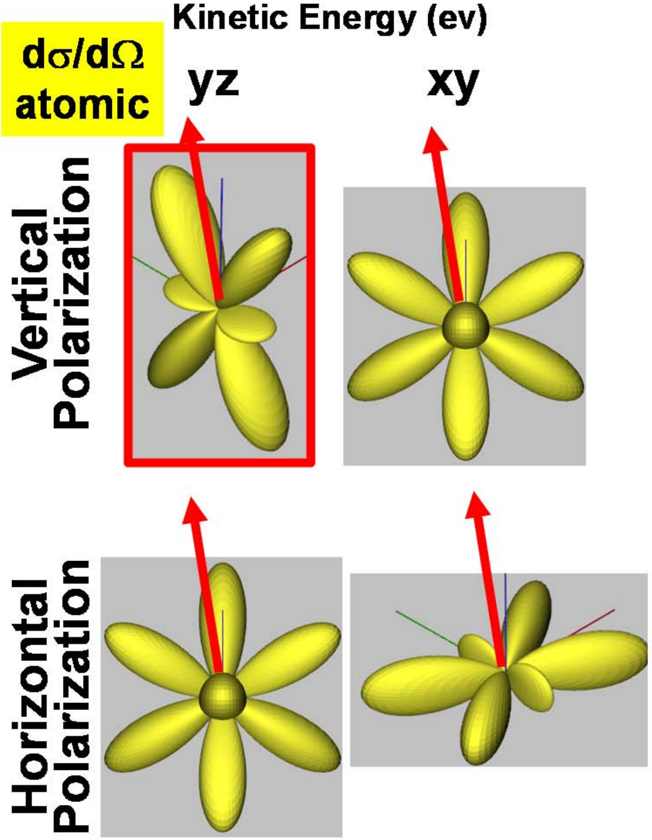

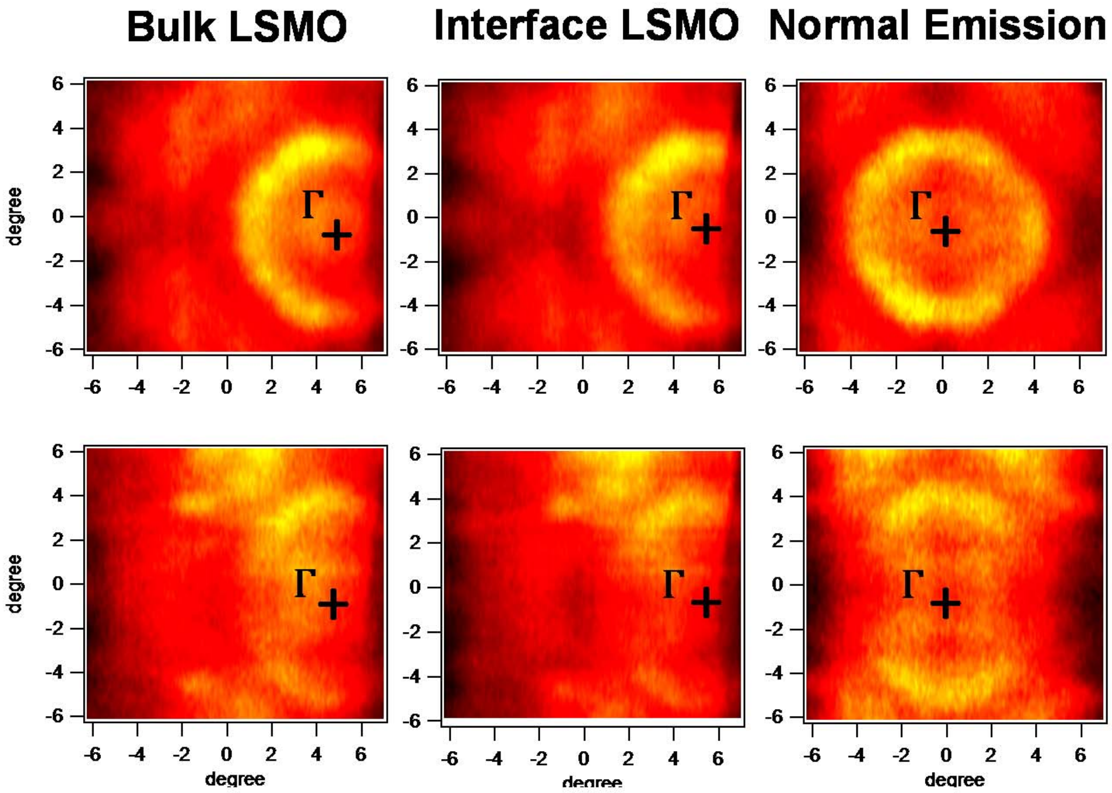

Gray, Nemšák et al., TBP

Conclusions: Soft and Hard X-Ray Standing-Wave PS and ARPES of $SrTiO_3/La_{0.7}Sr_{0.3}MnO_3$

- Measured the depth distribution of concentration and index of refraction through the interface with ca. ±2 Å resolution
- Detected interface Mn 3p binding energy shift consistent with crystal field distortion via AIM calculations
- Measured interface-specific changes in k-resolved electronic structure
- Results qualitatively in agreement with free-electron final state and one-step theory
- Variable polarization ARPES should yield d orbital character

Gray et al., Phys. Rev. B 82, 205116 (2010);
Europhysics Letters 104, 17004 (2013)

Photoemission from surfaces, complex bulk materials, buried layers, interfaces

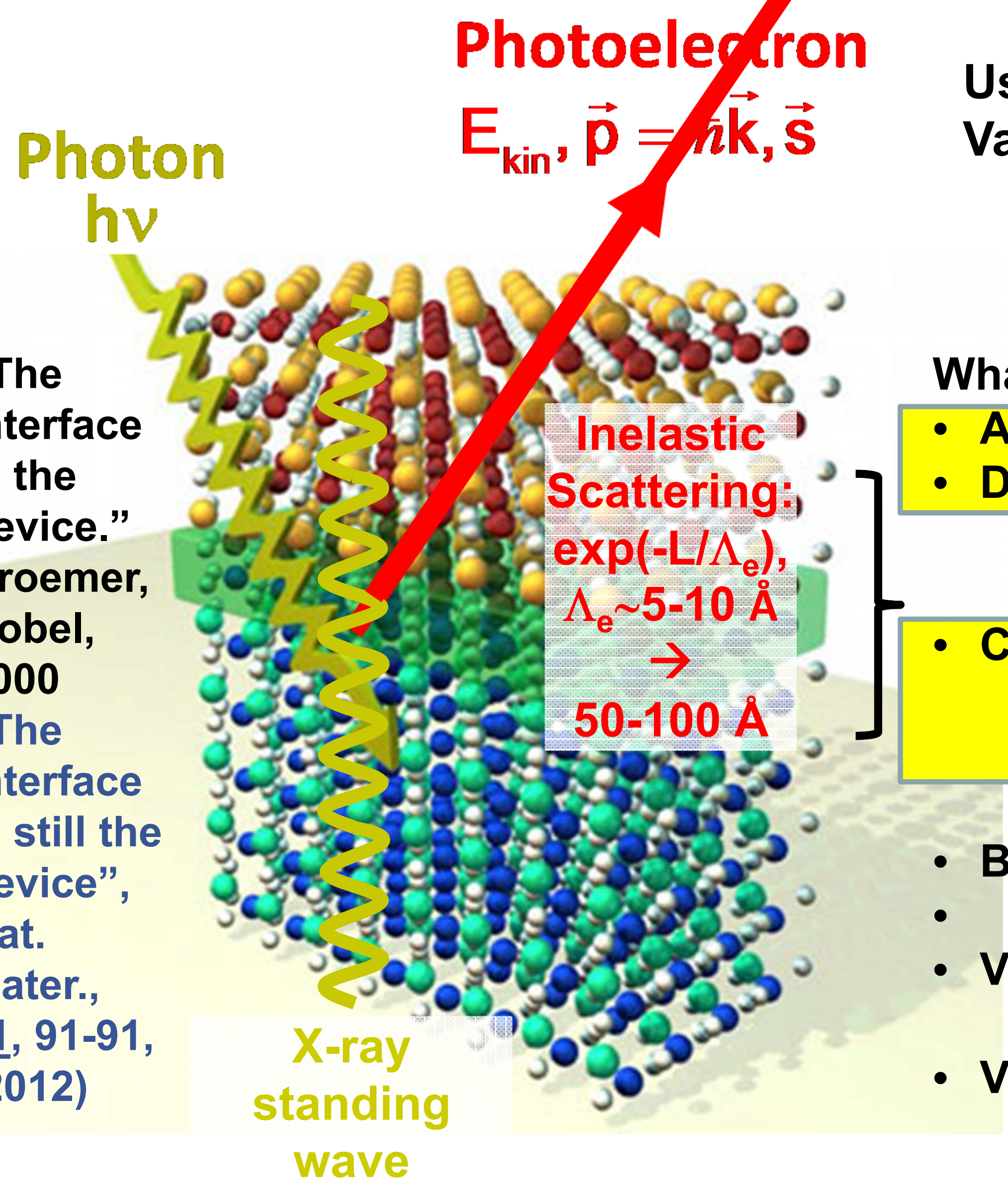

"The interface is the device." Kroemer, Nobel, 2000

"The interface is still the device", Nat. Mater., 11, 91-91, (2012)

Usually ~ultrahigh Vacuum→Multi-Torr

TEM+EELS+HAADF+…

What do we want to know?

- Atomic structure, lattice distortions
- Depth profiles of composition and optical properties, from surface inward
- Core-levels→element-specific binding energies, charge states electronic configurations, magnetic moments/magnetization
- Band offsets, band bending, depth-
- dependent pot'ls.
- Valence-band densities of states bandgaps, behavior near E_F (XPS)
- Valence-band dispersions, via depth-, angle-, spin- resolved photoemission (ARPES)

Photoemission from complex materials, heterostructures, and interfaces

Three ways to address the limitations of traditional photoemission:

- **Use of harder x-ray excitation (SXPS→2 keV, HXPS, HAXPES→10 keV) for deeper probing: core (HXPD) and valence DOSs or soft or hard x-ray ARPES**

- **Use of soft and hard x-ray standing waves, total reflection, other x-ray optical effects, resonant excitation, to selectively look below the surface, at buried interfaces, including soft x-ray ARPES**

- **Use of differentially-pumped systems to provide multi-Torr ambient pressure photoemission, more real-world conditions for studying surface chemical processes, catalysis, electrochemistry**

Lectures posted at Soleil website and group website:

http://www.physics.ucdavis.edu/fadleygroup/Soleil.Lectures.Fadley.pdf

Conclusions: Overall

- **Combining soft and hard x-ray photoemission, including core-level measurements and ARPES, with standing-wave excitation, total reflection, and resonant effects, represents a powerful new suite of techniques for studying bulk properties, as well as depth-resolved buried layers and interfaces in magnetic and strongly correlated materials, with other applications including solid/gas and solid/liquid interfaces at ambient pressures**
- **Future directions: higher ambient pressures, magnetic circular dichroism, spin-resolved studies, time-resolved studies, lateral resolution in PEEM, HAXPEEM**
- **And if you want to hear some more:**

Journée Scientifique:
Systèmes Quantiques Elementaires et Corrélés
Friday, 17 octobre 2014
Lieu: Amphi Blandin, batiment 510
8:45 Accueil – café